Universitat Autònoma de Barcelona

OPTIMIZING THE PROTOCOL FOR THE VITRIFICATION OF IN VITRO MATURED BOVINE OOCYTES

Tania García Martínez

Universitat Autònoma de Barcelona
Facultat de Veterinària

TESI DOCTORAL

OPTIMIZING THE PROTOCOL FOR THE VITRIFICATION OF *IN VITRO* MATURED BOVINE OOCYTES

PRESENTADA PER:

Tania García Martínez

SOTA LA DIRECCIÓ DE:

Dra. Teresa Mogas Amorós

Per accedir al grau de Doctor amb Menció Internacional dins el programa de Doctorat en Medicina i Sanitat Animals.

Departament de Medicina i Cirurgia Animals

UNIVERSITAT AUTÒNOMA DE BARCELONA

Bellaterra, juliol 2021

Universitat Autònoma de Barcelona

Departament de Medicina i Cirurgia Animals

Teresa Mogas Amorós, Catedràtica d'Universitat del Departament de Medicina i Cirurgia Animals de la Universitat Autònoma de Barcelona,

CERTIFICA:

Que la memòria titulada "**Optimizing the protocol for the vitrification of *in vitro* matured bovine oocytes**", presentada per **Tania García Martínez** amb la finalitat d'optar al grau de Doctor en Medicina i Sanitat Animals per la Universitat Autònoma de Barcelona, ha estat realitzada sota la seva direcció, i considerant-la acabada i complint tots els requisits per poder optar a la Menció Internacional, autoritzo la seva presentació per a què sigui jutjada per la comissió corresponent.

I per a què consti als efectes oportuns, signo aquest certificat a Bellaterra, a 25 de juliol de 2021.

Dra. Teresa Mogas Amorós

Edifici V- Campus de la UAB - 08193 Bellaterra(Cerdanyola del Vallès) - Barcelona. Spain
Tel: 34-93 581 10 91 – Fax: 34-93 581 20 06
d.med.cirurgia.animal@uab.es
www.uab.es

School of Chemical, Biological, & Environmental Engineering
Oregon State University
116 Johnson Hall
Corvallis, Oregon 97331

P 541-737-4791
F 541-737-4600
cbee.oregonstate.edu

11/1/2019

Dear Tania,

It was a pleasure working with you during your visit to the United States starting at the Cryobiology meeting in San Diego on July 22, 2019 and ending on November 1, 2019 after a 3 month stay at Oregon State University. We made significant progress with mathematical modeling and data analysis during your stay and I look forward to continuing to work with you after you return to Spain.

CERTIFICADO DE REALIZACIÓN DE ESTANCIA BREVE.

Apellidos, nombre: Tania García Martínez	**NIF/NIE:** 43191090B
Referencia de la ayuda: Beca FI (AGAUR): 2017_FI_00451	**Referencia del proyecto:** AGL2016-79802-P
Centro de I+D de la ayuda predoctoral: Universitat Autònoma de Barcelona	
ORGANISMO DE I+D RECEPTOR: Oregon State University	
CENTRO: College of Engineering	
DEPARTAMENTO: Chemical, biological and environmental Engineering	
PAÍS: United States	

El abajo firmante certifica que el/la investigador/a en formación a quien se refiere el presente document ha permanecido en el centro de trabajo desde el día 1 de agosto de 2019 hasta el día 1 de noviembre de 2019.

Nombre y apellidos del firmante: Adam Z. Higgins

Cargo: Associate Professor

Fecha: 1 de noviembre de 2019

Sincerely,

Adam Higgins, Associate Professor

School of Chemical, Biological, and Environmental Engineering
Oregon State University
116 Johnson Hall
105 SW 26th Street
Corvallis, OR 97331

This thesis has been supported by the Spanish Ministry of Economy and Competitiveness (Project AGL2016-79802-P) and the Generalitat de Catalunya (Project No. 2017 SGR 1229).

Tania García Martínez was supported by a Postgraduate Scholarship: "Ajuts per a la contractació de personal investigador novell" from the Generalitat de Catalunya (2017_FI_00451).

A mi familia

A todas las personas que forman parte de mi vida

TABLE OF CONTENTS

ABBREVIATIONS

2P	Two Parameter formalism
AQP	Aquaporin
C	Cooling rate
Cndv	Concentration non-devitrifiaction
CPA	Cryoprotectant agent
CR_{SF}	Cooling rate slow freezing
CR_v	Cooling rate vitrification
Cv	Concentration of vitrification
EG	Ethylene glycol
EGFP	Green fluorescence protein
ES	Equilibration solution
GV	Germinal vesicle
ICCP	Intracellular concentration of CPA
IIF	Intracellular ice formation
IIF	Intracellular ice formation
IVM	*In vitro* maturation
KK	Kedem-Katchalsky formalism
LN_2	Liquid nitrogen
Lp	Hydraulic conductivity
M	Molarity
Me_2SO	Dimethyl sulfoxide
MII	Metaphase II
npCPA	Non-permeating cryoprotectant agent
nVS	Non vitrification solution
pCPA	Permeating cryoprotectant agent

Ps	Cryoprotectant permeability
RT	Room temperature
T	Temperature
Tg	Glass transition temperature
Th	Homogeneous nucleation temperature
Tm	Melting temperature
Vol	Volume
VS	Vitrification solution
W	Warming rate

LIST OF ILLUSTRATIONS

Literature Review

Chapter I

Chapter II

Chapter III

LIST OF TABLES

Chapter I

Chapter II

Chapter III

Abstract

ABSTRACT

The cryopreservation of mammalian oocytes and embryos has become an integral part of assisted reproduction in both humans and veterinary species. However, the methods used to cryopreserve bovine oocytes and embryos still have significant shortcomings. Currently, vitrification has grown as an alternative option to traditional slow-cooling/rapid-thaw cryopreservation for oocytes of several species minimizing the formation of intracellular ice crystals when an oocyte and the surrounding vitrification solution are "glassified". During this process, controlling water flux as well as intracellular content plays an important role in minimizing cell injuries or lethal ice formation. For hence, optimization of cryopreservation protocols is, in part, dependent on cell membrane permeability characteristics. The development of optimal cryopreservation protocols requires accounting for these particular features, which makes rigorous experimental optimization impractical, as it would require a very large number of treatment combinations. By using fundamental principles and computer modeling, estimates of optimal methods can be achieved through rational analysis, with the potential to save a significant amount of resources by narrowing the choices to test *via* empirical methods.

Nevertheless, many of the transport formalisms currently used are based on limiting dilute-solution assumptions often appropriate under physiological conditions, but rarely appropriate in cryobiology where cryoprotectants are often used at high concentrations. Bearing this in mind, the first objective of this work was to examine the effects of increasing CPA concentrations on water and CPA membrane permeability in immature and *in vitro* matured bovine oocytes through two different mathematical approaches: the 2P formalism and the nondilute formalism. Results showed that CPA concentration affected membrane CPA permeability, with differential effects depending upon the maturation stage of the oocyte and the specific CPA type. Moreover, in order to compare both modeling approaches, the permeability parameters resulting from the previous experiments were used to model cell volume excursions for the CPA addition and removal process used in the Kuwayama protocol, which was designed for bovine and human oocyte vitrification. Results indicated that only slight differences exist between the two models' predictions during the CPA loading steps while a greater difference was observed between models during the first stage of CPA removal.

Because vitrification solutions contain a high concentration of cryoprotectant, permeability of the plasma membrane becomes an important aspect to minimize CPA toxicity. With an argument that cytotoxicity due to CPA exposure is time and concentration-sensitive, rational design strategies have also been extended to reduce toxic damage by minimizing the

duration of the CPA addition and removal procedures while still maintaining cell volumes between osmotic tolerance limits. Moreover, it has been shown that aquaglyceroporins could be involved in the movement of water and CPA in mouse and bovine oocytes. Thus, the second objective of this work aimed to study the expression of AQP3, AQP7 and AQP9 after exposure of *in vitro* matured bovine oocytes to hyperosmotic CPA solutions. And more specifically, we studied the role of AQP7 in the movement of water and cryoprotectants in bovine *in vitro* matured oocytes with artificially overexpressed AQP7 through cRNA injection. Our results demonstrated that MII bovine oocytes expressed AQP3 and AQP7 but not AQP9 when exposed to hyperosmotic solution being AQP3 expression up-regulated after exposure to Me_2SO while AQP7 was overexpressed after being in contact with EG hyperosmotic solutions. Moreover, we also demonstrated that exogenous expression of AQP7 is possible in *in vitro* matured oocytes, and it seems to facilitate water diffusion when bovine MII oocytes are in presence of sucrose or Me_2SO solutions but not EG solution. However, this aquaporin is not involved in the movement of Me_2SO and EG.

Finally, the efficiency of the theoretical model resulting from the first study was assessed. Based on *in silico* and *in vitro* osmotic observations, we proposed shorter dehydration-based protocols at different temperatures (25°C *vs* 38.5°C) as a first step towards defining an optimal cryopreservation method. *In vitro* observations of the oocytes' osmotic behavior indicated that the time required for the oocytes to reach the equilibrium cell volume upon exposure to standard equilibrium solution was 2 min 30 s at 38.5°C and at 5 min 30 s at 25°C. Subsequently, we tested the efficiency of the optimized cell-specific exposure times for each temperature prior to vitrification/warming on oocyte spindle configuration, DNA fragmentation and further embryo development. As a result, we were able to successfully reduce the necessary time to prepare bovine oocytes for vitrification to 2 min 30 s when vitrification was carried out at 38.5°C, obtaining similar results on spindle morphology, DNA fragmentation and embryo development than fresh control oocytes.

RESUMEN

La criopreservación de ovocitos y embriones de mamíferos se ha convertido en una parte integral de la reproducción asistida tanto en humanos como en especies veterinarias. Sin embargo, los métodos utilizados para criopreservar ovocitos y embriones bovinos todavía muestran deficiencias. Actualmente, la vitrificación ha crecido como una opción alternativa a la criopreservación tradicional de enfriamiento lento/descongelación rápida para ovocitos de varias especies ya que minimizan la formación de cristales de hielo intracelulares cuando un ovocito y la solución de vitrificación circundante se "glasifican". Durante este proceso, el control del flujo de agua y del contenido intracelular juega un papel importante para minimizar las lesiones celulares o la formación de hielo letal. Por tanto, la optimización de los protocolos de criopreservación depende, en parte, de las características de permeabilidad de la membrana celular. El desarrollo de protocolos óptimos de criopreservación requiere tener en cuenta estas características particulares, lo que hace que la optimización experimental rigurosa no sea práctica, ya que requeriría una gran cantidad de combinaciones de tratamientos. Mediante el uso de principios fundamentales y modelos informáticos, se pueden lograr las estimaciones de los métodos óptimos mediante un análisis racional, con el potencial de ahorrar una cantidad significativa de recursos al reducir las opciones para probar mediante métodos empíricos.

No obstante, muchos de los formalismos de transporte utilizados actualmente se basan en la limitación de supuestos de solución diluida, apropiada en condiciones fisiológicas pero no en criobiología, donde se utilizan a menudo altas concentraciones de CPA. Teniendo esto en cuenta, el primer objetivo de este trabajo fue examinar los efectos de concentraciones crecientes de CPA sobre la permeabilidad de la membrana al agua y al CPA en ovocitos bovinos inmaduros y madurados *in vitro* a través de dos enfoques matemáticos: el formalismo 2P y el formalismo no diluido. Los resultados mostraron que la concentración de CPA afectó la permeabilidad de la membrana del CPA, con efectos diferenciales según la etapa de maduración del ovocito y el tipo específico de CPA. Además, con el fin de comparar ambos enfoques de modelado, los parámetros de permeabilidad resultantes de los experimentos anteriores se utilizaron para modelar las excursiones de volumen celular para el proceso de adición y eliminación de CPA utilizado en el protocolo de Kuwayama, diseñado para la vitrificación de ovocitos bovinos y humanos. Los resultados indicaron que solo existen ligeras diferencias entre las predicciones de los dos modelos durante los pasos de adición de CPA, y una mayor diferencia entre los modelos durante la primera etapa de eliminación de CPA.

Debido a que las soluciones de vitrificación contienen una alta concentración de CPA, la permeabilidad de la membrana plasmática se convierte en un aspecto importante para minimizar la toxicidad del CPA. Con el argumento de que la citotoxicidad debida a la exposición a CPA es sensible al tiempo y a la concentración, las estrategias de diseño racional intentan reducir el daño tóxico minimizando la duración de los procedimientos de adición y eliminación de CPA mientras se mantienen los volúmenes de las células entre los límites de tolerancia osmótica. Además, se ha demostrado que las acuagliceroporinas podrían estar involucradas en el movimiento de agua y CPA en ovocitos de ratón y bovino. Es por eso, que el segundo objetivo de este trabajo se centró en estudiar la expresión de la AQP3, AQP7 y AQP9 después de la exposición de ovocitos bovinos madurados *in vitro* a soluciones hipertónicas de CPA. Y más específicamente, estudiamos el papel de la AQP7 en el movimiento de agua y crioprotectores en ovocitos bovinos madurados *in vitro* con la AQP7 sobreexpresada artificialmente mediante la microinyección del ARNc. Nuestros resultados demostraron que los ovocitos bovinos MII expresaron AQP3 y AQP7 pero no AQP9 cuando se expusieron a una solución hiperosmótica, con una expresión de la AQP3 regulada al alza después de la exposición a Me_2SO y de la AQP7 después de la exposición a EG. Además, demostramos que la expresión exógena de AQP7 es posible en ovocitos madurados *in vitro*, y parece facilitar la difusión de agua cuando los ovocitos bovinos MII están en presencia de soluciones de sacarosa o Me_2SO pero no de EG. Sin embargo, esta acuaporina no está involucrada en el movimiento de Me_2SO y EG.

Finalmente, se evaluó la eficiencia del modelo teórico resultante del primer estudio. Basándonos en observaciones osmóticas *in silico* e *in vitro*, propusimos protocolos de deshidratación más cortos a diferentes temperaturas (25°C frente a 38.5°C) como un primer paso hacia la definición de un método óptimo de criopreservación. Las observaciones *in vitro* del comportamiento osmótico de los ovocitos indicaron que el tiempo requerido para que los ovocitos alcancen el volumen celular de equilibrio tras la exposición a la solución de equilibrio estándar era de 2 min 30 s a 38.5°C y de 5 min 30 s a 25°C. Posteriormente, probamos la eficiencia de los tiempos optimizados de exposición específicos de la célula para cada temperatura antes de la vitrificación/calentamiento a través de la configuración del huso de los ovocitos, la fragmentación del ADN y el desarrollo embrionario. Como resultado, logramos reducir con éxito el tiempo necesario para preparar ovocitos bovinos para la vitrificación a 2 min 30 s cuando la vitrificación se realizó a 38.5°C, obteniendo resultados similares en morfología del huso, fragmentación del ADN y desarrollo embrionario comparado con los ovocitos control frescos.

RESUM

La criopreservació d'oòcits i embrions de mamífers s'ha convertit en una part integral de la reproducció assistida tant en humans com en espècies veterinàries. No obstant això, els mètodes utilitzats per a criopreservar oòcits i embrions bovins encara mostren deficiències. Actualment, la vitrificació ha crescut com una opció alternativa a la criopreservació tradicional de refredament lent/descongelació ràpida per a oòcits de diverses espècies ja que minimitzen la formació de cristalls de gel intracel·lulars quan un oòcit i la solució de vitrificació circumdant es "glassifiquen". Durant aquest procés, el control del flux d'aigua i del contingut intracel·lular juga un paper important per a minimitzar les lesions cel·lulars o la formació de gel letal. Per tant, l'optimització dels protocols de criopreservació depèn, en part, de les característiques de permeabilitat de la membrana cel·lular. El desenvolupament de protocols òptims de criopreservació requereix considerar aquestes característiques particulars, la qual cosa fa que l'optimització experimental rigorosa no sigui pràctica, ja que requeriria una gran quantitat de combinacions de tractaments. Mitjançant l'ús de principis fonamentals i models informàtics, es poden aconseguir les estimacions dels mètodes òptims mitjançant una anàlisi racional, amb el potencial d'estalviar una quantitat significativa de recursos en reduir les opcions per a provar mitjançant mètodes empírics.

No obstant això, molts dels formalismes de transport que s'utilitzen actualment es basen en la limitació de supòsits de solució diluïda, apropiada en condicions fisiològiques però menys apropiada en criobiologia, on s'utilitzen sovint els crioprotectors en altes concentracions. Tenint això en compte, el primer objectiu d'aquest treball va ser examinar els efectes de concentracions creixents de CPA sobre la permeabilitat de la membrana a l'aigua i al CPA en oòcits bovins immadurs i madurats *in vitro* a través de dos enfocaments matemàtics diferents: el formalisme 2P i el formalisme no diluït. Els resultats van mostrar que la concentració de CPA va afectar a la permeabilitat de la membrana del CPA, amb efectes diferencials segons l'etapa de maduració de l'oòcit i el tipus específic de CPA. A més, amb la finalitat de comparar tots dos enfocaments de modelatge, els paràmetres de permeabilitat resultants dels experiments anteriors es van utilitzar per a modelar les excursions de volum cel·lular per al procés d'addició i eliminació de CPA utilitzat en el protocol de Kuwayama, que va ser dissenyat per a la vitrificació d'oòcits bovins i humans. Els resultats van indicar que només existeixen lleugeres diferències entre les prediccions dels dos models durant els passos d'addició de CPA, mentre que es va observar una major diferència entre els models durant la primera etapa d'eliminació de CPA.

Pel fet que les solucions de vitrificació contenen una alta concentració de CPA, la permeabilitat de la membrana plasmàtica es converteix en un aspecte important per a minimitzar

la toxicitat del CPA. Amb l'argument que la citotoxicitat deguda a l'exposició a CPA és sensible al temps i a la concentració, les estratègies de disseny racional intenten reduir el dany tòxic minimitzant la durada dels procediments d'addició i eliminació de CPA mentre es mantenen els volums de les cèl·lules entre els límits de tolerància osmòtica. A més, s'ha demostrat que les aquagliceroporines podrien estar involucrades en el moviment d'aigua i CPA en oòcits de ratolí i boví. És per això que el segon objectiu d'aquest treball es va centrar en estudiar l'expressió de l'AQP3, AQP7 i AQP9 després de l'exposició d'oòcits bovins madurats *in vitro* a solucions hipertòniques de CPA. I més específicament, vam estudiar el paper de l'AQP7 en el moviment d'aigua i crioprotectors en oòcits bovins madurats *in vitro* amb l'AQP7 sobreexpressada artificialment mitjançant la microinjecció del ARNc. Els nostres resultats van demostrar que els oòcits bovins MII van expressar AQP3 i AQP7 però no AQP9 quan es van exposar a una solució hiperosmòtica, amb una expressió de l'AQP3 regulada a l'alça després de l'exposició a Me_2SO i de l'AQP7 després de l'exposició a EG. A més, vam demostrar que l'expressió exògena d'AQP7 és possible en oòcits madurats *in vitro*, i sembla facilitar la difusió d'aigua quan els oòcits bovins MII estan en presència de solucions de sacarosa o Me_2SO però no de EG. No obstant això, aquesta aquaporina no està involucrada en el moviment de Me_2SO i EG.

Finalment, es va avaluar l'eficiència del model teòric resultant del primer estudi. Basant-nos en observacions osmòtiques *in silico* i *in vitro*, vam proposar protocols de deshidratació més curts a diferents temperatures (25°C enfront de 38.5°C) com un primer pas cap a la definició d'un mètode òptim de criopreservació. Les observacions *in vitro* del comportament osmòtic dels oòcits van indicar que el temps requerit perquè els oòcits recuperin el volum cel·lular d'equilibri després de l'exposició a la solució d'equilibri estàndard era de 2 min 30 s a 38.5°C i de 5 min 30 s a 25°C. Posteriorment, vam provar l'eficiència dels temps optimitzats d'exposició específics de la cèl·lula per a cada temperatura abans de la vitrificació/escalfament a través de la configuració del fus dels oòcits, la fragmentació de l'ADN i el desenvolupament embrionari. Com a resultat, vam aconseguir reduir amb èxit el temps necessari per a preparar oòcits bovins per a la vitrificació a 2 min 30 s quan la vitrificació es va realitzar a 38.5°C, obtenint resultats similars en morfologia del fus, fragmentació de l'ADN i desenvolupament embrionari comparat amb els oòcits control frescos.

Literature Review

1. Cryopreservation of mammalian oocytes

Cryo-, a Greek word used in combination, means "very low temperature or freezing." Cryo-preservation is a technique in which biological living cells and tissues are preserved for extended periods of time, and from which they can be brought back to viability at some point in the future. The temperature that generally is used for storage of mammalian cells, -196°C, the temperature of liquid nitrogen, appears to be adequate for these purposes, although a precise threshold value for this temperature is not known. At very low subzero temperatures, the stored material enters in a state of "absolute quiescence" as all the physical and biochemical reactions are practically halted due to non-availability of water, a requirement of cell metabolism (Mazur 1984; Anzar 2017).

The ability to cryopreserve mammalian oocytes and embryos has become an integral part of assisted reproduction in both human and veterinary medicine. The possibility of cryopreservation in the field of reproduction was reported for the first time by Polge et al. (1949) (Polge *et al.* 1949), who accidentally discovered the cryoprotective properties of glycerol on human spermatozoa. Since then, many advances have been made in the field of gamete and embryo cryopreservation (Díez *et al.* 2012). In cattle, those originally developed in the decades of 50s to 70s include artificial insemination and multiple ovulations/embryo transfer combined with or without cryopreservation of spermatozoa and embryos. Nowadays, the combined use of reproductive technologies such as trans-vaginal ovum-pick up and *in vitro* embryo production followed by direct transfer of cryopreserved embryos has great potential for enhancing genetic selection and optimizing crossbreeding schemes in beef and dairy cattle production systems. This, along with an effective cryopreservation procedure for cow oocytes will enable the long-term conservation of female genetic traits and the advance of embryo biotechnology in this species.

Interest in oocyte cryopreservation has increased because of the wide use of oocytes for procedures such as *in vitro* embryo production, nuclear transfer or gene banking. The long-term storage of oocytes has benefits such as it allows the preservation of important genetic lineage; the ability to restock following out-breaks of diseases; the preservation of genetically modified strains, thereby reducing maintenance costs and providing safeguards against loss through infection, disease, genetic drift, and against catastrophic loss of rare or endangered animal genetic resources (Prentice and Anzar 2010). Therefore, these technologies have accelerated the progress of genetic improvement, the worldwide distribution of germplasm, and more efficient management of livestock and laboratory animal species (Holt 2008; Díez *et al.* 2012). In humans,

oocyte cryopreservation allows preserving fertility for individuals at risk of compromised oocyte quality due to cancer treatments or advanced maternal age; banking of excess oocytes produced as a result of *in vitro* fertilization treatments; and donation of oocytes to others. In certain circumstances, oocyte preservation is considered preferable to embryo preservation in humans because ethical concerns are fewer for unfertilized gametes (Paynter and Fuller 2007).

In veterinary species, cryopreservation of oocytes has short and less successful history when compared to the other reproductive cells as spermatozoa and embryos. Despite many efforts, advances on oocyte cryopreservation are rather slow and results on embryo development from slow-frozen or vitrified oocytes remain inefficient. The loss of developmental potential after cryopreservation makes mammalian oocytes probably one of the most difficult cell types to cryopreserve. The oocyte has very special structural and functional characteristics making the cell very sensitive to chilling and susceptible to intracellular ice formation (Moussa *et al.* 2014). After cryopreservation, the oocyte has both fertilization and embryo developmental competence already compromised. Hence, work is needed to develop an optimal cryopreservation protocol for unfertilized oocytes adapted to individual species requirements (Prentice *et al.* 2011).

2. The science of cryobiology

2.1. Water, ice and their importance to living cells

Since liquid water is considered essential to the structure and function of living cells, it is not surprising that the solidification of water as ice by freezing is usually lethal. Yet paradoxically, freezing can also preserve cells for long periods of time in a viable state, for hence the challenge is to determine how they can survive both the cooling to such temperatures and the subsequent return to physiological conditions (Mazur 1984).

Water appears in nature in all three common states of matter depending on the temperature and atmospheric pressure: solid, liquid, and vapor. Generally, when a dilute aqueous solution is cooled to subzero temperatures, the solidification (either spontaneously or when seeded artificially) of water is thought to be associated with the ice crystal formation (Pegg 2002; Leibo 2008). However, for the cryobiologist point of view, there are two distinct forms of water solidification. Water can either solidify from the liquid state to the *crystalline solid form of water* or it can undergo a second-order phase transition and become an amorphous solid without crystal formation when cooled under extremely rapid conditions (above 100 000°C/min) (Brüggeller

and Mayer 1980). Then it is referred to solidification of pure water, which is described as the *glassy solid-state of water* (Fahy *et al.* 1984).

2.1.1. Phase changes of pure water during the cooling process

a) The crystalline solid form of water

When the temperature drops below 0ºC, aqueous fluids do not freeze immediately but first "supercool" (Figure 1). Changes in thermal energy in the solution drive the mechanism for self-association of water molecules to form structures that can nucleate ice with a process termed homogenous nucleation (Zachariassen and Kristiansen 2000). Nevertheless, this process is surprisingly energetically unfavorable at high subzero temperatures (i.e. just below 0ºC) due to the extreme mobility and free rotation of water molecules. As long as the crystal formation has not reached a critical mass, the tendency to melt the newly formed ice crystal prevails, explaining why aqueous fluids do not freeze immediately but can remain supercooled down to temperatures as low as −40ºC (homogeneous nucleation temperature of pure water). The zone between the equilibrium melting temperature (Tm) and the homogeneous nucleation temperature (Th), is, therefore, characterized by the phenomenon of supercooling because there is a competition between the formation of crystallization nuclei and the disappearance of these same nuclei in the liquid. Moreover, in biological systems, the presence of particles in water can catalyze ice crystal formation at temperatures above Th by a process called heterogenous nucleation (Zachariassen and Kristiansen 2000; Zachariassen *et al.* 2004).

Both the formation of the nuclei and the subsequent growth of ice crystals are temperature dependent. Because the state of supercooling cannot indefinitely continue as the temperature drops, the movement of molecules of water slow down, and the critical mass of the crystal nucleus formation is finally sufficient to induce solidification as Th approaches (Franks 1986; Muldrew *et al.* 2004). Once seeds of ice nucleation are formed, the structure becomes more rigid, and seeds can gather together into larger crystals. When Th is attained, the complex structure ends up crystallizing uniformly even in the absence of any crystallization seeds and becomes a stable state as a crystalline solid. Rates of nucleation rise as temperature decreases, reaching a maximum near the glass transition temperature (Luyet 1957). Only below the glass transition temperature do astronomical and loss of rotational freedom begin to slow ice nucleation (Luyet and Gehenio 1947; Luyet 1957; Elliott *et al.* 2017).

b) The glassy solid-state of water

Glass solidification of pure water (vitrification) is possible when the temperature drops

sufficiently fast enough below the glass transition temperature (Tg) (Figure 1). Tg for pure water is −137°C (Angell 2002) and only possible with cooling (C) rates exceeding 100,000 °C/min to avoid spontaneous crystal nucleation when crossing the zone between Tm and Tg (Chian 2010).

Once below Tg, the movement of water molecules is too slow to organize the start of crystallization, and the solution solidifies with water molecules arranged in a completely disordered state achieving an amorphous or vitreous solid-state. In other words, the system is not merely a viscous liquid but is also a solid that is in a stable thermodynamic state that keeps almost intact intermolecular bonds typical of the liquid state. (Fahy *et al.* 1984). The probability of reaching the vitreous state can be expressed by the simple equation:

$$Probability\ of\ obtaining\ a\ vitrified\ state\ in\ pure\ water = \frac{Cooling\ rate\ (C)}{Volume\ (Vol)}$$

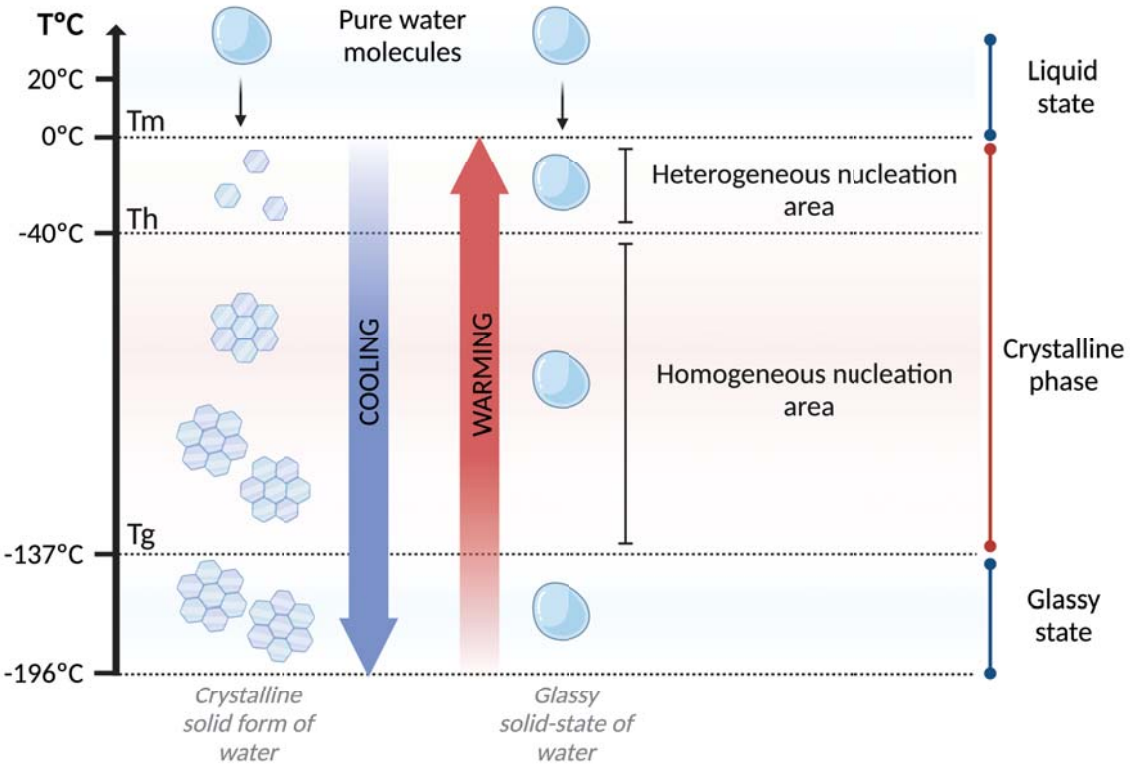

Figure 1. Changes in the physical states of pure water during cooling/warming. The physical states changes in the pure water as temperature (T°) decreases are presented on the left side of the diagram. Heterogeneous nucleation can occur below Tm (melting temperature). Ice crystal formation without the presence of nuclei of crystallization occurs only after reaching a temperature below Th (homogeneous nucleation temperature). When the T° decreases extremely

rapidly (cooling speed) below the glass transition temperature (Tg), pure water solidifies in a glassy solid form (vitrification) (right side). Image adapted from (Vanderzwalmen *et al.* 2020).

2.1.2. CPA concentration and temperature to control the solid-state of water

During the development of the different cryopreservation techniques, it was soon recognized that cryopreservation nearly always needs the use of one or more agents that confer protection to cell from freezing damage. These so-called cryoprotectant agents (CPA) are typically very simple, low molecular weight molecules with high water solubility and low toxicity. One feature that is common among these compounds is their ability to form hydrogen bonds with water molecules, through their hydroxyl residues (glycerol, ethylene glycol, 1-2 propanediol, propylene glycol) or sulfoxidegroups (dimethyl sulfoxide; Me_2SO) (Fuller 2004).

CPAs are highly soluble in the aqueous environment, and also intracellularly and can enter into the cell through both simple diffusion and through facilitated diffusion using specific aquaporin channels (Jin *et al.* 2011). When cells are exposed to solutions containing CPA, a part of the intracellular free water will be replaced by the CPA solution. CPAs increase the viscosity of the solution which causes the slowing down of the molecular movements of water (Mullen and Critser 2007). Besides, the increase in viscosity causes (i) a delay of the nucleation process, (ii) a decrease of the rate of growth of ice crystals, (iii) the limitation of the crystals size between Tm and Tg, and (iv) an impairment of crystal formation when a high increase in viscosity takes place while temperature drops (Vanderzwalmen *et al.* 2020).

For pure water, it has to be considered that Tm, Th, Tg are defined and constant (Figure 1). Nevertheless, aqueous solutions as culture media, containing salts, amino acids, and proteins, or cryopreservation solutions, supplemented with CPAs, exhibit altered Tm, Th, and Tg. The modification in these parameters depends on the respective concentration and composition of solved molecules and CPAs and it is displayed on a "dynamic" phase diagram (Figure 2) (Cocks and Brower 1974).

Both Tm and Th decrease as the CPA concentration increases, and Tg increases. As a result, and at some concentration (Cv), it becomes possible to cool from Tm to Tg and below without traditional homogeneous nucleation. The curve labeled Tg represents the glass transition temperature. At this temperature, liquid solutions will shift to a stable glass (vitrify) and will remain vitreous upon further cooling (Mullen and Critser 2007). However, it is practically impossible to achieve true vitrification at lower concentrations in region I, because both heterogeneous and homogeneous nucleation are unavoidable, at least with practical cooling rates

(Fahy *et al.* 1984). In the more concentrated region II, both heterogeneous and homogeneous nucleation markedly diminish, and those nuclei formed from homogeneous nucleation are too small to be detectable due to an extreme suppression of ice crystal growth caused by the very low temperatures at which the ice nuclei are formed. Moreover, the difference between the Th and Tg curves is small enough to allow vitrification with practical cooling rates. However, a solution that does attain a vitreous state in this region is thermodynamically unstable (Fahy *et al.* 1984; Tucker 2007).

At still higher concentrations, in the regions marked as III and IV, Th becomes equal to Tg and then actually falls below Tg and vitrification is easily achievable. Notice that the Th curve actually intersects Tg at the transition between regions II and III and therefore establishes the threshold or lowest possible concentration of CPA that might be used for sample vitrification. Heterogeneous ice formation will not occur at temperatures below Tg (Fahy *et al.* 1984; Tucker 2007).

If a sample with a composition described by regions II and III is cooled fast enough to vitrify, ice may still form during warming due to nucleation and ice growth. This is because cooling results in nuclei too small to visualize or to cause biological injury. However, when the solution is rewarmed, rapid ice growth becomes possible, and devitrification is observed. The temperature at which this happens is described by Td, the devitrification temperature (Boutron and Mehl 1990; Mullen and Critser 2007). This means that total ice development is much more rapid during warming, and hence warming rates required to avoid significant devitrification are found to be far higher than cooling rates initially required to achieve vitrification (Wolkers and Oldenhof 2015).

Finally, at region IV, as concentrations increase and nucleation density decreases, Td increases until, at some concentration (Cndv), the devitritication curve vanishes even at slow warming rates. Here all nucleation is prevented, and the system is virtually stable (Fahy *et al.* 1984).

Therefore, although vitrification is an appropriate goal, successful vitrification does not require that the whole system has completely achieved a glassy state. In fact, recovery is compatible with very small amounts of intracellular ice, and this is one reason why the warming rate has a profound effect. The behavior of very small intracellular ice crystals differs between slow and rapid warming. While it has been demonstrated that damage to the cells during slow warming is due to crystals recrystallization, there is insufficient time for this to happen during

rapid warming and the ice simply melts (Wolkers and Oldenhof 2015). As the solute concentration decreases, the cooling and warming rates necessary to avoid ice formation increase dramatically and may vary depending on the cell type because of their different water permeability and probably because of their different susceptibility to form intracellular ice (Toner *et al.* 1991).

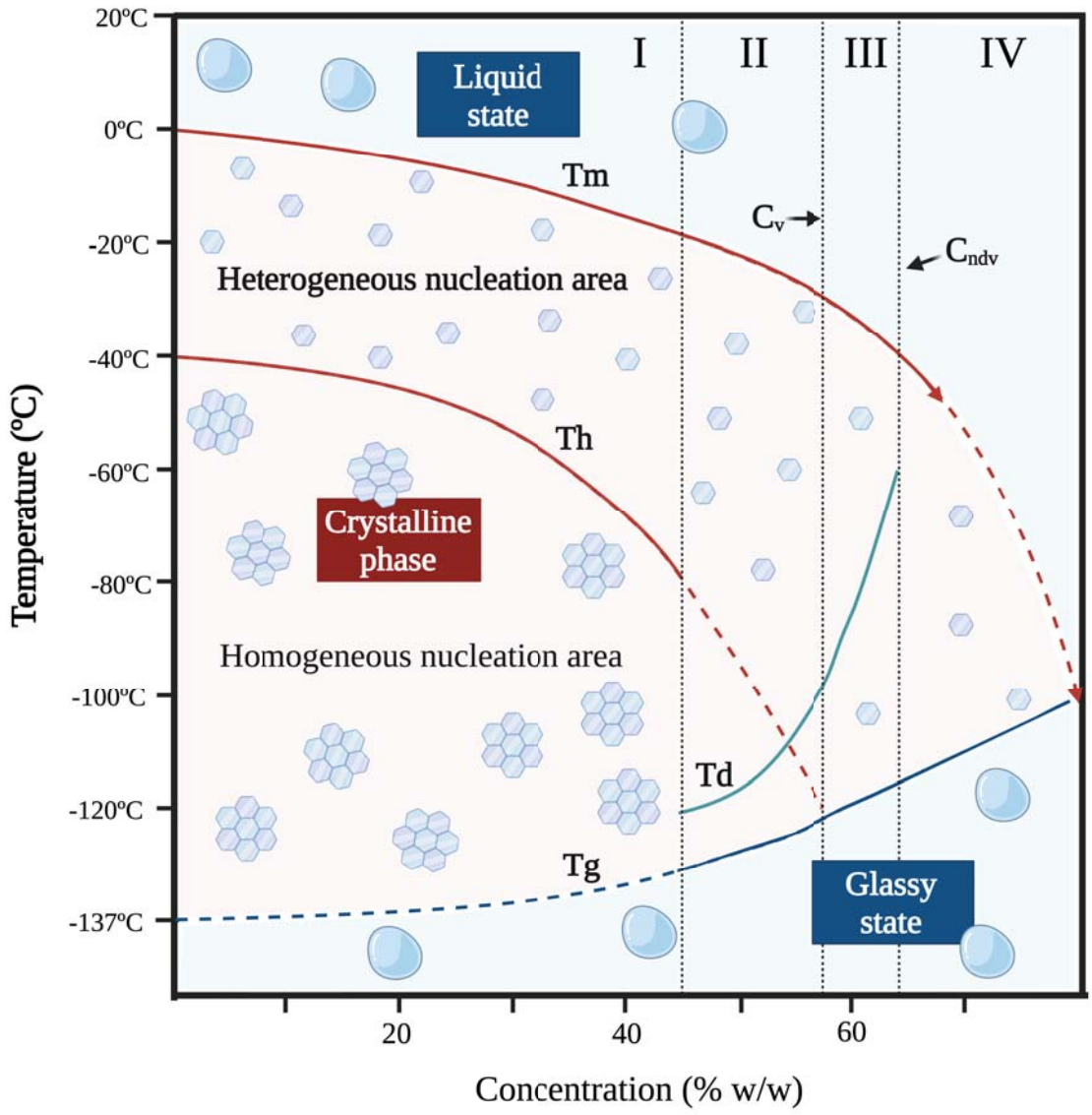

Figure 2. Supplemented phase diagram of a hypothetical cryoprotectant solution during cooling/warming. In solutions, the content of salts, proteins and other macromolecules, among cryoprotectants agents, lead to an increase in viscosity. Therefore, the melting temperature (Tm) decreases, and the glass transition temperature (Tg) increases. Thereby, the temperature where ice crystal formation occurs becomes substantially smaller, and the probability of obtaining a glassy state increases.

2.2. Mechanisms of damage during freezing: intracellular ice formation and solution effect

The main physical events occurring in cells during freezing are described schematically in Figure 3. The cells and their surrounding medium remain unfrozen down to -5°C because of supercooling and because of the decrease of the freezing point by the protective solutes frequently present in the solution (Mazur 1984). Ice is more likely to form in a large volume than a small volume. Because the volume of an individual cell is much smaller than the volume of the extracellular aqueous environment, ice will normally form in the extracellular space first (Karow 1969)[14]. However, as ice has insignificant ability to dissolve solutes, solutes are excluded from the growing ice matrix leading to increases in concentration in the remaining volume of unfrozen liquid and the depression of the colligative freezing point (Wolkers and Oldenhof 2015).

As the extracellular osmolality increases due to ice formation, the intracellular water flows out of the cell by an osmotic gradient, causing cell dehydration, which can lead to changes in the membrane phase and cell damage (Bryant 1995; Wolfe and Bryant 1999; Wolfe and Bryant 2001). The extracellular ice formation and subsequent cell dehydration depend upon cooling velocity (Mazur 1977). If cooling rate is lower than optimum (Figure 3, upper right), the extracellular ice crystals (large but innocuous) continue to form and cells keep dehydrating to maintain the chemical potential equilibrium between extra- and intracellular compartments. As a result, the cell dehydrates and does not freeze intracellularly due to its high intracellular osmolality (Mazur 1984). If cells are cooled slowly, they are exposed for prolonged periods to a hypertonic medium with higher salinity than isotonic exposure. This phenomenon is commonly known as "solution effect", and it is cell damage in a number of ways such as modifying the lipid bilayer of the plasma membrane, changing protein conformations or creating osmotic stress upon warming (Wolfe and Bryant 2001; Elliott *et al.* 2017).

Under too-fast cooling protocols (Figure 3, bottom right), cells do not have sufficient time to transport water out to maintain equilibrium and the reduction of the intracellular freezing point will not be enough to avoid intracellular ice formation (IIF) (Mazur 1977). The presence of pores such as aquaporins (Mazur 1965) or channels between cells such as gap junctions (Acker *et al.* 2001; Irimia and Karlsson 2005), and the proximity of extracellular ice may also influence IIF. The intracellular ice crystals are detrimental to cell organelles depending upon their size and number and so must be avoided. Both, intracellular ice formation and solution effect have lethal consequences on cell or tissue cryopreservation (Mazur 1963; Mazur *et al.* 1972).

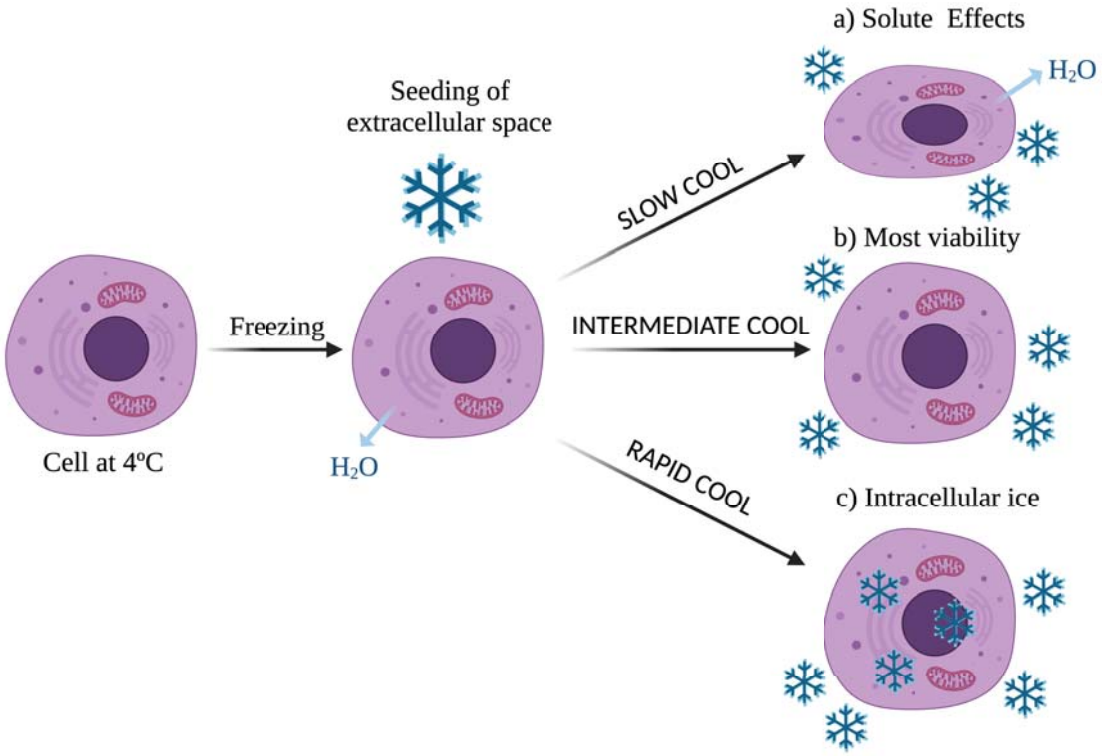

Figure 3. Schematic of physical events in cells depending upon different cooling rates during freezing. With slow cooling rate (A), the cell shrinks due to water loss and dehydration; solute concentration effects may produce cell death. With intermediate cooling rate (B) there is a balance between solute effects and intracellular ice formation, leading to maximum viability. With rapid cooling rate (C) the intracellular space supercooled, which leads to intracellular ice formation and cell death. Figure obtained from Raju et al (2021) (Raju *et al.* 2021).

At slow cooling rates the cells will be exposed to high concentrations of solutes and suffer dehydration, both of which can be toxic. However, when cooling rates are too fast, intracellular ice will form (Mazur *et al.* 1972). The "Two Factor Hypothesis" by Mazur (Mazur *et al.* 1972) suggests that there may be an ideal in-between cooling rate that confers maximum cell viability, represented by the classical inverted 'U' curve as illustrated in Figure 4 (black solid curve in the bottom figure). This 'ideal' intermediate cooling rate will differ between cell types determined by factors such as size and permeability (Mazur 1963; Mazur 1977).

However, this inverted 'U' curve cannot be applied for the thermal stabilization in the vitrification process, where low concentrations of CPAs and ultra-fast cooling are used to achieve the vitreous state phase, without any ice formation or freeze concentration. Therefore, the traditional inverted 'U' curve for cell viability vs. cooling rate can be changed and extended into the ultra-fast cooling region where cell viability increases with higher cooling rate (black dotted

line in Figure 4- Bottom). This is a phenomenon that usually occurs when the cooling rate is very high (thousands to millions of °C/Sec) and CPA concentration is very low (< 2–4 M) (He 2011).

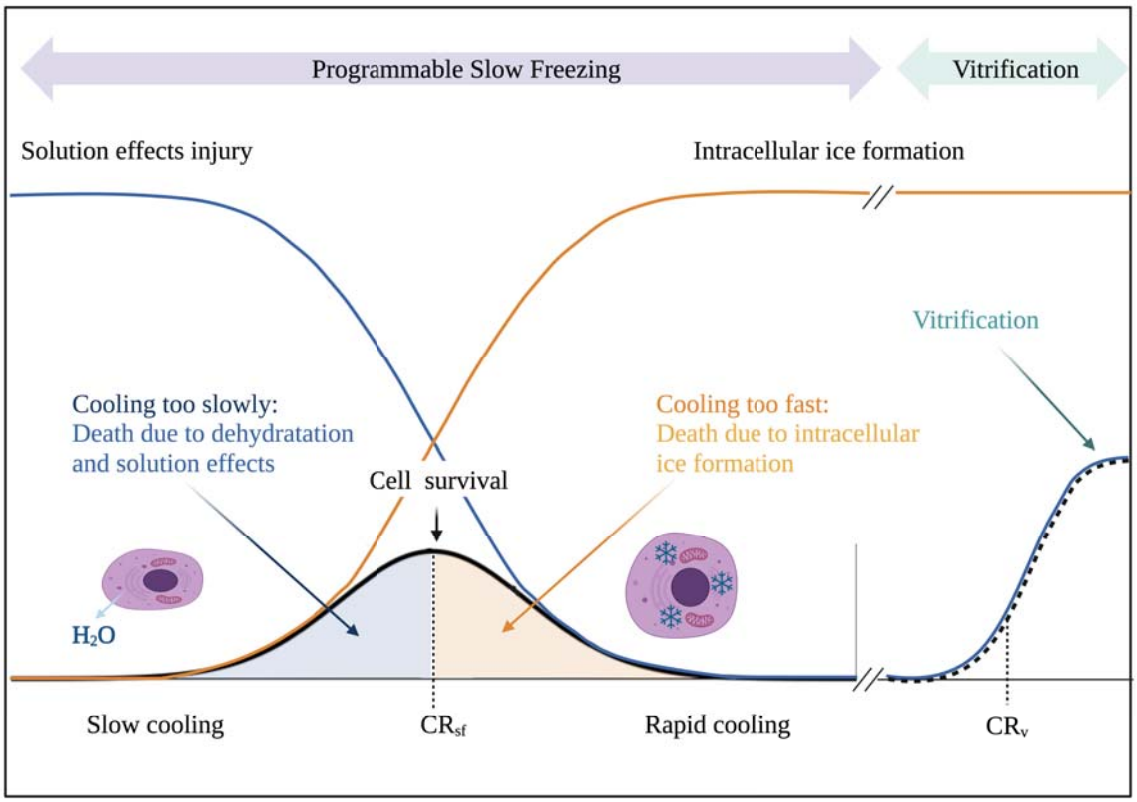

Figure 4. Graphical representation of Mazur's Two-Factor Hypothesis, underlining the cooling rate as a function of survival defined by competing effects for a generalized cell. During slow-freezing, the solute effect and intracellular ice formation determines cell survival at low and high cooling rates, respectively; the combined effect of intracellular ice formation and freeze concentration (i.e., solute effect) results in the classical inverted U curve of cell survival *versus* cooling rate and an optimal cooling rate (CR_{SF}) is observable for slow-freezing. The optimal cooling rate dependent on cell type and cryoprotectant concentration. When the cooling rate is higher than a critical cooling rate (CR_V), cells are vitrified without freezing (or ice formation) and high cell survival ensues. Adapted from (Mazur *et al.* 1972; Mazur 1977; He 2011; Raju *et al.* 2021).

It should be pointed out that cells' stability in the optimal cooling rate regime described above is due to both the combination of CPA and dehydration, which induces intracellular contents to become very viscous and eventually forming a glass – that is, the intracellular contents vitrify, thus avoiding further dehydration and providing lengthy stability. This regime is different to the "vitrification" regime, where the entire contents of the sample (intracellular and

extracellular) are vitrified due to ultra-fast cooling (Raju *et al.* 2021).

Thus there are two primary mechanisms that must be taken into consideration and controlled in order to minimize cell damage and death during cryopreservation: i) solute effects and dehydration, and ii) intracellular ice formation.

2.3. Mechanism of action of CPAs: protection versus toxicity

Cryoprotection usually involves treatment of the cells with cryoprotectant solutes that refers to 'any additive which can be provided to the cells before freezing and yields a higher post-thaw survival than can be obtained in its 'absence' (AM 1974). Although the mechanisms of action of CPA are not completely known, it is likely that the effects of CPA are multi-factorial, and the mechanism by which CPAs exerts its protective action against the stresses encountered during cryopreservation depends on the CPA itself (Elliott *et al.* 2017).

2.3.1. Beneficial effects

a) Preventing ice formation, solution effects and osmotic shock

Cryoprotective chemicals can be divided into two broad categories based on their ability to diffuse across cell membranes, permeating and non-permeating CPAs. Permeating cryoprotectants (pCPAs) are small molecules with low molecular mass and net charge that can easily diffuse through cell membranes, form hydrogen bonds with intracellular water molecules and lower the freezing temperature of the resulting mixture, preventing IIF (Pereira and Marques 2008). In addition, pCPAs play a second role in reducing cell injury due to solution effects by their colligative properties (Lovelock 1953). This effect is described by the phase rule, which states that in a two-phase system, such as liquid water and ice at a given pressure, the total solute concentration in the liquid phase is constant for a given temperature. Thus, as free water solidifies into ice, the remaining solution will contain progressively higher concentrations of both CPA and electrolytes. Because the total concentration of CPA and electrolytes must be constant, the higher the concentration of CPA, the lower the concentration of electrolytes. Thus, the CPA in solution effectively dilutes the electrolytes, thus limiting their toxicity (Friedler *et al.* 1988; Jain and Paulson 2006). Common groups of penetrating CPAs include molecules consisting of sulfoxides, alcohols, amides, and imides (Hubálek 2003).

On the other hand, non-permeating cryoprotectants (npCPAs) include small molecules with higher molecular mass (such as sugars) as well as large, long chain polymers that cannot penetrate membranes and remain extracellular drawing free water out of the cell by osmosis and

resulting in intracellular dehydration (Hubálek 2003; Fuller 2004). NpCPAs are usually less toxic than pCPAs at the same concentration. When used in combination with pCPAs, npCPAs increase extracellular osmolarity, which causes higher cell dehydration. Thus, npCPAs increase the net intracellular concentration of the pCPA, which, in turn, helps to prevent ice-crystal formation [40]. Moreover, npCPA reduce the amount of pCPAs needed by mimicking outside the cell the cryoprotective effects of proteins inside the cell.

b) Protein and membrane stabilization

The preferential exclusion theory may be a possible explanation of the possible mechanisms by which CPAs confer protection to cell biomolecules. According to this theory, interaction with co-solvents similar to water it is thermodynamically unfavorable for proteins (Gekko and Timasheff 1981; Arakawa *et al.* 1990; Timasheff 1993), or membranes (Westh 2003; Westh 2004; Andersen *et al.* 2011), leading to exclusion of the co-solvent from the hydration shell surrounding these biomolecules. When referring to proteins, this stabilizes the native state and increases the barrier of energy needed for protein denaturation (Arakawa and Timasheff 1982). Mention that the mechanism for protein stabilization is different to the 'water replacement hypothesis', which suggests that CPAs interact directly with the protein, thus undertaking the role of water (Clegg *et al.* 1982; Oldenhof *et al.* 2013). Whilst this does seems to be a potential mechanism for protection during dehydration, it has been argued that this bound water is not removed during freezing, and therefore CPA binding to the protein is irrelevant (Crowe *et al.* 1990).

One of the key requirements for cell survival is that the membrane must keep its integrity. The cell's contents will be released without a selectively permeable barrier, and the cell will die. Variation in temperature and/or hydration induces phase transitions in the lipids that provide the structure to cellular membranes. During freezing, the membrane is exposed to both (Steponkus 1984). These transitions cannot only lead to 'leakiness' of the membrane, but may also cause intramembrane protein aggregation or loss (Wolfe and Bryant 1999; Bryant *et al.* 2001). Preferential exclusion of co-solutes from the membrane surface modulates membrane phase behavior. Preferentially excluded co-solutes generate an osmotic stress at the membrane interface, which tends to stabilize lipid phases of low surface areas and to withdraw water from multilamellar stacks of membranes (Westh 2003; Westh 2004).

For the same reason, non-penetrating CPAs can be included in the warming media to prevent osmotic shock and lysis by slowing the return of water to cells and thus stopping traumatic expansion (Fuller 2004; Elliott *et al.* 2017). It has been postulated that non-penetrating

CPAs can be absorbed to the cell membrane surface, thus inhibiting ice formation in the immediate vicinity of the cell by preventing the necessary formation of crystal lattices and promoting vitrification (Wolfe and Bryant 1999; Koster *et al.* 2000; Bryant *et al.* 2001). However, at low hydrations, large molecules such as non-penetrating polymers are excluded from the bilayer region and have no effect on membrane phase transitions (Wolfe and Bryant 1999; Koster *et al.* 2000; Bryant *et al.* 2001; Raju *et al.* 2021).

2.3.2. Detrimental effects

a) Chemical toxicity

The positive effects of CPA on cryopreservation have so far been stressed. But it is easy to see how these solutes, which are able to permeate intracellular spaces and affect water interactions in general, can also have toxic effects within the highly organized molecular machinery supporting cell life processes. CPA toxicity is attributed to their ability to directly interact with a multitude of cellular activities such as enzymatic processes, transporter mechanisms, ion exchanges and the like (Elliott *et al.* 2017; Raju *et al.* 2021). CPA toxicity has been also explained by their capacity to disrupt protein interactions (Arakawa *et al.* 1990). They observed that CPA agents such as Me_2SO and ethylene glycol (EG) destabilize proteins through their hydrophobic interactions, at supra zero temperatures, in contrast to the stabilizing effect they produce on proteins by preferential exclusion at lower temperatures (Arakawa *et al.* 1990). Other CPA may have a membrane 'chaotropic' effect, resulting in membrane blebbing and disorganization; for example, butane diol was shown to produce membrane blebbing during exposure in mouse oocytes (Todorov 1993). Other studies on mammalian oocytes showed that CPA can have direct effects on organelle structures such as microtubules and microfilaments (Johnson and Pickering 1987), that could be reversed by shorter exposure times to CPA or CPA exposure at lower temperatures (Fuller and Paynter 2004).

Such concepts address to the complexity of defining CPA toxicity, and whether it is transitory, reversible, or long-lasting depending on the exposure conditions. Moreover, within the pragmatic division of CPAs into permeating and non-permeating agents, the potential for adverse events or reactions is heavily skewed towards permeating, especially when they are used in high concentrations because its permeating nature (Fahy 1986). This explain why only a very few toxicity events have been linked specifically with high molecular weight npCPA (Mazur 1984; Karlsson and Toner 1996). In practice it is found that the toxic limit concentration of CPAs that can be used without impairment of viability is strongly influenced by the temperature and the

conditions under which the CPAs are added and removed (Pegg 2002). Moreover, as the permeating speed of CPAs is also related directly to temperature, the major factors to be considered in assessing the toxicity of CPAs are their concentration, the exposure temperature, and the time in aqueous solution (Szurek and Eroglu 2011).

b) Osmotic damage

A second aspect that should be taken into account is the cell volume alteration due to osmotic events during equilibration to CPAs. The addition and removal of CPAs before and after cryopreservation also can cause damage to cells due to excessive osmotic forces (Meryman 1971). Because pCPAs typically enter and leave the cell with a membrane permeability several orders of magnitude slower than that for water, the initial response of a cell exposed to a cryoprotective solution is to lose water by exosmosis. Similarly, experience reverse osmotic damage or 'dilution shock' when returned to isotonic conditions after warming, a cell containing cryoprotective solutes will initially swell when placed in an isotonic environment, as water enters the cell by osmosis. Even though the cell volume will eventually return to its isotonic value as the CPAs permeates the cell membrane and equilibrates, excessive volumetric excursions and the attendant high osmotic water fluxes can result in cell rupture or sublethal damage that can hamper laboratory and clinical outcomes (Armitage and Mazur 1984; Karlsson and Toner 1996). It is therefore both logical and of proven efficacy to control changes in cell volume so that acceptable limits are not transgressed.

To avoid osmotic shock, two stratagems are available: the first is to add CPA in several small steps where concentration in progressively changing and carefully combined to appropriate cooling/warming rates (Mazur and Miller 1976b; Benson *et al.* 2012b); the other approach, which is applicable only to the more critical removal phase, is to incorporate solutes that do not penetrate the cells and therefore function as "osmotic buffers" by restricting the inflow of water as the concentration of CPAs is reduced (Pegg 2002).

3. How to attain the vitreous state: methods for mammalian oocytes cryopreservation

Oocyte cryopreservation is conducted mostly following methods developed for embryo cryopreservation. It is generally believed that cryopreservation of mammalian oocytes is difficult compared to embryo mainly due to their large size, low surface-to-volume ratio, high lipid content, low permeability, low conductivity, and sensitivity to chilling (Leibo 1980; Massip 2003; Rojas *et al.* 2004; Bogliolo *et al.* 2007; Succu *et al.* 2007; Saragusty and Arav 2011). Slow freezing

and vitrification are common oocyte cryopreservation methods. These methods differ in the concentration of CPAs used and cooling rate; otherwise, they are similar in storage, warming, and rehydration (Vajta and Kuwayama 2006). Recent studies showed that regardless of species, stage (GV or MII), cryopreservation method, the permeating and non-permeating CPAs, and thawing/warming methods, oocyte cryopreservation is not as successful as embryo cryopreservation in domestic animals (see review (Anzar 2017)).

3.1. Controlled rate freezing

Slow freezing is the conventional method for mammalian oocyte and embryo cryopreservation. In this procedure, cells are suspended in a freezing medium with a low initial concentration of CPAs (1–2 mol/L), loaded in a straw of 0.1-0.5 mL, which is cooled in a step-wise controlled programmable freezer: a common protocol is to use a cooling rate of 2 °C/min until the seeding (manual induction of ice formation in the extracellular solution, usually by touching the outer surface of straw with ice or very cold metal) temperature around −7°C. The seeding causes withdrawal of intracellular free water and cell dehydration in response to the concentration of the extracellular unfrozen fraction during the growth of extracellular ice before intracellular freezing takes place, called nonequilibrium freezing (Mazur 1963; Mazur 1990) (Figure 5). After seeding, a slower cooling rate of 0.3–1.0 °C/min is usually employed until temperatures between -30 and -65ºC are reached (Lassalle *et al.* 1985). Then, straws are quickly plunged in LN_2 for long-term storage (Jain and Paulson 2006; Cutting *et al.* 2009). This technique is based in the gradual depression of the freezing point resulting from the increase in viscosity that the solution experiences during cooling, and most importantly, the increase in solute concentration induced by extracellular ice formation. The temperature of the system is decreased just above the rate of depression of the freezing point, until the glass transition temperature is attained and the cytosol undergoes vitreous solidification. However, during slow freezing, cells undergo osmotic and phase changes, solution effect, and extra- and intracellular ice formation associated with dilution, initial cooling/freezing, and thawing processes. The success of cryopreservation mainly depends upon the severity of these changes and cells' ability to tolerate them (Anzar 2017).

3.2. Ultra-fast vitrification.

The vitreous state in this context can be considered as a solidified amorphous liquid state of extreme viscosity at low temperatures, obtained by specific conditions of cooling and solute concentration that inhibit ice crystal nucleation and growth. The procedure of ultra-fast vitrification is a more radical approach, as the temperature is lowered below the melting point, all

the way to the glass transition temperature which avoids the chilling injury (passing rapidly through the dangerous temperature zone between 0°C and -15°C) to mammalian oocytes associated with slow freezing method (Rall and Fahy 1985; Rall 1987). During vitrification, cells are exposed to a high concentration of pCPAs (~5-7 M) that binds with water, increase the intracellular viscosity, and depress the freezing point below Tg. Then cells are loaded on to open or closed device, and directly plunged into LN_2. Cooling and, most important, warming rate has to be performed at high rates (usually 10^3 to 10^6°C/min) so the water molecules in the cytosol, despite being below their melting point, do not have the necessary time to rearrange, form ice crystals and grow to a size that can produce cellular injury or death (Fahy *et al.* 1984; Rall and Fahy 1985). Consequently, the solution reaches the glass transition temperature and results in an amorphous solid of the extra- and intracellular compartments of cells, preserving the disordered molecular configuration of the living state (Fahy *et al.* 1984).

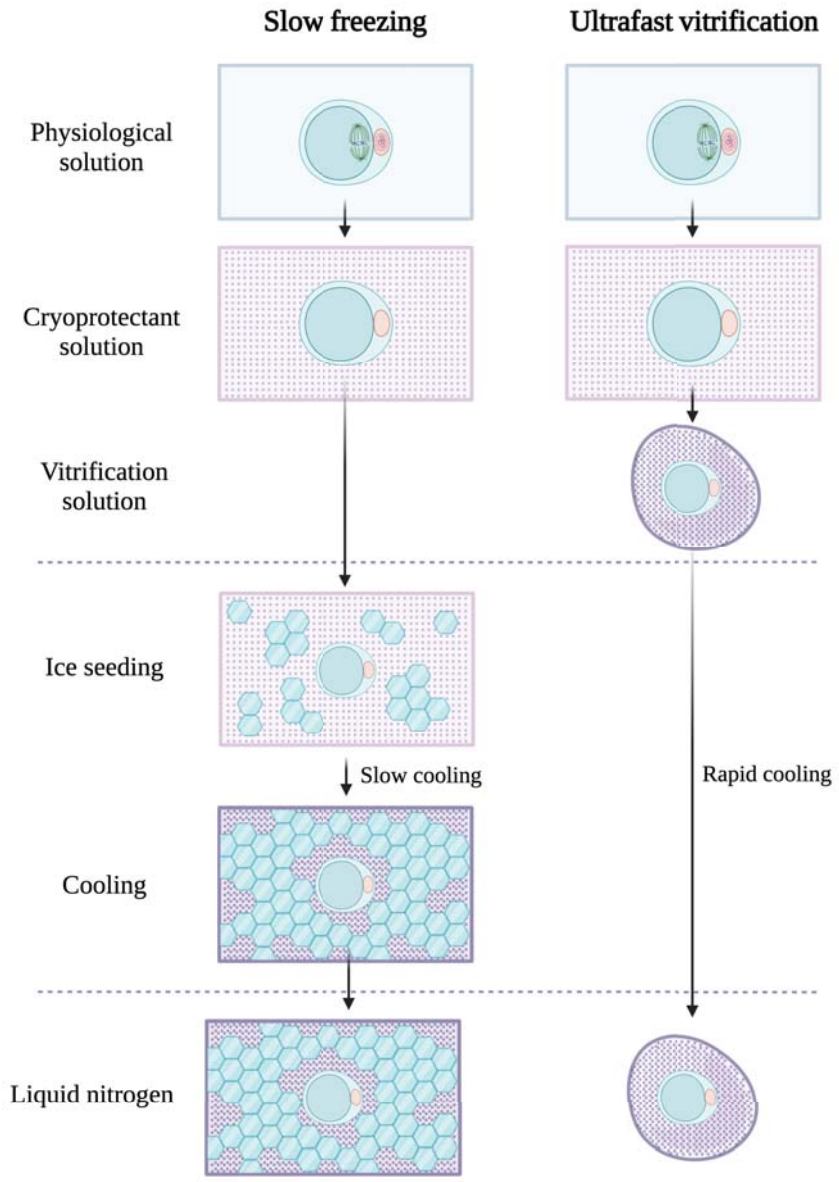

Figure 5. Schematic representation of an oocyte during slow freezing and ultrafast vitrification. Blue hexagons represent ice crystals. The concentration of cryoprotectant is shown by the darkness of shading. Adapted from (Mazur 1990).

From a practical point of view, vitrification is appreciated because it is a simple, time-saving and cheaper option. It does not require expensive automatic coolers and can be performed quite quickly in an insulated container. Moreover, several studies describe higher percentages of spindle abnormalities, low survival rates and implantation rates when human oocytes are cryopreserved by slow freezing (Bromfield *et al.* 2009). These negative effects have limited the widespread use of slow freezing techniques and give way to the widely use of vitrification for the cryopreservation of human oocytes (Smith *et al.* 2010) and a variety of domestic and laboratory animals (Vajta *et al.* 1998; Gupta *et al.* 2007; Vieira *et al.* 2008; Pope *et al.* 2012; Kohaya *et al.* 2013;

Moawad *et al.* 2013). Regardless of the methodology used for cryopreservation, pregnancy rate obtained from cryopreserved gametes and embryos is still below that obtained with their fresh counterparts (Forman *et al.* 2012).

3.2.1. Factors that determine the probability of vitrification

The fundamental issue in all vitrification methods is to achieve and maintain conditions inside and outside of the cells that guarantee an amorphous state throughout the cooling, as well as during the warming process. The success of vitrification is largely dependent on three factors: (1) cooling and warming rates; (2) viscosity of the sample; and (3) sample volume (Fahy *et al.* 1984; Yavin and Arav 2007; Saragusty and Arav 2011).

1) Cooling rate and warming rate: A high cooling rate is achieved with LN_2 or LN_2 slush and a warm water bath for warming. When using LN_2, the sample is plunged into LN_2, resulting in cooling rates of hundreds to tens of thousands degrees Celsius per minute, depending on the container, volume, thermal conductivity, solution composition, and so on (Yavin and Arav 2007). To achieve LN_2 slush, the LN_2 needs to be cooled close to its freezing point (-210°C), for example, by applying a negative pressure above liquid nitrogen (Steponkus *et al.* 1990). When liquid nitrogen slush is formed, the cooling rate is dramatically increased (Saragusty and Arav 2011).

2) Viscosity of the medium in which the oocytes are suspended or the glass transition coeffieciency of the solution at low temperatures is defined by the concentration and behavior of various CPAs and other additives during vitrification. The higher the concentration of CPAs, the higher the glass transition temperature (Tg), thus lowering the chance of ice nucleation and crystallization. Different CPAs and other additives have different toxicity, penetration rate, and Tg. Viscosity of the medium in which the oocytes are suspended is defined by the concentration and behavior of various CPAs and other additives during vitrification. The combination of different CPAs is often used to increase viscosity, increase Tg, and reduce the level of toxicity.

3. Volume: The smaller the volume, the higher the probability of vitrification (Arav *et al.* 2002; Yavin and Arav 2007). Smaller volumes allow better heat transfer, thus facilitating greater cooling rates. Many techniques have been developed to reduce sample volume with an explosion of methods appearing in the literature during the last decade. The Cryotop developed by Kuwayama and Kato (Kuwayama and Kato 2000) is now commonly used as a carrier for vitrification of oocytes because it allow to perform small size drops (<0.1mL) and due to these

systems are opened, high cooling and warming rates can be achieved because of the direct contact of the sample with the LN_2.

This is highlighted by the equation of Yavin and Arav (Yavin and Arav 2007) for the probability of obtaining a vitrified state:

$$Probability\ of\ obtaining\ a\ vitrified\ state\ in\ solutions = \frac{Cooling\ and\ warming\ rates\ \left(\frac{C}{W}\right) \times \text{viscosity (CPA conc.)}}{Volume\ (Vol)}$$

Whereas, in pure water, C determines the solidification in a glassy state, and in solutions, the content of solved molecules and CPA have to be considered. The faster the cooling rate, the lower the concentration of CPA in the solution is required to achieve vitrification.

3.2.2. Preparation of oocytes before plunging them into LN_2.

Before cooling of oocytes or embryos down to −196°C in LN_2, the intracellular compartment has to be prepared to allow the achievement and maintenance of an intracellular vitreous state (Macfarlane and Forsyth 1990). To reach this purpose, most of the vitrification protocols expose mammal oocyte to a minimum of two steps where CPA concentrations are gradually increased. First, oocytes are pre-incubated in the equilibrium medium or the non-vitrifying solution (nVS) containing 3-40% of CPA and, then, to the vitrifying solution (VS) containing higher concentration of CPA (30-40%). Thereby, intra- and extracellular viscosities are increased to a degree, which ensures that the liquid water molecules will solidify at an enough rate, so that a reorganization into a crystalline structure is particularly improbable (Fahy *et al.* 1987; Vanderzwalmen *et al.* 2009). Practically, the nVS contains a mixture of cell-penetrating CPA, being EG and Me_2SO the most commonly used in mammal oocytes (Vanderzwalmen *et al.* 2009; Vanderzwalmen *et al.* 2012). The duration of exposure to the nVS at a defined temperature is of greatest importance and determines the concentration of intracellular CPA. The exposure time is determined by several biophysical factors, such as the membrane properties (cellular permeability to water and CPA), the type, mixture, and concentration of CPA, the surface/volume ratio of the cells, and the speed of cooling and warming. For example, in Figure 6, an oocyte is exposed to the nVS until full equilibrium (recovery of the initial volume), meaning entrance of plenty of CPA molecules associated with water molecules.

Then, oocytes are exposed for a short period (45–90 s) to a second step (VS), containing very high concentrations of a mixture of penetrating CPA (4.8–6.4 M) and non-penetrating CPA (usually a polysaccharide at 0.5–0.75 M). This last solution is highly concentrated with an

osmolarity between 5500–6500 mOsm/L, which causes a fast shrinkage of the cytoplasm following dehydration (Figure 6). The soluble components of the cytoplasm (amino acids, proteins, polymers, nucleotides, and other macromolecules) and the CPA that have previously penetrated into the cell during pre-incubation in nVS concentrate generating an intracellular environment favorable to the formation of a vitreous state before the cells are rapidly plunged into LN_2 (Vanderzwalmen *et al.* 2020).

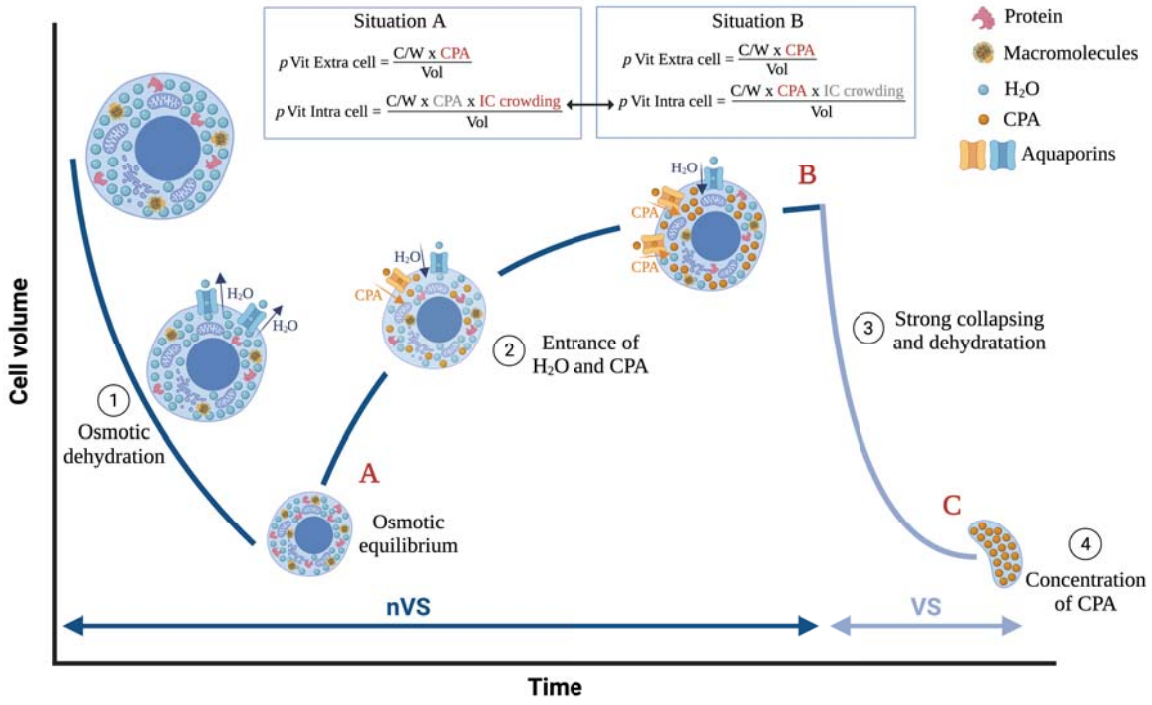

Figure 6. The biphasic reaction of a cell in the presence of non-vitrifying CPA solution (nVS; penetrating CPA) and vitrifying CPA solution (VS; penetrating and non-penetrating CPA). Changes in cell volume and molecular changes are shown. During incubation of oocytes with nVS, first the cells dehydrate as water flows out through the plasma membrane (1). After reaching an osmotic equilibrium (A), the entrance of CPA, and to a lesser extent, of H2O follows (2) which is characterized by a small increase in volume (B). In the VS, occurs a strong dehydration (3), leading to a concentration of CPA within the cell (4) and a strong decrease in cell volume (C). The probability of obtaining of a vitrified state in the extracellular fluid (P Vit extra cell) depends on the speed of cooling and warming (C/W), the concentration of CPA, and the volume (Vol). Inside the cell (P Vit intra cell), macromolecular crowding has to be added as another factor. The influence of IC crowding fluctuates, dependent on the type of cells and the extent of dehydration. Adapted from (Vanderzwalmen *et al.* 2020)

The probability of extracellular vitrification is in relation to the concentration of CPA and is represented by the following equation:

$$P\ vit\ extra\ cell = \frac{\left(\frac{C}{W}\right) \times \text{Extracellular CPA conc.}}{Vol}$$

a) The intracellular concentration of cryoprotectant and a revision of the classical equation on the probability of achieving a vitrifying state

One of the main concerns in vitrification was, and still is, the high concentrations of CPA in the VS because exceeds three- to four-fold the concentration of CPA in the previously applied slow freezing technique. For this reason, the vitrification protocol tries to minimize CPA toxicity by dramatically reducing incubation times in the nVS and VS, therefore limiting the time for CPA entrance. However, the hypothesis of high intracellular concentrations of CPA (ICCP) in vitrified cells was demystified in a recent study using cinematographic analysis where it was demonstrated that the real ICCP was approximately 2.14 M, far below the 6.4 M of CPA concentration of the VS solution (Vanderzwalmen *et al.* 2013). If we consider that an aqueous solution containing 2.14 M pCPA will directly crystallize, it is surprising how an oocyte/embryo is able to survive the vitrification process even when the ICCP is far below this threshold. This phenomenon has been recently review by Vanderzwalmen et al (2020) (Vanderzwalmen *et al.* 2020) who proposes the intracellular crowding and the colloidal vitrification as two physical arguments to explain the absence of intracellular crystallization. Osmotic dehydration process modifies the intracellular architecture in a way that the IIF is inhibited despite low ICCP (Zhou *et al.* 2009; Mochida *et al.* 2013). This is due to the cytosol of the cell that is a crowded fluid in which many macromolecules as proteins, amino acids, polymers and nucleotides, between others, are floating together with cell organelles and when freezing, an increase of intracellular macromolecules called "macromolecular crowding" is observed. Osmotic removal of water from the cytoplasm leads an increase in the packing density of macromolecules, which increase progressively the viscosity, and leads to a solidification by colloidal glass. This explains why amorphous extracellular and intracellular situations are different. When extracellularly CPA concentration dictates first the viscosity, intracellularly is the cytoplasmic dehydration and macromolecular crowding itself whose are essentially involved in increasing viscosity and form the amorphous state (Hunter and Weeks 2012; Mourão *et al.* 2014).

The intracellular milieu is depending on the number of CPAs that enter the cells during the exposure in the nVS. According to the time of exposure, the colloidal solidification may result in different architecture, and the probability of vitrification is dependent on the different factors that are more or less predominant, following short or longer exposure. As a consequence, the classical equation for the probability of obtaining a vitrified state takes into account the three

factors (i) speed of cooling and warming (2000 C/min to 20,000 C/min), (ii) solute viscosity, and (iii) the volume of the vitrification solution has to be updated. The equation needs to contain a distinction between the intracellular and extracellular compartments. While the extracellular compartment is influenced by the concentration of CPA, the intracellular compartment depends on the degree of crowding (dehydration) and the concentration of CPA (Figure 6) (Vanderzwalmen *et al.* 2020)

4. Cryopreservation-related injury to the bovine oocyte

Mammalian oocytes have a complex subcellular structure and most of the components are particularly sensitive to temperature and osmotic pressure. Oocytes are among the largest mammalian cells, thus decreasing to a considerable extent the surface to volume ratio, resulting in inefficient water exchange, and hence slower dehydration and rehydration and highly susceptible to intracellular ice formation (Fabbri *et al.* 2000). The plasma membrane of oocytes at the MII oocytes has a low permeability coefficient, making the movement of CPAs and water slower (Agca *et al.* 1998). Moreover, oocytes have high cytoplasmic lipid contents that increase chilling sensitivity and are also more susceptible to damage due to the formation of reactive oxygen species, very common during cryopreservation. Additionally, the developmental stage of the oocyte (from germinal vesicle (GV) to metaphase II (MII) stage) affects its cryobiological properties as the plasma membrane, the mitochondria, some cytoskeletal elements and other organelles relevantly change during maturation (Ambrosini *et al.* 2006). Surrounding the oocyte there is a continuous glycoprotein coat, the zona pellucida. Its role in the osmotic behavior of the oocyte is negligible. However, vitrification induces premature cortical granules exocytosis, leading to zona pellucida hardening, which impairs sperm penetration and hinders natural fertilization. Nonetheless, this drawback can be overcome by intracytoplasmic sperm injection (Gook *et al.* 1995).

During cryopreservation, cells first undergo chilling phase during initial cooling from body/room temperature to the freezing point and then freezing phase below freezing point to -196 °C. Mammalian oocytes undergo both chilling and freezing phases in slow freezing and only freezing phase in vitrification method. However, the extent of cryoinjury varies depending upon species, sensitivity of the cell structures to cooling, meiotic stage, lipid content, and origin (*in vitro* and *in vivo*) (Vajta and Kuwayama 2006; Pereira and Marques 2008). Injuries may occur at all phases of the cryopreservation procedure but in general exposure of oocytes to cooling (Aman and Parks 1994), CPAs (Vincent *et al.* 1989), or the freeze/thaw process (Aigner *et al.* 1992) may cause microtubule depolymerization and DNA fragmentation (Sharma *et al.* 2010), abnormal

spindle configurations (Boiso *et al.* 2002; Morato *et al.* 2008c), chromosomal abnormalities (Boiso *et al.* 2002), altered distribution or exocytosis of cortical granules (Morato *et al.* 2008c), and cytoplasmic membrane fracture (Zhou and Li 2009). Similarly, after oocyte cryopreservation, there is a negative influence on microfilament functions (Vincent *et al.* 1989). These developmental perturbations can lead to abnormal distributions of mitochondria in the oolemma (Nagai *et al.* 2006; Zander-Fox *et al.* 2013) and consequently result in reduced meiotic competence and fertilizability of oocytes, as well as developmental failure in the preimplantation embryo. Understanding the causes and mechanisms of damage may help the development of cryopreservation methods to avoid lethal or irreversible injuries.

4.1. Meiotic spindle dynamics in oocytes following cryopreservation

During initial cooling, the disassembly of meiotic spindles in MII oocytes is the most pronounced change in mouse (Pickering and Johnson 1987), human (Pickering *et al.* 1990), and bovine (Aman and Parks 1994) MII oocytes. The meiotic spindles consist of microtubules that are constructed by polymerization of tubulin dimmers of α- and β-tubulin (Zhou *et al.* 2002). Microtubules start from microtubular organizing centers at both poles and anchor chromosomes at the kinetochores, forming a barrel shape (Maro et al., 1986). The chromosomes align at the equatorial plane of the meiotic spindles. The tubulin dimmer would polymerize and depolymerize at various stages of a cell cycle. The meiotic spindles are crucial for the events following fertilization as completion of meiosis, second polar body formation, pronuclear development, migration and fusion, and formation of the first mitotic division (Schatten *et al.* 1985; Massip 2003). Studies have shown that subjecting oocytes to cooling temperatures, CPAs or vitrification (Albarracin *et al.* 2005a; Morato *et al.* 2008a; Morato *et al.* 2008b) may induce the depolymerisation and disorganisation of spindle microtubule. Subsequent impaired repolymerization on rewarming may lead to scattering of chromosomes or lesions in the reformed spindle resulting in misaggregation of chromatids following resumption of meiosis (Gook and Edgar 2007) thus, causing chromosomal anomalies after fertilization, such as aneuploidy and polyploidy (Wang *et al.* 2001b; Wang *et al.* 2001a; Chen *et al.* 2004; Stachecki *et al.* 2004; Coticchio *et al.* 2005; Rienzi *et al.* 2005; Shen *et al.* 2008; Bromfield *et al.* 2009). For hence, if performed inappropriately, slow cooling and vitrification may severely affect oocyte survival and physiology (Gardner *et al.* 2007), compromising irreversibly the ability to subsequent embryonic or fetal development (Fabbri 2006; Lei *et al.* 2014).

4.1.1. Effects of temperature and cryoprotectants on the meiotic spindle

The meiotic spindle has been shown to depolymerize when exposed to reduced temperatures or CPAs in oocytes from several mammal species, such as mature bovine (Aman and Parks 1994; Saunders and Parks 1999; Albarracin *et al.* 2005b; Spricigo *et al.* 2012) porcine (Liu *et al.* 2003; Wu *et al.* 2006; Galeati *et al.* 2011), equine (Tharasanit *et al.* 2006), murine (Pickering and Johnson 1987; Sathananthan *et al.* 1992a; Vincent and Johnson 1992; Larman *et al.* 2007; Chang *et al.* 2011; Gomes *et al.* 2012; Zhou *et al.* 2014), and human oocytes (Almeida and Bolton 1995; Wang *et al.* 2001a; Keefe *et al.* 2003).

The first report appeared in 1980 using mouse oocytes (Magistrini and Szöllösi 1980) where cooling on ice for 15, 30, 45, or 60 min resulted in progressive depolymerization of the spindle microtubules. The majority of the spindle fibers were depolymerized after the shortest treatment, and longer treatments completed the depolymerization process of the kinetochore microtubules. The effects of cooling on the spindle appeared to be reversible in the mouse oocyte, with normal spindle formation occurring after step-wise re-warming. On returning to 37°C, repolymerization was observed, but numerous chromosomes were observed scattered throughout the cytoplasm (Pickering and Johnson 1987; Sathananthan *et al.* 1992a). These effects were largely confirmed by later studies (Pickering and Johnson 1987; Sathananthan *et al.* 1992b). Nevertheless, one of the differences in the later studies is that direct warming to 37°C was able to restore a normal spindle structure in the ooplasm.

Cooling also has deleterious effects on the MII spindle of oocytes from other mammals (Tharasanit *et al.* 2006; Wu *et al.* 2006). However, one of the major differences is that the ability of the spindle to undergo normal repair (by which is meant the morphology of the spindle appears the same after warming as before cooling) is reduced. The repolymerization capacity of microtubules during the post-thawing incubation was related to the microtubular organizing centers, the concentration of free tubulin, the presence of chromosomes, and the associated kinetochores [156]. Most of the studies revealed that mammal oocytes analyzed immediately after thawing displayed severe disorganization or disappearance of spindles using slow, rapid, ultra-rapid, or vitrification methods [149, 157]. In general, incubation for 1-3 h after thawing/warming at 37 ºC resulted in recovery of spindles in diverse degrees.

Meanwhile microtubules in most mouse oocytes have the ability to repolymerize after about 1 h of returning back to 37°C from 4°C (Pickering and Johnson 1987), it appears that the human oocyte is exquisitely sensitive to cooling. Pickering et al. (Pickering *et al.* 1990) observed

that less than half of human oocytes had normal spindles after cooling to room temperature for either 10 or 30 min and warming to 37 °C for either 1 or 4 hours. Similarly, Wang et al. (Wang *et al.* 2001a) confirmed by direct visualization of the human oocyte that human oocyte spindles undergo depolymerization between 27.1°C and 31.9°C, and that cytoplasmic organelles and granules in oocytes show reduced movement at room temperature (RT). In fact, if oocytes were maintained at a cooled temperature (for 10 min) before being returned to 37°C, they failed to recover their spindle within the same time frame (Pickering *et al.* 1990; Wang *et al.* 2001a; Zenzes *et al.* 2001).

Complete disappearance of the spindle was observed *in vitro*-matured bovine oocytes after exposure to 4 ºC for 10-20 min. When mature bovine oocytes were exposed to 25ºC for 30 min, 90% of spindle appeared abnormal or absent. This damage was irreversible in most oocytes regardless of cooling temperature or rewarming scheme (Aman and Parks 1994).

Differences in the rate and extent of microtubule depolymeritzation following exposure to CPA might be related to different sensitivity among oocytes from different species (Vincent *et al.* 1990; George *et al.* 1996) and stages (Rojas *et al.* 2004) to different CPA concentrations (Cai *et al.* 2005) and exposure time and temperature (Rojas *et al.* 2004). At low doses (0/1.0 M) 1,2-propanediol induced disorganization of the meiotic spindles of mouse oocytes, but it had a stabilizing effect at 1.5 and 2.0 M (Joly *et al.* 1992), respectively. Chen et al. (Chen *et al.* 2000) found that the spindles of mouse oocytes disorganized or disappeared when exposed to a vitrification solution of 5.5 M EG and 1.0 M sucrose. In bovine oocytes, the sensitivity of the meiotic spindle to CPAs was different depending on the sexual maturity of the animal. Albarracin et al. (Albarracin *et al.* 2005b) found that oocytes retrieved from adult cows were more sensitive to the exposure to CPAs, while vitrification seemed to have worse effects on calf oocytes.

Moreover, Mullen et al. (Mullen SF 2004) demonstrated that damage to the oolemma and MII spindle in bovine oocytes occurs at a higher frequency as the solution concentrations diverge from isosmotic. High osmotic and hydrostatic pressure alters the hydration state of macromolecules leading to changes in conformation and activity in extreme cases. The changes in solute concentrations within cells associated with volume changes may lead to alterations in protein-protein interactions due to changes in intracellular ionic strength. This effect is particularly applicable to microtubules, since the α- and β-tubulin molecules associate through non-covalent interactions, and changes in solute conditions have been shown to alter microtubule assembly characteristics. Nevertheless, their tolerance to hypertonic conditions was

relatively high, with significant proportions of oocytes maintaining a normal spindle structure up to an 1800 mOsm exposure which open the possibility to design CPA addition protocols based on a few steps reducing the exposure time and for hence the associate CPA toxicity.

Therefore, the procedures of freezing and thawing at lower temperature or exposed to highly concentrated CPAs may lead to injury of the meiotic spindles. As in some of these experiments, the exposure to CPA had been performed at room temperature, it is difficult to discern the effect of CPAs in meiotic spindle from the effect that could exert the reduction of the physiological temperature to room temperature.

4.1.2. Effect of oocyte maturation status

Regarding to the maturation stage, oocytes have different specific physiological and biophysical properties that make them more or less sensitive to cryoinjury and CPA toxicity. Conventionally, prophase I (GV) oocytes have been considered more suitable for preservation than metaphase II (MII) oocytes because the risk of chromosome aberrations could be bypassed, since during meiosis arresting at GV, chromatin is protected by the nuclear membrane inside germinal vesicle and the microtubule assembly complex is not formed yet (Battaglia *et al.* 1996; Kim *et al.* 1998). Nevertheless, even when this problem was hypothetically avoided in GV oocytes, recent data have shown that other important cellular structures may be damaged. In particular, the cumulus cell compartment and transzonal processes are impaired (Brambillasca *et al.* 2013), as well as, alterations in the cortical granules distribution, cytoplasmic organelles, RNA, and proteins may compromise their maturation, fertilization and embryo developmental capacity (Gorbsky *et al.* 1990; Fabbri *et al.* 2001; Rho *et al.* 2002; Bromfield *et al.* 2009).

It has been documented that vitrified *in vitro* matured oocytes achieve a higher percentage cleavage rate after fertilization compared to when immature oocytes are vitrified/warmed at the GV stage (Spricigo *et al.* 2014; Chaves *et al.* 2017). By contrast, other studies reported lower tolerance of cattle matured oocytes to CPAs compared to oocytes at the germinal vesicle (GV) stage (Chaves *et al.* 2017) (Magnusson *et al.* 2008), with higher percentages of blastocysts from cumulus-enclosed oocytes vitrified at the GV stage compared with MII oocytes (Zhou *et al.* 2010). By contrast, Men et al. (2002) (Men *et al.* 2002) and Albarracin et al (2005) (Albarracin *et al.* 2005a) obtained higher percentages of blastocysts from bovine oocytes vitrified at the MII stage *vs* oocytes vitrified at the germinal vesicle breakdown stage.

Despite different vitrification schemes have been tested, the above-mentioned reports demonstrated that there is no consistent and uniform opinion about which maturation stage (mature/immature) is more suitable for oocyte cryopreservation.

4.2. Plasma membrane

The permeability of the plasma membrane affects cell survival after vitrification (Jin *et al.* 2011). Chilling injury occurs after exposure to low temperatures, but not freezing temperatures, and irreversibly affects the membrane integrity. When membranes are cooled, they tend to undergo phase transitions. Lipids tend to transition from a liquid-like state to a gel-like state, with the molecules being arranged in an orderly, crystalline fashion with a characteristic hexagonal arrangement (Chapman 1975). Unfortunately, changes that occur in this phase transition are usually not reversible, thus the cellular components are not reassembled correctly upon warming (Jung *et al.* 2014). The phase transition temperature is thought to happen between 13 to 20ºC and 10ºC for GV and MII bovine oocytes, respectively (Arav *et al.* 1996). Cholesterol is present in the plasma membrane, and its level and the ratio between cholesterol and the membranes' phospholipids determine to a great extent the membrane fluidity and thus its chilling sensitivity (Ghetler *et al.* 2005; Varghese *et al.* 2009) being membranes with high cholesterol content more fluid at low temperatures, and thus less susceptible to damage during cooling (Ghetler *et al.* 2005). This means that by incorporating cholesterol into the plasma membrane, the membrane will gain fluidity and permeability at low temperatures, thereby increasing oocyte tolerance to cryopreservation (Spricigo *et al.* 2012).

There are two pathways for the movement of water and CPAs across the plasma membrane: simple diffusion through the lipid bilayer, and facilitated diffusion through aquaporin water channels, a superfamily of membrane proteins that transport water across cell membranes (Jin *et al.* 2011). In addition to water, the members of the aquaporin superfamily aquaglyceroporins (e.g. aquaporin (AQP) 3, AQP7, AQP9 and AQP10) are able to transport small, neutral solutes, including some CPAs such as glycerol or EG (Pedro *et al.* 2005; Edashige *et al.* 2006). CPAs permeate oocytes and embryos through different pathways, which depend not only on the cell's developmental stage, but also on the CPA itself (Jin *et al.* 2011; Jin *et al.* 2013; Edashige 2016). In bovine, the permeability of oocytes to water and CPAs is lower than that of morulae and blastocysts (Edashige 2016). The plasma membranes of oocytes differ significantly from those of embryos, partially due to the lack of aquaporin expression, which affects the movement of water and CPAs. It was shown that water and CPA molecules move through mouse and bovine oocytes and early cleavage-stage embryos predominantly by simple diffusion,

but a smaller proportion of water moves via channel processes; thus, AQP3 was found to play a major role in aiding the diffusion of water, glycerol and EG in cow and mouse oocytes (Jin *et al.* 2011; Jin *et al.* 2013; Edashige 2016). Unlike in morulae, water and CPA move quickly, mainly by facilitated diffusion via channels (Jin *et al.* 2011; Jin *et al.* 2013; Hwang and Hochi 2014; Edashige 2016). When the movement of water and CPAs depends predominantly on simple diffusion across the plasma membrane, flow rates are reduced and affected by the temperature. Conversely, diffusion via channels implies a higher membrane permeability and higher independence on the temperature. These factors allow embryos to be relatively more tolerant to vitrification and warming than oocytes (Hwang and Hochi 2014).

More recently, Tan et al. (2015) (Tan *et al.* 2015) showed that expression of AQP7, but not that of AQP3 and AQP9, was increased in murine oocytes exposed to a hyperosmotic CPA solution containing EG, Me_2SO or sucrose. Similarly, exposure of bovine oocytes to hyperosmotic solutions containing EG, Me_2SO or sucrose increased AQP7 and AQP3 protein expression, whereas no AQP9 protein expression was observed. Treatment with EG significantly increased AQP7 protein expression in bovine oocytes, whereas exposure to Me_2SO significantly augmented AQP3 expression (Mogas 2018). To examine whether the ectopic expression of AQP3 could improve water and CPA permeability and oocyte survival after cryopreservation, exogenous expression of rat AQP3 in mouse oocytes or human and zebrafish AQP3 in porcine oocytes was measured (Edashige *et al.* 2003; Yamaji *et al.* 2011; Morató *et al.* 2014). In these studies, exogenous expression of AQP3 enhanced both the efflux of water and influx of CPAs into the cell, thus improving oocyte tolerance to chilling and survival and embryo development after warming of mouse oocytes (Edashige *et al.* 2003; Yamaji *et al.* 2011). However, there are no data in the literature regarding to this approach in bovine oocytes

The oocyte maturation stage determines some differences in oocyte membrane permeability. In bovine, GV oocytes present 2-fold lower hydraulic conductivity compared to matured MII oocytes (Ruffing *et al.* 1993; Agca *et al.* 1998). In other words, MII stage bovine oocytes have higher water and CPA permeability coefficients than GV stage oocytes. In this way, GV oocytes would be less able to tolerate potential water flux or shear force related damage during volume changes (Muldrew and McGann 1994). Conversely, at the same time this difference in plasma membrane permeability might make MII oocytes more sensitive, because changes of cell volume and intracellular CPA concentrations are more severe in MII than in GV bovine oocytes during CPA addition and dilution process (Zhou *et al.* 2010). It has to be into

account when a vitrification-warming protocol is designed, in order to ensure the optimal CPA concentration, temperature and exposure time.

5. The role of mathematical modeling

When developing a vitrification procedure focusing on technical methodologies, primary considerations include determining the appropriate solution to use (Levin and Miller 1981) and the manner in which it is to be used (Benson *et al.* 2012a). Regarding the appropriate solution, designing a vitrification solution requires knowing the appropriate proportions of each solute in relation to the total concentration of all solutes necessary to prevent ice formation during cooling and warming. As for the manner in which a solution is to be used, adding CPA to cells and removing it from cells can be osmotically damaging. CPA addition results in cell shrinkage when intracellular water exits in response to the increased extracellular osmolality, and then re-swells as the CPA and water permeate the cell membrane returning the cell to isotonic volume. During CPA removal, the cell first swells to greater than isotonic volume as water moves into the cell and then returns to isotonic volume as CPA and water exit the cell (Levin and Miller 1981). In order to reach the vitrification state, CPAs are used in concentrations usually exceeding 1 mol/kg. While the biophysics of the equilibration processes is dependent on many parameters including cell and CPA types, and temperature, among others, the protocol used to achieve equilibration can have a dramatically damaging effect on cell viability, even before any cooling has occurred. This damage is understood to be dominated by both physical and biochemical effects (Benson *et al.* 2012a). The former is linked to transport driven volume fluxes causing cells to exceed volume limits (Mullen *et al.* 2004; Woods *et al.* 2004), and the latter due to cytotoxicity, whether acute or by accumulation of CPAs, which can be due to many factors including the CPA type, time of exposure to CPA, CPA concentration, and temperature (Fahy *et al.* 1990; Elmoazzen *et al.* 2002; Wusteman *et al.* 2002; Fahy *et al.* 2004).

The development of optimal cryopreservation protocols requires accounting for all of these interdependent factors, which makes rigorous experimental optimization impractical, as it would require a very large number of experiments. Therefore, it is desirable to combine empirical and theoretical knowledge through the use of mathematical modeling to simplify experimental optimization (Leibo 2008). Rational design approaches combine mathematical models and cell biophysical parameters to predict optimized CPA addition and removal procedures. Because the damage due to extending cell volumes beyond osmotic tolerance limits is relatively well understood, the most common rational design method has been to use membrane transport equations and osmotic tolerance limits to predict multi-step procedures that prevent osmotic

damage (Mukherjee *et al.* 2007). With an argument that cytotoxicity due to CPA exposure is time-sensitive, rational design strategies have also been extended to reduce toxic damage by minimizing the duration of the CPA addition and removal procedures while still maintaining cell volumes between osmotic tolerance limits (Karlsson *et al.* 2009; Benson *et al.* 2011). While CPA cytotoxicity is time sensitive, it is also concentration sensitive (Fahy *et al.* 2004). Therefore, in order to account for this time and concentration dependence, mathematical methods that predict optimal procedures based on the minimization of a toxicity cost function, a term that describes the accrual of toxic damage, have been already described (Benson *et al.* 2012a), but its use to improve bovine oocyte and embryo vitrification still needs to be evaluated.

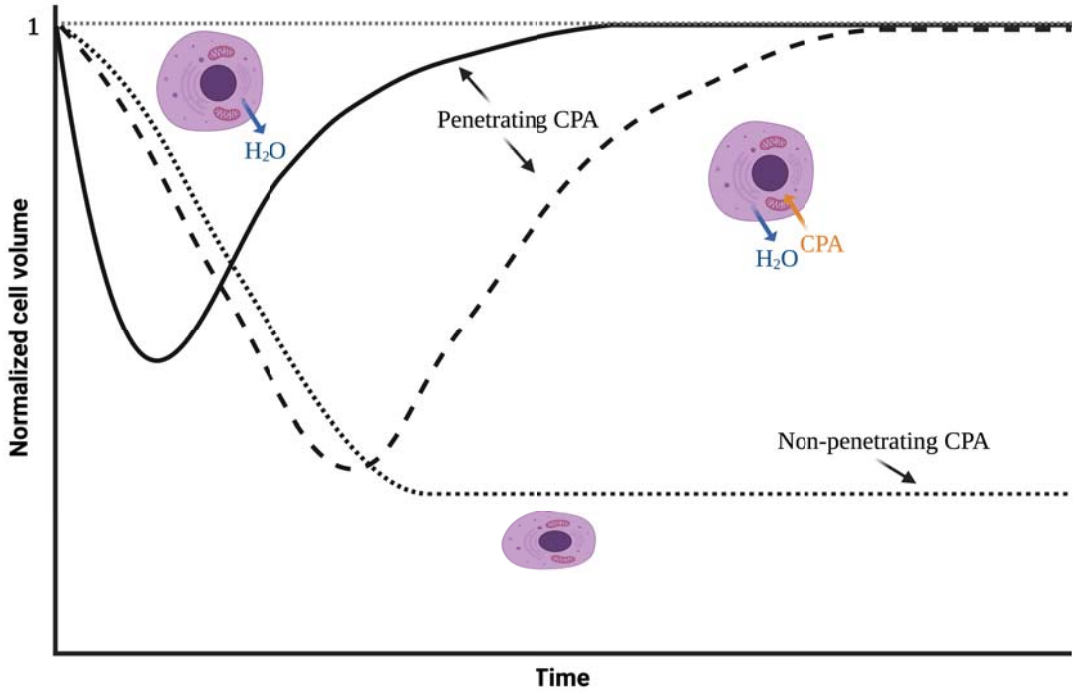

Figure 7. Change in cell volume during shrink-swell experiments as a result of osmotic changes with penetrating and small non-penetrating CPAs. The solid and long dash lines represent an example behavior of penetrating CPAs that have different permeabilities and osmolalities where the rate of shrink/swell are different. Adapted from (Raju *et al.* 2021).

In general, mathematical approaches rely on predictions of mass transfer across the cell membrane. Membrane transfer modeling has been used for decades to guide the design of cryopreservation methods for isolated cells. The backbone of these approaches is a mathematical model that describes the flow of water (hydraulic conductivity (Lp)) and CPA (cryoprotectant permeability (P_{CPA})) across the cell membrane. This membrane transport model allows prediction of changes in cell volume and intracellular CPA content during the addition and removal of CPA,

and determine whether water and solute movement occurs through channels or by simple diffusion through the lipid bilayer [13]. One of the simplest methods of measuring water and CPA penetration is a 'shrink-swell' light microscopy experiment, whereby changes in cell size are observed as the suspending solution is changed from an isotonic solution to one containing the CPA. If the CPA is permeable, the cell will initially shrink due to water leaving the cell, but will swell again as the CPA enters the cell and restores osmotic equilibrium (Weng *et al.* 2017). If the cell does not swell and return to near its starting size, then the CPA cannot penetrate (Levin and Miller 1981). Both of these cases are shown in Figure 8.

Nevertheless, the above microscopic method can be further improved by using microfluidic technologies. The shrink-swell behaviour can be modelled to extrapolate permeability parameters and related activation energies. A number of formalism exist for determing these permeability parameters. These include a one-parameter for calculating solute permeability model introduced by Mazur and colleagues (Mazur *et al.* 1974; Mazur and Miller 1976a). This was refined to a two-parameter model called 2P (Jacobs 1933; Kedem and Katchalsky 1958) for finding water and solute permeability. Kedem and Katchalsky (Kedem and Katchalsky 1958) developed the three-parameter model (also called the Kedem–Katchalsky (KK) formalism), which adds the term 'σ' representing the interaction between solute and solvent (Kleinhans 1998).

Historically, the two-parameter formalism (2P model) has been used to model membrane transport in MII oocytes (Jacobs and Stewart 1932; Jacobs 1933). This model makes limiting dilute-solution assumptions. The assumption of a dilute and ideal solution is often acceptable under physiological conditions, but it is rarely appropriate in most cryobiological cases where CPAs are often used at high concentrations and the presence of extracellular ice further concentrates the solutions. In 2009, Elmoazzen et al (Elmoazzen *et al.* 2009) developed a new nondilute solution model, which is comparatively more complex than the 2P model, but potentially more accurate. Nevertheless, this new mathematical approach has not been proved in MII oocytes.

Therefore, acquisition of the membrane permeability parameters by mathematical modelling allows the development of procedures which can minimize the time, concentration, and temperature-dependent cytotoxic effects of the CPAs during equilibration, cooling, warming, and dilution steps of the cryopreservation process.

6. Justification of the study

Despite many recent advances, the ideal protocol for the cryopreservation of cow oocytes has not yet been developed. During the past two decades, many research efforts have tried to overcome individual features of the bovine oocyte that make it notoriously difficult to cryopreserve. However, the embryo development rates obtained from cryopreserved oocytes have proved difficult and low pregnancy rates are achieved after transferring cryopreserved compared to fresh embryos. Being this said, the overall objective of the current study was to enhance bovine developmental competence of vitrified/warmed oocytes by means of mathematical modeling and optimization of CPA equilibration methods using a transport model and permeability parameters suitable for the high CPA concentrations required for vitrification. Moreover, this study aimed to facilitate the movement of water and CPAs in bovine *in vitro* matured oocytes in which AQP7 was artificially overexpressed through cRNA injection for better outcomes after vitrification/warming.

References

Acker, J.P., Elliott, J.A., and McGann, L.E. (2001) Intercellular ice propagation: experimental evidence for ice growth through membrane pores. *Biophys J* **81**(3), 1389-97

Agca, Y., Liu, J., Peter, A.T., Critser, E.S., and Critser, J.K. (1998) Effect of developmental stage on bovine oocyte plasma membrane water and cryoprotectant permeability characteristics. *Mol Reprod Dev* **49**(4), 408-15

Aigner, S., Van der Elst, J., Siebzehnrübl, E., Wildt, L., Lang, N., and Van Steirteghem, A.C. (1992) The influence of slow and ultra-rapid freezing on the organization of the meiotic spindle of the mouse oocyte. *Hum Reprod* **7**(6), 857-64

Albarracin, J.L., Morato, R., Izquierdo, D., and Mogas, T. (2005a) Vitrification of calf oocytes: effects of maturation stage and prematuration treatment on the nuclear and cytoskeletal components of oocytes and their subsequent development. *Mol Reprod Dev* **72**(2), 239-49

Albarracin, J.L., Morato, R., Rojas, C., and Mogas, T. (2005b) Effects of vitrification in open pulled straws on the cytology of *in vitro* matured prepubertal and adult bovine oocytes. *Theriogenology* **63**(3), 890-901

Almeida, P.A., and Bolton, V.N. (1995) The effect of temperature fluctuations on the cytoskeletal organisation and chromosomal constitution of the human oocyte. *Zygote* **3**(4), 357-65

AM, K. (1974) Cryopreservation: pharmacological considerations. In 'Organ Preservation for Transplantation.' (Ed. AG Karow AM, Humphries AL) pp. 86-107: Little Brown, Boston)

Aman, R.R., and Parks, J.E. (1994) Effects of cooling and rewarming on the meiotic spindle and chromosomes of *in vitro*-matured bovine oocytes. *Biol Reprod* **50**(1), 103-10

Ambrosini, G., Andrisani, A., Porcu, E., Rebellato, E., Revelli, A., Caserta, D., Cosmi, E., Marci, R., and Moscarini, M. (2006) Oocytes cryopreservation: state of art. *Reprod Toxicol* **22**(2), 250-62

Andersen, H.D., Wang, C., Arleth, L., Peters, G.H., and Westh, P. (2011) Reconciliation of opposing views on membrane-sugar interactions. *Proc Natl Acad Sci U S A* **108**(5), 1874-8

Angell, C.A. (2002) Liquid fragility and the glass transition in water and aqueous solutions. *Chem Rev* **102**(8), 2627-50

Anzar, M. (2017) Cryopreservation of Mammalian Oocytes. In '.' pp. 519-556)

Arakawa, T., Carpenter, J.F., Kita, Y.A., and Crowe, J.H. (1990) The basis for toxicity of certain cryoprotectants: A hypothesis. *Cryobiology* **27**(4), 401-415

Arakawa, T., and Timasheff, S.N. (1982) Preferential interactions of proteins with salts in concentrated solutions. *Biochemistry* **21**(25), 6545-52

Arav, A., Yavin, S., Zeron, Y., Natan, D., Dekel, I., and Gacitua, H. (2002) New trends in gamete's cryopreservation. *Mol Cell Endocrinol* **187**(1-2), 77-81

Arav, A., Zeron, Y., Leslie, S.B., Behboodi, E., Anderson, G.B., and Crowe, J.H. (1996) Phase transition temperature and chilling sensitivity of bovine oocytes. *Cryobiology* **33**(6), 589-99

Armitage, W.J., and Mazur, P. (1984) Osmotic tolerance of human granulocytes. *American Journal of Physiology-Cell Physiology* **247**(5), C373-C381

Battaglia, D.E., Klein, N.A., and Soules, M.R. (1996) Changes in centrosomal domains during meiotic maturation in the human oocyte. *Mol Hum Reprod* **2**(11), 845-51

Benson, J.D., Chicone, C.C., and Critser, J.K. (2011) A general model for the dynamics of cell volume, global stability, and optimal control. *J Math Biol* **63**(2), 339-59

Benson, J.D., Kearsley, A.J., and Higgins, A.Z. (2012a) Mathematical optimization of procedures for cryoprotectant equilibration using a toxicity cost function. *Cryobiology* **64**(3), 144-51

Benson, J.D., Woods, E.J., Walters, E.M., and Critser, J.K. (2012b) The cryobiology of spermatozoa. *Theriogenology* **78**(8), 1682-99

Bogliolo, L., Ariu, F., Fois, S., Rosati, I., Zedda, M.T., Leoni, G., Succu, S., Pau, S., and Ledda, S. (2007) Morphological and biochemical analysis of immature ovine oocytes vitrified with or without cumulus cells. *Theriogenology* **68**(8), 1138-49

Boiso, I., Marti, M., Santalo, J., Ponsa, M., Barri, P.N., and Veiga, A. (2002) A confocal microscopy analysis of the spindle and chromosome configurations of human oocytes cryopreserved at the germinal vesicle and metaphase II stage. *Hum Reprod* **17**(7), 1885-91

Boutron, P., and Mehl, P. (1990) Theoretical prediction of devitrification tendency: determination of critical warming rates without using finite expansions. *Cryobiology* **27**(4), 359-77

Brambillasca, F., Guglielmo, M.C., Coticchio, G., Mignini Renzini, M., Dal Canto, M., and Fadini, R. (2013) The current challenges to efficient immature oocyte cryopreservation. *Journal of assisted reproduction and genetics* **30**(12), 1531-1539

Bromfield, J.J., Coticchio, G., Hutt, K., Sciajno, R., Borini, A., and Albertini, D.F. (2009) Meiotic spindle dynamics in human oocytes following slow-cooling cryopreservation. *Hum Reprod* **24**(9), 2114-23

Brüggeller, P., and Mayer, E. (1980) Complete vitrification in pure liquid water and dilute aqueous solutions. *Nature* **288**(5791), 569-571

Bryant, G. (1995) DSC measurement of cell suspensions during successive freezing runs: implications for the mechanisms of intracellular ice formation. *Cryobiology* **32**(2), 114-28

Bryant, G., Koster, K.L., and Wolfe, J. (2001) Membrane behaviour in seeds and other systems at low water content: the various effects of solutes. *Seed Science Research* **11**(1), 17-25

Cai, X.Y., Chen, G.A., Lian, Y., Zheng, X.Y., and Peng, H.M. (2005) Cryoloop vitrification of rabbit oocytes. *Hum Reprod* **20**(7), 1969-74

Chang, C.-C., Lin, C.-J., Sung, L.-Y., Kort, H.I., Tian, X.C., and Nagy, Z.P. (2011) Impact of phase transition on the mouse oocyte spindle during vitrification. *Reproductive BioMedicine Online* **22**(2), 184-191

Chapman, D. (1975) Phase transitions and fluidity characteristics of lipids and cell membranes. *Q Rev Biophys* **8**(2), 185-235

Chaves, D.F., Corbin, E., Almiñana, C., Locatelli, Y., Souza-Fabjan, J.M.G., Bhat, M.H., Freitas, V.J.F., and Mermillod, P. (2017) Vitrification of immature and *in vitro* matured bovine cumulus-oocyte complexes: Effects on oocyte structure and embryo development. *Livestock Science* **199**, 50-56

Chen, C.K., Wang, C.W., Tsai, W.J., Hsieh, L.L., Wang, H.S., and Soong, Y.K. (2004) Evaluation of meiotic spindles in thawed oocytes after vitrification using polarized light microscopy. *Fertil Steril* **82**(3), 666-72

Chen, S.U., Lien, Y.R., Chen, H.F., Chao, K.H., Ho, H.N., and Yang, Y.S. (2000) Open pulled straws for vitrification of mature mouse oocytes preserve patterns of meiotic spindles and chromosomes better than conventional straws. *Hum Reprod* **15**(12), 2598-603

Chian, R.-C. (2010) Cryobiology: An overview. In 'Fertility Cryopreservation.' (Ed. RC Chian, Quinn, P.) pp. 1-9: Cambridge University Press: Cambridge, UK)

Clegg, J.S., Seitz, P., Seitz, W., and Hazlewood, C.F. (1982) Cellular responses to extreme water loss: the water-replacement hypothesis. *Cryobiology* **19**(3), 306-16

Cocks, F.H., and Brower, W.E. (1974) Phase diagram relationships in cryobiology. *Cryobiology* **11**(4), 340-58

Coticchio, G., Bonu, M.A., Bianchi, V., Flamigni, C., and Borini, A. (2005) Criteria to assess human oocyte quality after cryopreservation. *Reprod Biomed Online* **11**(4), 421-7

Crowe, J.H., Carpenter, J.F., Crowe, L.M., and Anchordoguy, T.J. (1990) Are freezing and dehydration similar stress vectors? A comparison of modes of interaction of stabilizing solutes with biomolecules. *Cryobiology* **27**(3), 219-231

Cutting, R., Barlow, S., and Anderson, R. (2009) Human oocyte cryopreservation: evidence for practice. *Hum Fertil (Camb)* **12**(3), 125-36

Díez, C., Muñoz, M., Caamaño, J.N., and Gómez, E. (2012) Cryopreservation of the bovine oocyte: current status and perspectives. *Reprod Domest Anim* **47 Suppl 3**, 76-83

Edashige, K. (2016) The movement of water and cryoprotectants across the plasma membrane of mammalian oocytes and embryos and its relevance to vitrification. *J Reprod Dev* **62**(4), 317-21

Edashige, K., Tanaka, M., Ichimaru, N., Ota, S., Yazawa, K., Higashino, Y., Sakamoto, M., Yamaji, Y., Kuwano, T., Valdez, D.M., Jr., Kleinhans, F.W., and Kasai, M. (2006) Channel-dependent permeation of water and glycerol in mouse morulae. *Biol Reprod* **74**(4), 625-32

Edashige, K., Yamaji, Y., Kleinhans, F.W., and Kasai, M. (2003) Artificial expression of aquaporin-3 improves the survival of mouse oocytes after cryopreservation. *Biol Reprod* **68**(1), 87-94

Elliott, G.D., Wang, S., and Fuller, B.J. (2017) Cryoprotectants: A review of the actions and applications of cryoprotective solutes that modulate cell recovery from ultra-low temperatures. *Cryobiology* **76**, 74-91

Elmoazzen, H.Y., Elliott, J.A., and McGann, L.E. (2002) The effect of temperature on membrane hydraulic conductivity. *Cryobiology* **45**(1), 68-79

Elmoazzen, H.Y., Elliott, J.A., and McGann, L.E. (2009) Osmotic transport across cell membranes in nondilute solutions: a new nondilute solute transport equation. *Biophys J* **96**(7), 2559-71

Fabbri, R. (2006) Cryopreservation of human oocytes and ovarian tissue. *Cell Tissue Bank* **7**(2), 113-22

Fabbri, R., Porcu, E., Marsella, T., Primavera, M.R., Rocchetta, G., Ciotti, P.M., Magrini, O., Seracchioli, R., Venturoli, S., and Flamigni, C. (2000) Technical aspects of oocyte cryopreservation. *Mol Cell Endocrinol* **169**(1-2), 39-42

Fabbri, R., Porcu, E., Marsella, T., Rocchetta, G., Venturoli, S., and Flamigni, C. (2001) Human oocyte cryopreservation: new perspectives regarding oocyte survival. *Hum Reprod* **16**(3), 411-6

Fahy, G.M. (1986) The relevance of cryoprotectant "toxicity" to cryobiology. *Cryobiology* **23**(1), 1-13

Fahy, G.M., Levy, D.I., and Ali, S.E. (1987) Some emerging principles underlying the physical properties, biological actions, and utility of vitrification solutions. *Cryobiology* **24**(3), 196-213

Fahy, G.M., Lilley, T.H., Linsdell, H., Douglas, M.S., and Meryman, H.T. (1990) Cryoprotectant toxicity and cryoprotectant toxicity reduction: in search of molecular mechanisms. *Cryobiology* **27**(3), 247-68

Fahy, G.M., MacFarlane, D.R., Angell, C.A., and Meryman, H.T. (1984) Vitrification as an approach to cryopreservation. *Cryobiology* **21**(4), 407-26

Fahy, G.M., Wowk, B., Wu, J., and Paynter, S. (2004) Improved vitrification solutions based on the predictability of vitrification solution toxicity. *Cryobiology* **48**(1), 22-35

Forman, E.J., Li, X., Ferry, K.M., Scott, K., Treff, N.R., and Scott, R.T., Jr. (2012) Oocyte vitrification does not increase the risk of embryonic aneuploidy or diminish the implantation potential of blastocysts created after intracytoplasmic sperm injection: a novel, paired randomized controlled trial using DNA fingerprinting. *Fertil Steril* **98**(3), 644-9

Franks, F. (1986) Metastable water at subzero temperatures. *Journal of Microscopy* **141**(3), 243-249

Friedler, S., Giudice, L.C., and Lamb, E.J. (1988) Cryopreservation of embryos and ova. *Fertil Steril* **49**(5), 743-64

Fuller, B., and Paynter, S. (2004) Fundamentals of cryobiology in reproductive medicine. *Reprod Biomed Online* **9**(6), 680-91

Fuller, B.J. (2004) Cryoprotectants: the essential antifreezes to protect life in the frozen state. *Cryo Letters* **25**(6), 375-88

Galeati, G., Spinaci, M., Vallorani, C., Bucci, D., Porcu, E., and Tamanini, C. (2011) Pig oocyte vitrification by cryotop method: effects on viability, spindle and chromosome configuration and *in vitro* fertilization. *Anim Reprod Sci* **127**(1-2), 43-9

Gardner, D.K., Sheehan, C.B., Rienzi, L., Katz-Jaffe, M., and Larman, M.G. (2007) Analysis of oocyte physiology to improve cryopreservation procedures. *Theriogenology* **67**(1), 64-72

Gekko, K., and Timasheff, S.N. (1981) Mechanism of protein stabilization by glycerol: preferential hydration in glycerol-water mixtures. *Biochemistry* **20**(16), 4667-76

George, M.A., Pickering, S.J., Braude, P.R., and Johnson, M.H. (1996) The distribution of alpha- and gamma-tubulin in fresh and aged human and mouse oocytes exposed to cryoprotectant. *Mol Hum Reprod* **2**(6), 445-56

Ghetler, Y., Yavin, S., Shalgi, R., and Arav, A. (2005) The effect of chilling on membrane lipid phase transition in human oocytes and zygotes. *Hum Reprod* **20**(12), 3385-9

Gomes, C., Merlini, M., Konheim, J., Serafini, P., Motta, E.L., Baracat, E.C., and Smith, G.D. (2012) Oocyte meiotic-stage-specific differences in spindle depolymerization in response to temperature changes monitored with polarized field microscopy and immunocytochemistry. *Fertil Steril* **97**(3), 714-9

Gook, D.A., and Edgar, D.H. (2007) Human oocyte cryopreservation. *Hum Reprod Update* **13**(6), 591-605

Gook, D.A., Schiewe, M.C., Osborn, S.M., Asch, R.H., Jansen, R.P., and Johnston, W.I. (1995) Intracytoplasmic sperm injection and embryo development of human oocytes cryopreserved using 1,2-propanediol. *Hum Reprod* **10**(10), 2637-41

Gorbsky, G.J., Simerly, C., Schatten, G., and Borisy, G.G. (1990) Microtubules in the metaphase-arrested mouse oocyte turn over rapidly. *Proc Natl Acad Sci U S A* **87**(16), 6049-53

Gupta, M.K., Uhm, S.J., and Lee, H.T. (2007) Cryopreservation of immature and *in vitro* matured porcine oocytes by solid surface vitrification. *Theriogenology* **67**(2), 238-48

He, X. (2011) Thermostability of biological systems: fundamentals, challenges, and quantification. *Open Biomed Eng J* **5**, 47-73

Holt, W.V. (2008) Cryobiology, wildlife conservation and reality. *Cryo Letters* **29**(1), 43-52

Hubálek, Z. (2003) Protectants used in the cryopreservation of microorganisms. *Cryobiology* **46**(3), 205-29

Hunter, G.L., and Weeks, E.R. (2012) The physics of the colloidal glass transition. *Rep Prog Phys* **75**(6), 066501

Hwang, I.S., and Hochi, S. (2014) Recent progress in cryopreservation of bovine oocytes. *Biomed Res Int* **2014**, 570647

Irimia, D., and Karlsson, J.O. (2005) Kinetics of intracellular ice formation in one-dimensional arrays of interacting biological cells. *Biophys J* **88**(1), 647-60

Jacobs, M.H. (1933) The simultaneous measurement of cell permeability to water and to dissolved substances. *Journal of Cellular and Comparative Physiology* **2**(4), 427-444

Jacobs, M.H., and Stewart, D.R. (1932) A simple method for the quantitative measurement of cell permeability. *Journal of Cellular and Comparative Physiology* **1**(1), 71-82

Jain, J.K., and Paulson, R.J. (2006) Oocyte cryopreservation. *Fertil Steril* **86**(4 Suppl), 1037-46

Jin, B., Higashiyama, R., Nakata, Y., Yonezawa, J., Xu, S., Miyake, M., Takahashi, S., Kikuchi, K., Yazawa, K., Mizobuchi, S., Niimi, S., Kitayama, M., Koshimoto, C., Matsukawa, K., Kasai, M., and Edashige, K. (2013) Rapid movement of water and cryoprotectants in pig expanded blastocysts via channel processes: its relevance to their higher tolerance to cryopreservation. *Biol Reprod* **89**(4), 87

Jin, B., Kawai, Y., Hara, T., Takeda, S., Seki, S., Nakata, Y., Matsukawa, K., Koshimoto, C., Kasai, M., and Edashige, K. (2011) Pathway for the movement of water and cryoprotectants in bovine oocytes and embryos. *Biol Reprod* **85**(4), 834-47

Johnson, M.H., and Pickering, S.J. (1987) The effect of dimethylsulphoxide on the microtubular system of the mouse oocyte. *Development* **100**(2), 313-24

Joly, C., Bchini, O., Boulekbache, H., Testart, J., and Maro, B. (1992) Effects of 1,2-propanediol on the cytoskeletal organization of the mouse oocyte. *Hum Reprod* **7**(3), 374-8

Jung, J., Shin, H., Bang, S., Mok, H.J., Suh, C.S., Kim, K.P., and Lim, H.J. (2014) Analysis of the phospholipid profile of metaphase II mouse oocytes undergoing vitrification. *PLoS One* **9**(7), e102620

Karlsson, J.O., and Toner, M. (1996) Long-term storage of tissues by cryopreservation: critical issues. *Biomaterials* **17**(3), 243-56

Karlsson, J.O.M., Younis, A.I., Chan, A.W.S., Gould, K.G., and Eroglu, A. (2009) Permeability of the rhesus monkey oocyte membrane to water and common cryoprotectants. *Molecular reproduction and development* **76**(4), 321-333

Karow, A.M., Jr. (1969) Cryoprotectants--a new class of drugs. *J Pharm Pharmacol* **21**(4), 209-23

Kedem, O., and Katchalsky, A. (1958) Thermodynamic analysis of the permeability of biological membranes to non-electrolytes. *Biochim Biophys Acta* **27**(2), 229-46

Keefe, D., Liu, L., Wang, W., and Silva, C. (2003) Imaging meiotic spindles by polarization light microscopy: principles and applications to IVF. *Reprod Biomed Online* **7**(1), 24-9

Kim, N.H., Chung, H.M., Cha, K.Y., and Chung, K.S. (1998) Microtubule and microfilament organization in maturing human oocytes. *Hum Reprod* **13**(8), 2217-22

Kleinhans, F.W. (1998) Membrane permeability modeling: Kedem-Katchalsky *vs* a two-parameter formalism. *Cryobiology* **37**(4), 271-89

Kohaya, N., Fujiwara, K., Ito, J., and Kashiwazaki, N. (2013) Generation of live offspring from vitrified mouse oocytes of C57BL/6J strain. *PLoS One* **8**(3), e58063

Koster, K.L., Lei, Y.P., Anderson, M., Martin, S., and Bryant, G. (2000) Effects of vitrified and nonvitrified sugars on phosphatidylcholine fluid-to-gel phase transitions. *Biophys J* **78**(4), 1932-46

Kuwayama, M., and Kato, O. (2000) All-round vitrification method for human oocytes and embryos. *J Assist Reprod Genet;* **17**

Larman, M.G., Minasi, M.G., Rienzi, L., and Gardner, D.K. (2007) Maintenance of the meiotic spindle during vitrification in human and mouse oocytes. *Reprod Biomed Online* **15**(6), 692-700

Lassalle, B., Testart, J., and Renard, J.P. (1985) Human embryo features that influence the success of cryopreservation with the use of 1,2 propanediol. *Fertil Steril* **44**(5), 645-51

Lei, T., Guo, N., Liu, J.-Q., Tan, M.-H., and Li, Y.-F. (2014) Vitrification of *in vitro* matured oocytes: effects on meiotic spindle configuration and mitochondrial function. *International Journal of Clinical and Experimental Pathology* **7**(3), 1159-1165

Leibo, S.P. (1980) Water permeability and its activation energy of fertilized and unfertilized mouse ova. *J Membr Biol* **53**(3), 179-88

Leibo, S.P. (2008) Cryopreservation of oocytes and embryos: optimization by theoretical versus empirical analysis. *Theriogenology* **69**(1), 37-47

Levin, R.L., and Miller, T.W. (1981) An optimum method for the introduction or removal of permeable cryoprotectants: isolated cells. *Cryobiology* **18**(1), 32-48

Liu, R.H., Sun, Q.Y., Li, Y.H., Jiao, L.H., and Wang, W.H. (2003) Effects of cooling on meiotic spindle structure and chromosome alignment within *in vitro* matured porcine oocytes. *Mol Reprod Dev* **65**(2), 212-8

Lovelock, J.E. (1953) The haemolysis of human red blood-cells by freezing and thawing. *Biochim Biophys Acta* **10**(3), 414-26

Luyet, B.J. (1957) On the growth of the ice phase in aqueous colloids. *Proc R Soc Lond B Biol Sci* **147**(929), 434-51

Luyet, B.J., and Gehenio, P.M. (1947) Thermoelectric recording of ice formation and of vitrification during ultra-rapid cooling of protoplasm. *Fed Proc* **6**(1 Pt 2), 157

Macfarlane, D.R., and Forsyth, M. (1990) Recent insights on the role of cryoprotective agents in vitrification. *Cryobiology* **27**(4), 345-358

Magistrini, M., and Szöllösi, D. (1980) Effects of cold and of isopropyl-N-phenylcarbamate on the second meiotic spindle of mouse oocytes. *Eur J Cell Biol* **22**(2), 699-707

Magnusson, V., Feitosa, W.B., Goissis, M.D., Yamada, C., Tavares, L.M.T., D'Avila Assumpção, M.E.O., and Visintin, J.A. (2008) Bovine oocyte vitrification: effect of ethylene glycol concentrations and meiotic stages. *Animal reproduction science* **106**(3-4), 265-273

Massip, A. (2003) Cryopreservation of bovine oocytes: current status and recent developments. *Reprod Nutr Dev* **43**(4), 325-30

Mazur, P. (1963) KINETICS OF WATER LOSS FROM CELLS AT SUBZERO TEMPERATURES AND THE LIKELIHOOD OF INTRACELLULAR FREEZING. *The Journal of general physiology* **47**(2), 347-369

Mazur, P. (1965) The role of cell membranes in the freezing of yeast and other single cells. *Ann N Y Acad Sci* **125**(2), 658-76

Mazur, P. (1977) The role of intracellular freezing in the death of cells cooled at supraoptimal rates. *Cryobiology* **14**(3), 251-72

Mazur, P. (1984) Freezing of living cells: mechanisms and implications. *Am J Physiol* **247**(3 Pt 1), C125-42

Mazur, P. (1990) Equilibrium, quasi-equilibrium, and nonequilibrium freezing of mammalian embryos. *Cell Biophys* **17**(1), 53-92

Mazur, P., Leibo, S.P., and Chu, E.H. (1972) A two-factor hypothesis of freezing injury. Evidence from Chinese hamster tissue-culture cells. *Exp Cell Res* **71**(2), 345-55

Mazur, P., Leibo, S.P., and Miller, R.H. (1974) Permeability of the bovine red cell to glycerol in hyperosmotic solutions at various temperatures. *J Membr Biol* **15**(2), 107-36

Mazur, P., and Miller, R.H. (1976a) Permeability of the human erythrocyte to glycerol in 1 and 2 M solutions at 0 or 20 degrees C. *Cryobiology* **13**(5), 507-22

Mazur, P., and Miller, R.H. (1976b) Survival of frozen-thawed human red cells as a function of the permeation of glycerol and sucrose. *Cryobiology* **13**(5), 523-536

Men, H., Monson, R.L., and Rutledge, J.J. (2002) Effect of meiotic stages and maturation protocols on bovine oocyte's resistance to cryopreservation. *Theriogenology* **57**(3), 1095-103

Meryman, H.T. (1971) Cryoprotective agents. *Cryobiology* **8**(2), 173-83

Moawad, A.R., Zhu, J., Choi, I., Amarnath, D., Chen, W., and Campbell, K.H. (2013) Production of good-quality blastocyst embryos following IVF of ovine oocytes vitrified at the germinal vesicle stage using a cryoloop. *Reprod Fertil Dev* **25**(8), 1204-15

Mochida, K., Hasegawa, A., Li, M.W., Fray, M.D., Kito, S., Vallelunga, J.M., Lloyd, K.C., Yoshiki, A., Obata, Y., and Ogura, A. (2013) High osmolality vitrification: a new method for the simple and temperature-permissive cryopreservation of mouse embryos. *PLoS One* **8**(1), e49316

Mogas, T. (2018) Update on the vitrification of bovine oocytes and invitro-produced embryos. *Reprod Fertil Dev* **31**(1), 105-117

Morató, R., Chauvigné, F., Novo, S., Bonet, S., and Cerdà, J. (2014) Enhanced water and cryoprotectant permeability of porcine oocytes after artificial expression of human and zebrafish aquaporin-3 channels. *Mol Reprod Dev* **81**(5), 450-61

Morato, R., Izquierdo, D., Albarracin, J.L., Anguita, B., Palomo, M.J., Jimenez-Macedo, A.R., Paramio, M.T., and Mogas, T. (2008a) Effects of pre-treating *in vitro*-matured bovine oocytes with the cytoskeleton stabilizing agent taxol prior to vitrification. *Mol Reprod Dev* **75**(1), 191-201

Morato, R., Izquierdo, D., Paramio, M.T., and Mogas, T. (2008b) Cryotops versus open-pulled straws (OPS) as carriers for the cryopreservation of bovine oocytes: effects on spindle and chromosome configuration and embryo development. *Cryobiology* **57**(2), 137-41

Morato, R., Mogas, T., and Maddox-Hyttel, P. (2008c) Ultrastructure of bovine oocytes exposed to Taxol prior to OPS vitrification. *Mol Reprod Dev* **75**(8), 1318-26

Mourão, M.A., Hakim, J.B., and Schnell, S. (2014) Connecting the dots: the effects of macromolecular crowding on cell physiology. *Biophys J* **107**(12), 2761-2766

Moussa, M., Shu, J., Zhang, X., and Zeng, F. (2014) Cryopreservation of mammalian oocytes and embryos: current problems and future perspectives. *Sci China Life Sci* **57**(9), 903-14

Mukherjee, I.N., Song, Y.C., and Sambanis, A. (2007) Cryoprotectant delivery and removal from murine insulinomas at vitrification-relevant concentrations. *Cryobiology* **55**(1), 10-18

Muldrew, K., Acker, J., Elliott, J.A.W., and Mcgann, L. The Water to Ice Transition: Implications for Living Cells. 2004,

Muldrew, K., and McGann, L.E. (1994) The osmotic rupture hypothesis of intracellular freezing injury. *Biophys J* **66**(2 Pt 1), 532-41

Mullen, S.F., Agca, Y., Broermann, D.C., Jenkins, C.L., Johnson, C.A., and Critser, J.K. (2004) The effect of osmotic stress on the metaphase II spindle of human oocytes, and the relevance to cryopreservation. *Hum Reprod* **19**(5), 1148-54

Mullen SF, A.Y., Critser JK (2004) Modeling the Probability of MII Spindle Disruption in Bovine Oocytes as a Function of Total Osmolality Using Logistic Regression and Its Application toward Improved CPA Addition and Removal Procedures. *Cell Preservation Technology* **2**(2), 145-155

Mullen, S.F., and Critser, J.K. (2007) The Science of Cryobiology. In 'Oncofertility Fertility Preservation for Cancer Survivors.' (Eds. TK Woodruff and KA Snyder) pp. 83-109. (Springer US: Boston, MA)

Nagai, S., Mabuchi, T., Hirata, S., Shoda, T., Kasai, T., Yokota, S., Shitara, H., Yonekawa, H., and Hoshi, K. (2006) Correlation of abnormal mitochondrial distribution in mouse oocytes with reduced developmental competence. *Tohoku J Exp Med* **210**(2), 137-44

Oldenhof, H., Gojowsky, M., Wang, S., Henke, S., Yu, C., Rohn, K., Wolkers, W.F., and Sieme, H. (2013) Osmotic stress and membrane phase changes during freezing of stallion sperm: mode of action of cryoprotective agents. *Biol Reprod* **88**(3), 68

Paynter, S.J., and Fuller, B.J. (2007) Cryopreservation of mammalian oocytes. *Methods Mol Biol* **368**, 313-24

Pedro, P.B., Yokoyama, E., Zhu, S.E., Yoshida, N., Valdez, D.M., Jr., Tanaka, M., Edashige, K., and Kasai, M. (2005) Permeability of mouse oocytes and embryos at various developmental stages to five cryoprotectants. *J Reprod Dev* **51**(2), 235-46

Pegg, D.E. (2002) The history and principles of cryopreservation. *Semin Reprod Med* **20**(1), 5-13

Pereira, R.M., and Marques, C.C. (2008) Animal oocyte and embryo cryopreservation. *Cell Tissue Bank* **9**(4), 267-77

Pickering, S.J., Braude, P.R., Johnson, M.H., Cant, A., and Currie, J. (1990) Transient cooling to room temperature can cause irreversible disruption of the meiotic spindle in the human oocyte. *Fertil Steril* **54**(1), 102-8

Pickering, S.J., and Johnson, M.H. (1987) The influence of cooling on the organization of the meiotic spindle of the mouse oocyte. *Hum Reprod* **2**(3), 207-16

Polge, C., Smith, A.U., and Parkes, A.S. (1949) Revival of spermatozoa after vitrification and dehydration at low temperatures. *Nature* **164**(4172), 666

Pope, C.E., Gómez, M.C., Kagawa, N., Kuwayama, M., Leibo, S.P., and Dresser, B.L. (2012) *In vivo* survival of domestic cat oocytes after vitrification, intracytoplasmic sperm injection and embryo transfer. *Theriogenology* **77**(3), 531-8

Prentice, J.R., and Anzar, M. (2010) Cryopreservation of Mammalian oocyte for conservation of animal genetics. *Vet Med Int* **2011**

Prentice, J.R., Singh, J., Dochi, O., and Anzar, M. (2011) Factors affecting nuclear maturation, cleavage and embryo development of vitrified bovine cumulus-oocyte complexes. *Theriogenology* **75**(4), 602-9

Raju, R., Bryant, S.J., Wilkinson, B.L., and Bryant, G. (2021) The need for novel cryoprotectants and cryopreservation protocols: Insights into the importance of biophysical investigation and cell permeability. *Biochim Biophys Acta Gen Subj* **1865**(1), 129749

Rall, W.F. (1987) Factors affecting the survival of mouse embryos cryopreserved by vitrification. *Cryobiology* **24**(5), 387-402

Rall, W.F., and Fahy, G.M. (1985) Ice-free cryopreservation of mouse embryos at -196 degrees C by vitrification. *Nature* **313**(6003), 573-5

Rho, G.J., Kim, S., Yoo, J.G., Balasubramanian, S., Lee, H.J., and Choe, S.Y. (2002) Microtubulin configuration and mitochondrial distribution after ultra-rapid cooling of bovine oocytes. *Mol Reprod Dev* **63**(4), 464-70

Rienzi, L., Ubaldi, F., Iacobelli, M., Minasi, M.G., Romano, S., and Greco, E. (2005) Meiotic spindle visualization in living human oocytes. *Reprod Biomed Online* **10**(2), 192-8

Rojas, C., Palomo, M.J., Albarracin, J.L., and Mogas, T. (2004) Vitrification of immature and *in vitro* matured pig oocytes: study of distribution of chromosomes, microtubules, and actin microfilaments. *Cryobiology* **49**(3), 211-20

Ruffing, N.A., Steponkus, P.L., Pitt, R.E., and Parks, J.E. (1993) Osmometric behavior, hydraulic conductivity, and incidence of intracellular ice formation in bovine oocytes at different developmental stages. *Cryobiology* **30**(6), 562-80

Saragusty, J., and Arav, A. (2011) Current progress in oocyte and embryo cryopreservation by slow freezing and vitrification. *Reproduction* **141**(1), 1-19

Sathananthan, A.H., Kirby, C., Trounson, A., Philipatos, D., and Shaw, J. (1992a) The effects of cooling mouse oocytes. *J Assist Reprod Genet* **9**(2), 139-48

Sathananthan, A.H., Kirby, C., Trounson, A., Philipatos, D., and Shaw, J. (1992b) The effects of cooling mouse oocytes. *Journal of Assisted Reproduction and Genetics* **9**(2), 139-148

Saunders, K.M., and Parks, J.E. (1999) Effects of cryopreservation procedures on the cytology and fertilization rate of *in vitro*-matured bovine oocytes. *Biol Reprod* **61**(1), 178-87

Schatten, G., Simerly, C., and Schatten, H. (1985) Microtubule configurations during fertilization, mitosis, and early development in the mouse and the requirement for egg microtubule-mediated motility during mammalian fertilization. *Proc Natl Acad Sci U S A* **82**(12), 4152-6

Sharma, G.T., Dubey, P.K., and Chandra, V. (2010) Morphological changes, DNA damage and developmental competence of *in vitro* matured, vitrified-thawed buffalo (Bubalus bubalis) oocytes: A comparative study of two cryoprotectants and two cryodevices. *Cryobiology* **60**(3), 315-21

Shen, Y., Betzendahl, I., Tinneberg, H.R., and Eichenlaub-Ritter, U. (2008) Enhanced polarizing microscopy as a new tool in aneuploidy research in oocytes. *Mutat Res* **651**(1-2), 131-40

Smith, G.D., Serafini, P.C., Fioravanti, J., Yadid, I., Coslovsky, M., Hassun, P., Alegretti, J.R., and Motta, E.L. (2010) Prospective randomized comparison of human oocyte cryopreservation with slow-rate freezing or vitrification. *Fertil Steril* **94**(6), 2088-95

Spricigo, J.F., Morais, K., Ferreira, A.R., Machado, G.M., Gomes, A.C., Rumpf, R., Franco, M.M., and Dode, M.A. (2014) Vitrification of bovine oocytes at different meiotic stages using the Cryotop method: assessment of morphological, molecular and functional patterns. *Cryobiology* **69**(2), 256-65

Spricigo, J.F., Morais, K.S., Yang, B.S., and Dode, M.A. (2012) Effect of the exposure to methyl-beta-cyclodextrin prior to chilling or vitrification on the viability of bovine immature oocytes. *Cryobiology* **65**(3), 319-25

Stachecki, J.J., Munne, S., and Cohen, J. (2004) Spindle organization after cryopreservation of mouse, human, and bovine oocytes. *Reprod Biomed Online* **8**(6), 664-72

Steponkus, P.L. (1984) Role of the Plasma Membrane in Freezing Injury and Cold Acclimation. *Annual Review of Plant Physiology* **35**(1), 543-584

Steponkus, P.L., Myers, S.P., Lynch, D.V., Gardner, L., Bronshteyn, V., Leibo, S.P., Rall, W.F., Pitt, R.E., Lin, T.T., and MacIntyre, R.J. (1990) Cryopreservation of Drosophila melanogaster embryos. *Nature* **345**(6271), 170-2

Succu, S., Leoni, G.G., Bebbere, D., Berlinguer, F., Mossa, F., Bogliolo, L., Madeddu, M., Ledda, S., and Naitana, S. (2007) Vitrification devices affect structural and molecular status of *in vitro* matured ovine oocytes. *Mol Reprod Dev* **74**(10), 1337-44

Szurek, E.A., and Eroglu, A. (2011) Comparison and avoidance of toxicity of penetrating cryoprotectants. *PLoS One* **6**(11), e27604

Tan, Y.J., Zhang, X.Y., Ding, G.L., Li, R., Wang, L., Jin, L., Lin, X.H., Gao, L., Sheng, J.Z., and Huang, H.F. (2015) Aquaporin7 plays a crucial role in tolerance to hyperosmotic stress and in the survival of oocytes during cryopreservation. *Sci Rep* **5**, 17741

Tharasanit, T., Colenbrander, B., and Stout, T.A. (2006) Effect of maturation stage at cryopreservation on post-thaw cytoskeleton quality and fertilizability of equine oocytes. *Mol Reprod Dev* **73**(5), 627-37

Timasheff, S.N. (1993) The control of protein stability and association by weak interactions with water: how do solvents affect these processes? *Annu Rev Biophys Biomol Struct* **22**, 67-97

Todorov, I., Bernard, A.G., McGrath, J.J., Fuller, B.J., and Shaw, R.W. (1993) Studies on 2,3-butanediol as a cryoprotectant for mouse oocytes: use of sucrose to avoid damage during exposure or removal. *Cryo Letters* **14**, 37-42

Toner, M., Cravalho, E.G., Karel, M., and Armant, D.R. (1991) Cryomicroscopic analysis of intracellular ice formation during freezing of mouse oocytes without cryoadditives. *Cryobiology* **28**(1), 55-71

Tucker, M., & Liebermann, J (2007) 'Vitrification in Assisted Reproduction: A User's Manual and Trouble-shooting Guide (1st ed.).' (CRC Press)

Vajta, G., Holm, P., Kuwayama, M., Booth, P.J., Jacobsen, H., Greve, T., and Callesen, H. (1998) Open Pulled Straw (OPS) vitrification: a new way to reduce cryoinjuries of bovine ova and embryos. *Mol Reprod Dev* **51**(1), 53-8

Vajta, G., and Kuwayama, M. (2006) Improving cryopreservation systems. *Theriogenology* **65**(1), 236-44

Vanderzwalmen, P., Connan, D., Grobet, L., Wirleitner, B., Remy, B., Vanderzwalmen, S., Zech, N., and Ectors, F.J. (2013) Lower intracellular concentration of cryoprotectants after vitrification

than after slow freezing despite exposure to higher concentration of cryoprotectant solutions. *Hum Reprod* **28**(8), 2101-10

Vanderzwalmen, P., Ectors, F., Grobet, L., Prapas, Y., Panagiotidis, Y., Vanderzwalmen, S., Stecher, A., Frias, P., Liebermann, J., and Zech, N.H. (2009) Aseptic vitrification of blastocysts from infertile patients, egg donors and after IVM. *Reprod Biomed Online* **19**(5), 700-7

Vanderzwalmen, P., Ectors, F., Panagiotidis, Y., Schuff, M., Murtinger, M., and Wirleitner, B. (2020) The Evolution of the Cryopreservation Techniques in Reproductive Medicine—Exploring the Character of the Vitrified State Intra- and Extracellularly to Better Understand Cell Survival after Cryopreservation. *Reproductive Medicine* **1**(2), 142-157

Vanderzwalmen, P., Zech, N.H., Ectors, F., Stecher, A., Lejeune, B., Vanderzwalmen, S., and Wirleitner, B. (2012) Blastocyst transfer after aseptic vitrification of zygotes: an approach to overcome an impaired uterine environment. *Reprod Biomed Online* **25**(6), 591-9

Varghese, A.C., Nagy, Z.P., and Agarwal, A. (2009) Current trends, biological foundations and future prospects of oocyte and embryo cryopreservation. *Reprod Biomed Online* **19**(1), 126-40

Vieira, A.D., Forell, F., Feltrin, C., and Rodrigues, J.L. (2008) Calves born after direct transfer of vitrified bovine *in vitro*-produced blastocysts derived from vitrified immature oocytes. *Reprod Domest Anim* **43**(3), 314-8

Vincent, C., Garnier, V., Heyman, Y., and Renard, J.P. (1989) Solvent effects on cytoskeletal organization and in-vivo survival after freezing of rabbit oocytes. *J Reprod Fertil* **87**(2), 809-20

Vincent, C., and Johnson, M.H. (1992) Cooling, cryoprotectants, and the cytoskeleton of the mammalian oocyte. *Oxf Rev Reprod Biol* **14**, 73-100

Vincent, C., Pickering, S.J., Johnson, M.H., and Quick, S.J. (1990) Dimethylsulphoxide affects the organisation of microfilaments in the mouse oocyte. *Mol Reprod Dev* **26**(3), 227-35

Wang, W.H., Meng, L., Hackett, R.J., Odenbourg, R., and Keefe, D.L. (2001a) Limited recovery of meiotic spindles in living human oocytes after cooling-rewarming observed using polarized light microscopy. *Hum Reprod* **16**(11), 2374-8

Wang, W.H., Meng, L., Hackett, R.J., Odenbourg, R., and Keefe, D.L. (2001b) The spindle observation and its relationship with fertilization after intracytoplasmic sperm injection in living human oocytes. *Fertil Steril* **75**(2), 348-53

Weng, L., Ellett, F., Edd, J., Wong, K.H.K., Uygun, K., Irimia, D., Stott, S.L., and Toner, M. (2017) A highly-occupied, single-cell trapping microarray for determination of cell membrane permeability. *Lab Chip* **17**(23), 4077-4088

Westh, P. (2003) Unilamellar DMPC vesicles in aqueous glycerol: preferential interactions and thermochemistry. *Biophys J* **84**(1), 341-9

Westh, P. (2004) Preferential interaction of dimethyl sulfoxide and phosphatidyl choline membranes. *Biochimica et Biophysica Acta (BBA) - Biomembranes* **1664**(2), 217-223

Wolfe, J., and Bryant, G. (1999) Freezing, drying, and/or vitrification of membrane- solute-water systems. *Cryobiology* **39**(2), 103-29

Wolfe, J., and Bryant, G. (2001) Cellular cryobiology: thermodynamic and mechanical effects. *International Journal of Refrigeration-revue Internationale Du Froid* **24**, 438-450

Wolkers, W., and Oldenhof, H. (2015) 'Cryopreservation and Freeze-Drying Protocols.'

Woods, E.J., Benson, J.D., Agca, Y., and Critser, J.K. (2004) Fundamental cryobiology of reproductive cells and tissues. *Cryobiology* **48**(2), 146-56

Wu, C., Rui, R., Dai, J., Zhang, C., Ju, S., Xie, B., Lu, X., and Zheng, X. (2006) Effects of cryopreservation on the developmental competence, ultrastructure and cytoskeletal structure of porcine oocytes. *Mol Reprod Dev* **73**(11), 1454-62

Wusteman, M.C., Pegg, D.E., Robinson, M.P., Wang, L.H., and Fitch, P. (2002) Vitrification media: toxicity, permeability, and dielectric properties. *Cryobiology* **44**(1), 24-37

Yamaji, Y., Seki, S., Matsukawa, K., Koshimoto, C., Kasai, M., and Edashige, K. (2011) Developmental ability of vitrified mouse oocytes expressing water channels. *J Reprod Dev* **57**(3), 403-8

Yavin, S., and Arav, A. (2007) Measurement of essential physical properties of vitrification solutions. *Theriogenology* **67**(1), 81-89

Zachariassen, K.E., and Kristiansen, E. (2000) Ice nucleation and antinucleation in nature. *Cryobiology* **41**(4), 257-79

Zachariassen, K.E., Kristiansen, E., Pedersen, S.A., and Hammel, H.T. (2004) Ice nucleation in solutions and freeze-avoiding insects-homogeneous or heterogeneous? *Cryobiology* **48**(3), 309-21

Zander-Fox, D., Cashman, K.S., and Lane, M. (2013) The presence of 1 mM glycine in vitrification solutions protects oocyte mitochondrial homeostasis and improves blastocyst development. *J Assist Reprod Genet* **30**(1), 107-16

Zenzes, M.T., Bielecki, R., Casper, R.F., and Leibo, S.P. (2001) Effects of chilling to 0 degrees C on the morphology of meiotic spindles in human metaphase II oocytes. *Fertil Steril* **75**(4), 769-77

Zhou, D., Shen, X., Gu, Y., Zhang, N., Li, T., Wu, X., and Lei, L. (2014) Effects of dimethyl sulfoxide on asymmetric division and cytokinesis in mouse oocytes. *BMC Developmental Biology* **14**, 28-28

Zhou, E.H., Trepat, X., Park, C.Y., Lenormand, G., Oliver, M.N., Mijailovich, S.M., Hardin, C., Weitz, D.A., Butler, J.P., and Fredberg, J.J. (2009) Universal behavior of the osmotically compressed cell and its analogy to the colloidal glass transition. *Proc Natl Acad Sci U S A* **106**(26), 10632-7

Zhou, G.B., and Li, N. (2009) Cryopreservation of porcine oocytes: recent advances. *Mol Hum Reprod* **15**(5), 279-85

Zhou, J., Shu, H.B., and Joshi, H.C. (2002) Regulation of tubulin synthesis and cell cycle progression in mammalian cells by gamma-tubulin-mediated microtubule nucleation. *J Cell Biochem* **84**(3), 472-83

Zhou, X.L., Al Naib, A., Sun, D.W., and Lonergan, P. (2010) Bovine oocyte vitrification using the Cryotop method: effect of cumulus cells and vitrification protocol on survival and subsequent development. *Cryobiology* **61**(1), 66-72

Hypothesis and objectives

1. Hypothesis

Successful vitrification of mammalian cells requires rapid transport of water and cryoprotectants across the plasma membrane. A more detailed understanding of the mechanisms necessary to rapidly move water and cryoprotectants across the plasma membrane of bovine oocytes is needed to help decrease osmotic stress and to minimize chilling injury. The development of a theoretical approach to determine the permeability of bovine oocytes to water and CPAs, towards the establishment of an optimal thermodynamic pathway, may be useful for developing suitable protocols for vitrification of bovine oocytes. In this way, the estimated permeability parameters could be used to predict CPA loading and dilution procedures that would minimize the exposure time to CPAs while limiting deleterious cell volume perturbations. Besides, artificially overexpression of aquaglyceroporins through cRNA injection may increase the permeability in bovine *in vitro* matured oocytes by facilitating water and CPA movement though their plasma membrane.

2. Objectives

To accomplish this general hypothesis, the following specific objectives have been addressed:

Objective 1: To assess the potential inaccuracies of typical modeling approaches used for oocytes by examining the concentration-dependent permeability characteristics for bovine immature (GV) oocytes and *in vitro* matured (MII) oocytes in the presence of increasing EG or Me_2SO concentrations, and compare the two different mathematical approaches for mass transport modeling.

Objective 2: To examine the expression of aquaglyceroporins AQP3, AQP7 and AQP9 after exposure of *in vitro* matured bovine oocytes to hyperosmotic CPA solutions and the role of AQP7 in the movement of water and CPAs when AQP7 was artificially overexpressed through cRNA injection.

Objective 3: To compare the osmotic tolerance of *in vitro* matured bovine oocytes in the presence of the equilibration solution at different temperatures (25°C *vs* 38.5°C) as a first step toward developing optimal cryopreservation method and compare the effect of the use of the optimized cell-specific step-wise adding and diluting protocol on oocyte spindle configuration, apoptosis index and further embryo development

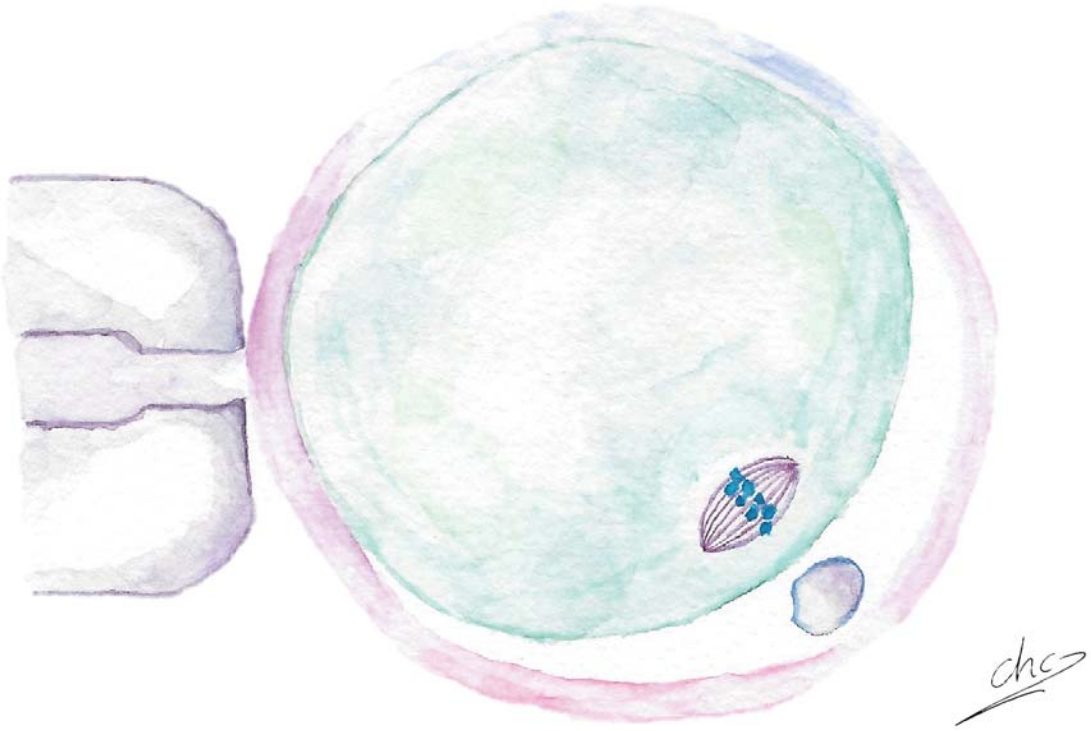

Chapter 1

Effect of cryoprotectant concentration on bovine oocyte permeability and comparison of two membrane permeability modelling approaches

Accepted in Scientific Reports July 2021

ABSTRACT

The plasma membrane permeability to water and cryoprotectant (CPA) significantly impacts vitrification efficiency of bovine oocytes. Our study was designed to determine the concentration-dependent permeability characteristics for immature (GV) and mature (MII) bovine oocytes in the presence of ethylene glycol (EG) and dimethyl sulphoxide (Me_2SO), and to compare two different modeling approaches: the two parameter (2P) model and a nondilute transport model. Membrane permeability parameters were determined by consecutively exposing oocytes to increasing concentrations of Me_2SO or EG. Higher water permeability was observed for MII oocytes than GV oocytes in the presence of both Me_2SO and EG, and in all cases the water permeability was observed to decrease as CPA concentration increased. At high CPA concentrations, the CPA permeability was similar for Me_2SO and EG, for both MII and GV oocytes, but at low concentrations the EG permeability of GV oocytes was substantially higher. Predictions of cell volume changes during CPA addition and removal indicate that accounting for the concentration dependence of permeability only has a modest effect, but there were substantial differences between the 2P model and the nondilute model during CPA removal, which may have implications for design of improved methods for bovine oocyte vitrification.

1. Introduction

Over the last few decades, simultaneously with the development of assisted reproductive technologies, gamete and embryo cryopreservation procedures have advanced rapidly. These technologies have made a significant impact on the progress of genetic improvement in livestock, the worldwide distribution of germplasm and conservation of endangered species (Holt 2008). However, despite many offspring of various species being produced after the application of these technologies, there still remain shortcomings with methods used to cryopreserve oocytes (Ambrosini *et al.* 2006; Wang *et al.* 2010). The reason for oocytes susceptibility to low temperatures is due to their sensitivity at different cellular levels, such as the zona pellucida, plasma membrane, meiotic spindles and cytoskeleton (see review (Mogas 2018)). These subcellular structures change during maturation, which means that the developmental stage of the oocyte affects its cryobiological properties (Díez *et al.* 2012). In addition, oocytes at different developmental stages have been shown to have different osmotic responses in the presence and absence of CPA (Ruffing *et al.* 1993; Agca *et al.* 1998).

Vitrification has been proven to be more efficient and reliable than slow freezing for bovine oocyte cryopreservation because it resolves two of the main reasons for oocyte damage during slow freezing: chilling injury (by using high cooling and warming rates (typically

>>100°C/min)), and lethal ice crystal formation (by using high CPA concentrations (typically > 5 mol/L)) (Vajta *et al.* 1998; Papis *et al.* 2000; Arav *et al.* 2002; Chian *et al.* 2004). CPAs have been demonstrated to dramatically suppress the freezing injuries suffered by cells. They promote the formation of a non-crystalline glassy state by increasing the viscosity of extra- and intracellular solutions and by interacting directly with water, which reduces ice nucleation and growth. CPAs are also beneficial by stabilizing the plasma membrane and reducing the harmful concentrated electrolytes through permeating into the cells (Karlsson and Toner 1996). However, there is a cost associated with their use as they dramatically increase the risk of damage due to osmotic stresses or death due to chemical toxicity (Agca *et al.* 2000; Lawson *et al.* 2011).

The process of adding and removing CPAs subjects the cells to an imbalanced osmotic pressure between the intra- and extracellular solutions. CPA addition results in cell shrinkage when water exits in response to the increased extracellular osmolality, and then re-swelling as the CPA and water permeate the cell returning the cell to isotonic volume. During CPA removal, the cell first swells to greater than isotonic volume as water moves into the cell and then returns to isotonic volume as CPA and water exit the cell (Levin and Miller 1981). These responses, if large enough, may drive the cell beyond critical volumes known as osmotic tolerance limits, outside of which irreversible cell damage occurs (Mullen *et al.* 2004; Woods *et al.* 2004). Typically, the use of stepwise addition and removal procedures can reduce concentration gradients enough to alleviate osmotic damage (Mullen *et al.* 2008).

It has been demonstrated that CPA toxicity is dependent on many factors including the CPA type, time of exposure to CPA, CPA concentration, and temperature (Fahy *et al.* 1990; Elmoazzen *et al.* 2002; Wusteman *et al.* 2002; Fahy *et al.* 2004). The development of optimal cryopreservation protocols requires accounting for all interdependent factors. This makes rigorous experimental optimization impractical, as it would require a very large number of experiments. Therefore, it is desirable to combine empirical and theoretical knowledge through the use of mathematical modeling to simplify experimental optimization (Leibo 2008). Frequently, the mathematical approaches rely on predictions of mass transfer across the cell membrane, which require an understanding of the cell membrane permeability to water (Lp) and CPA (Ps). Permeability parameters allow calculation of cellular osmotic responses during the addition and removal of CPA, and can provide evidence for whether water and solute movement occurs through channels or by simple diffusion through the lipid bilayer (Kleinhans 1998). Recently, it has been shown that the permeability of the erythrocyte cell membrane to water and CPA is dependent on concentration (Lahmann *et al.* 2018), contrary to what previous studies have assumed (Armitage 1986).

Historically, the two-parameter formalism (2P model) has been used to model membrane transport (Jacobs and Stewart 1932; Jacobs 1933). This model makes limiting dilute-solution assumptions. The assumption of a dilute and ideal solution is often acceptable under physiological conditions, but its accuracy is questionable in most cryobiological cases where CPAs are often used at high concentrations. In 2009, Elmoazzen et al (Elmoazzen *et al.* 2009) developed a new nondilute solution model, which is comparatively more complex than the 2P model, but potentially more accurate.

The present study was designed to assess the potential inaccuracies of typical modeling approaches used for oocytes by examining concentration-dependent permeability characteristics for GV and MII bovine oocytes in the presence of EG or Me_2SO, and comparing the two different mathematical approaches to mass transport modeling. To compare these different modeling approaches, we used the permeability parameters determined from the experiments to model cell volume excursions for the CPA addition and removal process used in the Kuwayama protocol (Kuwayama *et al.* 2005), which was designed for vitrification of bovine and human oocytes.

2. Material and method

2.1. Reagents

Unless otherwise specified, all chemicals and reagents were purchased from Sigma Chemical Co (St. Louis, MO, USA).

2.2. Oocyte collection and *in vitro* maturation

The *in vitro* maturation (IVM) procedure followed has been described previously (García-Martínez *et al.* 2020). Briefly, ovaries from slaughtered postpubertal heifers (12-18 months old) were transported from a local slaughterhouse to the laboratory in saline solution (0.9% NaCl) at 35-37ºC within 2h. Immature cumulus-oocyte complexes (COCs) were aspirated from 3–8 mm follicles using an 18-gauge needle attached to a 5 mL syringe. COCs with more than three layers of cumulus cells and a homogeneous cytoplasm were selected and washed three times in modified Dulbecco's PBS (PBS supplemented with 36 μg/mL pyruvate, 50 μg/mL gentamicin and 0.5 mg/mL bovine serum albumin). Groups of 40-50 COCs were placed in 500 μL of maturation medium covered with mineral oil in four-well plate and cultured for 24 h at 38.5°C in a 5% CO_2 humidified air atmosphere. The maturation medium (IVM medium) was tissue culture medium (TCM-199) supplemented with 10% (v/v) fetal bovine serum (FBS), 10 ng/mL epidermal growth factor and 50 μg/mL gentamicin.

2.3. Measurement of oocyte volumetric changes following increasing CPA exposure

GV bovine oocytes at time 0h or MII bovine oocytes after 24h of IVM were denuded of cumulus cells by gentle pipetting. Only GV showing a normal appearance and metaphase II oocytes with a normal appearance and a visible first polar body were used. An oocyte was placed in a 25 μl drop of holding medium (HM: TCM199-Hepes supplemented with 20% (v/v) FBS) covered with mineral oil, and was held with a holding pipette (outer diameter, 95-120 μm; MPH-MED-30, Origio, Denmark) connected to a micromanipulator on an inverted microscope (Zeiss Axio Vert A1, Germany). An initial photograph was taken of the oocyte in order to calculate the initial volume. The oocyte was then covered with another pipette with a larger inner diameter (600-μm diameter) (G-1 Narishigue, Tokyo, Japan) connected to a different micromanipulator. Then, by sliding the dish the oocyte was exposed consecutively to 25 μl drops containing increasing CPA concentrations at 25°C, as illustrated in Figure 1. Each oocyte was exposed consecutively to CPA concentrations of 0.30 mol/L, 0.68 mol/L, 1.55 mol/L, and 3.5 mol/L. These concentrations were chosen because they are expected to generate similar cell volume changes for each change in CPA concentration. In addition, the gradual increase in CPA concentration prevents excessive shrinkage which may result in osmotic damage. For the exposure times at each concentration it was considered the time needed for the oocyte to recover the isotonic cell volume and was set at 5 min for EG and 7 min for Me_2SO. CPA solutions consisted of EG or Me_2SO diluted in HM. The cell volume response of the oocyte during the experiments was recorded every 3.5 sec with a time-lapse video recorder (Zeiss Zen imaging software/Axiocam ERc 5s). The volume of the oocyte in each image was calculated from the area of the cross section using ImageJ software. Only those immature oocytes (EG: n=6; Me_2SO: n=5) and mature oocytes (EG: n=5; Me_2SO: n=7) that remained spherical on shrinkage were individually analyzed and used for calculation of permeability coefficients, with several oocytes in each group being discarded.

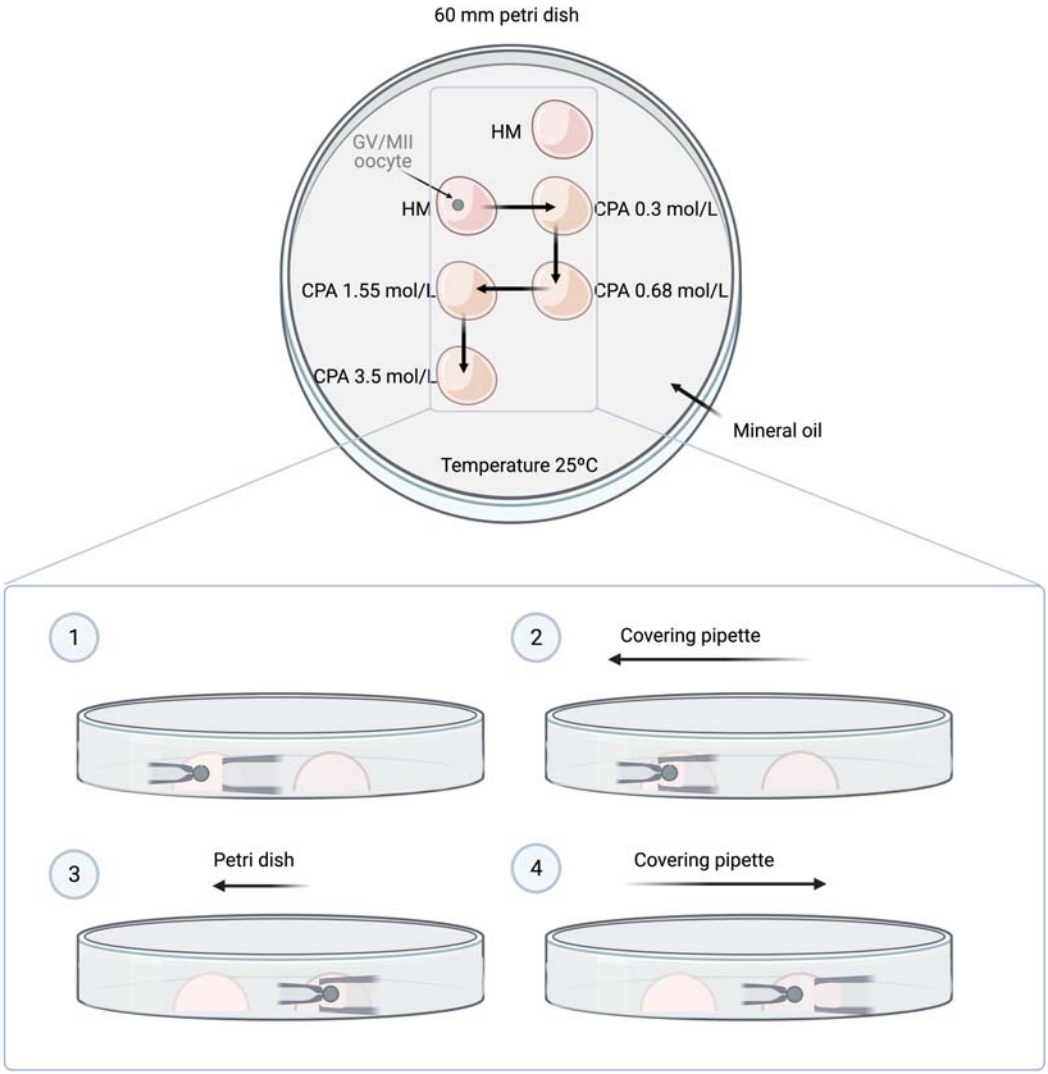

Figure 1. Schematic representation of the device and the procedure for direct transfer of GV or MII oocytes (solid circle) to an increasing CPA exposure (right hemisphere) from isotonic holding medium (left hemisphere) using a micromanipulator system.

2.4. Membrane transport models

2.4.1. Dilute solution model (two-parameter transport formalism)

The 2P model, which has its roots in work by Jacobs and Stewart (Jacobs and Stewart 1932; Jacobs 1933), provides a description of the osmotic responses of cells in solutions with both permeating and nonpermeating solutes. In this formalism, the water flux into the cell over time is expressed as:

$$\frac{dV_w}{dt} = -L_p ART(M^e - M^i) \quad (1)$$

where V_w is the cell water volume, L_p is the membrane hydraulic conductivity, A is the area of the plasma membrane, R is the universal gas constant, T is the absolute temperature, and M^e and M^i are the total external and internal osmolalities, respectively.

The rate of CPA transport is given by:

$$\frac{dN_s}{dt} = P_s A(M_s^e - M_s^i) \quad (2)$$

where N_s is the intracellular moles of CPA, P_s is the CPA permeability, M^i_s and M^e_s are the intracellular and extracellular CPA molality, respectively. To obtain the intracellular CPA volume, it is necessary to multiply by the partial molar volume of the CPA, υ_s, resulting in

$$V_s = \upsilon_s N_s \quad (3)$$

Then the total cell volume (V_c) is just the sum of the water (V_w), CPA (V_s), and solids (V_b) volumes:

$$V_c = V_w + V_s + V_b \quad (4)$$

2.4.2. Nondilute solution model

Elmoazzen et al (Elmoazzen *et al.* 2009) developed the nondilute solution model. The transport equations are based on the principle that the mass transfer is driven by the difference between the extra- and intracellular chemical potentials. This model was developed on the assumption that the extracellular solution contains water, permeating CPA and a nonpermeating solute (NaCl), while the intracellular environment contains water, a permeating CPA, and another nonpermeating solute (KCl). The changes in the moles of intracellular water and CPA as a function of time take the following forms:

$$\frac{dN_w^i}{dt} = -LART\left[(x_{CPA}^e + x_{NaCl}^e) + B_{CPA}^+(x_{CPA}^e) + B_{NaCl}^+(x_{NaCl}^e) + (B_{CPA}^+ + B_{NaCl}^+)x_{CPA}^e x_{NaCl}^e - \left(x_{CPA}^i + x_{KCl}^i\right) - B_{CPA}^+\left(x_{CPA}^i\right) - B_{KCl}^+\left(x_{KCl}^i\right) - (B_{CPA}^+ + B_{KCl}^+)x_{CPA}^i x_{KCl}^i\right] \quad (5)$$

$$\frac{dN_{CPA}^i}{dt} = PART\left[ln(x_{CPA}^e) + \left(\frac{1}{2} - B_{CPA}^+\right)(1 - x_{CPA}^e - x_{NaCl}^e)(1 - x_{CPA}^e) - \left(\frac{1}{2} - B_{NaCl}^+\right)(1 - x_{CPA}^e - x_{NaCl}^e)x_{NaCl}^e - ln\left(x_{CPA}^i\right) - \left(\frac{1}{2} - B_{CPA}^+\right)\left(1 - x_{CPA}^i - x_{KCl}^i\right)\left(1 - x_{CPA}^i\right) + \left(\frac{1}{2} - B_{KCl}^+\right)\left(1 - x_{CPA}^i - x_{KCl}^i\right)x_{KCl}^i\right] \quad (6)$$

2.5. Estimation of cell membrane permeability parameters

A randomized block design was used for this experiment, with the oocyte being the blocking factor (Kempthorne 1958). Each oocyte was used in the entire series of solutions for a single CPA. In other words, an oocyte was used to estimate the permeability of the CPA at each concentration, but for only one of the two CPAs. Volumetric data for each oocyte at each concentration was assessed as described and the first 3 minutes were fitted to the 2P and nondilute solution models to determine the water permeability (L_p and L, respectively) and CPA permeability (P_{CPA} and P, respectively). This was performed for both GV and MII oocytes. The differential equations (equations (1) and (2) for the 2P model; equations (5) and (6) for the nondilute solution model) were solved in Matlab software using the ode45 function, which implements an explicit Runge-Kutta formula (Dormand and Prince 1980; Shampine and Reichelt 1997). To estimate the permeability values, model predictions were fit to the data by minimizing the sum of the error squared in Matlab using the fminsearch function, which implements the Nelder-Mead simplex algorithm (Lagarias *et al.* 1998). For the first CPA concentration, the initial state was assumed to be the normal physiological state for oocytes in equilibrium with isotonic solution. For subsequent CPA concentrations, the initial state was assumed to be equal to the final state from model predictions for the previous CPA concentration. The concentrations used in these experiments are given in Table 1 in units of molarity, molality and mole fraction. The constants used for model predictions are given in Table 2.

Table 1. CPA concentration.

CPA	Molarity (M)	Molality (m)	Mole fraction (X^e_{CPA})
EG	0.3	0.31	0.06
	0.68	0.71	0.013
	1.55	1.7	0.030
	3.5	4.36	0.074
Me_2SO	0.3	0.3	0.06
	0.68	0.71	0.013
	1.55	1.74	0.031
	3.5	4.64	0.078

Abbreviations: CPA, cryoprotectant; EG, ethylene glycol; Me_2SO, dimethyl sulfoxide.

Table 2. Constant and parameters used in 2P model and nondilute solution model.

Description	Values	Symbol
Universal gas constant		
– 2P model:	8.314 m^3 Pa K^{-1} mol^{-1}	R
– Nondilute model:	8.206×10^{13} μm^3 atm mol^{-1} K^{-1}	
Absolute temperature	298 K	T
Partial molar volume of water	18.02 $x10^{12}\mu m^3 mol^{-1}$	υ_w
Partial molar volume of CPA:		
– EG [a]	55.8×10^{-6} m^3 mol^{-1}	υ_{CPA}
– Me_2SO [a]	71.3×10^{-6} m^3 mol^{-1}	
Osmotically inactive volume:		
– GV	0.16 (Ruffing *et al.* 1993; Wang *et al.* 2010)	V_b
– MII	0.25 (Ruffing *et al.* 1993; Jin *et al.* 2011)	
Second osmotic virial coefficient for CPA (in terms of mole fraction):	3.41	
– EG [b]	2.35	B^+_{CPA}
– Me_2SO [b]	8.68	
– Sucrose [b]		
Second osmotic virial coefficient for NaCl (in terms of mole fraction) [b]	3.80	B^+_{NaCl}
(Dissociation constant) [b]	1.644	
Second osmotic virial coefficient for KCl (in terms of mole fraction) [b]	0	B^+_{KCl}
(Dissociation constant) [b]	1.818	
Extracellular salt (NaCl) mole fraction	0.003	x^e_{NaCl}
Extracellular salt (KCl) mole fraction	0.0030	x^i_{KCl}

[a] Partial molar volumes of cryoprotectants from Vian et al (Vian and Higgins 2014).

[b] Second osmotic virial coefficient and dissociation constants from Zielinski et al (Zielinski *et al.* 2014). Abbreviations: CPA, cryoprotectant; EG, ethylene glycol; Me_2SO, dimethyl sulfoxide; GV, germinal vesicle; MII, metaphase II

To characterize the effects of CPA concentration, the permeability data was fit to the following concentration-dependent permeability models (Lahmann *et al.* 2018)

$$L_p = \frac{a}{bM_s + 1} \tag{7}$$

$$P_s = \frac{a}{bM_s + 1} \tag{8}$$

$$L = \frac{a}{bM_s + 1} \tag{9}$$

$$\frac{P}{M_s} = \frac{a}{bM_s + 1} \tag{10}$$

where a and b are best-fit constants. In equation (10), we use the ratio of the non-dilute model permeability coefficient P to the CPA molality M_s, for the reasons described in Elmoazzen et al (Elmoazzen *et al.* 2009). In particular, Elmoazzen et al (Elmoazzen *et al.* 2009) show that the nondilute model reduces to the 2P model under dilute conditions, where the parameter ratio P/M_{CPA} is proportional to the 2P model permeability P_{CPA}.

2.6. Prediction of cell volume changes during bovine oocyte vitrification

The following Kuwayama protocol (Kuwayama *et al.* 2005) for CPA addition and removal for vitrification of oocytes was used to predict the response of oocytes and compare different modeling approaches:

Two steps for loading CPA:

Step 1. 10 min in 1.6 mol/L EG in TCM199 medium at 22°C.

Step 2. 30 s in vitrification solution (6.8 mol/L EG + 1.0 mol/L sucrose in TCM199 medium).

Three steps for removal CPA:

Step 1. 1 min in 1.0 mol/L of sucrose in TCM199 medium at 37°C.

Step 2. 3 min in diluent solution (0.5 mol/L sucrose in TCM199 medium)

Step 3. 10 min in TCM199 medium (no CPA).

We compared volume excursion predictions during CPA addition and removal using four different modeling approaches:

1. Dilute (2P) model with constant water and CPA permeability.

2. Dilute (2P) model with water and CPA permeability changed with CPA concentration according to equations (7) and (8).

3. Nondilute model with constant water and CPA permeability.

4. Nondilute model with water and CPA permeability changed with CPA concentration according to equations (9) and (10).

Predictions for the CPA addition and removal process following these 4 conditions were carried out by numerically solving the model equations in Matlab as described above. To obtain predictions with constant permeability values, we used the permeability to water and EG obtained at 1.55 mol/L. This represents a baseline case that is consistent with the typical approach of estimating permeability for exposure to 1-2 mol/L CPA. To make predictions using concentration dependent permeability values, we used a different approach during CPA addition and removal. For CPA addition, we used the external CPA concentration in equations (7-10) to estimate the permeability values. For CPA removal, we used the intracellular CPA concentration to estimate the permeability values.

In order to simulate the cell volume response of the vitrification and warming Kuwayama's protocol, information on the isotonic cell volume of bovine oocytes at different developmental stages is required. The mean cell volumes for GV and MII bovine oocytes in isotonic medium were 8.17×10^5 and 7.40×10^5 μm^3, respectively; accordingly, the surface area was 4.22×10^4 and 3.95×10^4 μm^2.

2.7. Statistical analysis

Statistical tests were performed using the statistical package R, Version R 3.4.4. The normality of data distribution was checked using the Shapiro–Wilk test and homogeneity of variances through the Levene test. When required, data were linearly transformed into $\sqrt{x}$, arcsin $\sqrt{x}$ or log(x) prior to running statistical tests. An one-way analysis of variance (ANOVA) followed by a pairwise comparison test (Tukey-Kramer adjustment) was used to assess differences molarities within the same CPA and nuclear stage and differences in water or solute permeability between GV and MII stage within the same CPA. Significance was set at $p \leq 0.05$.

3. Results

3.1. Permeability parameters estimation

To determine concentration-dependent permeability characteristics for GV and MII bovine oocytes, cells were sequentially exposed to a series of increasing CPA concentrations, as

illustrated in Figure 2. When cells were transferred from an isotonic solution into a hypertonic CPA solution they immediately dehydrated and shrank in response to the higher solution osmolality, and then slowly re-gained iso-osmotic volume as the solute and water permeated the cell to maintain osmotic equilibrium with the extracellular medium. The rate of this shrink-swell response is a measure of the permeability of the cell membrane to the solute and water (Wang *et al.* 2010). As shown in Figure 2, model predictions are in good agreement with the experimental cell volume measurements.

We first examined the potential differences in permeability values between GV and MII oocytes for exposure to EG and Me_2SO. The resulting best-fit water and CPA permeability values from the 2P model are shown in Figure 3 and Table 3. Overall, the water permeability was about two-fold higher for MII oocytes than GV oocytes. This was true for the water permeability in the presence of both Me_2SO and EG, and the effect was statistically significant ($p < 0.05$). The CPA permeability was similar for Me_2SO and EG, for both MII and GV oocytes, with the exception of the EG permeability for GV oocytes, which was substantially higher at low EG concentrations.

We next examined the potential effects of CPA concentration on the permeability values. Results indicate that CPA concentration had a statistically significant effect on the water permeability in all cases ($p < 0.05$), and, in general, the water permeability decreased by about a factor of two as the CPA concentration increased from 0.3 mol/L to 3.5 mol/L (Table 3).

Only GV oocytes exposed to EG exhibited a continuous decrease in CPA permeability with increasing CPA concentration (Table 3). In this case, the effect of CPA concentration was statistically significant ($p = 0.002$), and the CPA permeability decreased by more than 3-fold from 1.31 μm/s at 0.3 mol/L EG to 0.35 μm/s at 3.5 mol/L EG. The effect of CPA concentration was also significant for MII oocytes exposed to Me_2SO ($p = 0.014$), but in this case, the CPA permeability did not exhibit a clear trend: the lowest permeability was 0.38 μm/s at 0.68 mol/L and the highest was 0.68 μm/s at 1.55 mol/L.

We also fit the data to the non-dilute model and analyzed the resulting best-fit permeability parameters. As shown in Figure 4 and Table 4, the trends for the non-dilute model were nearly identical to those observed for the 2P model. Similar to the water permeability from the 2P model, the best-fit water permeability values from the non-dilute model decreased by a more than a factor of two as the CPA concentration increased from 0.3 mol/L to 3.5 mol/L, and the effect of CPA concentration on the water permeability was statistically significant in all cases ($p < 0.004$). For the non-dilute model, only the CPA permeability parameter for GV oocytes

exposed to EG showed a continuous decrease with increasing concentration, which is consistent with the results for the 2P model. However, there was an even more substantial decrease in the CPA permeability parameter for the non-dilute model, which yielded a CPA permeability parameter at 3.5 mol/L that was about six times lower than the permeability parameter at 0.3 mol/L. Only the oocytes at the GV stage exposed to Me_2SO showed apparent constant permeability to that cryoprotectant across all concentrations. The oocytes in the other categories did exhibit apparent changes to CPA permeability between different concentrations, but the trend was not consistent.

To account for the effects of CPA concentration on water and CPA permeability, we fit the permeability data to a concentration-dependent model (Lahmann *et al.* 2018). This model is consistent with a transport mechanism that is limited by binding of CPA to a transporter protein such as an aquaporin. The resulting model fits are shown as lines in Figures 2 and 3, and the best-fit equations are provided in Tables 1 and 2. The concentration dependent model fits are in reasonable agreement with the permeability data.

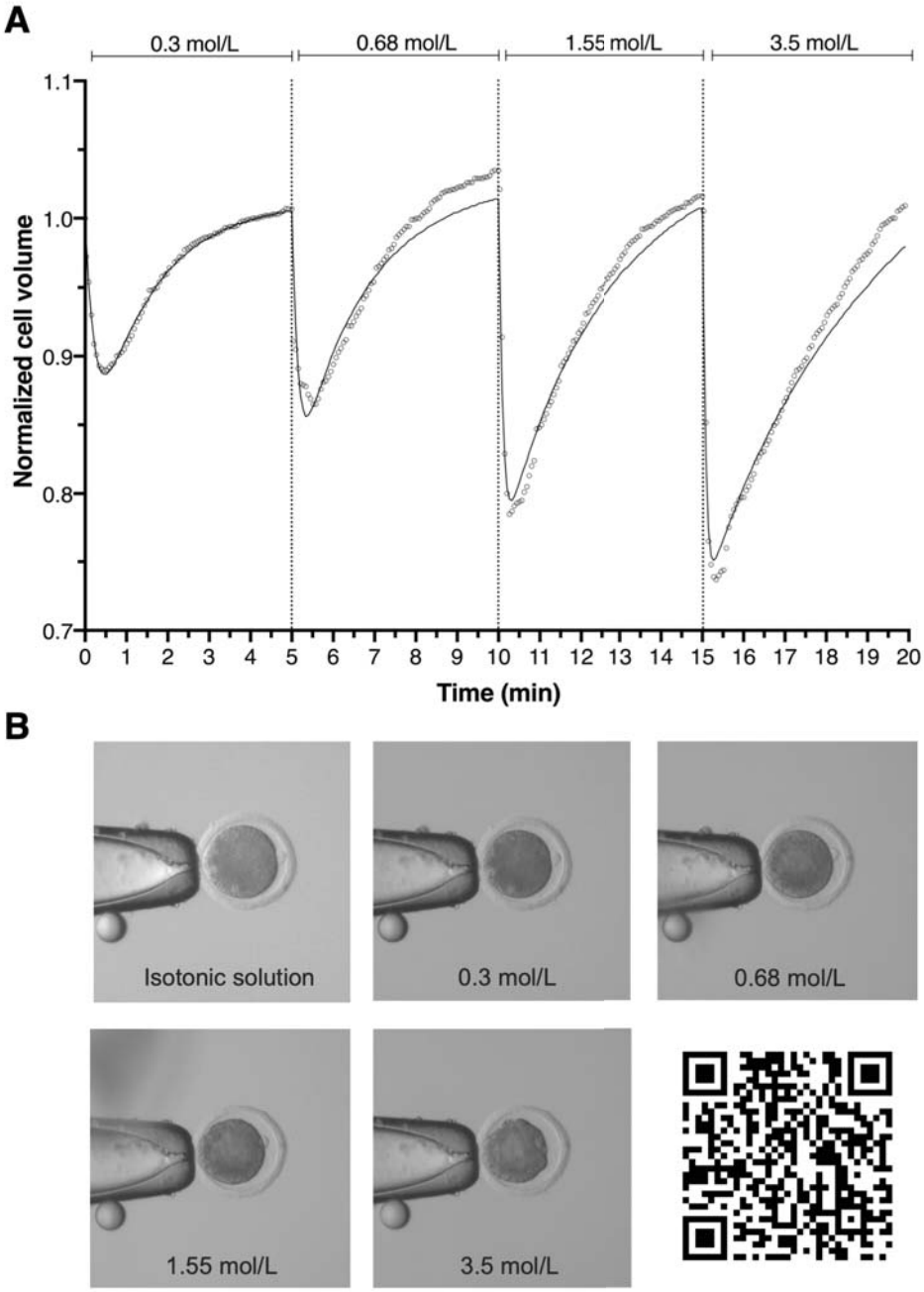

Figure 2. A representative sequence of the osmotic responses of MII bovine oocytes after exposure to increasing EG concentrations (0.3, 0.68, 1.55 and 3.5 mol/L). A) The normalized cell volume data (open circle) and their corresponding theoretical fitting curves (solid line) obtained with the 2P model. Exposure to 0.3 mol/L EG starts at t = 0, and the change every 5 min to subsequent increasing EG concentrations is demarcated in the X-axis with a vertical dotted line. B) An example of the oocyte's morphology at relevant timeframes (at the minimal volume) is shown below each graphic (magnification 20x). Note shrinkage in response to increasing EG concentration. QR code links to a representative video time-lapse for an MII oocyte exposed to increasing EG concentrations.

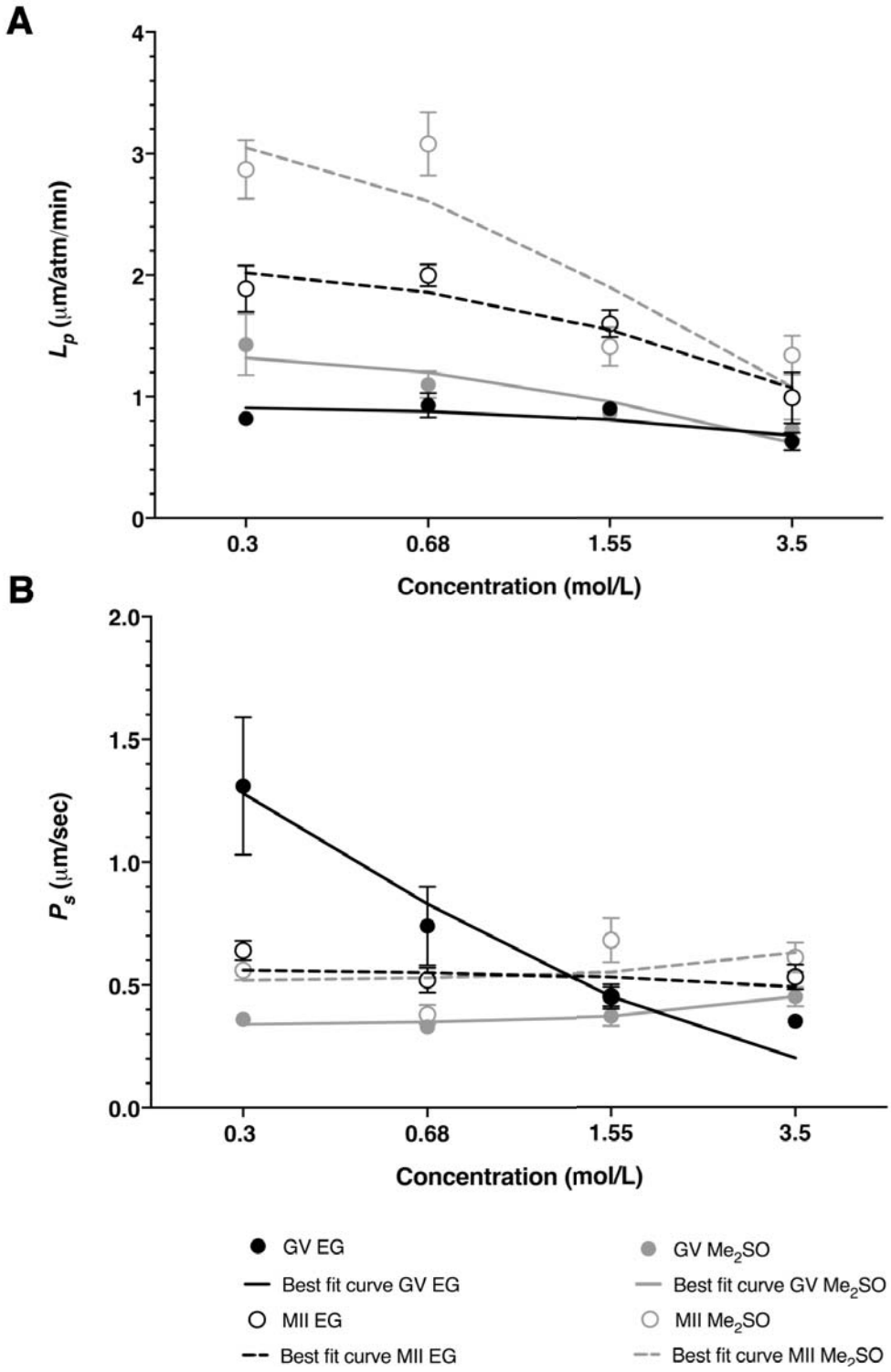

Figure 3. Water permeability and solute permeability GV (closed circles) and MII (open circles) oocytes in the presence of increasing concentration of CPA (EG (black) or Me_2SO (gray)) for the 2P model (a and b, respectively). Best-fit curve for the concentration dependent model represented by a solid black line (GV EG), dotted black line (MII EG), solid gray line (GV Me_2SO) and dotted gray line (MII Me_2SO). Unless indicated otherwise, data are given as the mean ± s.e.m.

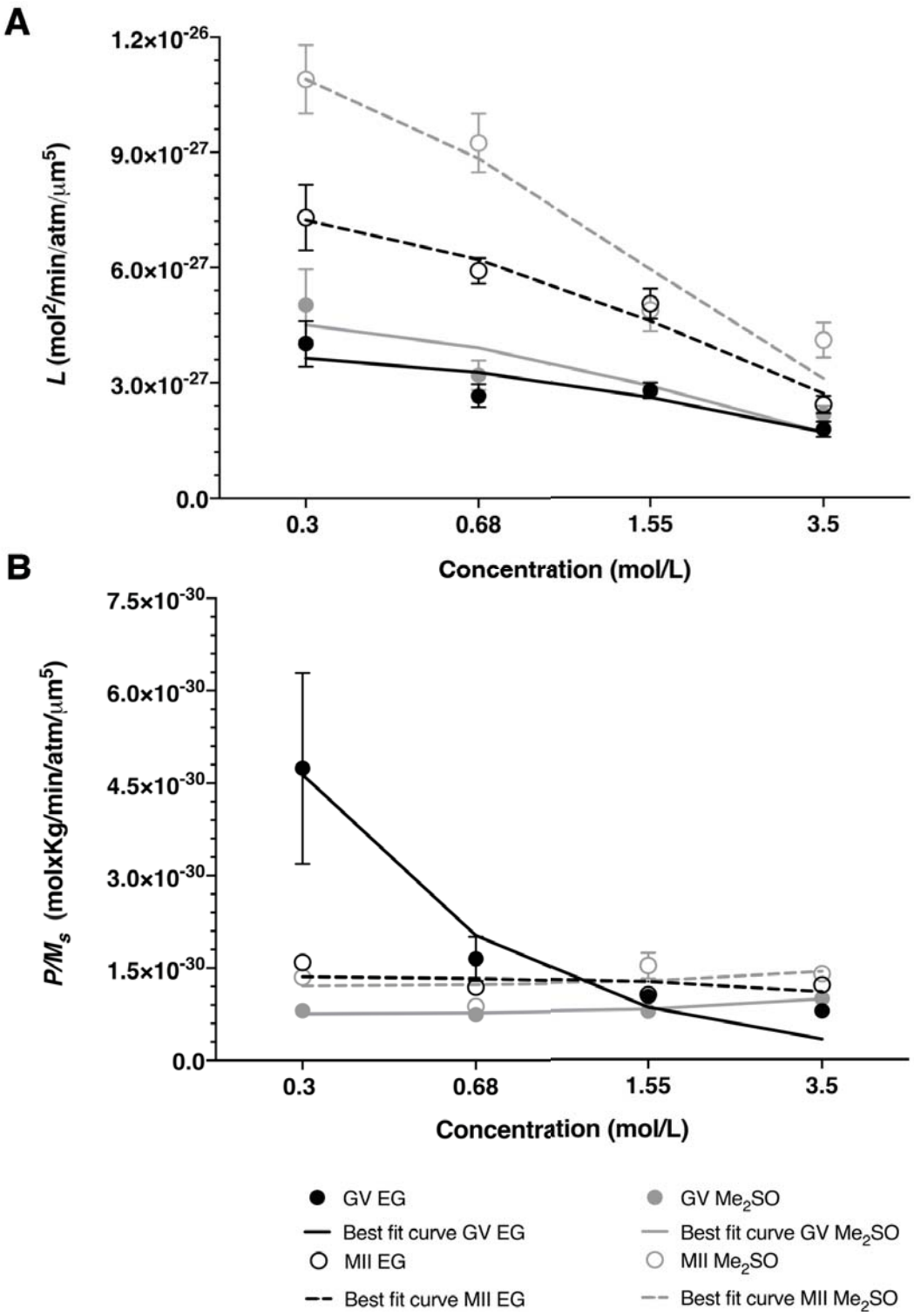

Figure 4. Water permeability and solute permeability GV (closed circles) and MII (open circles) oocytes in the presence of increasing concentrations of CPA (EG (black) or Me_2SO (gray)) for the nondilute solution model (a and b, respectively). Best-fit curve for the concentration dependent model is represented in solid black line (GV EG), dotted black line (MII EG), solid gray line (GV Me_2SO) and dotted gray line (MII Me_2SO). Unless indicated otherwise, data are given as the mean ± s.e.m.

	Stage	Solute	Concentration (mol/L) 0.3	0.68	1.55	3.5	Equation
L_p (µm/atm×min)	GV	Me_2SO	1.43 ± 0.25 ^{a,1}	1.10 ± 0.11 ^{ab,1}	0.86 ± 0.06 ^{ab,1}	0.73 ± 0.08 ^{b,1}	$L_p = 1.44/(0.29\times M_s + 1)$
	MII	Me_2SO	2.87 ± 0.24 ^{a,2}	3.08 ± 0.26 ^{a,2}	1.41 ± 0.16 ^{b,2}	1.33 ± 0.16 ^{b,2}	$L_p = 3.51/(0.49\times M_s + 1)$
	GV	EG	0.82 ± 0.05 ^{ab,1}	0.93 ± 0.10 ^{a,1}	0.90 ± 0.06 ^{a,1}	0.63 ± 0.07 ^{b,1}	$L_p = 0.93/(0.08\times M_s + 1)$
	MII	EG	1.89 ± 0.19 ^{a,2}	2.00 ± 0.09 ^{a,2}	1.60 ± 0.11 ^{a,2}	0.99 ± 0.21 ^{b,1}	$L_p = 2.17/(0.24\times M_s + 1)$
P_s (µm/sec)	GV	Me_2SO	0.36 ± 0.03 ^{a,1}	0.33 ± 0.03 ^{a,1}	0.37 ± 0.04 ^{a,1}	0.45 ± 0.04 ^{a,1}	$P_s = 0.34/(-0.05\times M_s + 1)$
	MII	Me_2SO	0.56 ± 0.04 ^{ab,2}	0.38 ± 0.04 ^{a,1}	0.68 ± 0.09 ^{b,2}	0.61 ± 0.06 ^{ab,1}	$P_s = 0.51/(-0.04\times M_s + 1)$
	GV	EG	1.31 ± 0.28 ^{a,1}	0.74 ± 0.16 ^{ab,1}	0.45 ± 0.05 ^{b,1}	0.35 ± 0.03 ^{b,1}	$P_s = 2.18/(2.28\times M_s + 1)$
	MII	EG	0.64 ± 0.04 ^{a,1}	0.52 ± 0.05 ^{a,1}	0.45 ± 0.04 ^{a,1}	0.53 ± 0.05 ^{a,2}	$P_s = 0.57/(0.04\times M_s + 1)$

Table 3. Bovine oocyte plasma membrane water permeability (L_p), solute permeability (P_s) of immature (GV) and mature (MII) oocytes in the presence of increasing CPA (EG or Me_2SO) concentrations. Permeability parameters obtained from 0.3, 0.68, 1.55 and 3.5 mol/L EG or Me_2SO data fit with the 2P model. The equation represents the best-fit model curve for each stage and CPA using the concentration dependent model described above. Unless indicated otherwise, data are given as the mean ± s.e.m. Different superscript letters indicate significant differences between different molarities within the same CPA and nuclear stage ($P < 0.05$). Different superscript numbers indicate significant differences in water or solute permeability between GV and MII stage within the same CPA ($P < 0.05$). GV, germinal vesicle; MII, metaphase II; Me_2SO, dimethyl sulfoxide; EG, ethylene glycol.

	Stage	Solute	Concentration (mol/L) 0.3	0.68	1.55	3.5	Equation
L x10^{-27} (mol^2/min/atm/µm^5)	GV	Me_2SO	5.03 ± 0.93 ^{a,1}	3.20 ± 0.38 ^{ab,1}	2.77 ± 0.20 ^{b,1}	2.17 ± 0.21 ^{b,1}	$L = 5.13/(0.44\times M_s + 1)$
	MII	Me_2SO	10.88 ± 0.89 ^{a,2}	9.24 ± 0.76 ^{a,2}	4.88 ± 0.56 ^{b,2}	4.10 ± 0.46 ^{b,2}	$L = 13.34/(0.71\times M_s + 1)$
	GV	EG	4.02 ± 0.59 ^{a,1}	2.66 ± 0.30 ^{ab,1}	2.79 ± 0.21 ^{ab,1}	1.78 ± 0.20 ^{b,1}	$L = 3.98/(0.31\times M_s + 1)$
	MII	EG	7.30 ± 0.85 ^{a,2}	5.92 ± 0.33 ^{a,2}	5.05 ± 0.40 ^{a,2}	2.42 ± 0.23 ^{b,1}	$L = 8.28/(0.47\times M_s + 1)$
P/M_s x10^{-30} (molxKg/min/atm/µm^5)	GV	Me_2SO	0.81 ± 0.07 ^{a,1}	0.74 ± 0.07 ^{a,1}	0.78 ± 0.09 ^{a,1}	0.99 ± 0.09 ^{a,1}	$P/M_s = 0.74/(-0.05\times M_s + 1)$
	MII	Me_2SO	1.35 ± 0.11 ^{a,2}	0.88 ± 0.09 ^{b,1}	1.52 ± 0.21 ^{a,2}	1.39 ± 0.12 ^{a,2}	$P/M_s = 1.20/(-0.04\times M_s + 1)$
	GV	EG	4.74 ± 1.55 ^{a,1}	1.65 ± 0.36 ^{ab,1}	1.02 ± 0.12 ^{b,1}	0.78 ± 0.07 ^{b,1}	$P/M_s = 43.1/(30\times M_s + 1)$*
	MII	EG	1.59 ± 0.12 ^{a,1}	1.19 ± 0.12 ^{b,1}	1.05 ± 0.10 ^{b,1}	1.21 ± 0.11 ^{ab,2}	$P/M_s = 1.38/(0.06\times M_s + 1)$

Table 4. Bovine oocyte plasma membrane water permeability (L), solute permeability (P) of immature (GV) and mature (MII) oocytes in the presence of increasing CPA (EG or Me_2SO) concentrations. Permeability parameters obtained from 0.3, 0.68, 1.55 and 3.5 mol/L EG or Me_2SO data fit with the nondilute model. The equation represents the best-fit model curve for each stage and CPA. Unless indicated otherwise, data are given as the mean ± s.e.m. Different superscript letters indicate significant differences between different molarities within the same CPA and nuclear stage ($P < 0.05$). Different superscript numbers indicate significant differences in water or solute permeability between GV and MII stage within the same CPA ($P < 0.05$). * In this case the fitting algorithm was unable to converge because the value of b was so large that the 1 in the denominator became negligible. This results in a constant ratio a/b, which can be satisfied using various combinations of a and b. The values of a and b in Table 4 were chosen arbitrarily among the possible values that match the best-fit value of a/b. GV, germinal vesicle; MII, metaphase II; Me_2SO, dimethyl sulfoxide; EG, ethylene glycol.

3.2. Model Comparison

To examine the potential practical implications of different modeling approaches, we simulated the cell volume response of both GV and MII bovine oocytes during CPA addition and removal following the Kuwayama vitrification protocol (Kuwayama *et al.* 2005), which was designed for and tested on bovine and human oocytes (see materials and methods for more details). Figures 5 and 6 show predictions for GV and MII oocytes for four different modeling approaches.

The most common approach for predicting cell volume changes during CPA addition and removal is to use the 2P model with constant water and CPA permeability values. This baseline case is shown by the solid black lines in Figures 5 and 6. For comparison, the dotted black lines show predictions for the 2P model using concentration dependent permeability values. The two modeling approaches yield nearly identical predictions, and the slight differences are small and not likely to have practical significance. The non-dilute model predictions are also similar to the 2P model baseline case, with the exception of the first step of CPA removal. The non-dilute model exhibits less swelling and faster equilibration during the first step of CPA removal than the 2P model.

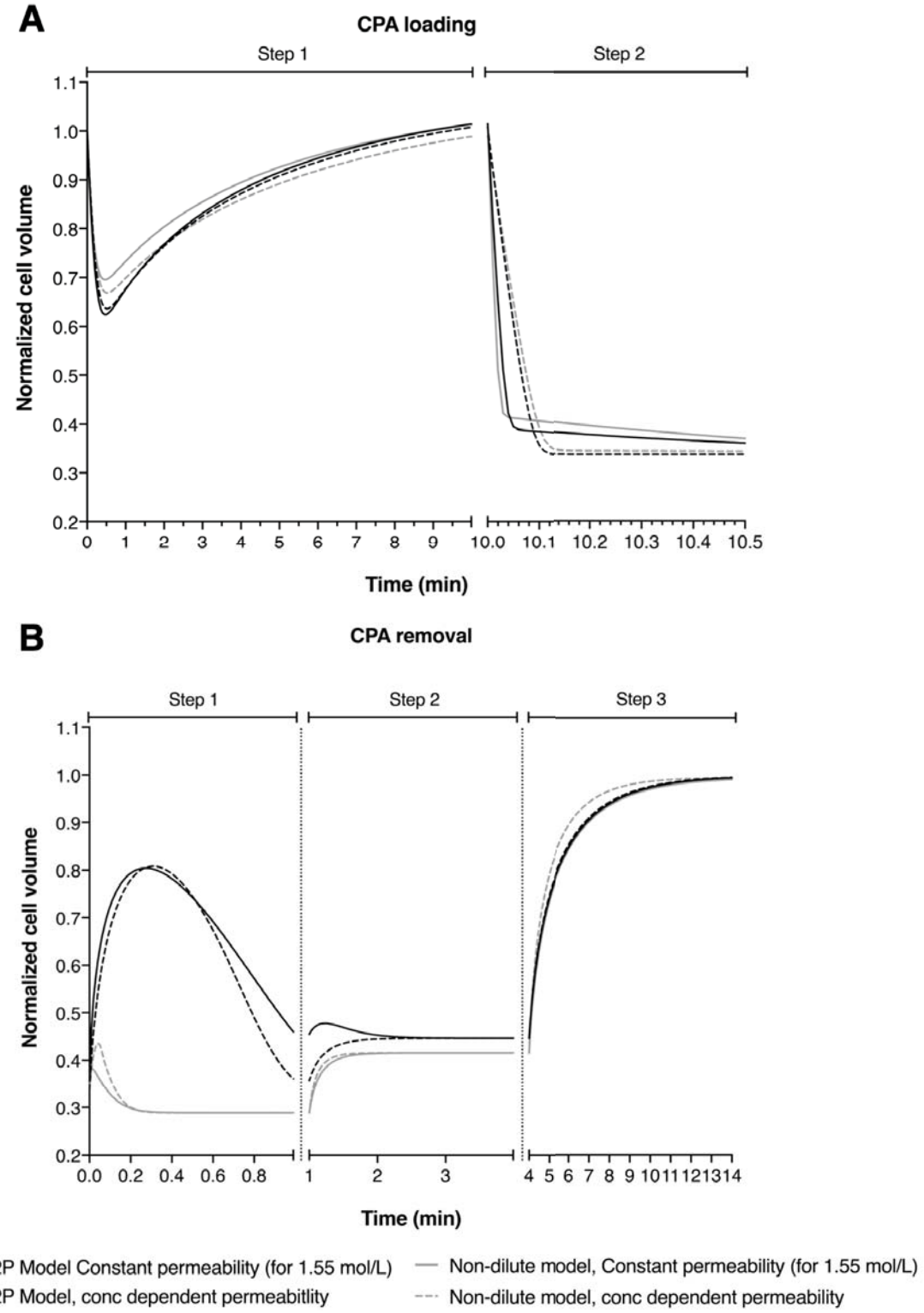

Figure 5. Comparative simulation of cell volume excursion of GV-stage bovine oocytes during CPA addition (a) and removal (b) following the Kuwayama protocol for the 2P model (black line) and nondilute model (gray line) using constant (solid line) and non-constant permeability parameters (dotted line).

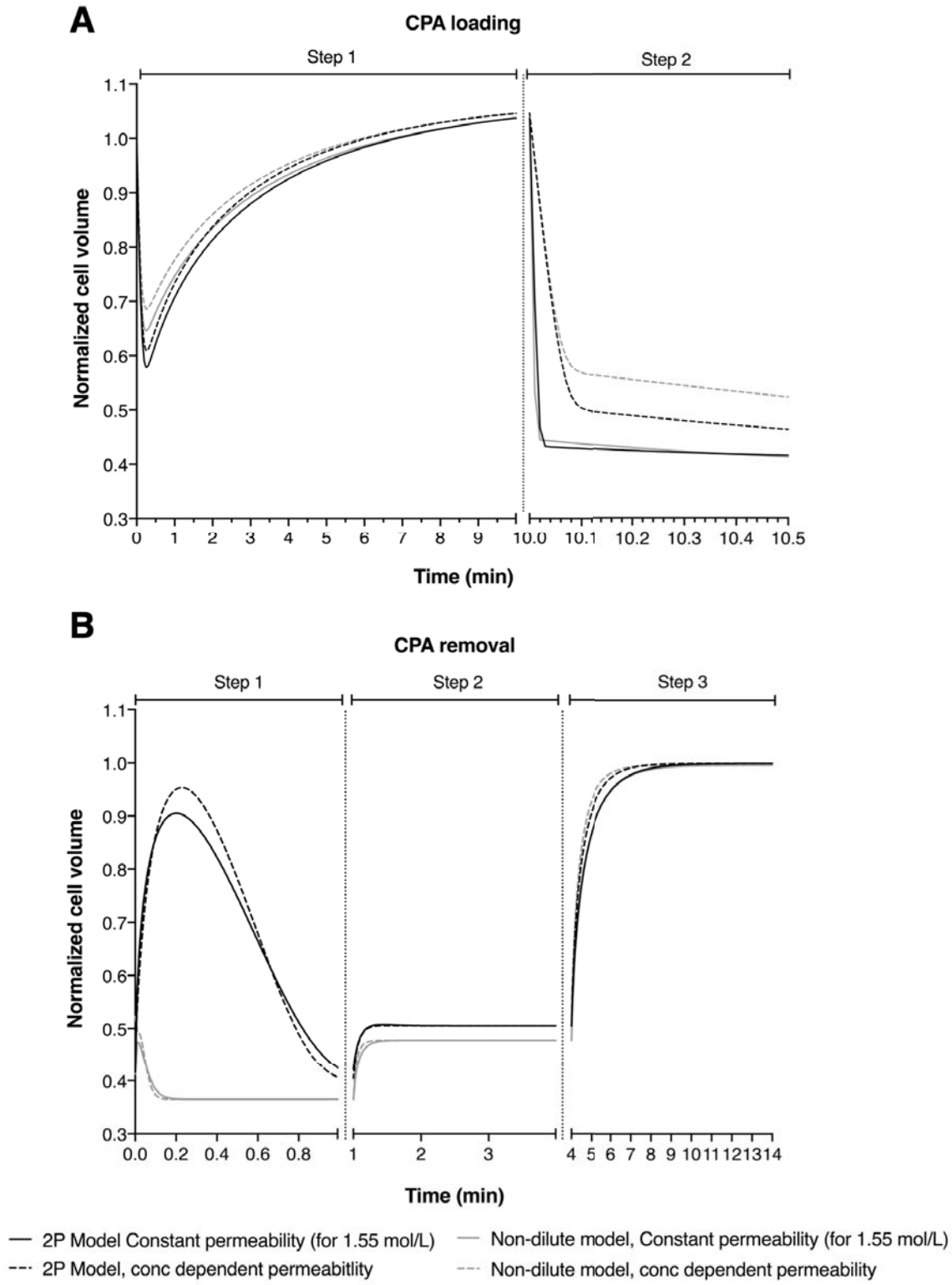

Figure 6. Comparative simulation of cell volume excursion of MII-stage bovine oocytes during CPA addition (a) and removal (b) following the Kuwayama protocol for the 2P model (black line) and nondilute model (gray line) using constant (solid line) and non-constant permeability parameters (dotted line).

4. Discussion

The development of a reliable method for the cryopreservation of mammalian oocytes is crucial for assisted reproduction in both human and domestic species (Hunter *et al.* 1995; Martino *et al.* 1996; Isachenko *et al.* 2001). However, in bovine species, the success rates are still limited due to the oocytes' unique structure and sensitivity to cooling (Mogas 2018; Dujíčková *et al.* 2021). One of the most important cryobiological properties that affects the survival of a cell after vitrification is the permeability of the plasma membrane to water and CPA (Edashige 2017). These permeability values determine the extent of cell volume changes and the time required for CPA equilibration. Therefore, knowledge of these permeability parameters is useful for predicting the likely optimal conditions during CPA addition and removal. Typically cell membrane permeability parameters are determined for exposure to a single CPA concentration (Agca *et al.* 1998; Wang *et al.* 2010; Jin *et al.* 2011). However, oocytes are exposed to various CPA concentrations during the vitrification process, and previous studies suggest that the water and CPA permeability may be concentration dependent (Lahmann *et al.* 2018). Therefore, in this study, we examined the potential effects of CPA concentration on the membrane permeability parameters and the implications for bovine oocyte vitrification.

Table 5 shows the water and CPA permeability values for bovine oocytes determined in previous studies (Agca *et al.* 1998; Wang *et al.* 2010; Jin *et al.* 2011). In these studies, the permeability parameters were estimated by measuring cell volume changes after exposure to a single CPA concentration ranging between 1.2 mol/L and 1.8 mol/L. In the current study, we measured the permeability for various CPA concentrations by sequentially exposing oocytes to increasing concentrations, but the most appropriate concentration for direct comparison to previous studies is 1.55 mol/L (see Table 1). Overall, our results are consistent with the trends observed in previous studies: the water permeability of MII oocytes was nearly twofold higher than that of GV oocytes, and the CPA permeability was similar for EG and Me_2SO and for GV and MII oocytes. However, the water permeability values determined in this study were higher than previous studies. The reason for this discrepancy is unclear but may be related to differences in the methods used to determine the permeability values (Li *et al.* 2017; Guo *et al.* 2020).

Table 5. Previously determined bovine oocyte plasma membrane water permeability (Lp) and cryoprotectant permeability (Ps) values in the presence of CPA at room temperature.

CPA	Molarity (mol/L)	Stage	L_P (μm/min/atm)	P_S (μm/sec)	References
Me_2SO	1.5	GV	0.69*	0.37*	Agca et al., 1993(Agca *et al.* 1998)
EG	1.5	GV	0.50*	0.22*	Agca et al., 1993(Agca *et al.* 1998)
Me_2SO	1.5	MII	1.16*	0.49*	Agca et al., 1993(Agca *et al.* 1998)
EG	1.5	MII	0.76*	0.42*	Agca et al., 1993(Agca *et al.* 1998)
EG	1.8	GV	0.11	0.55	Wang et al.,(Wang *et al.* 2010)
EG	1.8	MII	0.20	0.53	Wang et al.,(Wang *et al.* 2010)
Me_2SO	1.2	MII	1.24	0.25	Jin et al., (Jin *et al.* 2011)
EG	1.3	MII	0.84	0.58	Jin et al., (Jin *et al.* 2011)

GV, germinal vesicle; MII, metaphase II; EG, ethylene glycol; Me_2SO, dimethyl sulfoxide.

*Published L_p and P_s values were determined using the Kedem-Katchalsky (KK) model (Kedem and Katchalsky 1958). These KK parameters were converted to the corresponding L_p and P_s values for the 2P model as described previously (Chuenkhum and Cui 2006).

Our results demonstrate that the water permeability of bovine oocytes decreases as the CPA concentration increases. This trend has been observed previously for various other cell types (McGrath 1988; Gilmore *et al.* 1995; Lahmann *et al.* 2018), and has been explained in terms of steric hindrance caused by CPA binding to water-transporting channels (Toon and Solomon 1990). Bovine oocytes are known to express aquaporins (Jin *et al.* 2011; García-Martínez *et al.* 2018) and the observation that water permeability decreases as CPA concentration increases is consistent with such a mechanism. For some cell types, including mouse oocytes, the water permeability has been observed to increase

as CPA concentration increases (Li *et al.* 2017; Guo *et al.* 2020). The reason for this trend is unclear, but it does not appear to be relevant to bovine oocytes.

Our results also show that the EG permeability of bovine GV oocytes decreases as EG concentration increases. Bovine oocytes express both aquaporin 3 and aquaporin 7 (García-Martínez *et al.* 2018). These aquaglyceroporins have been shown to transport glycerol, ethylene glycol and possibly other CPAs (Jin *et al.* 2011) and are postulated to transport these molecules via successive binding to various sites on the aquaporin protein (Rodriguez *et al.* 2019; Moss *et al.* 2020). These binding sites can become saturated at high CPA concentrations, leading to slower CPA transport (Rodriguez *et al.* 2019; Moss *et al.* 2020). In contrast to glycerol and ethylene glycol, there is evidence that Me_2SO transport through aquaporin 3 is negligible in mammalian oocytes (Edashige 2017), which may explain why we did not observe a concentration dependence for the Me_2SO permeability. We also did not observe a concentration dependence of the EG permeability for MII oocytes, suggesting that changes in aquaporin expression or membrane composition during oocyte development may have impacted the EG transport mechanism (Jo *et al.* 2011).

One potential explanation for the observed effects of CPA concentration on the permeability parameters is the use of the 2P model for making predictions under non-dilute conditions. It has been suggested that the non-dilute transport model (equations (5) and (6)) can provide more accurate predictions, particularly at high CPA concentrations (Elmoazzen *et al.* 2009). Therefore, we also analyzed the permeability parameters for GV and MII bovine oocytes with the non-dilute transport model (Elmoazzen *et al.* 2009). Our results show nearly identical tendencies with both mathematical models: the water permeability decreases as EG or Me_2SO concentration increases in both GV and MII oocytes, and the EG permeability decreases as EG concentration increases in GV oocytes (see Tables 1 and 2). Elmoazzen et al (Elmoazzen *et al.* 2009) argued that when the permeability coefficient P is divided by concentration (as we have done in Table 4), the resulting ratio should not be dependent on CPA concentration. Nevertheless, our results indicate that GV oocytes exposed to EG exhibit a substantial decrease in the value of this ratio as the EG concentration increases. This indicates that the observed decreases in water and CPA permeability with increasing CPA concentration cannot be attributed only to use of the 2P model under non-dilute conditions, suggesting a physical transport process that is CPA concentration dependent.

Cell membrane transport predictions such as those shown in Figure 5 can be useful

for evaluating the potential for damage during CPA addition and removal and for design of less damaging methods. Many cell types have limited tolerance for changes in cell volume, with increasing volume changes causing additional loss of cell viability (Agca *et al.* 2000; Mullen *et al.* 2004). Thus, knowing the osmotic tolerance limits is essential for optimizing cryopreservation methods. Previously, Mullen et al (Mullen SF 2004) demonstrated that MII spindle damage in bovine oocyte occurs more frequently as the extracellular solution concentrations diverge from isosmotic. Moreover, they estimated that to prevent osmotic damage to the MII spindle with a probability of 90%, it is necessary to use CPA addition and removal procedure which maintains the cells within a volume range of 1.1 to 0.52 times the isotonic volume. Therefore, using the Kuwayama protocol (Kuwayama *et al.* 2005) for bovine oocytes is not expected to cause very much osmotic damage to the spindle during CPA loading based on predictions using any of the modeling approaches that we investigated (see Figure 5). However, during CPA removal, the non-dilute model predicts that GV and MII oocytes will shrink to an equilibrium value much faster than the 2P model predicts, which involves maintaining the cells in a more prolonged state of osmotic stress. Based on the osmotic damage model developed by Mullen et al (Mullen SF 2004), maintenance of the oocytes at a volume of 38% relative to isotonic is expected to cause about 35% of oocytes to experience osmotic damage to the spindle.

Exposure to CPA can also cause cell damage due to toxicity. Although toxicity is expected to be less of a problem during CPA removal, it is still important to design removal procedures with toxicity in mind. Benson et al (Benson *et al.* 2012) demonstrated that inducing swelling is beneficial because it decreases the intracellular CPA concentration and its associated toxicity. Human oocytes swell to more than their isotonic volume during the first step of the CPA removal process after vitrification (Davidson *et al.* 2014). In contrast, bovine oocytes are predicted to exhibit much less swelling (Figures 4 and 5), especially for the non-dilute model, which may increase CPA toxicity.

Overall, the predictions presented in Figure 5 suggest that modifying the first step of the CPA removal process may reduce damage to bovine oocytes. In particular, we observed that the non-dilute model predicts that the amount of osmotic swelling after vitrification relative to the starting (shrunken) volume is minor compared to the dilute model. To our knowledge, we are the first to demonstrate that the non-dilute model and dilute model predict such different volume responses during CPA removal, highlighting the need for future studies to examine the relative accuracy of the two different modeling approaches. If the non-dilute model predictions turn out to be more accurate than those

from the dilute model, this suggests that a very different protocol for CPA removal should be well tolerated (a lot less sucrose would be needed as an osmotic buffer in step 1). By reducing the amount of sucrose in the medium the oocytes would not be expected to shrink as much, keeping them within osmotic tolerance limits. This is expected to cause much less damage than the original protocol (Davidson *et al.* 2014).

Conclusions

Historically, cell permeabilities to water and CPA were assumed to be independent of CPA concentration. This is likely due to the predominance of slow cooling methods employed for cellular cryopreservation for the last half century, where a single concentration of CPA was used. In recent years, vitrification has become the preferred method for mammalian oocyte cryopreservation, requiring reconsideration of this assumption. In this study, we have examined the effects of CPA concentration on water and CPA membrane permeability for bovine oocytes. We have shown that water permeability is inversely related to CPA concentration. Furthermore, CPA concentration also affects membrane CPA permeability, with differential effects depending upon the maturation stage of the oocyte and the specific CPA type. Although both the water and CPA permeability change with concentration, accounting for the concentration dependence of permeability only had a slight effect on cell volume predictions during CPA addition and removal, suggesting that the typical assumption that permeability is independent of concentration is reasonable. We have also investigated two modeling approaches, one using dilute solution assumptions, and another that is not restricted to those assumptions. The results suggest that only slight differences exist in the predictions during the CPA loading steps of the procedure, but a greater difference was noted between the two models' predictions during the first stage of CPA removal. This may have important implications for developing improved procedures for the vitrification of mammalian oocytes.

References

Agca, Y., Liu, J., Peter, A.T., Critser, E.S., and Critser, J.K. (1998) Effect of developmental stage on bovine oocyte plasma membrane water and cryoprotectant permeability characteristics. *Mol Reprod Dev* **49**(4), 408-15

Agca, Y., Liu, J., Rutledge, J.J., Critser, E.S., and Critser, J.K. (2000) Effect of osmotic stress on the developmental competence of germinal vesicle and metaphase II stage bovine cumulus oocyte complexes and its relevance to cryopreservation. *Mol Reprod Dev* **55**(2), 212-9

Ambrosini, G., Andrisani, A., Porcu, E., Rebellato, E., Revelli, A., Caserta, D., Cosmi, E., Marci, R., and Moscarini, M. (2006) Oocytes cryopreservation: state of art. *Reprod Toxicol* **22**(2), 250-62

Arav, A., Yavin, S., Zeron, Y., Natan, D., Dekel, I., and Gacitua, H. (2002) New trends in gamete's cryopreservation. *Mol Cell Endocrinol* **187**(1-2), 77-81

Armitage, W.J. (1986) Effect of solute concentration on intracellular water volume and hydraulic conductivity of human blood platelets. *J Physiol* **374**, 375-85

Benson, J.D., Kearsley, A.J., and Higgins, A.Z. (2012) Mathematical optimization of procedures for cryoprotectant equilibration using a toxicity cost function. *Cryobiology* **64**(3), 144-51

Chian, R.C., Kuwayama, M., Tan, L., Tan, J., Kato, O., and Nagai, T. (2004) High survival rate of bovine oocytes matured *in vitro* following vitrification. *J Reprod Dev* **50**(6), 685-96

Chuenkhum, S., and Cui, Z. (2006) The parameter conversion from the Kedem-Katchalsky model into the two-parameter model. *Cryo Letters* **27**(3), 185-99

Davidson, A.F., Benson, J.D., and Higgins, A.Z. (2014) Mathematically optimized cryoprotectant equilibration procedures for cryopreservation of human oocytes. *Theor Biol Med Model* **11**, 13

Díez, C., Muñoz, M., Caamaño, J.N., and Gómez, E. (2012) Cryopreservation of the bovine oocyte: current status and perspectives. *Reprod Domest Anim* **47 Suppl 3**, 76-83

Dormand, J.R., and Prince, P.J. (1980) A family of embedded Runge-Kutta formulae. *Journal of Computational and Applied Mathematics* **6**(1), 19-26

Dujíčková, L., Makarevich, A.V., Olexiková, L., Kubovičová, E., and Strejček, F. (2021) Methodological approaches for vitrification of bovine oocytes. *Zygote* **29**(1), 1-11

Edashige, K. (2017) Permeability of the plasma membrane to water and cryoprotectants in mammalian oocytes and embryos: Its relevance to vitrification. *Reprod Med Biol* **16**(1), 36-39

Elmoazzen, H.Y., Elliott, J.A., and McGann, L.E. (2002) The effect of temperature on membrane hydraulic conductivity. *Cryobiology* **45**(1), 68-79

Elmoazzen, H.Y., Elliott, J.A., and McGann, L.E. (2009) Osmotic transport across cell membranes in nondilute solutions: a new nondilute solute transport equation. *Biophys J* **96**(7), 2559-71

Fahy, G.M., Lilley, T.H., Linsdell, H., Douglas, M.S., and Meryman, H.T. (1990) Cryoprotectant toxicity and cryoprotectant toxicity reduction: in search of molecular mechanisms. *Cryobiology* **27**(3), 247-68

Fahy, G.M., Wowk, B., Wu, J., and Paynter, S. (2004) Improved vitrification solutions based on the predictability of vitrification solution toxicity. *Cryobiology* **48**(1), 22-35

García-Martínez, T., Vendrell-Flotats, M., López-Béjar, M., and Mogas, T. (2018) Exposure to hyperosmotic solutions modifies expression of AQP3 and AQP7 on bovine oocytes. *Cryobiology* **85**, 143

García-Martínez, T., Vendrell-Flotats, M., Martínez-Rodero, I., Ordóñez-León, E.A., Álvarez-Rodríguez, M., López-Béjar, M., Yeste, M., and Mogas, T. (2020) Glutathione Ethyl Ester Protects *In Vitro*-Maturing Bovine Oocytes against Oxidative Stress Induced by Subsequent Vitrification/Warming. *Int J Mol Sci* **21**(20)

Gilmore, J.A., McGann, L.E., Liu, J., Gao, D.Y., Peter, A.T., Kleinhans, F.W., and Critser, J.K. (1995) Effect of cryoprotectant solutes on water permeability of human spermatozoa. *Biol Reprod* **53**(5), 985-95

Guo, X., Chen, Z., Memon, K., Chen, X., and Zhao, G. (2020) An integrated microfluidic device for single cell trapping and osmotic behavior investigation of mouse oocytes. *Cryobiology* **92**, 267-271

Holt, W.V. (2008) Cryobiology, wildlife conservation and reality. *Cryo Letters* **29**(1), 43-52

Hunter, J.E., Fuller, B.J., Bernard, A., Jackson, A., and Shaw, R.W. (1995) Vitrification of human oocytes following minimal exposure to cryoprotectants; initial studies on fertilization and embryonic development. *Hum Reprod* **10**(5), 1184-8

Isachenko, V., Alabart, J.L., Nawroth, F., Isachenko, E., Vajta, G., and Folch, J. (2001) The open pulled straw vitrification of ovine GV-oocytes: positive effect of rapid cooling or rapid thawing or both? *Cryo Letters* **22**(3), 157-62

Jacobs, M.H. (1933) The simultaneous measurement of cell permeability to water and to dissolved substances. *Journal of Cellular and Comparative Physiology* **2**(4), 427-444

Jacobs, M.H., and Stewart, D.R. (1932) A simple method for the quantitative measurement of cell permeability. *Journal of Cellular and Comparative Physiology* **1**(1), 71-82

Jin, B., Kawai, Y., Hara, T., Takeda, S., Seki, S., Nakata, Y., Matsukawa, K., Koshimoto, C., Kasai, M., and Edashige, K. (2011) Pathway for the movement of water and cryoprotectants in bovine oocytes and embryos. *Biol Reprod* **85**(4), 834-47

Jo, J.W., Jee, B.C., Suh, C.S., Kim, S.H., Choi, Y.M., Kim, J.G., and Moon, S.Y. (2011) Effect of maturation on the expression of aquaporin 3 in mouse oocyte. *Zygote* **19**(1), 9-14

Karlsson, J.O., and Toner, M. (1996) Long-term storage of tissues by cryopreservation: critical issues. *Biomaterials* **17**(3), 243-56

Kedem, O., and Katchalsky, A. (1958) Thermodynamic analysis of the permeability of biological membranes to non-electrolytes. *Biochim Biophys Acta* **27**(2), 229-46

Kempthorne, O. (1958) Experimental Designs (Second Edition). *Agronomy Journal* **50**(2), 115-115

Kleinhans, F.W. (1998) Membrane permeability modeling: Kedem-Katchalsky *vs* a two-parameter formalism. *Cryobiology* **37**(4), 271-289

Kuwayama, M., Vajta, G., Kato, O., and Leibo, S.P. (2005) Highly efficient vitrification method for cryopreservation of human oocytes. *Reprod Biomed Online* **11**(3), 300-8

Lagarias, J.C., Reeds, J.A., Wright, M.H., and Wright, P.E. (1998) Convergence Properties of the Nelder--Mead Simplex Method in Low Dimensions. *SIAM Journal on Optimization* **9**(1), 112-147

Lahmann, J.M., Benson, J.D., and Higgins, A.Z. (2018) Concentration dependence of the cell membrane permeability to cryoprotectant and water and implications for design of methods for post-thaw washing of human erythrocytes. *Cryobiology* **80**, 1-11

Lawson, A., Ahmad, H., and Sambanis, A. (2011) Cytotoxicity effects of cryoprotectants as single-component and cocktail vitrification solutions. *Cryobiology* **62**(2), 115-22

Leibo, S.P. (2008) Cryopreservation of oocytes and embryos: optimization by theoretical versus empirical analysis. *Theriogenology* **69**(1), 37-47

Levin, R.L., and Miller, T.W. (1981) An optimum method for the introduction or removal of permeable cryoprotectants: isolated cells. *Cryobiology* **18**(1), 32-48

Li, L., Chen, Z., Zhang, M., Panhwar, F., Gao, C., Zhao, G., Jin, B., and Ye, B. (2017) Cell membrane permeability coefficients determined by single-step osmotic shift are not applicable for optimization of multi-step addition of cryoprotective agents: As revealed by HepG2 cells. *Cryobiology* **79**, 82-86

Martino, A., Pollard, J.W., and Leibo, S.P. (1996) Effect of chilling bovine oocytes on their developmental competence. *Mol Reprod Dev* **45**(4), 503-12

McGrath, J.J. (1988) Membrane Transport Properties. In Low Temperature Biotechnology: Emerging Application and Engineering Contributions. In 'New York: American Society of Mechanical Engineers.' (Eds. J McGrath and K Diller) pp. 273-331)

Mogas, T. (2018) Update on the vitrification of bovine oocytes and invitro-produced embryos. *Reprod Fertil Dev* **31**(1), 105-117

Moss, F.J., Mahinthichaichan, P., Lodowski, D.T., Kowatz, T., Tajkhorshid, E., Engel, A., Boron, W.F., and Vahedi-Faridi, A. (2020) Aquaporin-7: A Dynamic Aquaglyceroporin With Greater Water and Glycerol Permeability Than Its Bacterial Homolog GlpF. *Front Physiol* **11**, 728

Mullen, S.F., Agca, Y., Broermann, D.C., Jenkins, C.L., Johnson, C.A., and Critser, J.K. (2004) The effect of osmotic stress on the metaphase II spindle of human oocytes, and the relevance to cryopreservation. *Hum Reprod* **19**(5), 1148-54

Mullen SF, A.Y., Critser JK (2004) Modeling the Probability of MII Spindle Disruption in Bovine Oocytes as a Function of Total Osmolality Using Logistic Regression and Its Application toward Improved CPA Addition and Removal Procedures. *Cell Preservation Technology* **2**(2), 145-155

Mullen, S.F., Li, M., Li, Y., Chen, Z.J., and Critser, J.K. (2008) Human oocyte vitrification: the permeability of metaphase II oocytes to water and ethylene glycol and the appliance toward vitrification. *Fertil Steril* **89**(6), 1812-25

Papis, K., Shimizu, M., and Izaike, Y. (2000) Factors affecting the survivability of bovine oocytes vitrified in droplets. *Theriogenology* **54**(5), 651-8

Rodriguez, R.A., Liang, H., Chen, L.Y., Plascencia-Villa, G., and Perry, G. (2019) Single-channel permeability and glycerol affinity of human aquaglyceroporin AQP3. *Biochim Biophys Acta Biomembr* **1861**(4), 768-775

Ruffing, N.A., Steponkus, P.L., Pitt, R.E., and Parks, J.E. (1993) Osmometric behavior, hydraulic conductivity, and incidence of intracellular ice formation in bovine oocytes at different developmental stages. *Cryobiology* **30**(6), 562-80

Shampine, L.F., and Reichelt, M.W. (1997) The MATLAB ODE Suite. *SIAM Journal on Scientific Computing* **18**(1), 1-22

Toon, M.R., and Solomon, A.K. (1990) Transport parameters in the human red cell membrane: solute-membrane interactions of hydrophilic alcohols and their effect on permeation. *Biochim Biophys Acta* **1022**(1), 57-71

Vajta, G., Holm, P., Kuwayama, M., Booth, P.J., Jacobsen, H., Greve, T., and Callesen, H. (1998) Open Pulled Straw (OPS) vitrification: a new way to reduce cryoinjuries of bovine ova and embryos. *Mol Reprod Dev* **51**(1), 53-8

Vian, A.M., and Higgins, A.Z. (2014) Membrane permeability of the human granulocyte to water, dimethyl sulfoxide, glycerol, propylene glycol and ethylene glycol. *Cryobiology* **68**(1), 35-42

Wang, X., Al Naib, A., Sun, D.W., and Lonergan, P. (2010) Membrane permeability characteristics of bovine oocytes and development of a step-wise cryoprotectant adding and diluting protocol. *Cryobiology* **61**(1), 58-65

Woods, E.J., Benson, J.D., Agca, Y., and Critser, J.K. (2004) Fundamental cryobiology of reproductive cells and tissues. *Cryobiology* **48**(2), 146-56

Wusteman, M.C., Pegg, D.E., Robinson, M.P., Wang, L.H., and Fitch, P. (2002) Vitrification media: toxicity, permeability, and dielectric properties. *Cryobiology* **44**(1), 24-37

Zielinski, M.W., McGann, L.E., Nychka, J.A., and Elliott, J.A. (2014) Comparison of non-ideal solution theories for multi-solute solutions in cryobiology and tabulation of required coefficients. *Cryobiology* **69**(2), 305-17

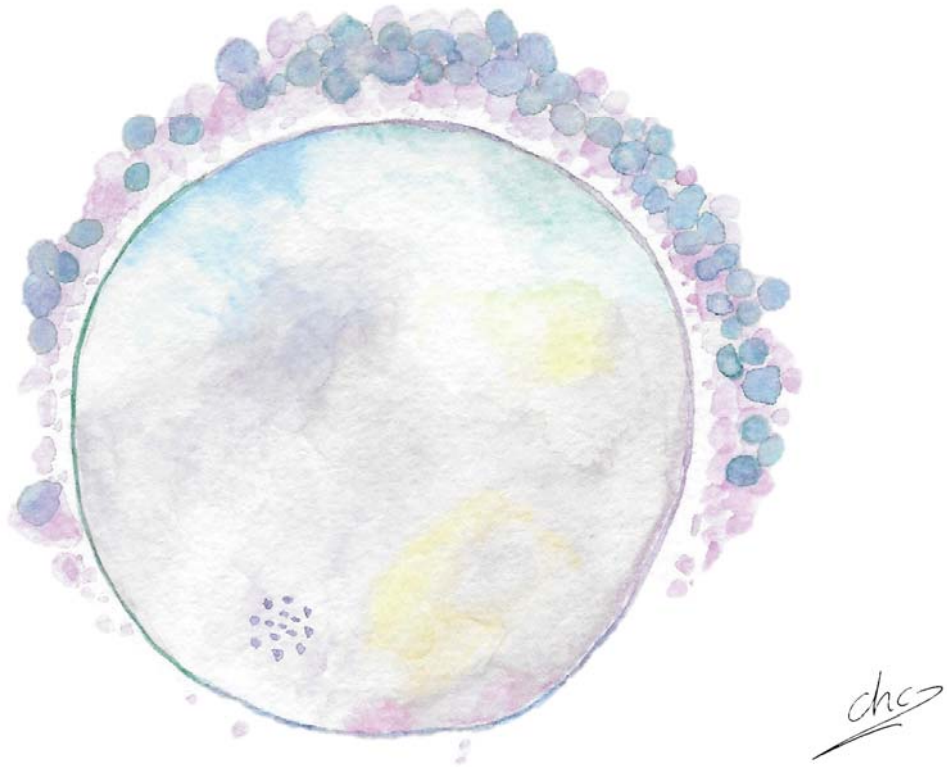

Chapter II

The role of aquaporin 7 in the movement of water and cryoprotectants in bovine *in vitro* matured oocytes

ABSTRACT: Mammalian oocytes are very sensitive to osmotic stress because of their reduced permeability to water and cryoprotectants, resulting in low survival and competence after cryopreservation. Successful vitrification of mammalian cells requires rapid transport of water and cryoprotectants across the plasma membrane. Aquaporins AQP3, AQP7 and AQP9 are known as channel proteins able to transport water and small neutral solutes. In this study, we evaluate the effect of exposure of *in vitro* matured bovine oocytes to hyperosmotic solutions containing ethylene glycol (EG), dimethyl sulfoxide (Me_2SO) or sucrose on the expression levels of AQP3, AQP7 and AQP9. Moreover, we studied whether artificial expression of AQP7 in bovine oocytes increases their permeability to water and cryoprotectants. Results showed that exposure to hyperosmotic solutions stimulated AQP3 and AQP7 but not AQP9 expression. Exposure of oocytes to hyperosmotic Me_2SO solution upregulated AQP3 while AQP7 expression was upregulated by EG hyperosmotic exposure. Microinjection of oocytes at germinal vesicle stage with enhanced green fluorescent protein (EGFP) or EGFP+AQP7 cRNAs resulted in the expression of the EGFP protein in ≈86% of the metaphase-II stage oocytes at 24 h of *in vitro* maturation. Although microinjection decreased the competence of oocytes to resume meiosis, 100% of oocytes expressing EGFP also co-expressed AQP7. AQP7 seems to facilitate water diffusion when bovine MII oocytes are in presence of sucrose or Me_2SO solution but not EG solution. However, this aquaporin is not involved in the movement of Me_2SO and EG, that principally move through simple diffusion across cell membranes. Therefore, a higher permeability to water of bovine oocytes through the overexpression of AQP7 channels may be a useful approach to improve cryopreservation of bovine MII oocytes.

1. Introduction

Cryopreservation of bovine gametes industry has grown worldwide, with an important impact on reproductive biotechnology (Díez *et al.* 2012; Mogas 2018). A major obstacle for cryopreservation of mammalian oocytes and early embryos is, however, their sensitivity to chilling and osmotic stress (Mullen and Fahy 2012). Vitrification requires the use of relatively high concentrations of cryoprotectants (CPAs) to decrease the probability of intracellular crystallization. However, CPAs are toxic and cause osmotic injury to the oocytes even before cooling them, mainly due to the cell volume excursions that the cells endure in extreme anisosmotic conditions (Rall 1987). These dehydratation-rehydratation processes caused by permeating CPAs place cumulative osmotic stress on the cell (Woods *et al.* 2004). Therefore, the movement of water and solutes across the cell membrane plays a

crucial role in cell viability because it influences the major forms of cell injury caused by cryopreservation, including damage from intracellular ice crystal formation, CPA toxicity, and osmotic swelling during removal of the CPA (Fahy *et al.* 2004; Mullen *et al.* 2004).

Two different pathways facilitate the movement of water and CPAs across the plasma membrane, simple diffusion through the lipid bilayer and facilitated diffusion through channels (Verkman *et al.* 2014). Movement through simple diffusion is characterized by low permeability to water (hydraulic conductivity [Lp]) or to a CPA (Ps), but permeability highly depends on the temperature. Therefore, it is necessary a longer exposure to the cryopreservation solution to allow cell to dehydrate and facilitate CPA diffusion and the period of exposure to the CPA will vary depending on the temperature (Agca *et al.* 1998a; Agca *et al.* 1999). Contrarily, the permeability would be higher when water and CPAs permeate the plasma membrane by facilitated diffusion through channels and for hence, this movement would be less affected by temperature. However, in both cases, exposure time to the cryopreservation solution needs to be limited to avoid damage from the chemical toxicity of the CPA (Benson *et al.* 2012). Therefore, rapid movement of water and CPAs through the plasma membranes is essential to minimize damaging exposure times to CPAs.

Aquaporins, present in all living organisms from bacteria to mammals, are a superfamily of small (25–34 kDa), hydrophobic, integral membrane proteins that facilitate rapid, passive movement of water across cellular membranes (King *et al.* 2004). To date, thirteen isoforms of aquaporins (AQP0–12) have been identified, and while most of them are water-selective, functional studies have identified a subgroup of channels termed as aquaglyceroporins (AQP3, AQP7, AQP9 and AQP10) that are non-selective water channels, and can transport glycerol, urea and other small non-electrolytes as well as water (Verkman and Mitra 2000; Huang *et al.* 2006).

Commonly, ethylene glycol (EG) and dimethyl sulfoxide (Me_2SO) are used as penetrating CPAs for vitrification of mammalian oocytes and sucrose as a nonpenetrating CPA to reduce the toxic effects of a vitrification solution (Raju *et al.* 2021). Previous studies demonstrated that water and CPAs move through plasma membrane of mouse and bovine oocytes predominantly by simple diffusion, but a smaller proportion of water moves via channel processes; thus, AQP3 was found to play a major role in aiding the diffusion of water, glycerol and EG in cow and mouse oocytes (Edashige *et al.* 2007; Jin *et al.* 2011). Moreover, to examine whether the artificial expression of AQP3 could improve water and

CPA permeability and oocyte survival after cryopreservation, exogenous expression of rat AQP3 in mouse oocytes or human and zebrafish AQP3 in porcine oocytes was measured (Edashige *et al.* 2003)'(Yamaji *et al.* 2011; Morató *et al.* 2014). In these studies, exogenous expression of AQP3 enhanced both the efflux of water and influx of CPAs into the cell, thus improving oocyte cryotolerance and survival and embryo development after warming of mouse oocytes (Edashige *et al.* 2003; Yamaji *et al.* 2011). However, there is no information in the literature regarding to the expression of other aquaglyceroporins and their effect on the permeability to water and CPAs in bovine oocytes.

The aim of this study was to examine the pathways for the movement of water and cryoprotectants through bovine *in vitro* matured oocytes with special reference to the role of AQP7. We first investigated the expression of AQP3, AQP7 and AQP9 after exposure of *in vitro* matured bovine oocytes to hyperosmotic CPA solutions. Then we examined the role of AQP7 in the movement of water and cryoprotectants in bovine *in vitro* matured oocytes in which AQP7 was artificially overexpressed through cRNA injection.

2. Materials and Methods

2.1. Chemicals

Unless indicated otherwise, all chemicals were purchased from Sigma Chemical Co. (St. Louis, MO, USA).

2.2. Oocyte collection and *in vitro* maturation

The methods used for the *in vitro* maturation (IVM), *in vitro* fertilization (IVF) and *in vitro* culture (IVC) of the bovine oocytes have been described elsewhere (García-Martínez *et al.* 2020). Cow ovaries were collected from a local slaughterhouse and transported to the laboratory in saline (0.9% w/v NaCl) at 35–37°C within 1h. The cumulus-oocyte complexes (COCs) were obtained by aspirating the 3- to 8-mm follicles, and only COCs with a compact cumulus and dark cytoplasm were selected for *in vitro* maturation (IVM). Groups of up to 50 COCs were transferred into each well of a 4-well multi-dish (Nunc, Roskilde, Denmark) containing 500 μL of maturation medium and cultured for 24 h at 38.5°C in a humidified CO_2 incubator (5% CO_2 in air). The maturation medium (IVM medium) consisted of tissue culture medium (TCM-199) supplemented with 10% (v/v) fetal bovine serum (FBS), 10 ng/mL epidermal growth factor and 50 μg/mL gentamicin.

2.3. Analysis of AQP3, AQP7 and AQP9 expression

After 24 h of IVM, bovine oocytes were completely denuded of cumulus cells by gentle pipetting and exposed to holding medium (HM: TCM199-Hepes supplemented with 20% (v/v) FBS) containing 9.5% Me_2SO (v/v 1.2 M), 8% (v/v 1.3 M) EG, or 0.5 M sucrose at 25ºC during 20 min (Jin *et al.* 2013; Tan *et al.* 2015). Oocytes keep in HM served as controls. Oocytes were then denuded of cumulus cells by gentle pipetting and fixed in 2% (w/v) paraformaldehyde–phosphate buffer saline (PFA-PBS) for 30 min; all steps were done at 38.5°C unless otherwise stated. After washing in PBS, oocytes were permeabilized in Triton X-100 (2.5% (v/v) in PBS) for 20 min and blocked in 3% bovine serum albumin (BSA) (w/v) in PBS for 30 min. After washing, oocytes were incubated either with rabbit anti-AQP3 antibody (70R-51452, Fitzgerald, USA) (1:200), rabbit anti-AQP7 antibody (NBP1–30862; Novus Biologicals, USA) (1:200) or rabbit anti-AQP9 antibody (GTX37783, GeneTex, USA) (1:200) overnight at 4°C, followed by incubation with goat Alexa Fluor™ 488-conjugated anti-rabbit IgG antibody (A11034, Life technologies, Carlsbad, CA, USA) (1:700) for 1 h. Following secondary antibody incubation, oocytes were washed three times in PBS supplemented with 0.005% (v/v) Triton X-100 for 20 min between incubations. Groups of 20 oocytes were mounted on poly L-lysine-treated coverslips fitted with a self-adhesive reinforcement ring in a 3-µL drop of Vectashield containing 125 ng/mL 4',6'-diamidino-2-phenylindole hydrochloride (DAPI) (Vysis Inc., Downers Grove, USA) and flattened with a coverslip. The preparation was sealed with nail varnish and stored at 4°C protected from light until observation within the following 2 days. For negative controls, primary antibodies were omitted. A laser-scanning confocal microscope (Leica TCS SP5, Leica Microsystems, Mannheim, Germany) was used to examine AQP3, AQP7 or AQP9 (Alexa Fluor™ 488; excitation 488 nm), and chromatin (DAPI; excitation 405nm) staining. In total, 20–30 oocytes were examined for each of the 3 primary antibodies.

After subtracting the background, fluorescence mean intensity expressed in arbitrary fluorescence units (pixel) was quantified using Image-J software (Version 2.0.0-rc-69/1.52p; National Institutes of Health, Bethesda, MD, USA). Fluorescence intensities in control oocytes were set at 100%, and the relative AQP levels of the samples were calculated with respect to this value.

2.4. Preparation of AQP7 cRNA

A circular plasmid constructed and packaged by VectorBuilder (Santa Clara, CA, USA) was used to drive the AQP7 expression in metaphase II (MII) oocytes following cytoplasmic microinjection at the germinal vesicle (GV) stage. The AQP7 vector (id: VB180522-1156Kgb) contained the active AQP7 gene sequence (GenBank accession number NM_001076378.2). The AQP7 gene sequence was under the control of the T7 promoter. Following the AQP7 sequence, the vector had a PolyA signal (SV30) that allows transcription termination and polyadenylation of mRNA transcribed by PolII RNA polymerase. In addition, the circular vector had the ampicillin resistance gene in a total sequence of 861 bp. The green fluorescent protein (EGFP) expression vector pcDNA3.2EGFP-poly(A83) (Yamagata *et al.* 2005) was used as reporter gene.

AQP7 expression vector was digested by AscI (New England Biolabs, Ipswich, MA, USA) and EGFP expression vector pcDNA3.2EGFP-poly(A83) was digested by XhoI and XbaI (New England Biolabs, Ipswich, MA, USA). Then, AQP7 and EGFP cRNAs were *in vitro* transcribed with mMESSAGE mMACHINE T7 Ultra Kit (Life technologies, Carlsbad, CA, USA) (Gómez-Redondo *et al.* 2020) and purified using FavorPrep™ Tissue Total RNA Mini Kit (Favorgen, Viena, Austria). The cRNAs were prepared at 50 ng/μL (AQP7 cRNA) and 30 ng/μL (EGFP cRNA) in water.

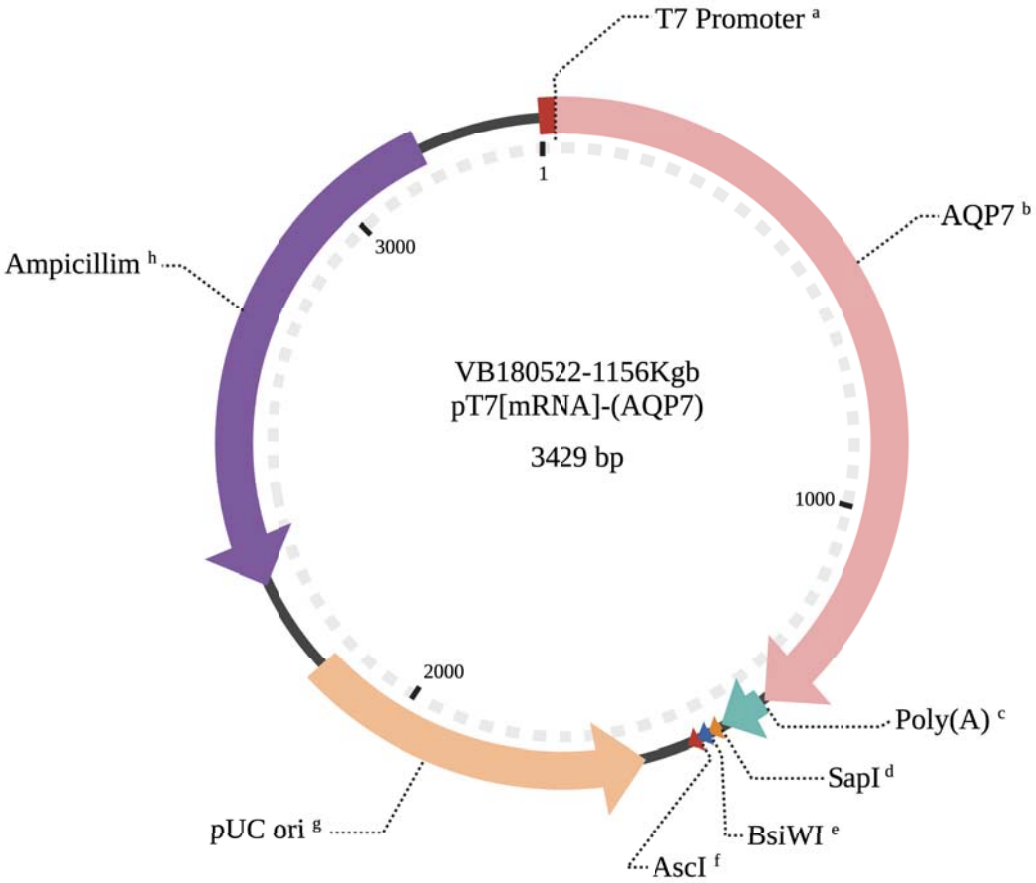

Figure 1. Composition of the pT7/bovine AQP7 plasmid. [a] T7 RNA polymerase promoter. [b] AQP7 transcribed sequence. [c] Synthetic poly(A)30 region. [d] SapI restriction site. [e] BsiWI restriction site. [f] AscI restriction site. [g]pUC origin of replication. [h]Ampicillin resistance gene.

2.5. Microinjection of AQP7 cRNA into bovine oocytes

Immature bovine oocytes at the GV stage were collected from ovaries bathed in PBS. Around 150 oocytes were pooled and used in each experiment. Cumulus cells surrounding oocytes were removed by repeatedly pipetting them in PBS medium, and groups of 20 COCs with normal size and color were placed in 25 μL drops of HM covered with mineral oil in a Petri dish (60 × 15 mm). An oocyte was immobilized with a holding pipette (outer diameter, 100 μm; MPHL-35, Life Global group, Guiford, United States) connected to a micromanipulator on an inverted microscope (Zeiss Axio Vert A1, Germany) and injected with an injection needle (MPIC-30L, Life Global group, Guiford, United States) connected to another micromanipulator. Oocytes were injected with ~10 pL of water solution containing EGFP cRNA alone (30 ng/μL), or together with AQP7 cRNA (50 ng/μL). Non-injected oocytes (intact oocytes) served as control. Both non-injected and injected

oocytes were cultured at 38.5°C in a humidified CO_2 incubator (5% CO_2) for up 24 h in IVM medium. Microinjected oocytes were supplemented with intact COCs (1:1 ratio) during *in vitro* maturation to improve the developmental capability of oocytes deprived of their CCs investment (Luciano *et al.* 2005). Oocyte survival was assessed at after IVM and only live oocytes showing a polar body were classified as matured and used as non-injected (control), EGFP cRNA-injected or EGFP+AQP7 cRNA-injected oocytes. Oocyte survival was evaluated on the basis of the integrity of the oocyte membrane and the zona pellucida together with the discoloration of the cytoplasm.

2.6. Expression of AQP7 in cRNA-Injected Oocytes

At 24 h of IVM, cumulus- free EGFP-positive and non-injected oocytes showing the first polar body were fixed in 2% (w/v) paraformaldehyde–phosphate buffer saline (PBS) for 30 min. Imnunostaining for AQP7 expression was carried out as described in section 2.3 except that oocytes were incubated with rabbit anti-AQP7 antibody (NBP1–30862; Novus Biologicals, USA) (1:200) overnight at 4°C, followed by incubation with goat Alexa Fluor™ 568-conjugated anti-rabbit IgG antibody (A11011, Life technologies, Carlsbad, CA, USA) (1:700) for 1 h. A laser-scanning confocal microscope (Leica TCS SP5, Leica Microsystems, Mannheim, Germany) was used to examine AQP7 (Alexa Fluor™ 568; excitation 568 nm) and chromatin (DAPI; excitation 405 nm) staining. The overlay image resulting from the capture of the different channels showed AQP7 and nuclei as red and blue, respectively. When EGFP was included, a 488-nm excitation was used for its detection and the ooplasm was stained in green. After subtracting the background, fluorescence mean intensity for AQP7 expressed in arbitrary fluorescence units (pixel) of 74 (30, 15, and 29) different cells of 3 representative experiments was quantified using Image-J software. Values for the fluorescence signal intensity of the cells stained with AQPs antibodies were normalized to the value of the corresponding control samples, arbitrarily set as 100%.

2.7. Measurement of permeability to water and cryoprotectants

After 22-24 h of culture, mature MII oocytes (i.e. with polar body) were freed of cumulus cells by gentle pipetting and used for permeability experiments following the methods described previously by Edashige et al. (Edashige *et al.* 2003) with some modifications. Only a limited number of matured oocytes were used for oocyte permeability assessment because measurement was done between 22-24 h of IVM to avoid the use of overmatured oocytes.

In brief, each oocyte was placed in a 25 μL drop of HM covered with mineral oil in, and was held with a holding pipette (outer diameter, 95-120 μm; MPH-MED-30, Origio, Denmark) connected to a micromanipulator on an inverted microscope (Zeiss Axio Vert A1, Germany). An initial photograph was taken of the oocyte in order to calculate the initial volume. The oocyte was then covered with another pipette with a larger inner diameter (600-μm diameter) (G-1 Narishigue, Tokyo, Japan) connected to a different micromanipulator. Then, by sliding the dish and removing the covering pipette the oocyte was abruptly exposed to 25 μL drop of HM containing 0.5 M sucrose, 9.5% (v/v 1.2 M) Me_2SO or 8% (v/v 1.3 M) EG at 25ºC during 5 min. Permeability values of non-injected and AQP7 cRNA-injected oocytes to water and CPAs were determined from changes in oocyte volume while suspended in HM containing sucrose, Me_2SO or EG for 5 min at 25ºC. The cell volume response of the oocyte during the experiments was recorded every 5 s with a time-lapse video recorder (Zeiss Zen imaging software/Axiocam ERc 5s). The volume of the oocyte in each image was calculated from the area of the cross section using ImageJ software (National Institutes of Health, Bethesda, MD, USA). Only oocytes that maintain an approximate spherical geometry were individually analyzed. The Lp and Ps of the bovine oocyte were estimated, based on the change in concentration of the solutes and the original volume of the oocyte, by fitting the movement of water and cryoprotectants by using a two-parameter (2P) formalism as described previously (Jacobs and Stewart 1932; Jacobs 1933; Kleinhans 1998).

Briefly, the 2P model provides a description of the osmotic responses of cells in solutions with both permeating and nonpermeating solutes. In this formalism, the water flux into the cell over time is expressed as:

$$\frac{dV_w}{dt} = -L_p ART(M^e - M^i) \quad (1)$$

where V_w is the cell water volume, L_p is the membrane hydraulic conductivity, A is the area of the plasma membrane, R is the universal gas constant, T is the absolute temperature, and M^e and M^i are the total external and internal osmolalities, respectively.

The rate of CPA transport is given by:

$$\frac{dN_s}{dt} = P_s A(M_s^e - M_s^i) \quad (2)$$

where N_s is the intracellular moles of CPA, P_s is the CPA permeability, M^i_s and M^e_s are the intracellular and extracellular CPA molality, respectively. To obtain the intracellular CPA volume, it is necessary to multiply by the partial molar volume of the CPA, υ_s, resulting in

$$V_s = \upsilon_s N_s \quad (3)$$

Then the total cell volume (V_c) is just the sum of the water (V_w), CPA (V_s), and solids (V_b) volumes:

$$V_c = V_w + V_s + V_b \quad (4)$$

The differential equations (equations (1) and (2) for the 2P model) were solved in Matlab software using the ode45 function, which implements an explicit Runge-Kutta formula (Dormand and Prince 1980; Shampine and Reichelt 1997). To estimate the permeability values, model predictions were fit to the data by minimizing the sum of the error squared in Matlab using the fminsearch function, which implements the Nelder-Mead simplex algorithm (Lagarias *et al.* 1998). The various constants and parameters appearing in the equations are listed in Table 1.

Table 1. Constant and parameters used in 2P model.

Description	**Values**	**Symbol**
Universal gas constant	8.314 m^3 Pa K^{-1} mol^{-1}	R
Absolute temperature	298 K	T
Partial molar volume of water	18.02 x10^{12}μm^3mol^{-1}	υ_w
Partial molar volume of CPA:		
– EG [a]	55.8×10-6 m^3 mol^{-1}	υ_s
– Me_2SO [a]	71.3×10-6 m^3 mol^{-1}	
Osmotically inactive volume (MII oocytes):	0.25 (Ruffing *et al.* 1993; Jin *et al.* 2011)	V_b

[a] Partial molar volumes of cryoprotectants from Vian et al (Vian and Higgins 2014).

Abbreviations: CPA, cryoprotectant; EG, ethylene glycol; Me_2SO, dimethyl sulfoxide; MII, metaphase II.

2.9. Experimental design

Experiment 1. Analysis of AQP3, AQP7 and AQP9 expression in oocytes after treatment with cryoprotection solutions

To analyze AQP3, AQP7 and AQP9 expression after exposure of *in vitro* bovine oocytes to hyperosmotic CPA solutions, IVM bovine oocytes were treated with holding medium containing 9.5% Me_2SO, 8% EG, or 0.5 M sucrose for 20 min at 25ºC. Oocytes in holding medium alone were used as controls. The oocytes were then collected and fixed immediately. The AQP3, AQP7 or AQP9 protein levels were analyzed with immunofluorescence

Experiment 2. Measurement of permeability to water and cryoprotectants of *in vitro* matured oocytes in which AQP7 was artificially overexpressed

To determine if bovine oocytes were able to translate the bovine AQP7, GV-stage oocytes were injected with EGFP or EGFP+AQP7 cRNA followed by assessment of AQP7 protein expression by immunofluorescence after *in vitro* oocyte maturation. A third group of non-injected oocytes was used as an additional control.

For permeability measurement, cumulus-free IVM oocytes from control (non-injected oocytes), EGFP, and EGFP+AQP7 groups were freed of cumulus cells by gentle pipetting and abruptly exposed to HM containing 0.5 M sucrose, 9.5% (v/v) Me_2SO or 8% (v/v) EG at 25ºC during 5 min. The cell volume response of the oocyte during the experiments was recorded every 5 s with a time-lapse video recorder. The volume of the oocyte in each image was calculated from the area of the cross section using ImageJ software.

2.10. Statistical analyses

All data sets were analyzed for normalcy and homoscedasticity using the Shapiro-Wilk normality test and Levene's test, respectively. Non-normal data distribution was restored using log(x+1) transformation prior analysis. To determine if there was a significant relationship between the maturation data and the groups of the study, data were analyzed by Fisher's exact test. Additionally, the relationship between the % survival and % EGFP in the microinjected groups was also analyzed. The immunofluorescent and permeability data were analyzed by one-way ANOVA tests, followed by Tukey's multiple comparison test. A non-parametric alternative (Kruskal-Wallis test) was used in data that did not meet the assumptions of the one-way ANOVA test, followed by pairwise Wilcoxon rank-sum

tests. R software version 3.6.1 (Team 2006) was used to conduct the statistical analyses. The threshold for significance was set at $p < 0.05$.

3. Results

3.1. Analysis of AQP3, AQP7 and AQP9 expression in oocytes after treatment with cryoprotection solutions

In this study, IVM bovine oocytes were exposed to hypertonic solutions of two permeable cryoprotectants (Me_2SO and EG) and a non-penetrating cryoprotectant (sucrose) to examine whether hyperosmotic stress induced changes on the expression of AQP3, AQP7 and AQP9. Immunofluorescence revealed that AQP7 protein expression increased ($p < 0.05$) when bovine oocytes were exposed to EG while no changes on AQP7 fluorescence intensity was observed when oocytes were exposed to Me_2SO or sucrose when compared to the control group. Besides, exposure to Me_2SO significantly ($p < 0.05$) increased AQP3 protein expression while no changes were observed after exposure to EG or sucrose (Figure 2B). No variations on AQP9 expression were observed after exposures of IVM bovine oocytes to EG, Me_2SO or sucrose (data not shown).

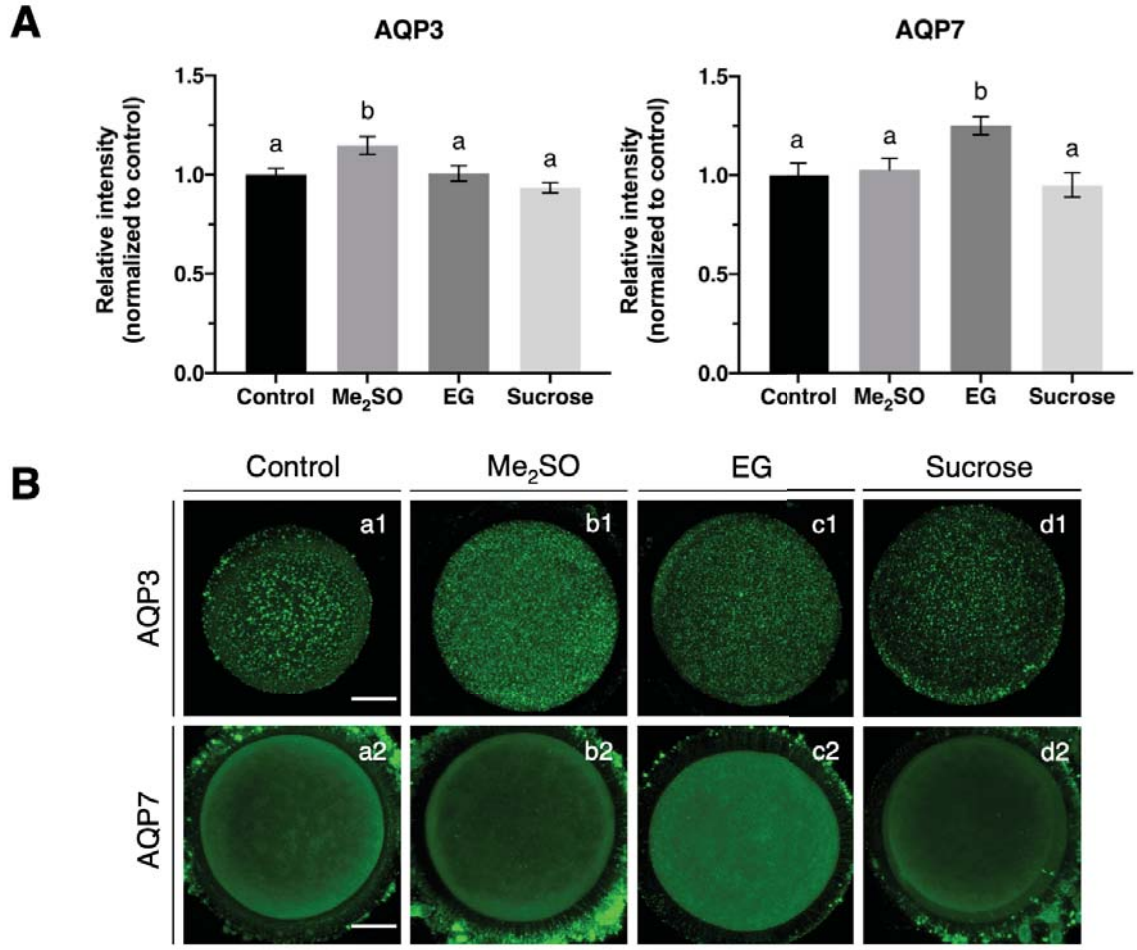

Figure 2. Effect of the exposure of IVM bovine oocytes to hyperosmotic CPA solutions on the levels of expression of AQP3 and AQP7. A) Relative immunofluorescence intensities for AQP3 (1) and AQP7 (2) expression in bovine oocytes when exposed to 9.5% Me_2SO, 8% EG or 0.5 M sucrose, respectively. Values for the fluorescence signal intensity of the cells stained with AQPs antibodies were normalized to the value of the corresponding control samples, arbitrarily set as 100%. Data are presented as the mean ± SEM. [a,b] Different letters within columns differ significantly ($P<0.05$). B) Laser scanning confocal microscopy images of AQP3 and AQP7 IVM bovine oocytes. Untreated MII oocytes (a) or IVM oocytes exposed to (b) 9.5% Me_2SO, (c) 8% EG, or (d) 0.5 M sucrose and stained with antibodies against AQP3 and AQP7. Scale bar, 30 μm.

3.2. Measurement of permeability to water and cryoprotectants of *in vitro* matured oocytes in which AQP7 was artificially overexpressed

Because the role of AQP3 in the movement of water and cryoprotectants in mouse and bovine oocytes has been already described (Edashige *et al.* 2003; Jin *et al.* 2011), we examined artificial over-expression of AQP7, through cRNA injection, to elucidate

whether aquaporin 7 is involved in the rapid movement of water and CPA in bovine *in vitro* matured oocytes.

Highly specific expression was observed in *in vitro* matured oocyte when APQ7 protein expression was assessed by immunofluorescence (Figure 3A). While immunofluorescence intensity for AQP7 in EGFP cRNA-injected bovine oocytes was similar to the non-injected, EGFP+AQP7 cRNA-injected bovine stained significantly stronger when compared to non-injected or EGFP cRNA-injected oocytes, indicating that AQP7 protein can be synthesized and overexpressed in bovine oocytes during *in vitro* maturation (Figure 3). Co-injection of EGFP cRNA with cRNA encoding AQP7 and further immunostaining for AQP7 demonstrated that 100% of oocytes expressing EGFP also co-expressed AQP7.

The percentage of oocytes that survived to the microinjection respect to the total number of injected oocytes was 71.48 ± 8.15% and 62.11 ± 2.25 % for EGFP and EGFP+AQP7 cRNA-injected oocytes, respectively (Table 2). When positive EGFP protein expression was assessed in lived oocytes after IVM, no differences between EGFP and EGFP-AQP7 cRNA-injected oocytes were observed (88.31% and 82.88%, respectively). The maturation rates of both EGFP and EGFP+AQP7 cRNA-injected oocytes after 24 h of culture, measured as the number of oocytes that reached the metaphase II stage over the total number of survived oocytes, was significantly reduced by approximately 20% with respect to the noninjected oocytes (Table 2).

Due to the similar efficiency expression of AQP7 and EGFP in bovine oocytes, we used an oocyte selection method based on the co-expression of enhanced green fluorescent protein (EGFP) (Ohashi et al., 2001).

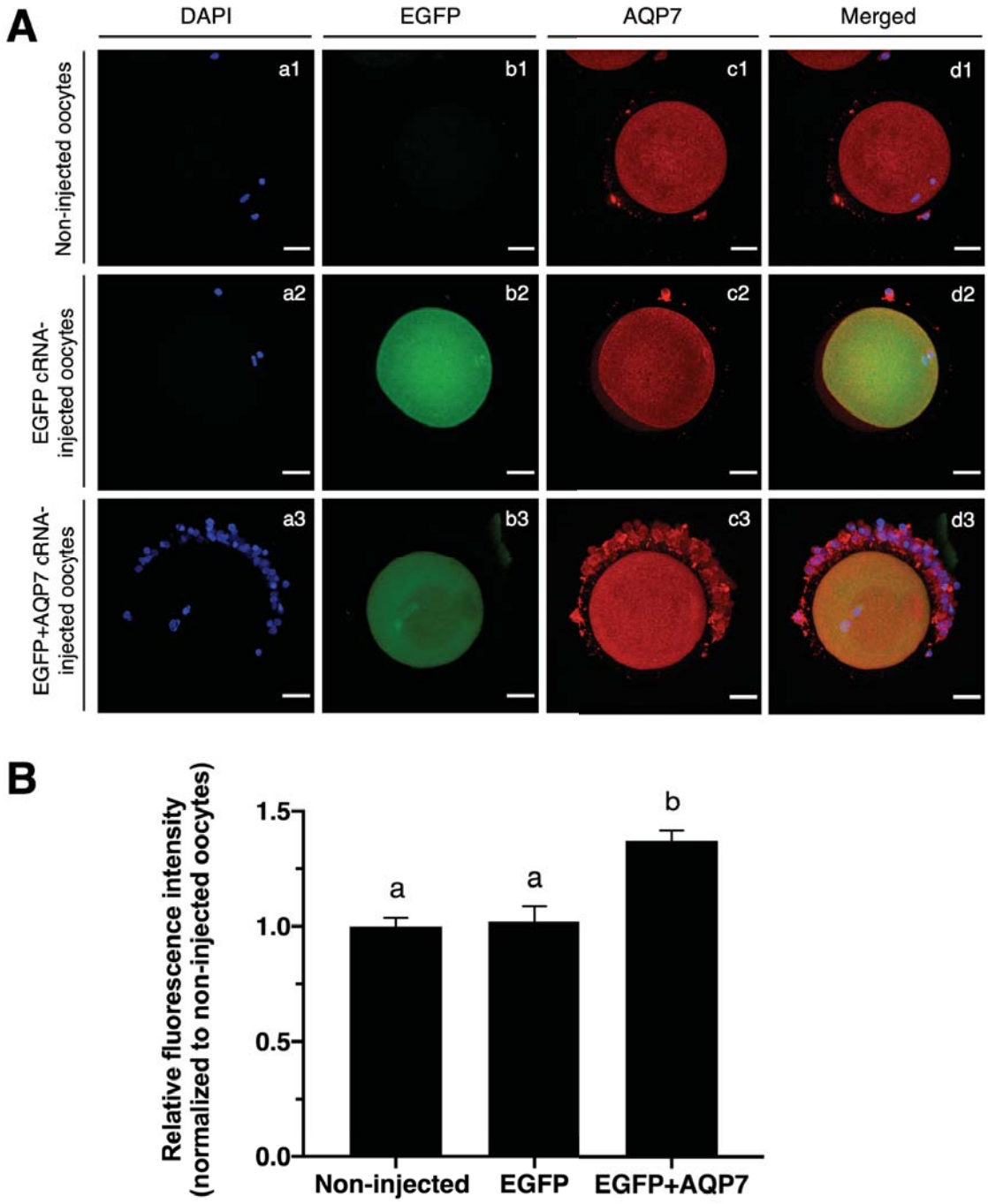

Figure 3. Exogenous expression of EGFP and AQP7 cRNA in bovine MII oocytes. (A) Representative confocal laser-scanning photomicrographs of non-injected (1), EGFP cRNA-injected (2) and EGFP+AQP7 cRNA-injected (3) oocytes. Nuclei counterstained with DAPI are displayed in blue (a1-a3), EGFP expression is displayed in green (b1-b3) and AQP7 protein expression is displayed in red (c1-c3). Overlayed images are presented in d1-d3. Scale bar, 30 μm. (B) Quantification of APQ7 signal intensities in control (non-injected), EGFP injected- and EGFP + AQP7 injected-oocytes. Labeling intensity was expressed relative to that of the control oocytes (set as 100%). Unless indicated otherwise,

data are given as the mean ± SEM. Values with different letters differ significantly ($P<0.05$). The experiments were replicated three times. In each replication, n=5-10 per group.

Table 2. Efficiency of injection of EGFP cRNA or together with AQP7 in GV bovine oocytes on the survival rate, EGFP protein expression and maturation rate at 24 of IVM.

Treatment	n	% Survival	% EGFP *	%AQP7§	% MII #
Non-injected	105	100 [a]	-	-	74.73 ± 1.93[a]
EGFP	84	71.48 ± 8.15 [b]	88.31 ± 9.36	100	56.55 ± 3.92[b]
EGFP+AQP7	135	62.11 ± 2.25 [b]	82.88 ± 4.25	100	56.54 ± 1.24[b]

Unless indicated otherwise, data are given as the mean ± SEM. Within columns, values with different superscript letters differ significantly ($P<0.05$).

*Rates of oocytes with positive EGFP expression were calculated from the total number of lived oocytes after microinjection.

§ Percentage of oocytes expressing AQP7, assessed by immunofluorescence microscopy, with respect to the oocytes expressing EGFP.

Maturation rate was calculated by using the ratio of oocytes attaining Metaphase II over the total number of lived oocytes.

3.3. Permeability to water and cryoprotectants of AQP7 cRNA-injected oocytes

To examine whether expression of EGFP alone or in combination with AQP7 increased the water permeability properties of bovine MII oocytes, we determined the changes in the cell volume of oocytes during 5 min of exposure to HM containing 0.5 M sucrose at 25°C (Figure 4). Overall, in a hypertonic sucrose solution, oocytes from all groups shrank quickly during the first minute and then decrease their shrinkage rate, indicating that they were slowly reaching equilibrium (Figure 4B). Nevertheless, comparing between treatment groups, both non-injected and EGFP cRNA-injected oocytes shrank quite slowly and did not differ in volume change (55% and 54%, respectively, in 1 min), suggesting that EGFP-injected oocytes have the same low-permeability as intact oocytes. On the other hand, EGFP+AQP7 cRNA-injected oocytes shrank very rapidly (50% in 30 s) (Figure 4B), indicating that the permeability to water of MII bovine oocytes was

markedly increased by the injection of AQP7 cRNA. Consequently, the hydraulic conductivity (Lp) calculated from the volume changes of the EGFP+AQP7 cRNA injected oocytes was 3.06± 0.24 μm/atm×min, about 1.7 times higher than that of the non-injected and EGFP cRNA injected oocytes (1.85 ± 0.10 and 1.80 ± 0.12 μm/atm×min, respectively) (Table 3). These results indicate that the AQP7 expressed in the oocytes functioned as a water channel and that exogenous expression of AQP7 enhanced the permeability to water of the MII bovine oocytes.

To evaluate if the exogenous expression of AQP7 in oocytes can also improve cryoprotectant permeability, changes in the cell volume of non-injected, EGFP cRNA or EGFP+AQP7cRNA-injected bovine oocytes during 5 min of suspension in HM containing 9.5% Me_2SO or 8% EG at 25ºC were assessed (Figure 5). In a dimethyl sulfoxide solution, EGFP+AQP7 cRNA-injected oocytes shrank quite rapidly to 60% of their isotonic volume in 12 s but regained their volume slowly (95% in 3 min). On the other hand, there was no appreciable difference in volumes between non-injected and EGFP cRNA-injected oocytes. Both shrank relatively slowly to 67% (in 12 s) of their isotonic volume and regained their volume slowly (94% in 3 min) (Figure 5B). In accordance with the changes in oocyte volume, the P_{Me2SO} values for non-injected, EGFP cRNA and EGFP+AQP7 cRNA-injected oocytes were similar (0.59 ± 0.05, 0.58 ± 0.05 and 0.57 ± 0.04 μm/sec, respectively) (Table 5). Nevertheless, the Lp value for EGFP+AQP7 cRNA-injected oocytes (4.01 ± 0.56 μm/atm×min) was much higher than that of non-injected (1.91 ± 0.13 μm/atm×min) and EGFP cRNA-injected (1.98 ± 0.24 μm/atm×min) oocytes (Table 4).

In an ethylene glycol solution, oocytes shrank slowly (72-76% in 22 s) and regained their volume slowly (93%– 96% in 3 min), regardless of the injection of EGFP or EGFP+AQP7 cRNA (Figure 5D). Therefore, the L_p and P_{EG} value for AQP7 cRNA-injected oocytes (1.39 ± 0.11 μm/atm×min and 0.76 ± 0.10 μm/s, respectively) was similar to that for non-injected (1.38 ± 0.12 μm/atm×min and 0.78 ± 0.09 μm/s, respectively) and EGFP cRNA-injected (1.44 ± 0.10 μm/atm×min and 1.04 ± 0.17 μm/s, respectively) oocytes (Table 4 and 5).

Table 3. Hydraulic conductivity (Lp) of bovine oocytes injected with EGFP alone or EGFP + AQP7 cRNA exposed to HM medium containing 0.5 M sucrose at 25ºC.

Treatment	Sucrose
Non-injected	1.85 ± 0.10 [a]
EGFP	1.80 ± 0.12 [a]
EGFP+AQP7	3.06 ± 0.24 [b]

The Lp (μm/atm×min) values were assessed from data shown in Figure 4. Data are given as the mean ± SEM. Within columns, values with different superscript letters differ significantly (P<0.05). Non-injected oocytes: n = 10; EGFP cRNA-injected oocytes: n= 12; and EGFP+AQP7 cRNA-injected oocytes: n= 12.

Table 4. Hydraulic conductivity (Lp) of bovine oocytes injected with EGFP alone or EGFP + AQP7 cRNA exposed to HM medium containing 9.5% Me_2SO or 8% EG at 25ºC.

Treatment	Me_2SO	EG
Non-injected	1.91 ± 0.13 [a]	1.38 ± 0.12 [a]
EGFP	1.98 ± 0.24 [a]	1.44 ± 0.10 [a]
EGFP+AQP7	4.01 ± 0.56 [b]	1.39 ± 0.11 [a]

The Lp (μm/atm×min) values were assessed from data shown in Figure 5. Data are given as the mean ± SEM. Within columns, values with different superscript letters differ significantly (P<0.05). Me_2SO: Non-injected oocytes: Me_2SO n = 13; EG n= 14; EGFP cRNA-injected oocytes: Me_2SO n = 10; EG n= 11; and EGFP+AQP7 cRNA-injected oocytes: Me_2SO n = 11; EG n= 13.

Table 5. Permeability to cryoprotectants (Ps) of bovine oocytes injected with EGFP alone or EGFP + AQP7 cRNA measured in HM medium containing 9.5% Me_2SO or 8% EG at 25ºC.

Treatment	Me_2SO	EG
Non-injected	0.59 ± 0.05	0.78 ± 0.09
EGFP	0.58 ± 0.05	1.04 ± 0.17
EGFP+AQP7	0.57 ± 0.04	0.76 ± 0.10

The Ps (μm/s) values were determined from the data shown in Figure 5. Data are given as the mean ± SEM. Within columns, values with different superscript letters differ significantly (P<0.05). Me_2SO: Non-injected oocytes: Me_2SO n = 13; EG n= 14; EGFP cRNA-injected oocytes: Me_2SO n = 10; EG n= 11; and EGFP+AQP7 cRNA-injected oocytes: Me_2SO n = 11; EG n= 13.

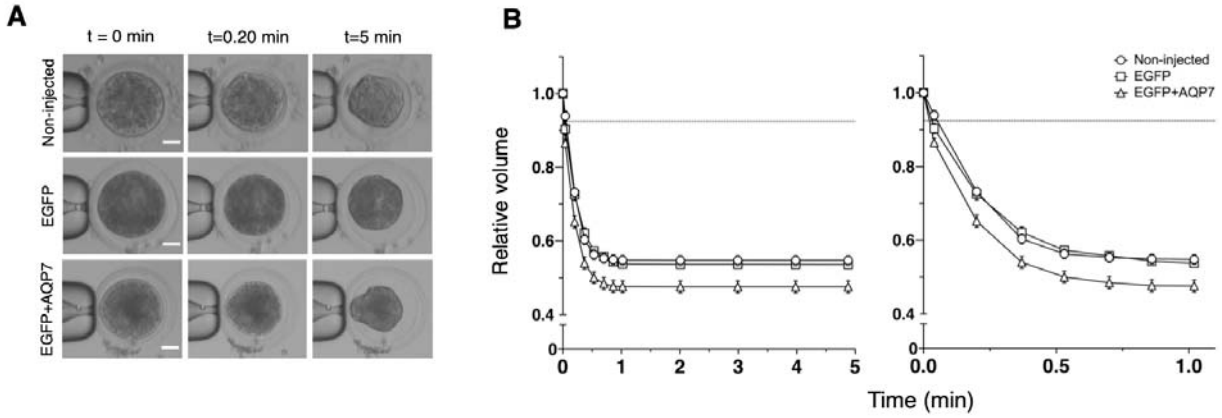

Figure 4. Osmotic behavior of non-injected MII bovine oocytes (circles), EGFP cRNA-injected (squares), or EGFP + AQP7 cRNA-injected-oocytes (triangles) exposed to 0.5 M sucrose for 5 min at 25ºC. (A) Representative phase-contrast microscopy images of oocytes measured in B. Scale bar, 30 μm. (B) Summary data represented as the relative mean volume ± SEM. Non-injected oocytes: n=10; EGFP cRNA-injected oocytes: n=12 and EGFP+AQP7 cRNA-injected oocytes: n=12.

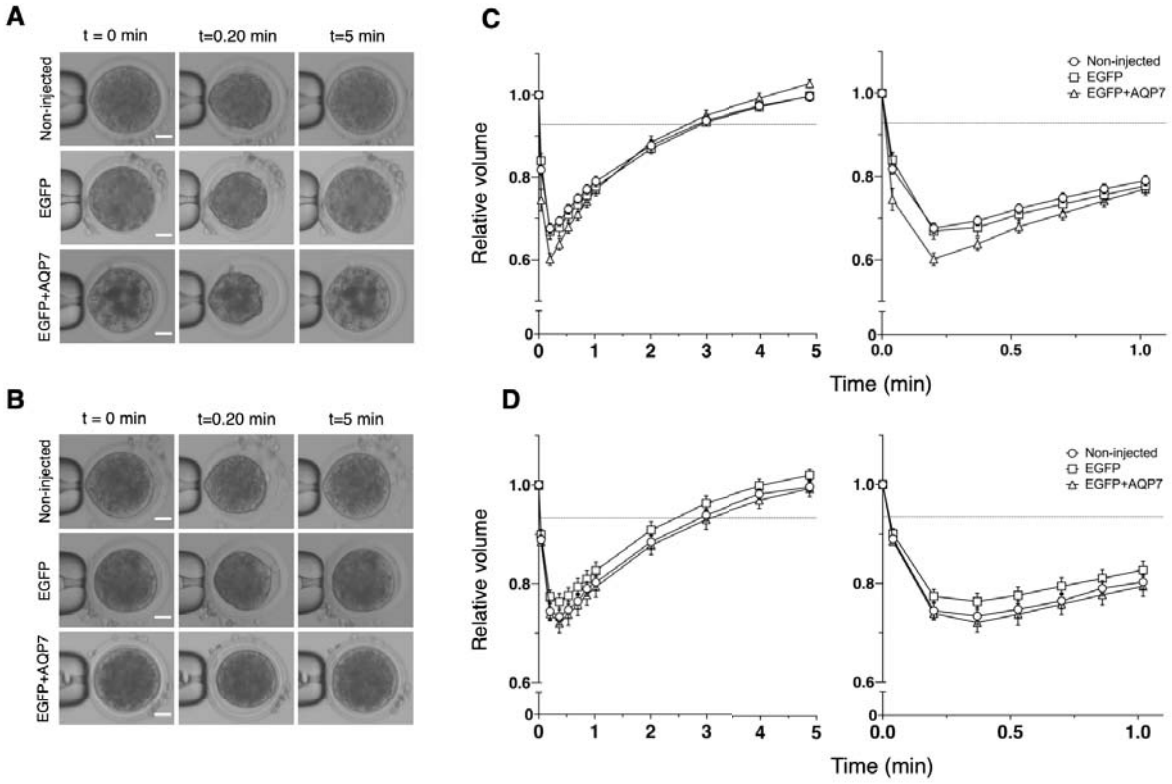

Figure 5. Osmotic behavior of non-injected MII bovine oocytes (circles), EGFP cRNA-injected (squares), or EGFP + AQP7 cRNA-injected-oocytes (triangles) exposed to 9.5% Me_2SO or 8% EG for 5 min at 25ºC (A and B respectively). (A, B) Representative phase-contrast microscopy images of oocytes measured in C and D are shown. Scale bar = 30 μm. (C,D) Summary data represented as the relative mean volume ± SEM. Non-injected oocytes: Me_2SO n = 13; EG n= 14; EGFP cRNA-injected oocytes: Me_2SO n = 10; EG n= 11; and EGFP+AQP7 cRNA-injected oocytes: Me_2SO n = 11; EG n= 13.

4. Discussion

Permeability of the plasma membrane to water and CPA is essential for cell survival during cryopreservation. Whereas transport rates of water and CPAs across the plasma membrane are low in simple diffusion, they are much higher in facilitated diffusion where AQPs are involved (Jin *et al.* 2011). In this context, AQPs are crucial to prevent osmotic-induced damage, one of the major risks of cryopreservation protocols. Aquaporins in the plasma membrane and mainly those members of the aquaglyceroporin subfamily, which includes AQP3, AQP7 and AQP9, play an important role in facilitating water and CPA movement because aquaglyceroporins are permeable not only to water but also to small neutral solutes (Huang *et al.* 2006; Sales *et al.* 2013; Edashige 2017). In the present study, we demonstrated that cryoprotectants stimulated AQP3 and AQP7 but not AQP9 expression in mature

bovine oocytes. In particular, we observed that exposure of oocytes to hyperosmotic Me_2SO solution could upregulate AQP3 while AQP7 expression was upregulated after EG hyperosmotic exposure. The aquaglyceroporin expression in oocytes after exposure to CPA has previously been reported. Murine oocytes exposed to a hyperosmotic CPA solution containing EG, Me_2SO or sucrose increased the expression of AQP7, but not of AQP3 and AQP9 (Tan *et al.* 2013; Tan *et al.* 2015). Results obtained so far both in bovine and mouse oocytes may indicate that aquaporin upregulation in oocytes due to hyperosmosis it is not only species-specific, but also depends on the cryoprotectant itself.

Upregulation of AQP3 expression in oocytes induced by Me_2SO is not only due to hyperosmolarity, because up-regulation of AQP3 by Me_2SO was much greater than that induced by sucrose or by EG at the same osmolarity. The same applies to the up-regulation of AQP7 expression by EG. These results suggest that Me_2SO may stimulate AQP3 expression or EG may promote AQP7 expression in oocytes not only by increasing osmolarity but also by direct effects on AQP3 or AQP7 gene transcription and/or translation (Tan *et al.* 2013). The mechanisms involved in CPA-induced AQP expression are unclear. The fully grown oocyte itself is essentially transcriptionally silent, although recent data do suggest that some small degree of transcriptional activity may still occur in this period (Balboula *et al.* 2010). The oocytes rely on regulation of pre-existing transcripts to precisely regulate the maturation process, therefore, oocyte developmental competence relies on both the constitution of an adequate pool of RNA in immature oocytes and highly orchestrated regulation of the stability and processing of these mRNAs during maturation before transcription resumes during embryonic genome activation (Kang and Han 2011). The stability of mRNA has been shown to be regulated by the mitogen-activated protein kinase (MAPK) signaling pathway (Sugiura *et al.* 2011). Hyperosmotic treatment activates the MAPK14/11 pathway in the embryo and in other cell types (Arima *et al.* 2003; Fong *et al.* 2007). Moreover, MAPK signaling regulates aquaporin 3 and 9 expression and localization in preimplantation embryos regulation (Bell *et al.* 2009). It is not clear whether the mechanisms involved in the upregulation of aquaporins by CPAs in MII bovine oocytes are similar to those in preimplantation embryos. Tan et al study demonstrated that AQP7 in mouse oocytes may mediate tolerance to hyperosmotic stress during cryopreservation through the activation of the Aurora A/CPEB pathway mediated by PI3K and PKC to upregulate AQP7 expression. Moreover, F-actin may play an important role in AQP7 intracellular trafficking from the cytoplasm to the cell membrane (Tan *et al.* 2015).

Upregulation of the water transport capacity of the cell membrane with aquaporins can improve the osmotic flow generated by an osmotic gradient. In order to determine whether ectopic expression of AQP7 could increase water and CPA permeability, exogenous expression of bovine AQP7 in MII bovine oocytes was examined. In our study, we successfully over-expressed bovine AQP7 channel in bovine MII oocytes by cRNA microinjection at the germinal vesicle stage. Thus, bovine oocytes are able to translate and integrate exogenous aquaporins in the plasma membrane during IVM, as found for murine, amphibian, and porcine oocytes (Edashige *et al.* 2003; Chauvigné *et al.* 2011; Jin *et al.* 2011; Valdez *et al.* 2013; Morató *et al.* 2014). Viability or competence of oocytes to resume meiosis *in vitro* was lower for microinjected oocytes compared to non-injected oocytes, probably caused by the microinjection injury or to the presence of an exogenous cRNA. However, the rate of EGFP protein expression in the injected bovine oocytes was high (≈86%) when compared to previous studies in which AQP3 was microinjected in immature porcine oocytes (Ohashi *et al.* 2001; Morató *et al.* 2014), suggesting a higher capacity of bovine oocytes to translate and integrate exogenous aquaporins. Moreover, EGFP is a good proxy for the expression of other proteins because all of the EGFP-positive oocytes also contained high levels of AQP7 protein located in the cytoplasm and around the plasma membrane.

The aquaglyceroporin role on CPA permeability during dehydration and swelling of IVM bovine oocytes has previously been reported (Edashige *et al.* 2003). Edashige´s research group showed that permeability of bovine oocytes to water and cryoprotectants was low but higher than in mouse oocytes. The Lp and Ps values for MII bovine oocytes determined in this study were higher than those determined by Agca et al(Agca *et al.* 1998b) and Jin et al(Jin *et al.* 2011) in the presence of Me_2SO and EG. However, permeability to water in the presence of sucrose was similar to other studies (Jin *et al.* 2011) meaning a higher difference in water and CPA permeability between bovine and mouse MII oocytes (Jin *et al.* 2011). Moreover, in this study, the authors observed that water and CPAs move through cow oocytes predominantly by simple diffusion but suggested that other water and CPA channels could be involved in the relatively high membrane permeability of bovine oocytes. When exogenous expression of bovine AQP3 in mouse oocytes was examined (Jin *et al.* 2011), the authors demonstrated that bovine AQP3 increased water permeability in a hypertonic sucrose solution, a glycerol solution, and a Me_2SO solution but not in an ethylene glycol solution and a propylene glycol solution, as occurred in mouse AQP3 (Edashige *et al.* 2007). Similarly, our study demonstrated that after injection of

EGFP+AQP7 cRNA and 24 h of IVM, water permeability increased almost 2 times compared to non-injected oocytes when oocytes were exposed to sucrose and Me_2SO solution. However, this tendency was not observed in an EG solution, similar to previous results (Jin *et al.* 2011). Our results together with those observed by Jin et al (Jin *et al.* 2011) suggest that both, AQP3 and AQP7, are involved in water movement when oocytes are exposed to sucrose or Me_2SO solution, whereas water diffusion mainly happens through simple diffusion when oocytes are exposed to EG.

Moreover, it has seen that overexpression of AQPs not only enhance water permeability but also CPA permeability, thus improving oocyte survival after warming mouse oocytes (Edashige *et al.* 2003; Morató *et al.* 2014). In fact, Jin et al (Jin *et al.* 2011) demonstrated that the exogenous expression of bovine AQP3, also increase the permeability to EG (P_{EG}) showing 13 times higher permeability than that for non-injected oocytes contrarily to our results, where P_{EG} was not altered after microinject oocytes with AQP7 cRNA, which suggest that some EG molecules moves through AQP3 but not AQP7 channels when the oocyte is suspended in a EG solution. Similar to our results, AQP3 (Jin *et al.* 2011) or AQP7 cRNA-injected oocytes had similar permeability to Me_2SO than non-injected oocytes, suggesting that Me_2SO move by simple diffusion across oocyte plasma membrane.

In conclusion, *in vitro* matured oocytes express AQP3 and AQP7 but not AQP9 when exposed to hyperosmotic solution. Me_2SO up-regulates AQP3 expression while EG up-regulates AQP7 expression in oocytes in an CPA-dependent fashion. We also demonstrated that exogenous expression of aquaglyceroporins such as AQP7 is possible in *in vitro* matured oocytes, and that these oocytes are more permeable to water. Therefore, a higher permeability to water of bovine oocytes through the overexpression of AQP7 channels may be a useful approach to decrease osmotic stress induced by the vitrification-warming process. Further studies are underway to investigate if overexpression of AQP7 improves the survival rates and further embryo development of vitrified/warmed *in vitro* bovine oocytes.

References

Agca, Y., Liu, J., Critser, E.S., McGrath, J.J., and Critser, J.K. (1999) Temperature-dependent osmotic behavior of germinal vesicle and metaphase II stage bovine oocytes in the presence of Me2SO in relationship to cryobiology. *Mol Reprod Dev* **53**(1), 59-67

Agca, Y., Liu, J., McGrath, J.J., Peter, A.T., Critser, E.S., and Critser, J.K. (1998a) Membrane permeability characteristics of metaphase II mouse oocytes at various temperatures in the presence of Me2SO. *Cryobiology* **36**(4), 287-300

Agca, Y., Liu, J., Peter, A.T., Critser, E.S., and Critser, J.K. (1998b) Effect of developmental stage on bovine oocyte plasma membrane water and cryoprotectant permeability characteristics. *Mol Reprod Dev* **49**(4), 408-15

Arima, H., Yamamoto, N., Sobue, K., Umenishi, F., Tada, T., Katsuya, H., and Asai, K. (2003) Hyperosmolar mannitol simulates expression of aquaporins 4 and 9 through a p38 mitogen-activated protein kinase-dependent pathway in rat astrocytes. *J Biol Chem* **278**(45), 44525-34

Balboula, A.Z., Yamanaka, K., Sakatani, M., Hegab, A.O., Zaabel, S.M., and Takahashi, M. (2010) Intracellular cathepsin B activity is inversely correlated with the quality and developmental competence of bovine preimplantation embryos. *Mol Reprod Dev* **77**(12), 1031-9

Bell, C.E., Lariviere, N.M., Watson, P.H., and Watson, A.J. (2009) Mitogen-activated protein kinase (MAPK) pathways mediate embryonic responses to culture medium osmolarity by regulating Aquaporin 3 and 9 expression and localization, as well as embryonic apoptosis. *Hum Reprod* **24**(6), 1373-86

Benson, J.D., Kearsley, A.J., and Higgins, A.Z. (2012) Mathematical optimization of procedures for cryoprotectant equilibration using a toxicity cost function. *Cryobiology* **64**(3), 144-51

Chauvigné, F., Lubzens, E., and Cerdà, J. (2011) Design and characterization of genetically engineered zebrafish aquaporin-3 mutants highly permeable to the cryoprotectant ethylene glycol. *BMC Biotechnol* **11**, 34

Díez, C., Muñoz, M., Caamaño, J.N., and Gómez, E. (2012) Cryopreservation of the bovine oocyte: current status and perspectives. *Reprod Domest Anim* **47 Suppl 3**, 76-83

Dormand, J.R., and Prince, P.J. (1980) A family of embedded Runge-Kutta formulae. *Journal of Computational and Applied Mathematics* **6**(1), 19-26

Edashige, K. (2017) Permeability of the plasma membrane to water and cryoprotectants in mammalian oocytes and embryos: Its relevance to vitrification. *Reprod Med Biol* **16**(1), 36-39

Edashige, K., Ohta, S., Tanaka, M., Kuwano, T., Valdez, D.M., Jr., Hara, T., Jin, B., Takahashi, S., Seki, S., Koshimoto, C., and Kasai, M. (2007) The role of aquaporin 3 in the movement of water and cryoprotectants in mouse morulae. *Biol Reprod* **77**(2), 365-75

Edashige, K., Yamaji, Y., Kleinhans, F.W., and Kasai, M. (2003) Artificial expression of aquaporin-3 improves the survival of mouse oocytes after cryopreservation. *Biol Reprod* **68**(1), 87-94

Fahy, G.M., Wowk, B., Wu, J., and Paynter, S. (2004) Improved vitrification solutions based on the predictability of vitrification solution toxicity. *Cryobiology* **48**(1), 22-35

Fong, B., Watson, P.H., and Watson, A.J. (2007) Mouse preimplantation embryo responses to culture medium osmolarity include increased expression of CCM2 and p38 MAPK activation. *BMC Dev Biol* **7**, 2

García-Martínez, T., Vendrell-Flotats, M., Martínez-Rodero, I., Ordóñez-León, E.A., Álvarez-Rodríguez, M., López-Béjar, M., Yeste, M., and Mogas, T. (2020) Glutathione Ethyl Ester Protects *In Vitro*-Maturing Bovine Oocytes against Oxidative Stress Induced by Subsequent Vitrification/Warming. *Int J Mol Sci* **21**(20)

Gómez-Redondo, I., Ramos-Ibeas, P., Pericuesta, E., Fernández-González, R., Laguna-Barraza, R., and Gutiérrez-Adán, A. (2020) Minor Splicing Factors Zrsr1 and Zrsr2 Are Essential for Early Embryo Development and 2-Cell-Like Conversion. *Int J Mol Sci* **21**(11)

Huang, H.F., He, R.H., Sun, C.C., Zhang, Y., Meng, Q.X., and Ma, Y.Y. (2006) Function of aquaporins in female and male reproductive systems. *Hum Reprod Update* **12**(6), 785-95

Jacobs, M.H. (1933) The simultaneous measurement of cell permeability to water and to dissolved substances. *Journal of Cellular and Comparative Physiology* **2**(4), 427-444

Jacobs, M.H., and Stewart, D.R. (1932) A simple method for the quantitative measurement of cell permeability. *Journal of Cellular and Comparative Physiology* **1**(1), 71-82

Jin, B., Higashiyama, R., Nakata, Y., Yonezawa, J., Xu, S., Miyake, M., Takahashi, S., Kikuchi, K., Yazawa, K., Mizobuchi, S., Niimi, S., Kitayama, M., Koshimoto, C., Matsukawa, K., Kasai, M., and Edashige, K. (2013) Rapid movement of water and cryoprotectants in pig expanded blastocysts via channel processes: its relevance to their higher tolerance to cryopreservation. *Biol Reprod* **89**(4), 87

Jin, B., Kawai, Y., Hara, T., Takeda, S., Seki, S., Nakata, Y., Matsukawa, K., Koshimoto, C., Kasai, M., and Edashige, K. (2011) Pathway for the movement of water and cryoprotectants in bovine oocytes and embryos. *Biol Reprod* **85**(4), 834-47

Kang, M.K., and Han, S.J. (2011) Post-transcriptional and post-translational regulation during mouse oocyte maturation. *BMB Rep* **44**(3), 147-57

King, L.S., Kozono, D., and Agre, P. (2004) From structure to disease: the evolving tale of aquaporin biology. *Nat Rev Mol Cell Biol* **5**(9), 687-98

Kleinhans, F.W. (1998) Membrane permeability modeling: Kedem-Katchalsky *vs* a two-parameter formalism. *Cryobiology* **37**(4), 271-89

Lagarias, J.C., Reeds, J.A., Wright, M.H., and Wright, P.E. (1998) Convergence Properties of the Nelder--Mead Simplex Method in Low Dimensions. *SIAM Journal on Optimization* **9**(1), 112-147

Luciano, A.M., Lodde, V., Beretta, M.S., Colleoni, S., Lauria, A., and Modina, S. (2005) Developmental capability of denuded bovine oocyte in a co-culture system with intact cumulus-oocyte complexes: role of cumulus cells, cyclic adenosine 3',5'-monophosphate, and glutathione. *Mol Reprod Dev* **71**(3), 389-97

Mogas, T. (2018) Update on the vitrification of bovine oocytes and invitro-produced embryos. *Reprod Fertil Dev* **31**(1), 105-117

Morató, R., Chauvigné, F., Novo, S., Bonet, S., and Cerdà, J. (2014) Enhanced water and cryoprotectant permeability of porcine oocytes after artificial expression of human and zebrafish aquaporin-3 channels. *Mol Reprod Dev* **81**(5), 450-61

Mullen, S.F., Agca, Y., Broermann, D.C., Jenkins, C.L., Johnson, C.A., and Critser, J.K. (2004) The effect of osmotic stress on the metaphase II spindle of human oocytes, and the relevance to cryopreservation. *Hum Reprod* **19**(5), 1148-54

Mullen, S.F., and Fahy, G.M. (2012) A chronologic review of mature oocyte vitrification research in cattle, pigs, and sheep. *Theriogenology* **78**(8), 1709-1719

Ohashi, S., Naito, K., Liu, J., Sheng, Y., Yamanouchi, K., and Tojo, H. (2001) Expression of Exogenous Proteins in Porcine Maturing Oocytes after mRNA Injection: Kinetic Analysis and Oocyte Selection Using EGFP mRNA. *Journal of Reproduction and Development* **47**(6), 351-357

Raju, R., Bryant, S.J., Wilkinson, B.L., and Bryant, G. (2021) The need for novel cryoprotectants and cryopreservation protocols: Insights into the importance of biophysical investigation and cell permeability. *Biochim Biophys Acta Gen Subj* **1865**(1), 129749

Rall, W.F. (1987) Factors affecting the survival of mouse embryos cryopreserved by vitrification. *Cryobiology* **24**(5), 387-402

Ruffing, N.A., Steponkus, P.L., Pitt, R.E., and Parks, J.E. (1993) Osmometric behavior, hydraulic conductivity, and incidence of intracellular ice formation in bovine oocytes at different developmental stages. *Cryobiology* **30**(6), 562-80

Sales, A.D., Lobo, C.H., Carvalho, A.A., Moura, A.A., and Rodrigues, A.P. (2013) Structure, function, and localization of aquaporins: their possible implications on gamete cryopreservation. *Genet Mol Res* **12**(4), 6718-32

Shampine, L.F., and Reichelt, M.W. (1997) The MATLAB ODE Suite. *SIAM Journal on Scientific Computing* **18**(1), 1-22

Sugiura, R., Satoh, R., Ishiwata, S., Umeda, N., and Kita, A. (2011) Role of RNA-Binding Proteins in MAPK Signal Transduction Pathway. *J Signal Transduct* **2011**, 109746

Tan, Y.J., Xiong, Y., Ding, G.L., Zhang, D., Meng, Y., Huang, H.F., and Sheng, J.Z. (2013) Cryoprotectants up-regulate expression of mouse oocyte AQP7, which facilitates water diffusion during cryopreservation. *Fertil Steril* **99**(5), 1428-35

Tan, Y.J., Zhang, X.Y., Ding, G.L., Li, R., Wang, L., Jin, L., Lin, X.H., Gao, L., Sheng, J.Z., and Huang, H.F. (2015) Aquaporin7 plays a crucial role in tolerance to hyperosmotic stress and in the survival of oocytes during cryopreservation. *Sci Rep* **5**, 17741

Team, R. (2006) A language and environment for statistical computing. *Computing* **1**

Valdez, D.M., Jr., Tsuchiya, R., Seki, S., Saida, N., Niimi, S., Koshimoto, C., Matsukawa, K., Kasai, M., and Edashige, K. (2013) A trial to cryopreserve immature medaka (Oryzias latipes) oocytes after enhancing their permeability by exogenous expression of aquaporin 3. *J Reprod Dev* **59**(2), 205-13

Verkman, A.S., Anderson, M.O., and Papadopoulos, M.C. (2014) Aquaporins: important but elusive drug targets. *Nat Rev Drug Discov* **13**(4), 259-77

Verkman, A.S., and Mitra, A.K. (2000) Structure and function of aquaporin water channels. *Am J Physiol Renal Physiol* **278**(1), F13-28

Verkman, A.S., van Hoek, A.N., Ma, T., Frigeri, A., Skach, W.R., Mitra, A., Tamarappoo, B.K., and Farinas, J. (1996) Water transport across mammalian cell membranes. *Am J Physiol* **270**(1 Pt 1), C12-30

Vian, A.M., and Higgins, A.Z. (2014) Membrane permeability of the human granulocyte to water, dimethyl sulfoxide, glycerol, propylene glycol and ethylene glycol. *Cryobiology* **68**(1), 35-42

Woods, E.J., Benson, J.D., Agca, Y., and Critser, J.K. (2004) Fundamental cryobiology of reproductive cells and tissues. *Cryobiology* **48**(2), 146-56

Yamagata, K., Yamazaki, T., Yamashita, M., Hara, Y., Ogonuki, N., and Ogura, A. (2005) Noninvasive visualization of molecular events in the mammalian zygote. *Genesis* **43**(2), 71-9

Yamaji, Y., Seki, S., Matsukawa, K., Koshimoto, C., Kasai, M., and Edashige, K. (2011) Developmental ability of vitrified mouse oocytes expressing water channels. *J Reprod Dev* **57**(3), 403-8

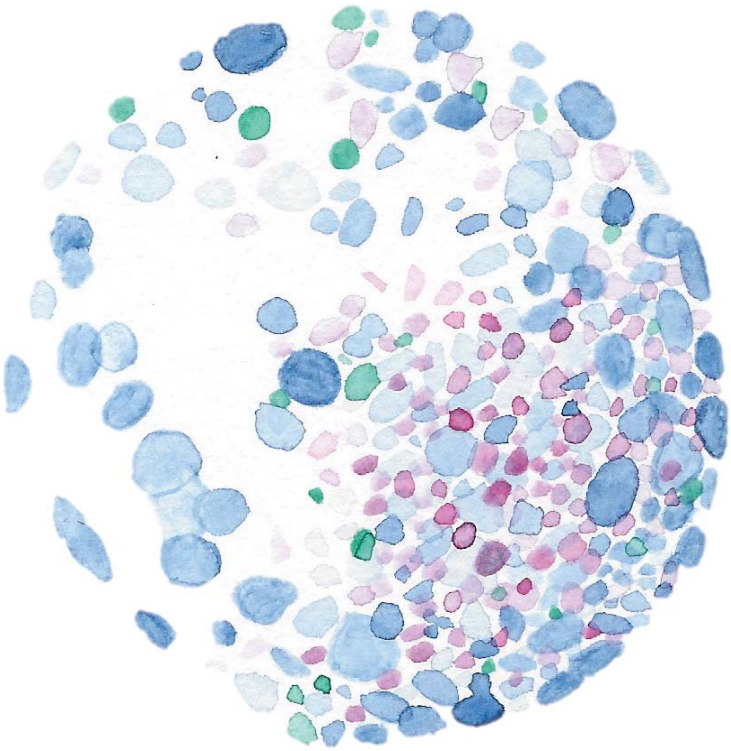

Chapter III

Impact of equilibration duration combined with temperature on the outcome of bovine oocyte vitrification

Under review in Biology of Reproduction, July 2021

ABSTRACT: While the cryopreservation of bovine oocytes has several shortcomings, few protocols have considered the osmotic response of cells according to the temperature and time of cryoprotectant (CPA) addition. Based on *in silico* and *in vitro* osmotic observations, we propose shorter dehydration-based protocols at different temperatures (25°C *vs* 38.5°C) as a first step towards defining an optimal cryopreservation method. IVM oocytes were exposed to ES at 25°C and 38.5°C and effects of optimized exposure times for each temperature were determined prior to vitrification/warming on oocyte spindle configuration, DNA fragmentation and further embryo development. Upon exposure to standard ES (7.5% Me_2SO + 7.5% EG in TCM199 medium + 20% FBS), original oocyte volume was recovered within 2 min 30 s at 38.5°C and 5 min 30 s at 25°C. IVM oocytes were then exposed to the aforementioned CPAs at both temperature/duration conditions and vitrified/warmed. While similar percentages of oocytes exhibiting a normally configured spindle and DNA fragmentation were observed in the fresh control group (66.69 ± 2.28% and 6.17 ± 2.57%, respectively) and oocytes vitrified at 38.5°C (53.49 ± 4.00% and 11.32 ± 3.21%, respectively), in oocytes vitrified at 25°C the apoptosis rate was significantly higher (32.37 ± 4.87%) and the normal spindle configuration rate was lower (38.38 ± 1.52%). Similar cleavage rates and blastocyst yields were observed in the vitrified/38.5°C and fresh controls, while these rates were lower in vitrified/25°C. Thus, the time needed to prepare bovine oocytes for vitrification was successfully reduced to 2 min 30 s at 38.5°C.

1. Introduction

Oocyte cryopreservation is today the most promising and cost-effective option for the storage of female germplasm. In domestic animals, cryopreservation of oocytes to create banks is a way of preserving female genetically valuable material or avoiding the loss of rare genotypes in the event of an unexpected catastrophe. The value and feasibility of genome resource banking becomes even more important for the preservation of ancient breeds, as over the last decades, farm animal genetic diversity has rapidly declined due to changing market demands and intensification of agriculture (Prentice and Anzar 2010). Cryopreserved oocyte banks could also help improve research endeavors by providing accessible and repeatable supplies and reduce the effects of seasonal variation in oocyte quality. Despite these benefits, bovine oocyte cryopreservation is much more challenging compared to other species such as mice or humans (Ledda *et al.* 2007; Hwang and Hochi 2014) and this has been attributed to several cryoinjuries/stresses caused by exposure to cryoprotective agents (CPAs), cooling, and the combination of both processes.

Currently, there is no universal vitrification protocol for bovine oocytes. Several procedures to load CPAs into oocytes have been proposed. Some are time-specific and require a given treatment duration with an equilibration solution (ES) whose composition is similar to the vitrification solution (VS) but less concentrated, and a given exposure time to VS before plunging the oocytes into liquid nitrogen; some require observation of oocyte volume response when in the ES; some demand exposure to ES and VS be conducted at room temperature (RT), biological temperatures or higher than biological temperatures (reviewed by (Dujickova *et al.* 2020)). These empirically derived protocols for bovine oocyte cryopreservation need to be improved.

During the vitrification of bovine oocytes, osmotic damage, chemical toxicity, and the formation of intracellular ice crystals are likely to compromise oocyte viability if the procedure is not well optimized. The injury induced is usually irreversible plasma membrane damage, depolymerization/disruption of the oocyte cytoskeleton and spindle microtubule, low membrane permeability, premature exocytosis of cortical granules and zona hardening, high rates of polyspermy and altered gene expression (Mogas 2018). Most vitrification protocols initially involve a long exposure stage to a non-vitrifying solution lasting 8 to 15 min followed by a short time of exposure (~1 min) to the VS (Dujickova *et al.* 2020). These procedures, however, rarely consider the osmotic tolerance of the cells according to temperature and time of CPA addition and removal. When this characteristic is taken into account, the time needed to prepare oocytes for vitrification can be shortened while maintaining the critical cytosolic solute content necessary for successful vitrification. Optimization of cryopreservation techniques can be pursued by a wholly empirical methodology or by using fundamental cryobiology theory and mathematical simulations (Leibo 2008; Gallardo *et al.* 2019), which requires knowledge of the biophysical parameters of the oocytes and also of the effects of osmotic stress (both magnitude and duration) on the developmental potential of oocytes. In the context of optimization of cryopreservation procedures for vitrification in the presence of combined CPAs, one goal is to determine the best exposure time to the equilibration solution at a specific temperature (Wang *et al.* 2011). So, the aims of the present study were: 1) to determine both predictively and experimentally the osmotic behavior of metaphase II (MII) bovine oocytes in terms of membrane permeability parameters (L_p and P_s) in response to ES CPAs at 25°C and 38.5°C and 2) to assess the optimized CPA addition procedure by examining induced toxicity/osmotic stress and the whole vitrification process by analyzing oocyte spindle morphology, DNA fragmentation and subsequent embryo development.

2. Material and Methods

2.1. Chemicals and suppliers

All chemicals and reagents used in this study were purchased from Sigma Chemical Co (St. Louis, MO, USA) except where otherwise indicated.

2.2. Oocyte collection and *in vitro* maturation

The methods used for the *in vitro* maturation (IVM), *in vitro* fertilization (IVF) and *in vitro* culture (IVC) of the bovine oocytes have been described elsewhere (Rizos *et al.* 2001). Briefly, ovaries were collected from cows at a local abattoir (Escorxador Sabadell, S.A., Sabadell, Spain) and immediately transported to the laboratory in pre-warmed (35–37°C) saline solution (0.9% NaCl). Cumulus-oocyte complexes (COCs) were obtained by aspirating 3–8 mm diameter follicles using an 18 g needle, and washed three times in modified Dulbecco's PBS (PBS supplemented with 0.036 mg/mL sodium pyruvate, 0.05 mg/mL gentamicin and 0.5 mg/mL bovine serum albumin, BSA). Only COCs with at least three compact layers of cumulus cells and a homogeneous cytoplasm were used. After three washes in PBS, groups of 50 COCs were transferred to 500 μL of maturation medium in four-well dishes and cultured for 24 h at 38.5°C in a 5% CO_2 humidified air atmosphere. The maturation medium was composed of tissue culture medium (TCM-199) supplemented with 10% (v/v) fetal bovine serum (FBS), 10 ng/mL epidermal growth factor, and 50 μg/mL gentamicin.

2.3. Modeling the membrane permeability of bovine MII oocytes

2.3.1. Measurement of oocyte volumetric changes following CPA exposure at 25°C and 38.5°C

After 22 h of IVM, oocytes were denuded of cumulus cells by gentle pipetting. Only mature oocytes showing a normal appearance and a visible first polar body were used. An oocyte was placed in a 25 μL-drop of holding medium (HM: TCM199-Hepes supplemented with 20% (v/v) FBS) covered with mineral oil, and held with a holding pipette (outer diameter, 100 μm) (MPHL-35, Life Global group, Guiford, United States) connected to a micromanipulator on an inverted microscope (Zeiss Axio Vert A1, Germany). An initial photograph was taken of the oocyte to calculate its initial volume. The oocyte was then covered with another pipette of larger inner diameter (600 μm) (G-1 Narishigue, Tokyo, Japan) connected to a different micromanipulator. Then, by sliding the dish, the oocyte was introduced in a 25 μL drop containing 1.55 M dimethyl sulfoxide

(Me_2SO) or 1.55 M ethylene glycol (EG) (Kuwayama 2007) at 25°C or 38.5°C and left for 5 min. The volumetric response of the oocyte during the experiments was recorded every 5 s using a time-lapse video recorder (Zeiss Zen imaging software/Axiocam ERc 5s). The video was converted into image frames and a series of images taken at 5 s-intervals utilized for analysis. Oocyte volume was measured through its cross sectional area using ImageJ software. An average of 10-14 mature oocytes that remained close to spherical in shape were individually analyzed for each CPA and temperature. Osmotic responses of the oocyte were calculated by measuring oocyte volume changes when exposed to 1.55 M Me_2SO or 1.55 M EG at the different temperatures.

2.3.2. Membrane permeability parameters

The experimental data were fitted to a two-parameter (2P) transport formalism to determine the permeability of bovine MII oocytes to water (L_p) and solutes (P_s). The 2P model assesses mass transfer dynamics through the cell over time by assuming there is no intramembrane interaction between water and permeable solutes. This model uses a pair of coupled differential equations to describe cell volume changes and moles of intracellular permeating solute when the cell is exposed to a ternary solution consisting of a permeable solute (CPA), an impermeable solute (NaCl), and solvent (water).

Water flux into the cell over time is expressed as:

$$\frac{dV_w}{dt} = -L_p ART(M^e - M^i) \quad (1)$$

where V_w is the cell water volume, L_p is the membrane permeability to water (hydraulic conductivity), A is the area of the plasma membrane, R is the universal gas constant, T is the absolute temperature, and M^e and M^i are the total external and internal osmolalities, respectively.

The rate of CPA transport is given by:

$$\frac{dN_s}{dt} = P_s A(M_s^e - M_s^i) \quad (2)$$

where N_s is the intracellular moles of CPA, P_s is CPA permeability, and M^i_s and M^e_s are intracellular and extracellular CPA molality, respectively.

Volumetric data for each oocyte at each concentration and temperature were fitted to the 2P model to determine L_p and P_s. The differential equations (equations (1) and (2)) were solved in Matlab software using the ode45 function, which implements an explicit Runge-Kutta formula (Dormand and Prince 1980; Shampine and Reichelt 1997). To

estimate permeabilities, model predictions were fitted to the data by minimizing the sum of the error squared in Matlab using the fminsearch function, which implements the Nelder-Mead simplex algorithm (Lagarias *et al.* 1998).

2.3.3. Prediction of cell volume changes during exposure of bovine oocytes to the equilibration solution at 25°C and 38.5°C

To predict the cell volume response and intracellular CPA concentration when oocytes are exposed to ES (the first step of CPA addition), it is essential to define two solute equations, one for Me_2SO and another for EG. Accordingly, a system of three linear ordinary differential equations needs to be solved for the three variables (V_w, N_{Me2SO} and N_{EG}). These three differential equations were solved as described above in Matlab software using the ode45 function, which implements an explicit Runge-Kutta formula (Dormand and Prince 1980; Shampine and Reichelt 1997).

In this study, the water and solute permeability used for the CPA addition predictions at 25°C or 38.5°C were previously estimated (see section 2.3.2). Water permeability was assumed to be the average value for the individual L_p values obtained when the oocytes where exposed to 1.55 M Me_2SO or 1.55 M EG at 25°C or 38.5°C (2.41 and 1.64 μm/atm×min, respectively). The values for P_{Me2SO} and P_{EG} were 0.59 and 0.78μm/s, respectively at 25°C, and 1.38 and 1.94 μm/s, respectively at 38.5°C. The oocyte was assumed to be a perfect sphere with a radius of 56.1 μm in isotonic medium, and an osmotically inactive volume of 25% of its initial volume.

Predictions for the CPA addition process (equilibration solution) were run at 25°C or 38.5°C for bovine MII oocytes, for which the exposure time was limited to 9 min. Key parameters for oocyte survival of vitrification, such as the volumetric excursion of the oocyte and total cytoplasmic solute concentration were determined and compared between the two temperatures.

2.4. *In vitro* osmotic behavior following ES exposure at 25°C and 38.5°C

To determine if the model predictions were accurate, our *in silico* dehydration profiles obtained with the theoretical models were tested *in vitro* by observing the osmotic behavior of bovine MII oocytes exposed to the equilibration solution at 25°C or 38.5°C. The methodology used was the same as described in section 2.3.1 with the difference that oocytes were exposed for 9 min to the equilibration solution (ES; 7.5% (v/v) EG and 7.5%

(v/v) Me_2SO in TCM-199 Hepes) at 25°C or 38.5°C. An average of 20 mature oocytes that remained close to spherical in shape were individually analyzed for each temperature.

2.5. Oocyte vitrification and warming

In vitro matured oocytes were vitrified/warmed as previously described (García-Martínez *et al.* 2020). After 22 h of IVM, oocytes were partially denuded by gently pipetting in PBS. Based on the results obtained in the previous experiments, oocytes with only corona radiata cells were transferred to ES containing 7.5% (v/v) Me_2SO and 7.5% (v/v) EG for different periods of time depending on the temperature (see experimental design). Oocytes were then transferred to the vitrification solution (VS: 15% (v/v) Me_2SO, 15% (v/v) EG, and 0.5 M sucrose). After incubating for 30–40 s, up to five oocytes were loaded onto a Cryotop and almost all the solution was removed to leave only a thin layer covering the oocytes. Oocytes were immediately plunged into liquid nitrogen. The entire process from exposure to the vitrification solution to plunging in liquid nitrogen was completed within 60 s.

Warming was performed by quickly immersing the tip of the Cryotop in warming solution 1 (WS1: HM supplemented with 1 M sucrose) at 38.5°C. After 1 min, oocytes were transferred into WS2 (HM supplemented with 0.5 M sucrose) for 3 min and then to HM for 5 min. Oocytes were then transferred back into the maturation medium and allowed to mature for 2 additional hours at 38.5°C in humidified air containing 5% CO_2.

2.6. *In vitro* fertilization and embryo culture

In vitro-matured oocytes were *in vitro* fertilized (IVF) at 38.5°C in a 5% CO_2 atmosphere and cultured as previously described by Arcarons et al. (Arcarons *et al.* 2019). Briefly, high motility and good morphology spermatozoa from Asturian bulls (ASEAVA, Llanera, Asturias, Spain) were obtained by centrifuging frozen/thawed sperm at 300×g for 10 min at RT on a discontinuous gradient consisting of 1 mL of 40% and 1 mL of 80% BoviPure (Nidacon Laboratories AB, Göteborg, Sweden) according to the manufacturer's instructions. Viable spermatozoa collected from the bottom were washed with 3 mL of BoviWash (Nidacon International, Göteborg, Sweden) and pelleted by centrifugation at 300×g for 5 min at RT. Spermatozoa were counted in a Neubauer chamber and diluted in an appropriate volume of fertilization medium to give a final concentration of 1×10^6 spermatozoa/mL. One-hundred-microliter droplets of diluted sperm were prepared under mineral oil and 20 oocytes/droplet were co-incubated at 38.5°C, 5% CO_2 and high

humidity. The fertilization medium consisted of Tyrode's medium supplemented with 25 mM bicarbonate, 22 mM sodium lactate, 1 mM sodium pyruvate, 6 mg/mL fatty acid-free BSA and 1 mg/mL heparin-sodium salt.

At 18–20 h post-insemination, oocyte survival was evaluated morphologically. The criteria used to classify oocytes as surviving or degenerated have been described elsewhere (Chian *et al.* 2004). Briefly, oocytes with intact oolemma, intact zona pellucida, and homogenous and dark cytoplasm were considered as surviving oocytes. Only surviving oocytes were transferred to 25-μL drops of the culture medium (1 embryo/μL) covered by 3.5 mL of mineral oil. The culture medium was synthetic oviduct fluid (Caisson Labs, Smithfield, UT, USA) supplemented with 0.96 μg/mL BSA, 88.6 μg/mL sodium pyruvate, 2% (v/v) non-essential amino acids, 1% (v/v) essential amino acids, 0.5% gentamicin and 2% (v/v) FBS. Presumptive zygotes were incubated at 38.5°C in a humidified 5% CO_2 and 5% O_2 atmosphere for 8 days. Embryo development was recorded at 48 h post-insemination (cleavage) and at Days 7 and 8 (blastocysts) post-insemination (pi). Day 8 blastocysts were fixed and immunostained to assess total cell number (TCN), inner cell mass (ICM) number, trophectoderm (TE) cell number and apoptosis rate (AR).

2.7. Spindle configuration

After 24 h of IVM, oocytes were completely denuded of cumulus cells by gentle pipetting before immunostaining for tubulin and chromatin detection as described previously by García-Martínez et al. (García-Martínez *et al.* 2020). Briefly, oocytes were fixed in 2% (w/v) paraformaldehyde–phosphate buffer saline (PFA-PBS) for 30 min at 38.5°C. Oocytes were then permeabilized in Triton X-100 (2.5% (v/v) in PBS) for 20 min and blocked in 3% BSA (w/v) in PBS for 30 min at 38.5 °C. The fixed oocytes were incubated with mouse anti-α-tubulin monoclonal antibody (TU-01, Invitrogen, CA, USA; 1:250 dilution) overnight at 4°C, followed by incubation with the anti-mouse IgG antibody Alexa Fluor™ 488 (Molecular Probes, Paisley, UK; 1:5000) at 38.5°C for 1 h. Oocytes were washed three times in pre-warmed PBS supplemented with 0.005% (v/v) of Triton X-100 at 38.5°C for 20 min after each incubation. Groups of 20 oocytes were mounted on poly L-lysine-treated coverslips fitted with a self-adhesive reinforcement ring in a 3-μL drop of Vectashield containing 125 ng/mL 4',6'-diamidino-2-phenylindole hydrochloride (DAPI) (Vysis Inc., Downers Grove, USA) and flattened with a coverslip. Preparations were sealed with clear nail varnish and stored at 4°C protected from light until observation within the following 2 days. An epifluorescence microscope (Axioscop 40FL; Carl Zeiss, Göttingen, Germany)

was used to examine tubulin (Alexa Fluor™ 488; excitation 488 nm) and chromatin (DAPI; excitation 405 nm). The criteria used to classify chromosome and microtubule distributions have been described elsewhere (Morato *et al.* 2008). In brief, the meiotic spindle was defined as normal when the classic symmetrical barrel shape was observed, with chromosomes aligned regularly in a compact group along the equatorial plane. In contrast, abnormal spindles were recorded when there was microtubule decondensation or partial or total disorganization, or as absent when there was a complete lack of microtubules. Chromosome organization was considered abnormal when chromosomes were dispersed or had an aberrant, less condensed appearance or lacking when chromosomes were missing. Detailed images of these normal and abnormal patterns are shown in Figure 1.

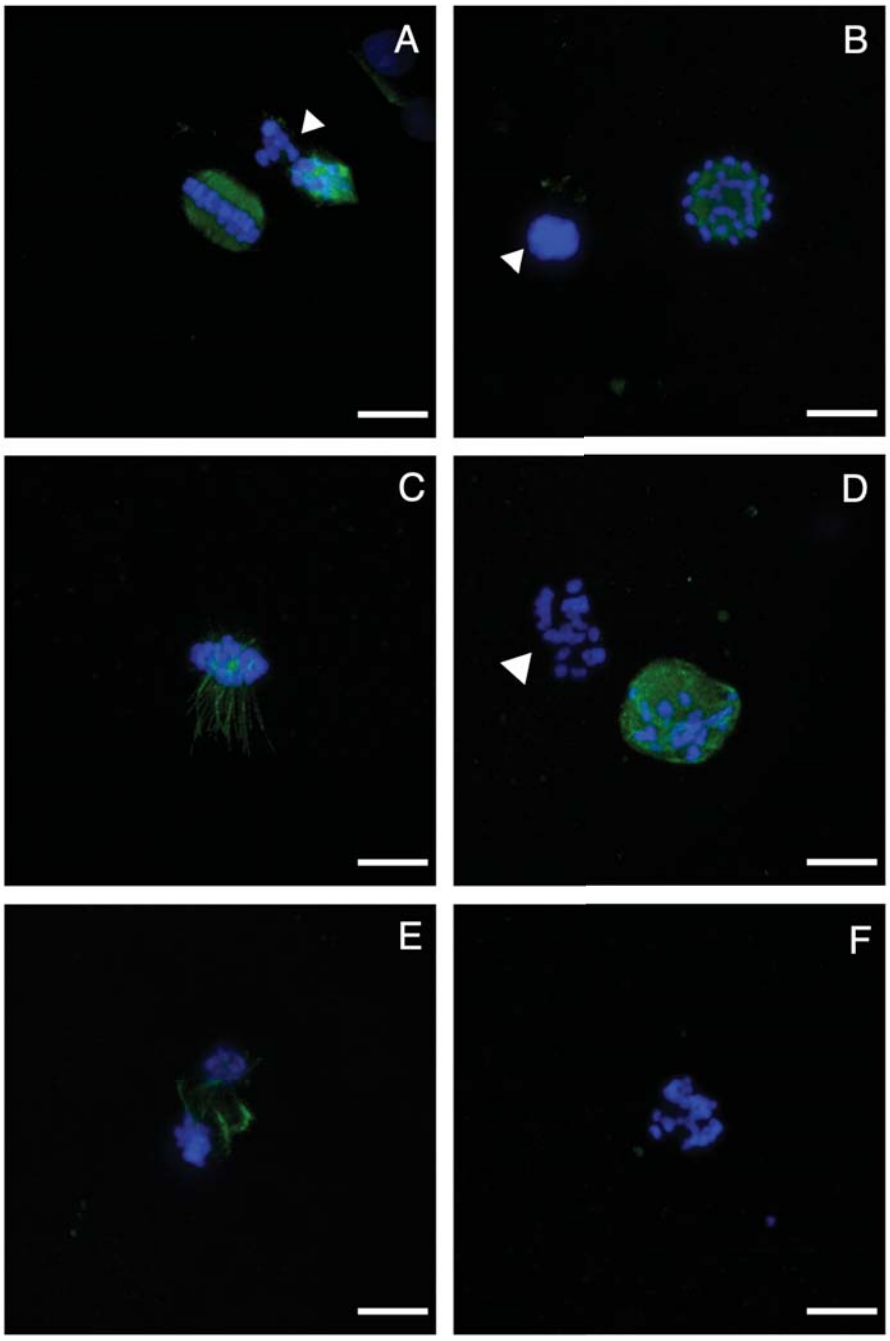

Figure 1. Representative confocal laser-scanning photomicrographs of spindle microtubule and chromosome configurations in IVM bovine oocytes after CPA exposure or vitrification. (**A**) Normal barrel-shaped MII spindle with microtubules forming a clear meiotic spindle with compact chromosomes arranged at the equator of the structure. (**B**) Abnormal spindle morphology showing partly disorganized chromosomes. (**C**) Abnormal spindle structures with completely disorganized microtubules and partly disorganized chromosomes. (**D**) Abnormal spindle structure associated with completely disorganized microtubules and chromosomes. (**E**) Abnormal spindle structure associated with a

disrupted microtubule arrangement and chromosomes appearing condensed. (**F**) Chromosomes with an aberrant, less condensed appearance. Note the absence of microtubules. Scale bar = 10 μm. Green, tubulin (Alexa Fluor™ 488); blue, chromosomes (DAPI). The white arrowheads indicate polar bodies.

2.8. TUNEL detection of fragmented oocyte DNA

Oocyte DNA fragmentation was detected by terminal deoxynucleotidyl transferase (TdT) mediated dUTP-digoxigenin nick end-labeling (TUNEL) using a kit (in situ Cell Death Detection Kit, Fluorescein) according to the manufacturer's instructions (as described in Vendrell-Flotats et al. (Vendrell-Flotats *et al.* 2020) with some modifications). Briefly, after 24 h of maturation, oocytes were completely denuded of cumulus cells by gentle pipetting and fixed in 2% (w/v) paraformaldehyde in PBS for 30 min at 38.5°C. After three washes in PBS with 0.3% polyvinylpyrrolidone (PVP), fixed oocytes were permeabilized with 0.5% (v/v) Triton X-100 containing 0.1% (w/v) sodium citrate for 1 h at RT. The oocytes were then washed again in PBS-PVP solution and incubated in the TUNEL reaction cocktail at 38.5°C for 1 h in the dark. Positive and negative control samples were included in each assay. Oocytes exposed to DNase I (50 mL of RQ1 RNase-free Dnase (50 U/mL)) for 1 h at RT served as positive controls, and oocytes incubated in the absence of the terminal TdT enzyme served as negative controls. After washing in PBS-PVP, controls and samples were mounted on poly L-lysine-treated coverslips fitted with a self-adhesive reinforcement ring in a 3-μL drop of Vectashield containing 125 ng/mL of DAPI (Vectorlabs, Burlingame, CA, USA) and flattened with a coverslip. Preparations were sealed with clear nail varnish and stored at 4°C in the dark until their observation within the following 2 days. An epifluorescence microscope (Axioscop 40FL; Carl Zeiss, Göttingen, Germany) was used to detect TUNEL-positive nuclei (fluorescein isothiocyanate-conjugated TUNEL label; excitation 488 nm) while nuclei were localized using the DAPI filter (DAPI; excitation 405 nm). Nuclei were scored as having either intact (TUNEL [-]; blue stain) or fragmented (TUNEL [+]; green stain) DNA (Figure 4B). The percentage of TUNEL-positive oocytes was calculated as the ratio between TUNEL(+) oocytes and the total number of oocytes analyzed in each group.

2.9. Differential staining of blastocysts and DNA fragmentation

Day 8 bovine blastocysts were immunostained for differential cell counts and apoptosis analysis as previously described by Martinez-Rodero et al.(Martínez-Rodero *et al.* 2021)

with some modifications. Unless otherwise stated, all steps were conducted at 38.5°C. After fixation in 2% (v/v) paraformaldehyde diluted in PBS for 15 min, embryos were washed three times in PBS. For permeabilization, embryos were incubated with 0.01% Triton X-100 in PBS supplemented with 5% normal donkey serum (PBS-NDS) for 1 h at RT. Then, the embryos were washed in PBS (×3) and incubated at 4°C overnight with mouse anti-SOX2 primary antibody (1:100; MA1-014, Invitrogen, CA, USA) and rabbit anti-caspase 3 primary antibody (1:250, CST9664S, Cell Signaling Technologies, CA, USA) in a humidified chamber. Afterwards, once washed in 0.005% Triton X-100 in PBS-NDS for 20 min, the embryos were incubated with the secondary antibody goat anti-mouse IgG Alexa Fluor™ 568 (1:500; A-11004, ThermoFisher, Waltham, MA, USA) and a goat anti-rabbit IgG Alexa Fluor™ 488 antibody (1:500, A-11001, ThermoFisher, Waltham, MA, USA) for 1 h in a humidified chamber. Embryos were then washed thoroughly in 0.005% Triton X-100 in PBS-NDS for 5 min, mounted on poly-L-lysine treated coverslips fitted with a self-adhesive reinforcement ring in a 3-μL drop of Vectashield containing 125 ng/ml DAPI (Vectorlabs, Burlingame, CA, USA), and flattened with a slide. The preparation was sealed with clear nail varnish and stored at 4°C protected from light until observation within the following 2 days. Confocal images of 0.5 μm-serial sections were captured with a confocal laser-scanning microscope (Leica TCS SP5, Leica Microsystems CMS GmbH, Mannheim, Germany) to examine the ICM nucleus (SOX2-Alexa Fluor™ 568; excitation 561 nm), cell nucleus (DAPI; excitation 405 nm) and DNA fragmentation (caspase 3-Alexa Fluor™ 488; excitation 488 nm). TCN, ICM cell number, and apoptotic cells were analyzed using Imaris 9.2 software (Oxford Instruments, UK). Individual nuclei were counted and assessed as intact (caspase-3(−); blue/red stain) or fragmented (caspase-3(+), green stain) DNA, TE cells (SOX2(−OX2(, green stain) DNA, TE cells (SOXs, UK). (Figure 2). The AR was calculated as the ratio of caspase-3(+) cells/total number of cells.

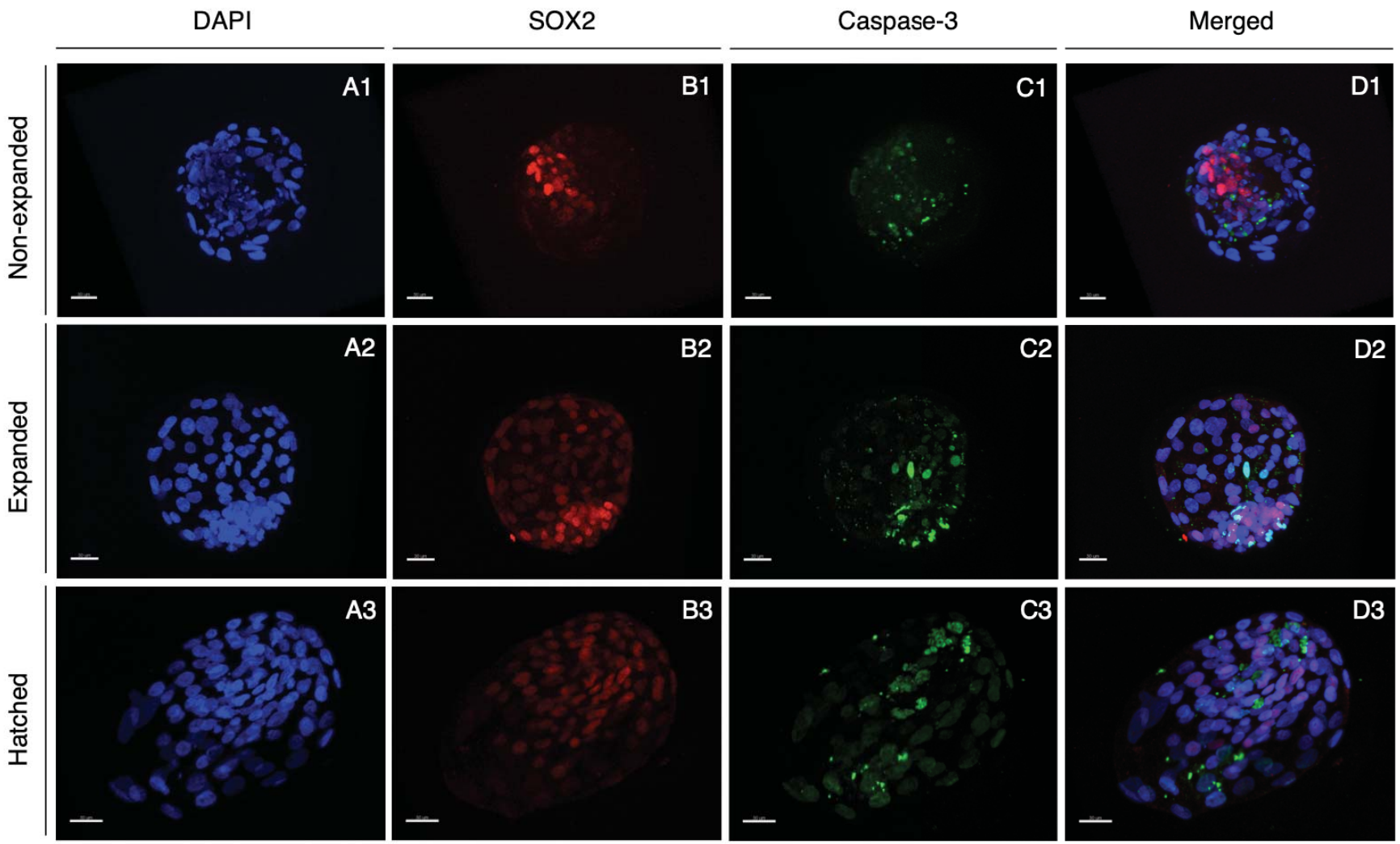
DAPI
SOX2
Caspase-3
Merged
Non-expanded
Expanded
Hatched
A1
B1
C1
D1
A2
B2
C2
D2
A3
B3
C3
D3

Figure 2. Representative images of D8 non-expanded, expanded, and hatched blastocysts derived from oocytes vitrified/warmed in the 25°C and 38.5°C equilibration protocols. Fluorescence of anti-SOX2 (red) was examined using the Alexa Fluor™ 568 filter to detect ICM cells (B1-B3). Fluorescence of anti-active-caspase-3 antibody (green) was examined by the Alexa Fluor™ 488 filter to detect caspase activity (C1-C3), while DAPI staining (blue) was examined by the DAPI filter for total cell counts (A1-A3). An overlay is provided in (D1-D3). (A1,B1,C1,D1) Non-expanded blastocyst; (A2,B2,C2,D2) Expanded blastocyst; (A3,B3,C3,D3) Hatched blastocyst. Scale bar: 30 μm.

2.10. Experimental Design

To assess the effect of oocyte exposure or vitrification/warming in the 25°C or 38.5°C protocol and based on the results obtained in the oocyte osmotic behavior study at 25°C and 38.5°C, bovine oocytes *in vitro* matured for 22 h were randomly assigned to two groups: 1) oocytes exposed to ES for 5 min 30 s followed by exposure to VS, WS2 and HM media at 25°C as previously described; and 2) oocytes exposed to ES for 2 min and 30 s followed by exposure to VS, WS2 and HM media at 38.5°C as previously described. In both experimental groups, exposure to WS1 was performed at 38.5°C. A sample of the oocytes in each IVM group was vitrified/warmed using the Cryotop method and allowed to recover for 2 h (VIT25 and VIT35.8, respectively) while the other half were only exposed to the vitrification and warming solutions without plunging them in liquid nitrogen to assess CPA toxicity (CPA25 and CPA38.5, respectively). Fresh, non-vitrified *in vitro* matured oocytes served as the Control group. After 24 h of IVM, a sample of oocytes from each of the five treatment groups (Control, CPA25, CPA38.5, VIT25 and VIT38.5) was collected to assess spindle and chromosome configurations (6 replicates) and DNA fragmentation (4 replicates) (see Supplemental Figure S1).

To assess the effect on embryo development of oocyte vitrification/warming in the 25°C or 38.5°C protocol, oocytes in the groups Control, VIT25 and VIT38.5 were inseminated and *in vitro* cultured for 8 days. Cleavage rates were determined 48 hpi and blastocysts rates at 168 hpi (day 7) and 192 hpi (day 8) and are provided as the percentage of zygotes cultured. Early and non-expanded blastocysts (mid blastocysts) were graded as blastocysts, while expanded, hatching, and hatched blastocysts were termed advanced blastocysts (Gutierrez-Anez *et al.* 2021). Day 8 blastocysts were fixed and immunostained to assess TCN, ICM cell number, TE cell number and AR (3 replicates).

2.11. Statistical Analysis

All statistical tests were performed using R software (V 4.0.3, R Core Team, Vienna, Austria). The Kolmogorov-Smirnov test and the Levene test were first used to check the normality of the data and homogeneity of variance, respectively. When required, data were linearly transformed into the arcsin √x function prior to running statistical tests. However, if after applying this function, the data continued to show a non-normal distribution, they were analyzed using a non-parametric test. For the *in vitro* osmotic behavior experiment, an ANOVA of repeated measures was used, considering the given oocyte examined as a random factor. A parametric test (one-way ANOVA) was used to examine differences between groups in spindle configuration, DNA fragmentation and embryo development. Non-normally distributed data were analyzed with a non-parametric test (Kruskal-Wallis). For the permeability estimates and the TCN, ICM and TE cell number and AR experiments, a two-way ANOVA was used. Secondly, we conducted a pairwise comparison using the Bonferroni test for parametric analyzes and the Wilcoxon test for non-parametric analyzes. Results are expressed as means ± standard error of the mean (SEM). Significance was set at $P \leq 0.05$.

3. Results

3.1. Modeling membrane permeability of bovine MII oocytes.

3.1.1. Membrane permeability parameters

Our calculated L_p and P_s for MII bovine oocytes in the presence of Me_2SO or EG at different temperatures are given in Table 1. Overall, L_p values varied significantly between the temperatures ($P < 0.05$) for each CPA. In general, values of L_p for MII oocytes exposed to 1.55 M Me_2SO or 1.55 M EG at 25°C (1.91 ± 0.13 and 1.38 ± 0.12 μm/atm×min, respectively) were much smaller than for MII oocytes in the presence of Me_2SO or EG at 38.5°C (2.47 ± 0.18 and 2.34 ± 0.16 μm/atm×min, respectively). Moreover, we also found that temperature had a significant effect on the permeability of solutes in both CPAs ($P < 0.05$). In general, solute permeability increased by a factor of about two as the temperature increased from 25°C to 38.5°C (Table 1). Also, the L_p for Me_2SO was higher than for EG at 25°C (1.91 ± 0.13 and 1.38 ± 0.12 μm/atm×min, respectively) ($P < 0.05$) whereas at 38.5°C no differences in water permeability were detected between the CPAs. When solute permeability was compared between CPAs at

each temperature, only at 38.5°C was P_s for EG higher than for Me_2SO (1.94 ± 0.24 and 1.38 ± 0.11 μm/s, respectively) ($P < 0.05$).

Table 1. Water permeability (L_p) and solute permeability (P_s) of bovine MII oocytes in the presence of 1.55 M Me_2SO or 1.55 M EG at 25°C or 38.5°C.

			Membrane permeability parameters	
CPA	**Temperature**	**n° oocytes**	**L_p (μm/atm×min)**	**P_s (um/sec)**
Me_2SO	25°C	13	1.91 ± 0.13[a,1]	0.59 ± 0.05[a,1]
	38.5°C	10	2.47 ± 0.18[b,1]	1.38 ± 0.11[b,1]
EG	25°C	14	1.38 ± 0.12[a,2]	0.78 ± 0.09[a,1]
	38.5°C	10	2.34 ± 0.16[b,1]	1.94 ± 0.24[b,2]

Unless indicated otherwise, data are given as the mean ± SEM. [a,b]Different superscript letters indicate significant differences between temperatures for the same CPA ($P < 0.05$). [1,2] Different superscript numbers indicate significant differences in water or solute permeability between Me_2SO and EG CPA for the same temperature ($P < 0.05$). Me_2SO, dimethyl sulfoxide; EG, ethylene glycol.

3.1.2. In silico versus in vitro results

For our comparison of the effects of temperature on the cell osmotic response, mature oocytes were both predictively and experimentally exposed to a hyperosmotic gradient by exposing them to a solution containing 7.5% Me_2SO + 7.5% EG at the two temperatures (25°C and 38.5°C). As these CPAs are permeable, there is simultaneous water transport (because of the osmotic gradient) and CPA influx (because of concentration gradients) and this produces cell volume changes.

Predicted relative volumes and total intracellular solute concentrations in oocytes subjected to ES at 25°C or 38.5°C, as a function of time, are shown in Figure 3. Our model predictions show that oocytes exposed to ES shrink to a minimum of 53% of their isotonic volume after 8 s of exposure, whereas at 38.5°C the oocytes are predicted to shrink to 60% within 5 s. Moreover, simulations predict that oocytes at 38.5°C swell back to their isotonic volume faster than at 25°C, recovering their original volume after 2.33 min or 5 min, respectively. Total intracellular solute molarity is achieved faster at 38.5°C than at 25°C.

However, in both cases the solute concentration gets close to the equilibrium value within the first minute of exposure to ES (Figure 3).

As in the simulations, the *in vitro* oocyte osmotic response of bovine MII oocytes exposed to ES depicted in Figure 3 indicates when oocytes attained their minimum volume (Vmin ~61% at 25°C after 15 s and 65% at 38.5°C after 10 s) and when they reach their new final equilibrium volume (5 min 30 s at 25°C and 2 min 30 s at 38.5°C).

As expected, we observed the reduced volume of oocytes in all groups attributable to water outflow. However, after this initial shrinkage, the cells swell as CPA permeates the cell membrane driven by the concentration gradient (Figure 3). These relative volume changes are dependent on temperature and were in good agreement with the model predictions.

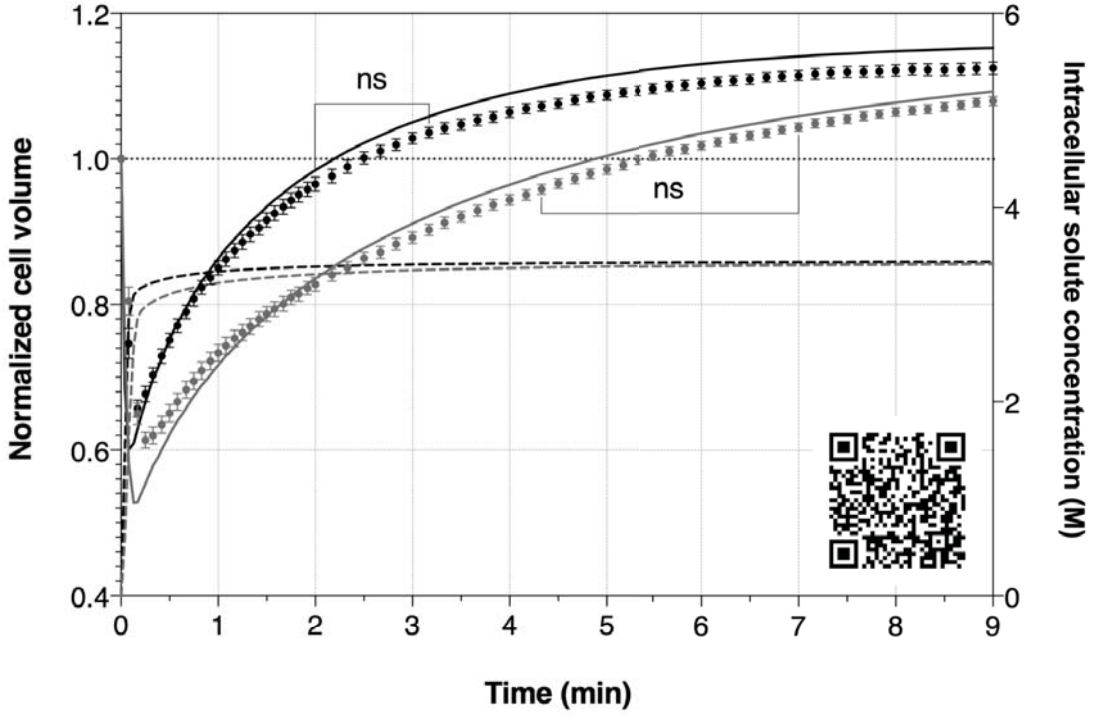

Figure 3. Comparison between model predictions and *in vitro* results obtained in bovine MII oocytes exposed for 9 min to ES at 25°C or 38.5°C. Simulation of the osmotic response (solid line) of bovine MII oocytes when transferred to ES and predicted intracellular CPA concentration (dotted line) at 25°C (gray) and 38.5°C (black). The figure also shows experimental volume changes produced in bovine MII oocytes after exposure to ES at 25°C (gray circles) and 38.5°C (black circles). Data are the means of relative volumes ± SEM. Ns: means of relative volumes that do not differ statistically from the

volume in isotonic solution. QR code links to a representative time-lapse video for MII bovine oocytes exposed to ES at 25°C or 38.5°C.

3.2. Spindle configurations observed in IVM bovine oocytes vitrified/warmed in the 25°C or 38.5°C equilibration protocols

To assess whether reducing the preparation time of oocytes for vitrification at a certain temperature would modify oocyte morphofunctionality, oocytes were exposed to the ES for 5 min 30 s at 25°C and for 2 min 30 s at 38.5°C and then analyzed for their spindle configurations compared to those of non-treated controls. In this set of experiments, we used 987 oocytes. Results are summarized in Table 2.

Percentages of bovine oocytes reaching the MII stage did not differ between treatments, except for oocytes exposed to ES at 25°C for 5 min 30 s which showed a significantly lower percentage of nuclear maturation than fresh, non-vitrified oocytes. Neither were differences observed in the percentages of oocytes exhibiting a normally configured spindle between the control group and oocytes exposed or vitrified at 38.5°C. However, oocytes exposed or vitrified at 25°C showed a significantly lower proportion of oocytes with normal spindle and chromosome configurations compared to the control group, due primarily to a higher proportion of oocytes with decondensed or disorganized microtubules or chromosomes in the treated groups.

No significant differences among the treatment groups were observed in proportions of oocytes with a disorganized, decondensed or absent spindle configuration, except in the VIT25 group, in which a significantly higher proportion of oocytes featured disorganized spindle and chromosome configurations compared to the control group.

3.3. Percentages of TUNEL-positive oocytes observed in IVM bovine oocytes vitrified/warmed in the 25°C or 38.5°C equilibration protocols

CPA exposure or vitrification/warming of bovine oocytes after exposure to the equilibration solution for 5 min 30 s at 25°C significantly increased the percentage of oocytes with fragmented DNA compared to the fresh control group. Although without significance, percentages of TUNEL-positive oocytes in the 38.5°C vitrified group were similar to those in the fresh non-vitrified treatments (Figure 4A).

Table 2. Spindle morphology and chromosome alignments observed in IVM bovine oocytes vitrified/warmed in the 25°C or 38.5°C equilibration protocols.

Treatment	N° oocytes	MII (%)	Normal spindle configuration (%)	Microtubule distribution (%)			Chromosome distribution (%)		
				Dispersed	Decondensed	Absent	Dispersed	Decondensed	Absent
Control	227	79.19 ± 1.59^{a}	66.69 ± 2.28^{a}	22.19 ± 2.00^{a}	9.53 ± 3.87	1.59 ± 1.30	22.19 ± 2.00^{a}	11.12 ± 3.52	0.00 ± 0.00
CPA25	183	62.16 ± 4.26^{b}	42.00 ± 2.63^{b}	33.21 ± 5.46^{ab}	16.85 ± 6.27	7.94 ± 3.75	34.49 ± 5.31^{ab}	23.51 ± 4.68	0.00 ± 0.00
CPA38.5	211	70.30 ± 2.64^{ab}	61.16 ± 5.40^{a}	27.54 ± 4.18^{a}	8.05 ± 2.90	3.26 ± 1.76	27.54 ± 4.18^{a}	11.30 ± 2.98	0.00 ± 0.00
VIT25	164	66.54 ± 3.53^{ab}	38.38 ± 1.52^{b}	45.76 ± 2.61^{b}	12.79 ± 2.78	3.07 ± 1.46	45.76 ± 2.61^{b}	15.86 ± 3.10	0.00 ± 0.00
VIT38.5	198	71.42 ± 5.22^{ab}	53.49 ± 4.00^{ab}	32.26 ± 1.62^{ab}	10.19 ± 1.49	4.07 ± 2.61	32.26 ± 1.62^{ab}	14.25 ± 3.91	0.00 ± 0.00

Unless indicated otherwise, data are given as the mean ± SEM. ^{a,b} Within columns, values with different superscript letters differ significantly ($P < 0.05$). Rates of oocytes with the given morphology were calculated from the total number of oocytes reaching the MII stage. Control, fresh, non-vitrified oocytes; CPA25: non-vitrified oocytes exposed to the equilibration solution at 25°C for 5 min 30 s; CPA38.5: non-vitrified oocytes exposed to the equilibration solution at 38.5°C for 2 min 30 s; VIT25: oocytes exposed to the equilibration solution at 25°C for 5 min 30 s and vitrified/warmed; VIT38.5: oocytes exposed to the equilibration solution at 38.5°C for 2 min 30 s and vitrified/warmed.

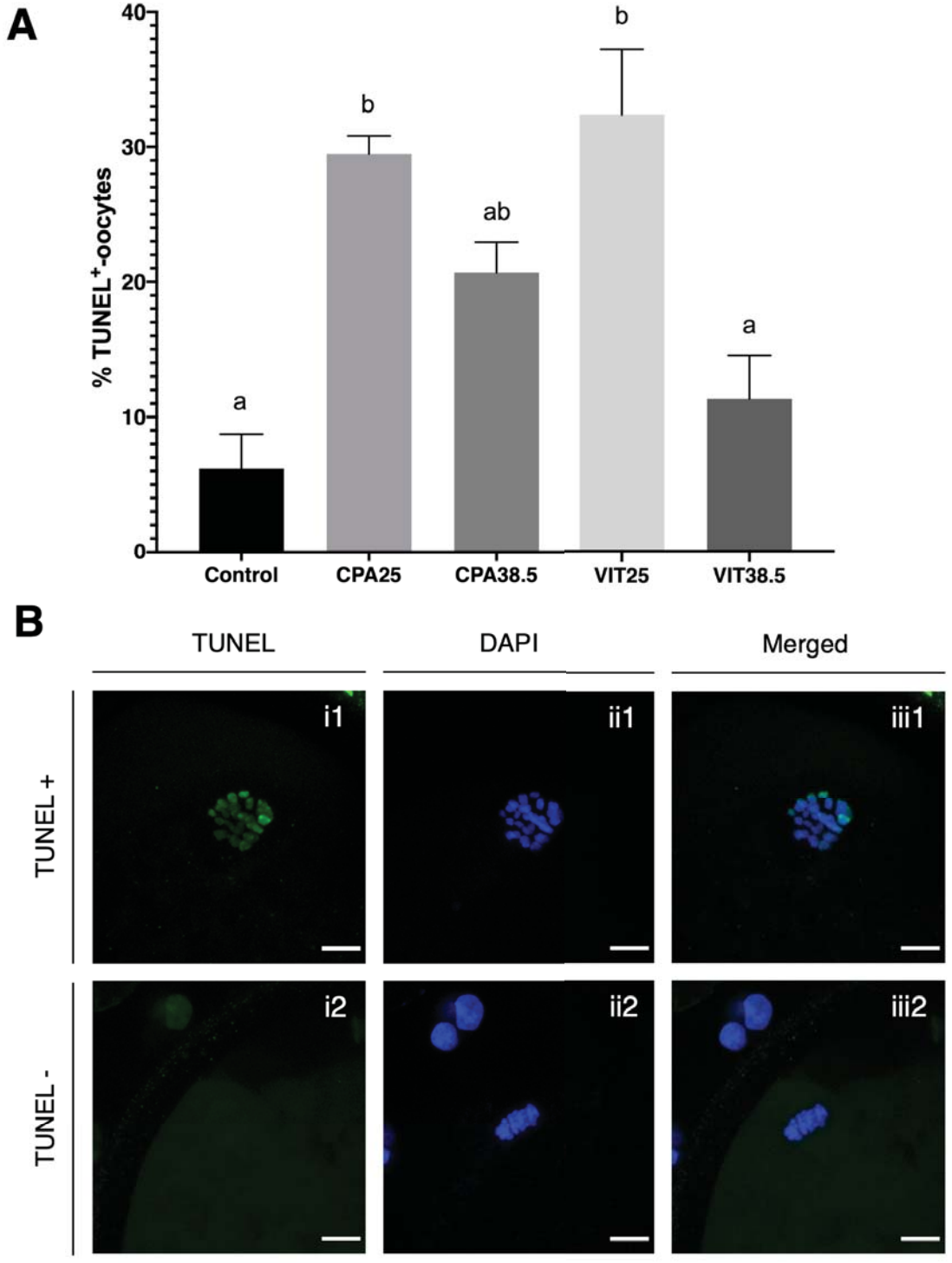

Figure 4. TUNEL detection of fragmented oocyte DNA. (A) Effects of exposing IVM bovine oocytes to the equilibration solution for 5 min 30 s at 25°C or 2 min 30 s at 38.5°C before vitrification/warming on percentages of TUNEL-positive oocytes. Data are presented as the mean ± SEM. [a,b] Values with different letters differ significantly ($P < 0.05$). Treatment groups: Control: fresh, non-vitrified oocytes; CPA25: non-vitrified

oocytes exposed to the equilibration solution at 25°C for 5 min 30 s; CPA38.5: non-vitrified oocytes exposed to the equilibration solution at 38.5°C for 2 min 30 s; VIT25: oocytes exposed to the equilibration solution at 25°C for 5 min 30 s and vitrified/warmed; VIT38.5: oocytes exposed to the equilibration solution at 38.5°C for 2 min 30 s and vitrified/warmed. (B) Representative images of IVM bovine oocytes stained with TUNEL ((i1,i2); green) and DAPI ((ii1,ii2); blue). (i1,ii1): TUNEL-positive oocyte; (i2,ii2): TUNEL-negative oocyte. An overlay is given in (iii1,iii2). Scale bar: 10 μm.

3.4. Embryo development in IVM bovine oocytes vitrified/warmed in the 25°C or 38.5°C equilibration protocols

Table 3 compares the effects on early *in vitro* embryo development of exposing IVM bovine oocytes to CPA solutions at 25°C or 38.5°C prior to vitrification/warming. Vitrification after exposure of oocytes to CPA solutions at 25°C resulted in significantly lower cleavage rates and D7 and D8 blastocyst yields when compared to the control non-vitrified oocyte group. Although not significantly different from those obtained after exposure at 25°C, cleavage rate and percentages of day 7 and day 8 blastocysts resulting from vitrified oocytes previously exposed to CPAs at 38.5°C were similar to those obtained from fresh control oocytes. Further, the impact of the temperature of exposure to CPAs during vitrification/warming on kinetics blastocyst formation was examined. Vitrification/warming using the 38.5°C protocol tended to increase ($P \leq 0.1$) the proportion of advanced blastocysts (expanded, hatching, and hatched) despite no significant differences detected among the experimental groups.

Table 3. Developmental competence of embryos derived from IVM bovine oocytes vitrified/warmed after the 25°C or 38.5°C equilibration protocol

					D8 blastocysts	
	n	**Cleavage rate**	**D7 blastocysts**	**D8 blastocysts**	**n_{D8}**	**Blastocysts**	**Advanced**
Control	170	83.06 ± 2.07[a]	28.17 ± 3.34[a]	33.78 ± 5.07[a]	60	17.44 ± 1.89[a]	16.33 ± 3.90
VIT25	108	55.18 ± 5.09[b]	12.35 ± 2.54[b]	13.23 ± 1.81[b]	14	7.31 ± 1.40[b]	5.92 ± 2.19
VIT38.5	78	64.92 ± 6.54[ab]	18.83 ± 2.23[ab]	23.94 ± 4.88[ab]	17	10.38 ± 2.71[ab]	13.56 ± 2.42

Unless indicated otherwise, data are given as the mean ± SEM. [a.b] Within columns, values with different superscript letters differ significantly ($P < 0.05$). Cleavage rates (48 hpi) and D7 and D8 blastocyst yields were based on the number of oocytes that survived at Day 1 postinsemination. Oocyte survival was assessed on the basis of integrity of the oocyte membrane and zona pellucida, along with discoloration of the cytoplasm. Blastocysts: early and non-expanded blastocysts (intermediate-stage blastocysts); Advanced: expanded, hatching, and hatched blastocysts. Control: embryos derived from fresh, non-vitrified oocytes; VIT25: embryos derived from oocytes exposed to the equilibration solution at 25°C for 5 min 30 s and vitrified/warmed; VIT38.5: embryos derived from oocytes exposed to the equilibration solution at 38.5°C for 2 min 30 s and vitrified/warmed.

3.5. Differential staining of blastocysts and DNA fragmentation.

In Table 4 we provide total cell numbers (TCN), numbers of ICM cells, numbers of TE cells and apoptotic rates (AR) recorded in Day 8 blastocysts derived from oocytes vitrified/warmed in the 25°C and 38.5°C equilibration protocols. Photographs obtained after differential cell staining of blastocysts are displayed in Figure 2. While no differences were observed in TCN and numbers of TE cells in blastocysts derived from vitrified/warmed oocytes in the 38.5°C protocol, advanced blastocysts were produced with similar TCN and TE and ICM cell numbers than those derived from control oocytes. Although not significantly different from advanced blastocysts derived from vitrified/warmed oocytes subjected to the 38.5°C protocol, those vitrified/warmed in the 25°C equilibration protocols gave rise to advanced blastocysts with significantly lower ICM cell counts and higher TCN and TE cell counts than blastocysts derived from the non-vitrified group. Further, a significant increase was observed in TCN, ICM cell numbers and TE cell numbers as the blastocyst stage progressed from blastocyst to advanced blastocyst, regardless of the treatment group. Although blastocysts derived from vitrified (38.5°C) oocytes showed significantly higher apoptosis rates than those derived from fresh non-vitrified oocytes, blastocysts derived from oocytes vitrified in the 25°C protocol showed the highest AR compared to the other treatment groups, regardless of blastocyst stage.

Table 4. Total cell numbers, number of cells in the ICM and TE, and rate of apoptotic cells recorded in Day 8 blastocysts derived from oocytes vitrified/warmed after the 25°C and 38.5°C equilibration protocols

	Day 8 blastocysts									
	n		TCN ± SEM		ICM cell number ± SEM		TE cell number ± SEM		AR± SEM	
	Blast	Adv	Blast	Adv	Blast	Adv	Blast	Adv	Blast	Adv
Control	31	29	95.2 ± 2.2[1]	155.7 ± 5.6[a,2]	12.5 ± 0.7[a,1]	24.3 ± 1.0[a,2]	82.7 ± 2.1[1]	131.45 ± 5.2[a,2]	6.8 ± 0.4[a,1]	6.0 ± 0.5[a,1]
VIT25	8	6	87.8 ± 3.2[1]	180.5 ± 5.4[b,2]	8.9 ± 0.5[b,1]	18.5 ± 2.9[b,2]	79.0 ± 3.1[1]	162.0 ± 6.2[b,2]	19.9 ± 3.1[b,1]	15.3 ± 1.4[b,2]
VIT38.5	7	10	92.0 ± 4.5[1]	162.8 ± 8.1[ab,2]	10.8 ± 1.9[ab,1]	20.5 ± 2.3[ab,2]	81.1 ± 4.2[1]	142.3 ± 7.9[ab,2]	13.3 ± 1.3[c,1]	10.3 ± 1.0[c,1]

Unless indicated otherwise, data are given as mean ± SEM. [a.b.c] Values within columns with different superscripts differ significantly ($P < 0.05$); [1,2] Values within rows with different superscripts differ significantly ($P < 0.05$). Blast: early and non-expanded blastocysts (intermediate stage blastocysts); Adv: expanded, hatching, and hatched blastocysts. TCN: total cell number; ICM: inner cell mass; TE: trophectoderm; AR: apoptosis rate. Control: embryos derived from fresh, non-vitrified oocytes. VIT25: embryos derived from oocytes exposed to the equilibration solution at 25°C for 5 min 30 s and vitrified/warmed. VIT38.5: embryos derived from oocytes exposed to the equilibration solution at 38.5°C for 2 min 30 s and vitrified/warmed.

4. Discussion

Procedures designed to prepare bovine oocytes for vitrification strive to attain both appropriate intracellular glass-forming conditions and prevent an impaired capacity for fertilization and development into viable embryos. Because of the possible effects of numerous factors during the equilibration stage such as the CPAs employed and their concentrations, as well as the temperature and time of exposure to these CPAs, success with bovine oocyte survival and development has been limited and variable among studies (reviewed by (Dujickova *et al.* 2020)). This has determined that much research is still being devoted to improve the vitrification/warming of oocytes in cattle production. Rational design approaches combine mathematical models and cell biophysical parameters to predict optimized CPA addition and removal procedures. As the damage induced by extending cell volumes beyond osmotic tolerance limits is relatively well understood, the most common approach has been to use membrane transport equations and osmotic tolerance limits to predict multi-step procedures that prevent osmotic damage (Mukherjee *et al.* 2007).

The *in silico* and *in vitro* analysis of the osmotic behavior of MII oocytes has several limitations. To calculate the relative volume of an oocyte from a 2D image of the shrinking-swelling process, several assumptions are made, so predicted permeability parameters may not be accurate (Paynter *et al.* 1999b; Mullen *et al.* 2008). Also osmotic behavior has been determined separately for low concentrations of each CPA (Newton *et al.* 1999; Paynter *et al.* 1999a; Zhao *et al.* 2017) and under different CPA conditions, this behavior is likely to vary (Mazur and Schneider 1986). At the CPA concentrations needed for oocyte vitrification, CPAs could affect cytoplasmic phospholipid bilayer permeability (Sydykov *et al.* 2018). Also, the biophysical parameters of individual oocytes seem highly variable (Paynter 2005). Hence, permeability models and *in vitro* observations may not accurately reflect the physiological situation.

Despite these limitations, our *in silico* and *in vitro* results were fairly consistent. The time required for the oocytes to reach the equilibrium cell volume upon exposure to standard ES increased as the temperature decreased, such that 2 min 30 s was needed at 38.5°C and 5 min 30 s at 25°C. This is important because during this interval intracellular water ejection is close to completion and the permeation of low molecular weight cryoprotectants leads to similar intracellular and extracellular solute concentrations. Hence, lengthening exposure to CPAs solutions does not improve the cytosolic glass-forming

tendency and toxicity derived for longer CPA exposures could be avoided. This determines that rather than the usual 9 to 15 min of CPA exposure time used for bovine oocytes, a better approach could be the exposure of oocytes to non-vitrifying hypertonic solutions just until the equilibrium cell volume is reached to prepare them for vitrification. In the present study, we modified the equilibration protocol of a new vitrification/warming method designed to represent the current standard practice to prepare bovine oocytes (Kuwayama 2007) according to the *in vitro* osmotic behavior of oocytes at different temperatures. These modifications to the protocol were validated by examining oocyte spindle status, oocyte DNA fragmentation and further embryo development after vitrification/warming of MII bovine oocytes.

The main hurdle in developing successful protocols for the cryopreservation of mammalian oocytes is preserving the integrity of the meiotic spindle when oocytes are cooled below physiological temperature. Temperature fluctuations directly affect the cytoskeletal and microtubular system of mature bovine (Aman and Parks 1994) and human (Almeida and Bolton 1995) oocytes. While the effects of cooling on the spindle seem reversible in the mouse oocyte, with normal spindle formation occurring after step-wise re-warming (Pickering and Johnson 1987), bovine and human oocytes are less resilient because of the irreversibility of temperature-induced spindle disruption (Pickering *et al.* 1990; Aman and Parks 1994; Almeida and Bolton 1995). In our study, exposure of oocytes to CPAs at 25°C for 5 min 30 s yielded the lowest percentage of oocytes reaching the MII stage. Aman and Parks (Aman and Parks 1994) reported that the spindles of MII bovine oocytes started to depolymerize when cooled to 25°C for 1 min or more, and the extent of depolymerization (or disassembly) was also directly related to CPA exposure duration (Aman and Parks 1994). We also observed that CPA exposure or vitrification after equilibration at 25°C for 5 min 30 s also resulted in reduced proportions of oocytes displaying normal spindle configurations. Other authors have described higher proportions of spindle alterations in MII bovine oocytes vitrified after similar or longer exposures times to the equilibration solution at 25°C (Arcarons *et al.* 2015; Chaves *et al.* 2016) when compared to their fresh counterparts. However, no significant increase was noted here in chromosomal abnormalities after CPA exposure at 38.5°C for 2 min 30 s before vitrification, suggesting that the bovine oocytes were able to recover from cooling or CPA-induced damage to the oocytes' spindle microtubules. In prior work, we observed that bovine oocytes vitrified after 10 min of exposure to ES at 38.5°C led to similar rates of maturation and normal spindle configurations to those detected here at 38.5°C (Arcarons *et*

al. 2019; García-Martínez *et al.* 2020). This may indicate that IVM bovine oocytes are more sensitive to the temperature of exposure to ES and VS than to the detrimental effects of CPA toxicity.

In this study, vitrification after CPA exposure at 38.5°C for 2 min 30 s did not significantly affect the occurrence of DNA fragmentation in oocytes when compared to fresh controls. Contrarily, exposure or vitrification of oocytes at 25°C significantly increased the percentage of DNA fragmentation after warming. Using the same methodology, studies by our group (Spricigo *et al.* 2017; Vendrell-Flotats *et al.* 2020) detected significantly higher apoptosis rates through TUNEL analysis in bovine oocytes vitrified after being exposed for a longer time to ES (10 min or 9 min, respectively) at 38.5°C. Hence, the toxicity of CPAs in terms of DNA fragmentation can be reduced by modifying equilibration times and temperatures (Raju *et al.* 2021). Some authors have questioned whether CPA toxicity is related to the osmotic stress of adding and removing CPAs. Although osmotic stress can indeed cause cytotoxicity, experimental evidence suggests that CPAs are more chemically toxic (Lawson *et al.* 2012). While the mechanisms of CPA toxicity remain to be clearly established (Best 2015), hydrophobic interactions between CPAs and proteins, and a longer lifetime of CPA–water hydrogen bonds (Kirchner and Reiher 2002) have been proposed. These agents have also been accused of varying intracellular pH (Damien *et al.* 1990), increasing intracellular calcium contents (Gardner *et al.* 2007) and causing formaldehyde formation in cryopreservation solutions (Karran and Legge 1996) (or reviewed by (Best 2015)).

The results of our embryo development experiments designed to assess oocyte competence after vitrification/warming indicate comparable cleavage and blastocyst rates of vitrified bovine oocytes after exposure to CPA solutions at 38.5°C to those of control fresh oocytes. Moreover, although not significant, shorter CPA exposures at 38.5°C gave rise to almost double the percentage of blastocysts obtained after longer CPA exposure at 25°C. Our results clearly indicate the importance of temperature and time of CPA addition prior to vitrification. Cytotoxicity has been shown to increase with increased temperatures for relatively long exposure times (Lawson *et al.* 2011; Davidson *et al.* 2015). This has led to the general assumption that CPA exposure should be carried out at low temperatures (25°C). However, the temperature of addition significantly affects the time needed to achieve full equilibration. At a higher temperature, equilibration occurs much more quickly, allowing for shorter incubation times and reducing cell exposure to CPAs during their addition and removal. Due to faster mass transport across cell membrane at 38.5°C,

equilibration of the oocyte occurs earlier than at 25°C and less time is required for CPA addition. If we bear in mind that CPA exposure at 38.5°C had fewer deleterious effects on the meiotic spindle and oocyte apoptosis, CPA exposure at 38.5°C for 2 min 30 s may have allowed the oocyte to achieve the minimum intracellular glass-forming conditions so as not to fully impair the ability of vitrified/warmed oocytes to be successfully fertilized and develop into viable embryos.

When this same vitrification/warming methodology was used to vitrify MII bovine oocytes (Kuwayama 2007), a longer exposure (9 or 15 min) to ES at 25°C produced lower (Azari *et al.* 2017) or similar (Zhou *et al.* 2010; Vendrell-Flotats *et al.* 2020) cleavage and blastocyst rates to the ones observed in this study in the VIT25 group. However, blastocyst yields were reduced when IVM bovine oocytes were exposed to ES at 38.5°C-39°C for 9 or more minutes prior to vitrification (Ortiz-Escribano *et al.* 2016; Arcarons *et al.* 2017; Arcarons *et al.* 2019; García-Martínez *et al.* 2020). These findings highlight the fact that the effects of temperature on cytotoxicity are clearly dependent on exposure times (Lawson *et al.* 2011). Thus, reports exist of significantly decreased rates of embryo development when oocytes were overexposed to CPAs at 38.5°C (Ortiz-Escribano *et al.* 2016; Arcarons *et al.* 2017; Arcarons *et al.* 2019; García-Martínez *et al.* 2020) while prolonged exposure (9 or 15 min) at 25°C also impaired embryo development (Zhou *et al.* 2010; Vendrell-Flotats *et al.* 2020) but this effect was much less dramatic than at 38.5°C.

It has been well established that for embryo survival and post-implantation development, blastocyst cells need to be optimally allocated to the ICM and TE. Studies have shown that a defined minimal number of ICM cells correlates strongly with normal fetal development and an adequate ICM:TE cell ratio seems essential for embryo viability and pregnancy (Van Soom *et al.* 1996). Moreover, excessive allocation of cells to the TE possibly leads to early pregnancy loss (Van Soom *et al.* 1996; Loureiro *et al.* 2009). Our blastocyst kinetics experiments revealed a clear trend towards a higher hatching ability of blastocysts derived from oocytes vitrified/warmed in the 38.5°C protocol. Further, blastocysts in the 38.5°C vitrification group featured similar TCN, ICM and TE cell counts as in the non-vitrified groups, regardless of blastocyst stage. In contrast, higher TE and apoptotic cell numbers and lower ICM cell counts were observed in blastocysts derived from oocytes vitrified at 25°C. While in preimplantation embryos apoptosis serves to eliminate compromised cells, a high incidence of apoptosis results in a morphologically abnormal embryo (Hardy *et al.* 1989). This may explain why the lower apoptosis rate

observed here in blastocysts derived from oocytes vitrified/warmed in the 38.5°C protocol gave rise to higher ($P<0.1$) percentages of advanced blastocysts.

In conclusion, in this study we validate new CPA equilibration procedures at two different temperatures as a first step to optimize vitrification/warming methods for bovine IVM oocytes. Based on *in silico* data on the biophysical permeability of oocytes and *in vitro* osmotic observations, we here propose a shorter vitrification/warming protocol for MII bovine oocytes. Using a standardized combination of vitrification solutions, exposure to the equilibration solution was constrained to 5 min 30 s or to 2 min 30 s when ES exposure was done at 25°C or 38.5°C, respectively. After validating oocyte morphofunctionality and embryo development, our results indicate that exposure to ES for 2 min 30 s and vitrification/warming at 38.5°C could improve the quality of vitrified/warmed oocytes improving blastocyst rates and quality by protecting spindle integrity and reducing DNA fragmentation. These data also indicate that toxic damage at a given temperature may be reduced by minimizing the duration of CPA addition and removal while maintaining cell volumes within osmotic tolerance limits. Our findings also pave the way for using a similar approach to improve vitrification of other mammalian oocytes.

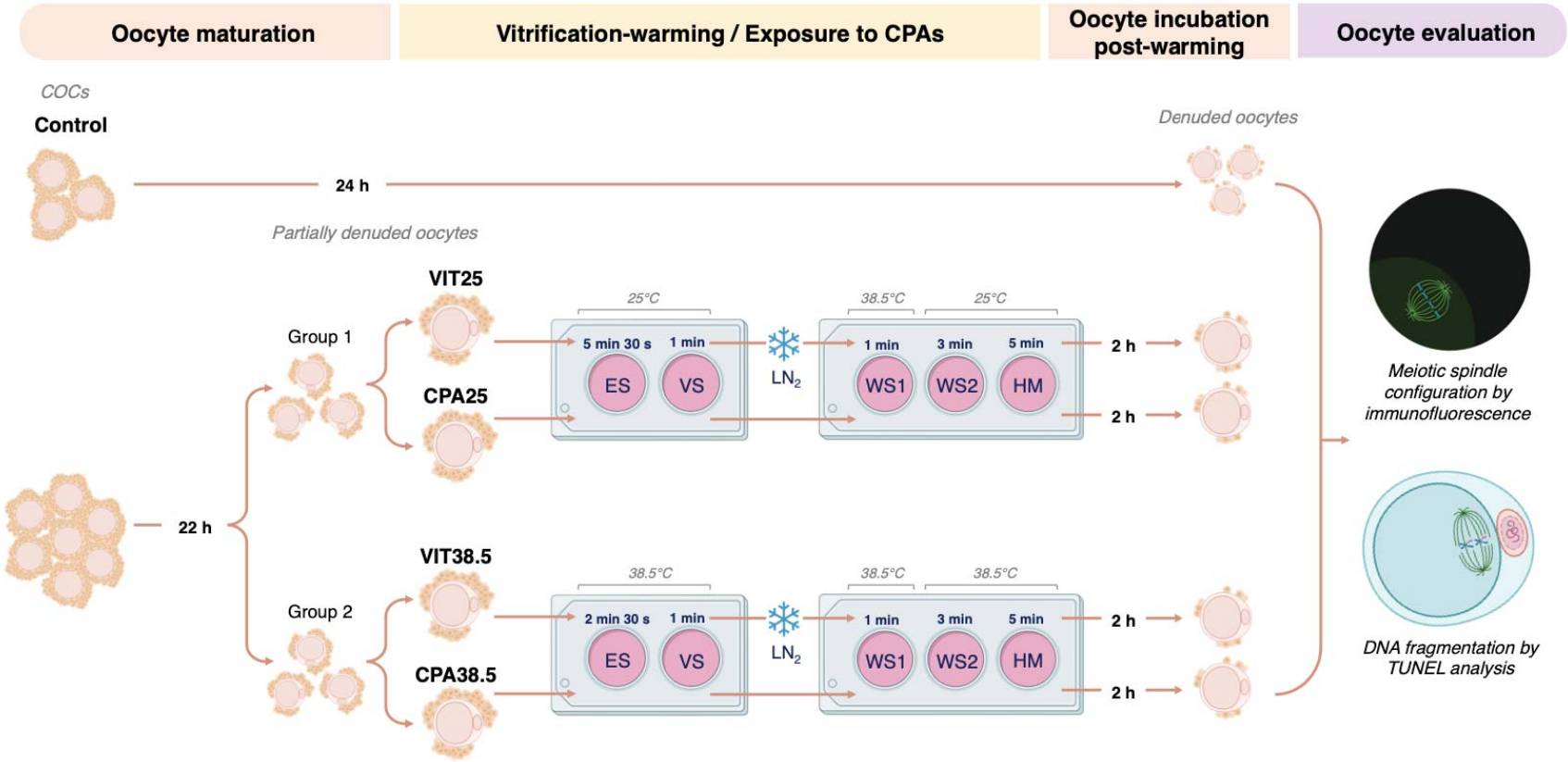

Supplemental Figure S1. Experimental design. IVM oocytes were randomly assigned to five groups: 1) Control, fresh, non-vitrified oocytes; 2) VIT25: oocytes exposed to ES for 5 min 30 s at 25°C and vitrified/warmed; 3) CPA25: non-vitrified oocytes exposed to ES for 5 min 30 s at 25°C; 4) VIT38.5: oocytes exposed to ES for 2 min 30 s at 38.5°C and vitrified/warmed; and 5) CPA38.5: non-vitrified oocytes exposed to ES for 2 min 30 s at 38.5°C. At 24 h of IVM, oocytes from each of the five treatment groups were denuded and immunostained to assess spindle morphology and DNA fragmentation.

References

Almeida, P.A., and Bolton, V.N. (1995) The effect of temperature fluctuations on the cytoskeletal organisation and chromosomal constitution of the human oocyte. *Zygote* **3**(4), 357-65

Aman, R.R., and Parks, J.E. (1994) Effects of cooling and rewarming on the meiotic spindle and chromosomes of *in vitro*-matured bovine oocytes. *Biol Reprod* **50**(1), 103-10

Arcarons, N., Morato, R., Spricigo, J.F., Ferraz, M.A., and Mogas, T. (2015) Spindle configuration and developmental competence of *in vitro*-matured bovine oocytes exposed to NaCl or sucrose prior to Cryotop vitrification. *Reprod Fertil Dev*

Arcarons, N., Vendrell-Flotats, M., Yeste, M., Mercade, E., Lopez-Bejar, M., and Mogas, T. (2019) Cryoprotectant role of exopolysaccharide of Pseudomonas sp. ID1 in the vitrification of IVM cow oocytes. *Reprod Fertil Dev* **31**(9), 1507-1519

Arcarons, N., Vendrell-Flotats, M., Yeste, M., Mercadé, E., and Mogas, T. (2017) Spindle configuration of *in vitro* matured bovine oocytes vitrified and warmed in media supplemented with a biopolymer produced by an Antarctic bacterium. *Animal Reproduction* **14**(3), 972

Azari, M., Kafi, M., Ebrahimi, B., Fatehi, R., and Jamalzadeh, M. (2017) Oocyte maturation, embryo development and gene expression following two different methods of bovine cumulus-oocyte complexes vitrification. *Vet Res Commun* **41**(1), 49-56

Best, B.P. (2015) Cryoprotectant Toxicity: Facts, Issues, and Questions. *Rejuvenation Res* **18**(5), 422-36

Chaves, D.F., Campelo, I.S., Silva, M.M., Bhat, M.H., Teixeira, D.I., Melo, L.M., Souza-Fabjan, J.M., Mermillod, P., and Freitas, V.J. (2016) The use of antifreeze protein type III for vitrification of *in vitro* matured bovine oocytes. *Cryobiology* **73**(3), 324-328

Chian, R.C., Kuwayama, M., Tan, L., Tan, J., Kato, O., and Nagai, T. (2004) High survival rate of bovine oocytes matured *in vitro* following vitrification. *J Reprod Dev* **50**(6), 685-96

Damien, M., Luciano, A.A., and Peluso, J.J. (1990) Propanediol alters intracellular pH and developmental potential of mouse zygotes independently of volume change. *Hum Reprod* **5**(2), 212-6

Davidson, A.F., Glasscock, C., McClanahan, D.R., Benson, J.D., and Higgins, A.Z. (2015) Toxicity Minimized Cryoprotectant Addition and Removal Procedures for Adherent Endothelial Cells. *PLoS One* **10**(11), e0142828

Dormand, J.R., and Prince, P.J. (1980) A family of embedded Runge-Kutta formulae. *Journal of Computational and Applied Mathematics* **6**(1), 19-26

Dujickova, L., Makarevich, A.V., Olexikova, L., Kubovicova, E., and Strejcek, F. (2020) Methodological approaches for vitrification of bovine oocytes. *Zygote*, 1-11

Gallardo, M., Saenz, J., and Risco, R. (2019) Human oocytes and zygotes are ready for ultra-fast vitrification after 2 minutes of exposure to standard CPA solutions. *Sci Rep* **9**(1), 15986

García-Martínez, T., Vendrell-Flotats, M., Martínez-Rodero, I., Ordóñez-León, E.A., Álvarez-Rodríguez, M., López-Béjar, M., Yeste, M., and Mogas, T. (2020) Glutathione Ethyl Ester Protects *In Vitro*-Maturing Bovine Oocytes against Oxidative Stress Induced by Subsequent Vitrification/Warming. *Int J Mol Sci* **21**(20)

Gardner, D.K., Sheehan, C.B., Rienzi, L., Katz-Jaffe, M., and Larman, M.G. (2007) Analysis of oocyte physiology to improve cryopreservation procedures. *Theriogenology* **67**(1), 64-72

Gutierrez-Anez, J.C., Lucas-Hahn, A., Hadeler, K.G., Aldag, P., and Niemann, H. (2021) Melatonin enhances *in vitro* developmental competence of cumulus-oocyte complexes collected by ovum pick-up in prepubertal and adult dairy cattle. *Theriogenology* **161**, 285-293

Hardy, K., Handyside, A.H., and Winston, R.M. (1989) The human blastocyst: cell number, death and allocation during late preimplantation development *in vitro*. *Development* **107**(3), 597-604

Hwang, I.S., and Hochi, S. (2014) Recent progress in cryopreservation of bovine oocytes. *BioMed research international* **2014**, 570647

Karran, G., and Legge, M. (1996) Non-enzymatic formation of formaldehyde in mouse oocyte freezing mixtures. *Hum Reprod* **11**(12), 2681-6

Kirchner, B., and Reiher, M. (2002) The secret of dimethyl sulfoxide-water mixtures. A quantum chemical study of 1DMSO-nwater clusters. *J Am Chem Soc* **124**(21), 6206-15

Kuwayama, M. (2007) Highly efficient vitrification for cryopreservation of human oocytes and embryos: the Cryotop method. *Theriogenology* **67**(1), 73-80

Lagarias, J.C., Reeds, J.A., Wright, M.H., and Wright, P.E. (1998) Convergence Properties of the Nelder--Mead Simplex Method in Low Dimensions. *SIAM Journal on Optimization* **9**(1), 112-147

Lawson, A., Ahmad, H., and Sambanis, A. (2011) Cytotoxicity effects of cryoprotectants as single-component and cocktail vitrification solutions. *Cryobiology* **62**(2), 115-22

Lawson, A., Mukherjee, I.N., and Sambanis, A. (2012) Mathematical modeling of cryoprotectant addition and removal for the cryopreservation of engineered or natural tissues. *Cryobiology* **64**(1), 1-11

Ledda, S., Bogliolo, L., Succu, S., Ariu, F., Bebbere, D., Leoni, G.G., and Naitana, S. (2007) Oocyte cryopreservation: oocyte assessment and strategies for improving survival. *Reprod Fertil Dev* **19**(1), 13-23

Leibo, S.P. (2008) Cryopreservation of oocytes and embryos: optimization by theoretical versus empirical analysis. *Theriogenology* **69**(1), 37-47

Loureiro, B., Bonilla, L., Block, J., Fear, J.M., Bonilla, A.Q., and Hansen, P.J. (2009) Colony-stimulating factor 2 (CSF-2) improves development and posttransfer survival of bovine embryos produced *in vitro*. *Endocrinology* **150**(11), 5046-54

Martínez-Rodero, I., García-Martínez, T., Ordóñez-León, E.A., Vendrell-Flotats, M., Olegario Hidalgo, C., Esmoris, J., Mendibil, X., Azcarate, S., López-Béjar, M., Yeste, M., and Mogas, T. (2021) A Shorter Equilibration Period Improves Post-Warming Outcomes after Vitrification and in Straw Dilution of *In Vitro*-Produced Bovine Embryos. *Biology (Basel)* **10**(2)

Mazur, P., and Schneider, U. (1986) Osmotic responses of preimplantation mouse and bovine embryos and their cryobiological implications. *Cell Biophys* **8**(4), 259-85

Mogas, T. (2018) Update on the vitrification of bovine oocytes and invitro-produced embryos. *Reprod Fertil Dev* **31**(1), 105-117

Morato, R., Izquierdo, D., Paramio, M.T., and Mogas, T. (2008) Cryotops versus open-pulled straws (OPS) as carriers for the cryopreservation of bovine oocytes: effects on spindle and chromosome configuration and embryo development. *Cryobiology* **57**(2), 137-41

Mukherjee, I.N., Song, Y.C., and Sambanis, A. (2007) Cryoprotectant delivery and removal from murine insulinomas at vitrification-relevant concentrations. *Cryobiology* **55**(1), 10-8

Mullen, S.F., Li, M., Li, Y., Chen, Z.J., and Critser, J.K. (2008) Human oocyte vitrification: the permeability of metaphase II oocytes to water and ethylene glycol and the appliance toward vitrification. *Fertil Steril* **89**(6), 1812-25

Newton, H., Pegg, D.E., Barrass, R., and Gosden, R.G. (1999) Osmotically inactive volume, hydraulic conductivity, and permeability to dimethyl sulphoxide of human mature oocytes. *J Reprod Fertil* **117**(1), 27-33

Ortiz-Escribano, N., Smits, K., Piepers, S., Van den Abbeel, E., Woelders, H., and Van Soom, A. (2016) Role of cumulus cells during vitrification and fertilization of mature bovine oocytes: Effects on survival, fertilization, and blastocyst development. *Theriogenology* **86**(2), 635-41

Paynter, S.J. (2005) A rational approach to oocyte cryopreservation. *Reprod Biomed Online* **10**(5), 578-86

Paynter, S.J., Cooper, A., Gregory, L., Fuller, B.J., and Shaw, R.W. (1999a) Permeability characteristics of human oocytes in the presence of the cryoprotectant dimethylsulphoxide. *Hum Reprod* **14**(9), 2338-42

Paynter, S.J., Fuller, B.J., and Shaw, R.W. (1999b) Temperature dependence of Kedem-Katchalsky membrane transport coefficients for mature mouse oocytes in the presence of ethylene glycol. *Cryobiology* **39**(2), 169-76

Pickering, S.J., Braude, P.R., Johnson, M.H., Cant, A., and Currie, J. (1990) Transient cooling to room temperature can cause irreversible disruption of the meiotic spindle in the human oocyte. *Fertil Steril* **54**(1), 102-8

Pickering, S.J., and Johnson, M.H. (1987) The influence of cooling on the organization of the meiotic spindle of the mouse oocyte. *Hum Reprod* **2**(3), 207-16

Prentice, J.R., and Anzar, M. (2010) Cryopreservation of Mammalian oocyte for conservation of animal genetics. *Vet Med Int* **2011**

Raju, R., Bryant, S.J., Wilkinson, B.L., and Bryant, G. (2021) The need for novel cryoprotectants and cryopreservation protocols: Insights into the importance of biophysical investigation and cell permeability. *Biochim Biophys Acta Gen Subj* **1865**(1), 129749

Rizos, D., Ward, F., Boland, M.P., and Lonergan, P. (2001) Effect of culture system on the yield and quality of bovine blastocysts as assessed by survival after vitrification. *Theriogenology* **56**(1), 1-16

Shampine, L.F., and Reichelt, M.W. (1997) The MATLAB ODE Suite. *SIAM Journal on Scientific Computing* **18**(1), 1-22

Spricigo, J.F., Morato, R., Arcarons, N., Yeste, M., Dode, M.A., Lopez-Bejar, M., and Mogas, T. (2017) Assessment of the effect of adding L-carnitine and/or resveratrol to maturation medium before vitrification on *in vitro*-matured calf oocytes. *Theriogenology* **89**, 47-57

Sydykov, B., Oldenhof, H., de Oliveira Barros, L., Sieme, H., and Wolkers, W.F. (2018) Membrane permeabilization of phosphatidylcholine liposomes induced by cryopreservation and vitrification solutions. *Biochim Biophys Acta Biomembr* **1860**(2), 467-474

Van Soom, A., Boerjan, M., Ysebaert, M.T., and De Kruif, A. (1996) Cell allocation to the inner cell mass and the trophectoderm in bovine embryos cultured in two different media. *Mol Reprod Dev* **45**(2), 171-82

Vendrell-Flotats, M., Garcia-Martinez, T., Martinez-Rodero, I., Lopez-Bejar, M., LaMarre, J., Yeste, M., and Mogas, T. (2020) *In Vitro* Maturation with Leukemia Inhibitory Factor

Prior to the Vitrification of Bovine Oocytes Improves Their Embryo Developmental Potential and Gene Expression in Oocytes and Embryos. *Int J Mol Sci* **21**(19)

Wang, L., Liu, J., Zhou, G.B., Hou, Y.P., Li, J.J., and Zhu, S.E. (2011) Quantitative investigations on the effects of exposure durations to the combined cryoprotective agents on mouse oocyte vitrification procedures. *Biol Reprod* **85**(5), 884-94

Zhao, G., Zhang, Z., Zhang, Y., Chen, Z., Niu, D., Cao, Y., and He, X. (2017) A microfluidic perfusion approach for on-chip characterization of the transport properties of human oocytes. *Lab Chip* **17**(7), 1297-1305

Zhou, X.L., Al Naib, A., Sun, D.W., and Lonergan, P. (2010) Bovine oocyte vitrification using the Cryotop method: effect of cumulus cells and vitrification protocol on survival and subsequent development. *Cryobiology* **61**(1), 66-72

General Discussion

Successful cryopreservation of mammalian oocytes has numerous practical, economical and ethical benefits, and will positively impact animal breeding programs and assisted conception in humans (Fabbri 2006; Leibo 2008). However, despite many offspring of various species being produced after the application of these technologies, there still remain shortcomings of methodologies used to cryopreserve oocytes (Ambrosini *et al.* 2006; Wang *et al.* 2010). Vitrification is a process of cryopreservation during which solidification of a solution occurs without the formation of ice crystals. This phenomenon requires either rapid cooling and warming rates or the use of concentrated CPAs solutions. CPAs have been proven to dramatically suppress the freezing injuries suffered by the cells because they decelerate the water molecule diffusion by increasing the viscosity of the solution, and thus greatly reduce the ice nucleation and growth (Karlsson and Toner 1996; Yi *et al.* 2014). CPAs are also potentially useful in stabilizing the plasma membrane through electrostatic interactions (Anchordoguy *et al.* 1991) or reducing the harmful concentrated electrolytes by permeating into the cells (Karlsson and Toner 1996). However, CPAs themselves are harmful to cells because its chemical toxicity at high concentrations (Yang *et al.* 2011) and the excessive osmotic damage that oocytes would suffer through adding or removing the CPAs during cryopreservation (Karlsson and Toner 1996). As a consequence, to optimize the cryopreservation procedure for oocytes, it is of great importance to understand mass transport across the cell membrane completely (Zhang *et al.* 2016).

A wide variety of methodologies have been used to improve and optimize procedures of bovine-oocyte vitrification. The majority of studies tend to use "trial-and-error" to examine the effects of various protective compounds (Morato *et al.* 2008; García-Martínez *et al.* 2020), macromolecular supplements (Chian *et al.* 2004; Checura and Seidel 2007) and to compare different cooling and warming conditions. However, in recent years, the development of bovine vitrification seemed to reach a plateau phase and researchers achieved disparate survival and developmental rates when using similar or different protocols. Theoretical analysis of membrane transport characteristics of oocytes has been considered to be an efficacious approach to optimization of oocyte cryopreservation, because it allows design the vitrification protocols in a rational manner and reduce the times of replicate experiment greatly. For this purpose, a plethora of mathematical models have been developed (Jacobs and Stewart 1932; Jacobs 1933; Kedem and Katchalsky 1958; Elmoazzen *et al.* 2009). The two-parameter (2P) model, which was proposed by Jacobs and Stewart (Jacobs and Stewart 1932; Jacobs 1933), is very popular, simple and makes a dilute

solution assumption that may not be suitable for CPAs solutions. For that reason, in 2009, Elmoazzen et al. (Elmoazzen *et al.* 2009) presented a new nondilute solution model, which is comparatively more complex than the 2P model .

For this purpose, this thesis aimed as a first objective to investigate if the use of mathematical models could help to provide a better understanding of the osmotic transport across the cell membranes, to design less damaging methods for the vitrification of bovine oocytes. Typically cell membrane permeability parameters are determined after exposure to a single CPA concentration (Agca *et al.* 1998; Wang *et al.* 2010; Jin *et al.* 2011). However, because oocytes are exposed to increasing CPA concentrations during the vitrification process, previous studies suggested that oocyte permeability to water and CPA may be concentration dependent (Lahmann *et al.* 2018). Therefore, in the first study, we determined the concentration-dependent permeability characteristics of immature (at GV stage) oocytes and *in vitro* matured (at MII stage) oocytes sequentially exposed to increasing concentrations of EG and Me_2SO (0.30 mol/L, 0.68 mol/L, 1.55 mol/L, and 3.5 mol/L)

Results demonstrate that water permeability of bovine oocytes decreases as the CPA concentration increases. This trend has been observed previously in other cell types (McGrath 1988; Gilmore *et al.* 1995; Lahmann *et al.* 2018), and has been explained in terms of steric hindrance caused by CPA binding to water-transporting channels (Toon and Solomon 1990). Bovine oocytes are known to express aquaporins (Jin *et al.* 2011) and the fact that water permeability decreases as CPA concentration increases is consistent with such a mechanism. Our results also show that the EG permeability of bovine GV oocytes decreases as EG concentration increases. Bovine oocytes express both aquaporin 3 and aquaporin 7 (García-Martínez *et al.* 2018). These aquaglyceroporins have been shown to transport glycerol, EG and possibly other CPAs (Jin *et al.* 2011) and are postulated to transport these molecules via successive binding to various sites on the aquaporin protein (Rodriguez *et al.* 2019; Moss *et al.* 2020). These binding sites can become saturated at high CPA concentrations, leading to slower CPA transport (Rodriguez *et al.* 2019; Moss *et al.* 2020). In contrast to glycerol and EG, there is evidence that Me_2SO transport through aquaporin 3 is negligible in mammalian oocytes (Edashige 2017), which may explain why Me_2SO permeability was not concentration dependent. Similarly, permeability to EG turned out to be not concentration dependent in *in vitro* matured oocytes. This suggests that maturation may have caused changes in the expression of aquaporins or in the composition of the membrane, modifying the transport mechanism of EG. (Jo *et al.* 2011).

Results observed on membrane permeability when oocytes were exposed to 1.55 mil/L are consistent with the trends observed in previous studies, where permeability parameters were estimated by measuring cell volume changes after exposure of bovine oocytes to a single CPA concentration ranging between 1.2 mol/L and 1.8 mol/L (Agca *et al.* 1998; Wang *et al.* 2010; Jin *et al.* 2011). In these studies, the water permeability of MII oocytes was nearly twofold higher than that of GV oocytes, and the CPA permeability was similar for EG and Me_2SO and for GV and MII oocytes. That means the changes of cell volume and intracellular CPA concentrations are more severe in MII than GV bovine oocytes during CPA addition and dilution process, which make it more sensitive to CPA addition and removal.

Moreover, the use of the 2P model for making predictions under non-dilute conditions may be one potential explanation for the observed effects of CPA concentration on the permeability parameters. It has been suggested that the non-dilute transport model can provide more accurate predictions, particularly at high CPA concentrations (Elmoazzen *et al.* 2009). Therefore, we also analyzed the permeability parameters for GV and MII bovine oocytes with the non-dilute transport model (Elmoazzen *et al.* 2009) which showed nearly identical tendencies in both mathematical models: water permeability decreases as EG or Me_2SO concentration increases in both GV and MII oocytes, and the EG permeability decreases as EG concentration increases in GV oocytes. Thus, the fact the water and CPA permeability decreases as CPA concentration increases cannot be only attributed to use of the 2P model under non-dilute conditions, suggesting the existence of a transport process dependent on CPA concentration.

Cell membrane transport predictions can be useful to predict the potential damage during CPA addition and removal and to design less damaging methods. For that reason, the potential practical implications of different modeling approaches was examined. For that purpose, and using the permeability parameters determined from the previous experiments, to model cell volume excursions of both GV and MII bovine oocytes during CPA addition and removal following the Kuwayama vitrification protocol (Kuwayama *et al.* 2005), which was designed for and tested on bovine and human oocytes. The two modeling approaches yield nearly identical predictions, and the slight differences are small and not likely to have practical significance. The non-dilute model predictions are also similar to the 2P model baseline case, with the exception of the first step of CPA removal. The non-dilute model exhibits less swelling and faster equilibration during the first step of CPA removal than the 2P model.

Overall, the predictions suggest that modifying the first step of the CPA removal process may reduce damage to bovine oocytes. In particular, we observed that the non-dilute model predicts that the amount of osmotic swelling after vitrification relative to the starting (shrunken) volume is minor compared to the dilute model. To our knowledge, we are the first to demonstrate that the non-dilute model and dilute model predict such different volume responses during CPA removal, highlighting the need for future studies to examine the relative accuracy of the two different modeling approaches. If the non-dilute model predictions turn out to be more accurate than those from the dilute model, a very different protocol for CPA removal should be well tolerated such as much less sucrose would be needed as an osmotic buffer in step 1. By reducing the amount of sucrose in the medium the oocytes would not be expected to shrink as much, keeping them within osmotic tolerance limits. This is expected to cause much less damage than the original protocol (Davidson *et al.* 2014).

To account for the effects of CPA concentration on water and CPA permeability, we fit the permeability data to a concentration-dependent model (Lahmann *et al.* 2018). This model is consistent with a transport mechanism that is limited by binding of CPA to a transporter protein such as an aquaporin. The concentration dependent model fits were in reasonable agreement with our permeability data. These results leads us to bring up a new experimental design in which the main objective was to study the importance of the aquaglyceroporins on the movement of water and CPA across cell membrane in bovine MII oocytes. For that purpose, we first investigated whether hyperosmotic stress induced changes on the protein expression of AQP3, AQP7 and AQP9 by exposing *in vitro* matured bovine oocytes to hypertonic solutions of two permeable CPAs (9.5% Me_2SO and 8% EG) and a non-penetrating CPAs (0.5 M sucrose) for 20 min at 25ºC. We demonstrated that CPAs stimulated AQP3 and AQP7 but not AQP9 expression in mature bovine oocytes. In particular, we observed that exposure of oocytes to hyperosmotic Me_2SO solution could upregulate AQP3 while AQP7 expression was upregulated after EG hyperosmotic exposure. Instead, murine oocytes exposed to a hyperosmotic CPA solution containing EG, Me_2SO or sucrose increased the expression of AQP7, but not of AQP3 and AQP9 (Tan *et al.* 2013; Tan *et al.* 2015). Results obtained so far both in bovine and mouse oocytes may indicate that aquaporin upregulation in oocytes due to hyperosmosis it is not only species-specific, but also depends on the CPA itself.

Previous studies demonstrated that water and CPAs move through plasma membrane of mouse and bovine oocytes predominantly by simple diffusion, but a smaller

proportion of water moves via channel processes; thus, AQP3 was found to play a major role in aiding the diffusion of water, glycerol and EG in cow and mouse oocytes (Edashige *et al.* 2007; Jin *et al.* 2011). Moreover, to examine whether the artificial expression of AQP3 could improve water and CPA permeability and oocyte survival after cryopreservation, exogenous expression of rat AQP3 in mouse oocytes or human and zebrafish AQP3 in porcine oocytes was measured (Edashige *et al.* 2003)·(Yamaji *et al.* 2011; Morató *et al.* 2014). In these studies, exogenous expression of AQP3 enhanced both the efflux of water and influx of CPAs into the cell, thus improving oocyte tolerance to survival and embryo development after warming of mouse oocytes (Edashige *et al.* 2003; Yamaji *et al.* 2011). However, there was no information in the literature regarding to the overexpression of AQP7 and its effect on the permeability to water and CPAs in bovine oocytes. Thus, the second objective of the chapter II was to examine the role of AQP7 in the movement of water and CPAs in bovine *in vitro* matured oocytes in which AQP7 was artificially overexpressed through cRNA injection. In our study, we successfully over-expressed bovine AQP7 channel in bovine MII oocytes by cRNA microinjection at the GV stage. Bovine oocytes were able to translate and integrate exogenous aquaporins in the plasma membrane during IVM, as found for murine, amphibian, and porcine oocytes (Edashige *et al.* 2003; Chauvigné *et al.* 2011; Jin *et al.* 2011; Valdez *et al.* 2013; Morató *et al.* 2014). Viability or competence of oocytes to resume meiosis *in vitro* was lower for microinjected oocytes compared to non-injected oocytes, probably caused by the microinjection injury or to the presence of an exogenous cRNA. However, the rate of EGFP protein expression in the injected bovine oocytes was high (≈86%) when compared to previous studies in which AQP3 was microinjected in immature porcine oocytes (Ohashi *et al.* 2001; Morató *et al.* 2014), suggesting a higher capacity of bovine oocytes to translate and integrate exogenous aquaporins. Moreover, EGFP is a good proxy for the expression of other proteins because all of the EGFP-positive oocytes also contained high levels of AQP7 protein located in the cytoplasm and around the plasma membrane.

The aquaglyceroporin role on CPA permeability during dehydration and swelling of IVM bovine oocytes has previously been reported (Edashige *et al.* 2003). Edashige´s research group showed that permeability of bovine oocytes to water and CPAs was low but higher than in mouse oocytes. Our results for Lp and Ps in the presence of EG or Me_2SO were higher than those determined by Agca et al (Agca *et al.* 1998) and Jin et al (Jin *et al.* 2011) meanwhile the permeability to water in the presence of sucrose was similar to other studies (Jin *et al.* 2011). Moreover, Jin et al (Jin *et al.* 2011) observed that water and CPAs

move through cow oocytes predominantly by simple diffusion but suggested that other water and CPA channels could be involved in the relatively high membrane permeability of bovine oocytes. When exogenous expression of bovine AQP3 in mouse oocytes was examined (Jin *et al.* 2011), the authors demonstrated that bovine AQP3 increased water permeability in a hypertonic sucrose solution, a glycerol solution, and a Me_2SO solution but not in an ethylene glycol solution and a propylene glycol solution, as occurred in mouse AQP3 (Edashige *et al.* 2007). Similarly, our study demonstrated that after injection of EGFP+AQP7 cRNA and 24 h of IVM, water permeability increased almost 2 times compared to non-injected oocytes when oocytes were exposed to sucrose and Me_2SO solution. However, this tendency was not observed in an EG solution, similar to previous results (Jin *et al.* 2011). Our results together with those observed by Jin et al (Jin *et al.* 2011) suggest that both, AQP3 and AQP7, are involved in water movement when oocytes are exposed to sucrose or Me_2SO solution, whereas water diffusion mainly happens through simple diffusion when oocytes are exposed to EG.

Moreover, it has observed that overexpression of AQPs not only enhance water permeability but also CPA permeability, thus improving oocyte tolerance to survival after warming mouse oocytes (Edashige *et al.* 2003; Morató *et al.* 2014). Jin et al (Jin *et al.* 2011) demonstrated that the exogenous expression of bovine AQP3 also increase the permeability to EG showing 13 times higher permeability than that for non-injected oocytes. Because permeability to EG was not altered in AQP7 microinjected oocyte, it may be hypostatized that EG molecules moves through AQP3 but not AQP7 channels when the bovine oocyte is suspended in a EG solution. Similar to our results, AQP3 (Jin *et al.* 2011) or AQP7 cRNA-injected oocytes had similar permeability to Me_2SO than non-injected oocytes, suggesting that Me_2SO move by simple diffusion across oocyte plasma membrane.

However, despite the mathematical approaches and a better knowledge of the movement of water and CPA across oocyte cell membrane, there is no universal vitrification protocol for bovine oocytes. Most vitrification protocols initially involve a long exposure stage to a non-vitrifying solution lasting 8 to 15 min followed by a short time of exposure (~1 min) to the VS (Dujickova *et al.* 2020). These procedures, however, rarely consider the osmotic tolerance of the cells according to temperature and time of CPA addition and removal. When this characteristic is taken into account, the time needed to prepare oocytes for vitrification can be shortened while maintaining the critical cytosolic solute content necessary for successful vitrification. Thus, optimization of cryopreservation

techniques can be pursued by a wholly empirical methodology or by using fundamental cryobiology theory and mathematical simulations (Leibo 2008; Gallardo *et al.* 2019), which requires knowledge of the biophysical parameters of the oocytes and also of the effects of osmotic stress (both magnitude and duration) on the developmental potential of oocytes. In the context of optimization of cryopreservation procedures for vitrification in the presence of combined CPAs, the main goal in chapter III was to determine the best exposure time to the equilibration solution at a specific temperature (Wang *et al.* 2011). For that purpose, we first determined both predictively and experimentally the osmotic behavior of metaphase II (MII) bovine oocytes in terms of membrane permeability parameters (L_p and P_s) in response to ES CPAs at 25°C and 38.5°C. Despite the own limitations of the *in silico* and *in vitro* analysis of the osmotic behavior of MII oocytes, our results were fairly consistent. The time required for the oocytes to reach the equilibrium cell volume upon exposure to standard ES increased as the temperature decreased, such that 2 min 30 s was needed at 38.5°C and 5 min 30 s at 25°C. This is important because during this interval intracellular water ejection is close to completion and the permeation of low molecular weight CPAs leads to similar intracellular and extracellular solute concentrations. Hence, lengthening exposure to CPAs solutions does not improve the cytosolic glass-forming tendency and toxicity derived for longer CPA exposures could be avoided. This determines that rather than the usual 9 to 15 min of CPA exposure time used for bovine oocytes, a better approach could be the exposure of oocytes to non-vitrifying hypertonic solutions just until the equilibrium cell volume is reached to prepare them for vitrification. In the present study, we modified the equilibration protocol of a new vitrification/warming method designed to represent the current standard practice to prepare bovine oocytes (Kuwayama 2007) according to the *in vitro* osmotic behavior of oocytes at different temperatures. These modifications to the protocol were validated by examining oocyte spindle status, oocyte DNA fragmentation and further embryo development after vitrification/warming of MII bovine oocytes.

The main hurdle in developing successful protocols for the cryopreservation of mammalian oocytes is preserving the integrity of the meiotic spindle when oocytes are cooled below physiological temperature. Temperature fluctuations directly affect the cytoskeletal and microtubular system of mature bovine (Aman and Parks 1994) and human (Almeida and Bolton 1995) oocytes. While the effects of cooling on the spindle seem reversible in the mouse oocyte, with normal spindle formation occurring after step-wise re-warming (Pickering and Johnson 1987), bovine and human oocytes are less resilient

because of the irreversibility of temperature-induced spindle disruption (Pickering *et al.* 1990; Aman and Parks 1994; Almeida and Bolton 1995). In our study, exposure of oocytes to CPAs at 25°C for 5 min 30 s yielded the lowest percentage of oocytes reaching the MII stage. Aman and Parks (Aman and Parks 1994) reported that the spindles of MII bovine oocytes started to depolymerize when cooled to 25°C for 1 min or more, and the extent of depolymerization (or disassembly) was also directly related to CPA exposure duration (Aman and Parks 1994). We also observed that CPA exposure or vitrification after equilibration at 25°C for 5 min 30 s also resulted in reduced proportions of oocytes displaying normal spindle configurations. Other authors have described higher proportions of spindle alterations in MII bovine oocytes vitrified after similar or longer exposures times to the equilibration solution at 25°C (Arcarons *et al.* 2015; Chaves *et al.* 2016) when compared to their fresh counterparts. However, no significant increase was noted here in chromosomal abnormalities after CPA exposure at 38.5°C for 2 min 30 s before vitrification, suggesting that the bovine oocytes were able to recover from cooling or CPA-induced damage to the oocytes' spindle microtubules. In prior work, we observed that bovine oocytes vitrified after 10 min of exposure to ES at 38.5°C led to similar rates of maturation and normal spindle configurations to those detected here at 38.5°C (Arcarons *et al.* 2019; García-Martínez *et al.* 2020). This may indicate that IVM bovine oocytes are more sensitive to the temperature of exposure to ES and VS than to the detrimental effects of CPA toxicity.

Moreover, vitrification after CPA exposure at 38.5°C for 2 min 30 s did not significantly affect the rate of DNA fragmentation in oocytes when compared to fresh controls. Contrarily, exposure or vitrification of oocytes at 25°C significantly increased the percentage of DNA fragmentation after warming. Using the same methodology, studies by our group (Spricigo *et al.* 2017; Vendrell-Flotats *et al.* 2020) detected significantly higher apoptosis rates through TUNEL analysis in bovine oocytes vitrified after being exposed for a longer time to ES (10 min or 9 min, respectively) at 38.5°C. Hence, the toxicity of CPAs in terms of DNA fragmentation can be reduced by modifying equilibration times and temperatures (Raju *et al.* 2021).

Embryo development experiments were designed to assess oocyte competence after vitrification/warming. The results indicate comparable cleavage and blastocyst rates of vitrified bovine oocytes after exposure to CPA solutions at 38.5°C to those of control fresh oocytes. Moreover, although not significant, shorter CPA exposures at 38.5°C gave rise to almost double the percentage of blastocysts obtained after longer CPA exposure at 25°C.

These results make evident the importance of temperature and time of CPA addition prior to vitrification. Cytotoxicity has been shown to increase with increased temperatures for relatively long exposure times (Lawson *et al.* 2011; Davidson *et al.* 2015). This has led to the general assumption that CPA exposure should be carried out at low temperatures (25°C). However, the temperature of addition significantly affects the time needed to achieve full equilibration. At a higher temperature, equilibration occurs much more quickly, allowing for shorter incubation times and reducing cell exposure to CPAs during their addition and removal. Due to faster mass transport across cell membrane at 38.5°C, equilibration of the oocyte occurs earlier than at 25°C and less time is required for CPA addition. If we bear in mind that CPA exposure at 38.5°C had fewer deleterious effects on the meiotic spindle and oocyte apoptosis, CPA exposure at 38.5°C for 2 min 30 s may have allowed the oocyte to achieve the minimum intracellular glass-forming conditions so as not to fully impair the ability of vitrified/warmed oocytes to be successfully fertilized and develop into viable embryos.

When this same vitrification/warming methodology was used to vitrify MII bovine oocytes (Kuwayama 2007), a longer exposure (9 or 15 min) to ES at 25°C produced lower (Azari *et al.* 2017) or similar (Zhou *et al.* 2010; Vendrell-Flotats *et al.* 2020) cleavage and blastocyst rates to the ones observed in our study in the VIT25 group. However, blastocyst yields were reduced when IVM bovine oocytes were exposed to ES at 38.5°C-39°C for 9 or more minutes prior to vitrification (Ortiz-Escribano *et al.* 2016; Arcarons *et al.* 2017; Arcarons *et al.* 2019; García-Martínez *et al.* 2020). These findings highlight the fact that the effects of temperature on cytotoxicity are clearly dependent on exposure times (Lawson *et al.* 2011). Thus, reports exist of significantly decreased rates of embryo development when oocytes were overexposed to CPAs at 38.5°C (Ortiz-Escribano *et al.* 2016; Arcarons *et al.* 2017; Arcarons *et al.* 2019; García-Martínez *et al.* 2020) while prolonged exposure (9 or 15 min) at 25°C also impaired embryo development (Zhou *et al.* 2010; Vendrell-Flotats *et al.* 2020) but this effect was much less dramatic than at 38.5°C.

Taking into account these results, we have demonstrated that the *in silico* data on the biophysical permeability of oocytes and *in vitro* osmotic observations risen in similar results. So we could use mathematical modeling to optimize vitrification/warming methods for bovine IVM oocytes. Moreover, we proposed a shorter vitrification/warming protocol for MII bovine oocytes by reducing the exposure time to ES CPA according to the temperature, validated by better outcomes in oocyte morphofunctionality and embryo development.

Conclusions

Conclusions

- CPA concentration affects membrane permeability of bovine oocytes, with different effects depending on the maturation stage of the oocyte and the specific CPA type. *In vitro* matured oocytes showed a higher permeability to water than immature oocytes when exposed to increasing concentrations of Me_2SO and EG. However, membrane permeability to water decreased as CPA concentration increased, regardless of the maturation stage. At higher CPA concentrations, CPA permeability of MII and GV oocytes was similar for Me_2SO and EG, while EG permeability at low concentrations was substantially higher in GV oocytes.

- When two modeling approaches were compared, the first one using dilute solution assumptions, and the second one not restricted to those assumptions, results indicated that only slight differences exist between the two models' predictions during the CPA loading steps while a greater difference was observed between models during the first stage of CPA removal. .

- *In vitro* matured oocytes expressed AQP3 and AQP7 but not AQP9 when exposed to hyperosmotic solutions. Exposure of oocytes to hyperosmotic Me_2SO solution upregulated AQP3 while AQP7 expression was upregulated by EG hyperosmotic exposure in oocytes in a CPA-dependent fashion.

- AQP7 channel was successfully over-expressed in bovine *in vitro* matured bovine oocytes by cRNA microinjection at the germinal vesicle stage

- AQP7 seems to facilitate water diffusion when bovine MII oocytes are exposed to hyperosmotic sucrose or Me_2SO solutions but not when exposed to a hyperosmotic EG solution. However, AQP7 is not involved in the movement of Me_2SO and EG, which mainly move through cell membranes by simple diffusion.

- When the permeability parameters previously determined were used, the two parameter model was effective to predict the osmotic response of bovine *in vitro* matured oocytes at different temperatures in a similar approach than the *in vitro* experiments.

- Based on *in silico* and *in vitro* osmotic observations, exposure of bovine *in vitro* matured oocytes to the equilibration solution was constrained to 5 min 30 s or to 2 min 30 s when ES exposure was done at 25°C or 38.5°C, respectively.

- Exposure to equilibration solution for 2 min 30 s and vitrification/warming at 38.5°C improved the quality of vitrified/warmed bovine *in vitro* matured oocytes improving blastocyst rates and quality by protecting spindle integrity and reducing DNA fragmentation. These data also indicate that toxic damage at a given temperature may be reduced by minimizing the duration of CPA addition and removal while maintaining cell volumes within osmotic tolerance limits.

References

Agca, Y., Liu, J., Peter, A.T., Critser, E.S., and Critser, J.K. (1998) Effect of developmental stage on bovine oocyte plasma membrane water and cryoprotectant permeability characteristics. *Mol Reprod Dev* **49**(4), 408-15

Almeida, P.A., and Bolton, V.N. (1995) The effect of temperature fluctuations on the cytoskeletal organisation and chromosomal constitution of the human oocyte. *Zygote* **3**(4), 357-65

Aman, R.R., and Parks, J.E. (1994) Effects of cooling and rewarming on the meiotic spindle and chromosomes of *in vitro*-matured bovine oocytes. *Biol Reprod* **50**(1), 103-10

Ambrosini, G., Andrisani, A., Porcu, E., Rebellato, E., Revelli, A., Caserta, D., Cosmi, E., Marci, R., and Moscarini, M. (2006) Oocytes cryopreservation: state of art. *Reprod Toxicol* **22**(2), 250-62

Anchordoguy, T.J., Cecchini, C.A., Crowe, J.H., and Crowe, L.M. (1991) Insights into the cryoprotective mechanism of dimethyl sulfoxide for phospholipid bilayers. *Cryobiology* **28**(5), 467-73

Arcarons, N., Morato, R., Spricigo, J.F., Ferraz, M.A., and Mogas, T. (2015) Spindle configuration and developmental competence of *in vitro*-matured bovine oocytes exposed to NaCl or sucrose prior to Cryotop vitrification. *Reprod Fertil Dev*

Arcarons, N., Vendrell-Flotats, M., Yeste, M., Mercade, E., Lopez-Bejar, M., and Mogas, T. (2019) Cryoprotectant role of exopolysaccharide of Pseudomonas sp. ID1 in the vitrification of IVM cow oocytes. *Reprod Fertil Dev* **31**(9), 1507-1519

Arcarons, N., Vendrell-Flotats, M., Yeste, M., Mercadé, E., and Mogas, T. (2017) Spindle configuration of *in vitro* matured bovine oocytes vitrified and warmed in media supplemented with a biopolymer produced by an Antarctic bacterium. *Animal Reproduction* **14**(3), 972

Azari, M., Kafi, M., Ebrahimi, B., Fatehi, R., and Jamalzadeh, M. (2017) Oocyte maturation, embryo development and gene expression following two different methods of bovine cumulus-oocyte complexes vitrification. *Vet Res Commun* **41**(1), 49-56

Chauvigné, F., Lubzens, E., and Cerdà, J. (2011) Design and characterization of genetically engineered zebrafish aquaporin-3 mutants highly permeable to the cryoprotectant ethylene glycol. *BMC Biotechnol* **11**, 34

Chaves, D.F., Campelo, I.S., Silva, M.M., Bhat, M.H., Teixeira, D.I., Melo, L.M., Souza-Fabjan, J.M., Mermillod, P., and Freitas, V.J. (2016) The use of antifreeze protein type III for vitrification of *in vitro* matured bovine oocytes. *Cryobiology* **73**(3), 324-328

Checura, C.M., and Seidel, G.E., Jr. (2007) Effect of macromolecules in solutions for vitrification of mature bovine oocytes. *Theriogenology* **67**(5), 919-30Chian, R.C., Kuwayama,

M., Tan, L., Tan, J., Kato, O., and Nagai, T. (2004) High survival rate of bovine oocytes matured *in vitro* following vitrification. *J Reprod Dev* **50**(6), 685-96

Davidson, A.F., Benson, J.D., and Higgins, A.Z. (2014) Mathematically optimized cryoprotectant equilibration procedures for cryopreservation of human oocytes. *Theor Biol Med Model* **11**, 13

Davidson, A.F., Glasscock, C., McClanahan, D.R., Benson, J.D., and Higgins, A.Z. (2015) Toxicity Minimized Cryoprotectant Addition and Removal Procedures for Adherent Endothelial Cells. *PLoS One* **10**(11), e0142828

Dujickova, L., Makarevich, A.V., Olexikova, L., Kubovicova, E., and Strejcek, F. (2020) Methodological approaches for vitrification of bovine oocytes. *Zygote*, 1-11

Edashige, K. (2017) Permeability of the plasma membrane to water and cryoprotectants in mammalian oocytes and embryos: Its relevance to vitrification. *Reprod Med Biol* **16**(1), 36-39

Edashige, K., Ohta, S., Tanaka, M., Kuwano, T., Valdez, D.M., Jr., Hara, T., Jin, B., Takahashi, S., Seki, S., Koshimoto, C., and Kasai, M. (2007) The role of aquaporin 3 in the movement of water and cryoprotectants in mouse morulae. *Biol Reprod* **77**(2), 365-75

Edashige, K., Yamaji, Y., Kleinhans, F.W., and Kasai, M. (2003) Artificial expression of aquaporin-3 improves the survival of mouse oocytes after cryopreservation. *Biol Reprod* **68**(1), 87-94

Elmoazzen, H.Y., Elliott, J.A., and McGann, L.E. (2009) Osmotic transport across cell membranes in nondilute solutions: a new nondilute solute transport equation. *Biophys J* **96**(7), 2559-71

Fabbri, R. (2006) Cryopreservation of human oocytes and ovarian tissue. *Cell Tissue Bank* **7**(2), 113-22

Gallardo, M., Saenz, J., and Risco, R. (2019) Human oocytes and zygotes are ready for ultra-fast vitrification after 2 minutes of exposure to standard CPA solutions. *Sci Rep* **9**(1), 15986

García-Martínez, T., Vendrell-Flotats, M., López-Béjar, M., and Mogas, T. (2018) Exposure to hyperosmotic solutions modifies expression of AQP3 and AQP7 on bovine oocytes. *Cryobiology* **85**, 14

García-Martínez, T., Vendrell-Flotats, M., Martínez-Rodero, I., Ordóñez-León, E.A., Álvarez-Rodríguez, M., López-Béjar, M., Yeste, M., and Mogas, T. (2020) Glutathione Ethyl Ester Protects *In Vitro*-Maturing Bovine Oocytes against Oxidative Stress Induced by Subsequent Vitrification/Warming. *Int J Mol Sci* **21**(20)

Gilmore, J.A., McGann, L.E., Liu, J., Gao, D.Y., Peter, A.T., Kleinhans, F.W., and Critser, J.K. (1995) Effect of cryoprotectant solutes on water permeability of human spermatozoa. *Biol Reprod* **53**(5), 985-95

Jacobs, M.H. (1933) The simultaneous measurement of cell permeability to water and to dissolved substances. *Journal of Cellular and Comparative Physiology* **2**(4), 427-444

Jacobs, M.H., and Stewart, D.R. (1932) A simple method for the quantitative measurement of cell permeability. *Journal of Cellular and Comparative Physiology* **1**(1), 71-82

Jin, B., Kawai, Y., Hara, T., Takeda, S., Seki, S., Nakata, Y., Matsukawa, K., Koshimoto, C., Kasai, M., and Edashige, K. (2011) Pathway for the movement of water and cryoprotectants in bovine oocytes and embryos. *Biol Reprod* **85**(4), 834-47

Jo, J.W., Jee, B.C., Suh, C.S., Kim, S.H., Choi, Y.M., Kim, J.G., and Moon, S.Y. (2011) Effect of maturation on the expression of aquaporin 3 in mouse oocyte. *Zygote* **19**(1), 9-14

Karlsson, J.O., and Toner, M. (1996) Long-term storage of tissues by cryopreservation: critical issues. *Biomaterials* **17**(3), 243-56

Kedem, O., and Katchalsky, A. (1958) Thermodynamic analysis of the permeability of biological membranes to non-electrolytes. *Biochim Biophys Acta* **27**(2), 229-46

Kuwayama, M. (2007) Highly efficient vitrification for cryopreservation of human oocytes and embryos: the Cryotop method. *Theriogenology* **67**(1), 73-80

Kuwayama, M., Vajta, G., Kato, O., and Leibo, S.P. (2005) Highly efficient vitrification method for cryopreservation of human oocytes. *Reprod Biomed Online* **11**(3), 300-8

Lahmann, J.M., Benson, J.D., and Higgins, A.Z. (2018) Concentration dependence of the cell membrane permeability to cryoprotectant and water and implications for design of methods for post-thaw washing of human erythrocytes. *Cryobiology* **80**, 1-11

Lawson, A., Ahmad, H., and Sambanis, A. (2011) Cytotoxicity effects of cryoprotectants as single-component and cocktail vitrification solutions. *Cryobiology* **62**(2), 115-22

Leibo, S.P. (2008) Cryopreservation of oocytes and embryos: optimization by theoretical versus empirical analysis. *Theriogenology* **69**(1), 37-47

McGrath, J.J. (1988) Membrane Transport Properties. In Low Temperature Biotechnology: Emerging Application and Engineering Contributions. In 'New York: American Society of Mechanical Engineers.' (Eds. J McGrath and K Diller) pp. 273-331)

Morató, R., Chauvigné, F., Novo, S., Bonet, S., and Cerdà, J. (2014) Enhanced water and cryoprotectant permeability of porcine oocytes after artificial expression of human and zebrafish aquaporin-3 channels. *Mol Reprod Dev* **81**(5), 450-61

Morato, R., Izquierdo, D., Albarracin, J.L., Anguita, B., Palomo, M.J., Jimenez-Macedo, A.R., Paramio, M.T., and Mogas, T. (2008) Effects of pre-treating *in vitro*-matured bovine oocytes with the cytoskeleton stabilizing agent taxol prior to vitrification. *Mol Reprod Dev* **75**(1), 191-201

Moss, F.J., Mahinthichaichan, P., Lodowski, D.T., Kowatz, T., Tajkhorshid, E., Engel, A., Boron, W.F., and Vahedi-Faridi, A. (2020) Aquaporin-7: A Dynamic Aquaglyceroporin With Greater Water and Glycerol Permeability Than Its Bacterial Homolog GlpF. *Front Physiol* **11**, 728

Ohashi, S., Naito, K., Liu, J., Sheng, Y., Yamanouchi, K., and Tojo, H. (2001) Expression of Exogenous Proteins in Porcine Maturing Oocytes after mRNA Injection: Kinetic Analysis and Oocyte Selection Using EGFP mRNA. *Journal of Reproduction and Development* **47**(6), 351-357

Ortiz-Escribano, N., Smits, K., Piepers, S., Van den Abbeel, E., Woelders, H., and Van Soom, A. (2016) Role of cumulus cells during vitrification and fertilization of mature bovine oocytes: Effects on survival, fertilization, and blastocyst development. *Theriogenology* **86**(2), 635-41

Pickering, S.J., Braude, P.R., Johnson, M.H., Cant, A., and Currie, J. (1990) Transient cooling to room temperature can cause irreversible disruption of the meiotic spindle in the human oocyte. *Fertil Steril* **54**(1), 102-8

Pickering, S.J., and Johnson, M.H. (1987) The influence of cooling on the organization of the meiotic spindle of the mouse oocyte. *Hum Reprod* **2**(3), 207-16

Raju, R., Bryant, S.J., Wilkinson, B.L., and Bryant, G. (2021) The need for novel cryoprotectants and cryopreservation protocols: Insights into the importance of biophysical investigation and cell permeability. *Biochim Biophys Acta Gen Subj* **1865**(1), 129749

Rodriguez, R.A., Liang, H., Chen, L.Y., Plascencia-Villa, G., and Perry, G. (2019) Single-channel permeability and glycerol affinity of human aquaglyceroporin AQP3. *Biochim Biophys Acta Biomembr* **1861**(4), 768-775

Spricigo, J.F., Morato, R., Arcarons, N., Yeste, M., Dode, M.A., Lopez-Bejar, M., and Mogas, T. (2017) Assessment of the effect of adding L-carnitine and/or resveratrol to maturation medium before vitrification on *in vitro*-matured calf oocytes. *Theriogenology* **89**, 47-57

Tan, Y.J., Xiong, Y., Ding, G.L., Zhang, D., Meng, Y., Huang, H.F., and Sheng, J.Z. (2013) Cryoprotectants up-regulate expression of mouse oocyte AQP7, which facilitates water diffusion during cryopreservation. *Fertil Steril* **99**(5), 1428-35

Tan, Y.J., Zhang, X.Y., Ding, G.L., Li, R., Wang, L., Jin, L., Lin, X.H., Gao, L., Sheng, J.Z., and Huang, H.F. (2015) Aquaporin7 plays a crucial role in tolerance to hyperosmotic stress and in the survival of oocytes during cryopreservation. *Sci Rep* **5**, 17741

Toon, M.R., and Solomon, A.K. (1990) Transport parameters in the human red cell membrane: solute-membrane interactions of hydrophilic alcohols and their effect on permeation. *Biochim Biophys Acta* **1022**(1), 57-71

Valdez, D.M., Jr., Tsuchiya, R., Seki, S., Saida, N., Niimi, S., Koshimoto, C., Matsukawa, K., Kasai, M., and Edashige, K. (2013) A trial to cryopreserve immature medaka (Oryzias latipes) oocytes after enhancing their permeability by exogenous expression of aquaporin 3. *J Reprod Dev* **59**(2), 205-13

Vendrell-Flotats, M., Garcia-Martinez, T., Martinez-Rodero, I., Lopez-Bejar, M., LaMarre, J., Yeste, M., and Mogas, T. (2020) *In Vitro* Maturation with Leukemia Inhibitory Factor Prior to the Vitrification of Bovine Oocytes Improves Their Embryo Developmental Potential and Gene Expression in Oocytes and Embryos. *Int J Mol Sci* **21**(19)

Wang, L., Liu, J., Zhou, G.B., Hou, Y.P., Li, J.J., and Zhu, S.E. (2011) Quantitative investigations on the effects of exposure durations to the combined cryoprotective agents on mouse oocyte vitrification procedures. *Biol Reprod* **85**(5), 884-94

Wang, X., Al Naib, A., Sun, D.W., and Lonergan, P. (2010) Membrane permeability characteristics of bovine oocytes and development of a step-wise cryoprotectant adding and diluting protocol. *Cryobiology* **61**(1), 58-65

Yamaji, Y., Seki, S., Matsukawa, K., Koshimoto, C., Kasai, M., and Edashige, K. (2011) Developmental ability of vitrified mouse oocytes expressing water channels. *J Reprod Dev* **57**(3), 403-8

Yang, G., Veres, M., Szalai, G., Zhang, A., Xu, L.X., and He, X. (2011) Biotransport phenomena in freezing mammalian oocytes. *Ann Biomed Eng* **39**(1), 580-91

Yi, J., Tang, H., and Zhao, G. (2014) Influence of hydroxyapatite nanoparticles on the viscosity of dimethyl sulfoxide-H2O-NaCl and glycerol-H2O-NaCl ternary systems at subzero temperatures. *Cryobiology* **69**(2), 291-8

Zhang, Y., Zhao, G., Yi, J., Shu, Z., Zhou, P., Cao, Y., and Gao, D. (2016) Comparison of the Fitting Validity Between the 2P Model and the Nondilute Solution Model Using Statistical Methods in Modeling Cell Membrane Permeabilities. *Biopreserv Biobank* **14**(1), 39-44

Zhou, X.L., Al Naib, A., Sun, D.W., and Lonergan, P. (2010) Bovine oocyte vitrification using the Cryotop method: effect of cumulus cells and vitrification protocol on survival and subsequent development. *Cryobiology* **61**(1), 66-72